

**MECHANISTIC STUDIES ON THE LIGAND
SUBSTITUTION REACTIONS OF Fe(II),
Fe(III), Pd(II) AND Cd(II) COMPLEXES**

A Thesis Submitted
In Partial Fulfilment of the Requirements
for the Degree of

DOCTOR OF PHILOSOPHY

By
Ms. NISHI GUPTA

to the

DEPARTMENT OF CHEMISTRY

INDIAN INSTITUTE OF TECHNOLOGY, KANPUR
APRIL, 1988

*Dedicated to
My Parents
As a token of
Love and Regards*

CHM-1985-D-GUD-M.

- 8 NOV 1989

CENTRAL LIBRARY

I.I.T. KANPUR

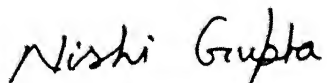
Acc. No. 106263

Th
541.2242
G 959m

STATEMENT

I, hereby, state that the matter embodied in this thesis is the result of investigations carried out by me in the Department of Chemistry, Indian Institute of Technology, Kanpur, under the supervision of Professor P.C. Nigam.

In keeping with the general practice of reporting scientific observations, due acknowledgement has been given wherever the work described is based on the findings of other investigators.



Nishi Gupta

DEPARTMENT OF CHEMISTRY
INDIAN INSTITUTE OF TECHNOLOGY, KANPUR, INDIA

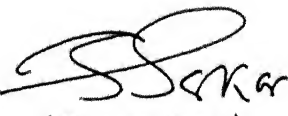
CERTIFICATE-I

This is to certify that Ms. Nishi Gupta has satisfactorily completed all the courses required for the Ph.D. programme. These courses are listed below:

Chm 505 Principles of Organic Chemistry
Chm 521 Chemical Binding
Chm 524 Modern Methods in Physical Chemistry
Chm 525 Principles of Physical Chemistry
Chm 545 Principles of Inorganic Chemistry
Chm 622 Chemical Kinetics
Chm 646 Bio-Inorganic Chemistry
Chm 800 General Seminar
Chm 801 Graduate Seminar
Chm 900 Post Graduate Research

Ms. Nishi Gupta was admitted to the candidacy of the Ph.D. degree on January 21, 1985 after she successfully completed the written and oral qualifying examinations.


(P.S. Goel)
Professor and Head
Dept. of Chemistry
IIT-KANPUR


(S. Sarkar)
Convener
Departmental Post Graduate Committee
Department of Chemistry
IIT-KANPUR

CERTIFICATE II

Certified that the work contained in this thesis titled, 'MECHANISTIC STUDIES ON THE LIGAND SUBSTITUTION REACTIONS OF Fe(II), Fe(III), Pd(II) and Cd(II) CENTRES' has been carried out by Ms. Nishi Gupta under my supervision and the same has not been submitted elsewhere for a degree.

P. C. Nigam
(P.C. Nigam)
Thesis Supervisor

Kanpur
May 1988

ACKNOWLEDGEMENTS

It is a very difficult task to acknowledge the gratitude of one's own benefactors and well wishes. To enlist all of them is not an easy task. To repay them is beyond my capacity. Yet I must attempt to express my sentiments in a modest way.

First of all, I wish to record my profound gratitude to Prof. P.C. Nigam who inspired and encouraged me through his scholarly guidance, constructive suggestions, critical comments and detailed instructions at every stage of my research programme. He has been sympathetic and affectionate in moments of despair. The second person whom I feel compelled to express my gratitude is Mrs. Madhuri Nigam for her kind hospitality, understanding and motherly treatment during my stay in campus.

I owe a lot to my senior research colleague Dr. R.M. Naik (now at C.S.M.C.R.I., Bhavnagar) who introduced me to the ways and language of laboratory discipline and helped me in various other ways in the completion of my work. I am highly grateful to my other laboratory mates Ms. Pratima Mishra, Mr. S. Prasad, Mr. S. Asthana and Ms. Seema Tiwari for their kind cooperation and consideration. It is also my privilege to thank Mr. S.R. Naidu for various helps, Ms. Bedamati Das and Ms. Swati Mohanty who enlivened many hours which would have been unbearably dull.

I am highly indebted to Prof. U.C. Agarwala for helpful discussions, Prof. N. Sathyamurthy, Prof. P.K. Ghosh, Prof. S.K. Dogra and my other teachers in the department for their encouragement from time to time.

I am highly thankful to Mr. M.L. Sharma for maintenance of laboratory and other help and Mr. R.K. Sharma and his team for upkeep of electronic equipments. I wish to thank Mr. Anil Johari for meticulous typing, Mr. R.K. Bajpai for tracing the drawings.

I find myself at a loss for words in expressing my heartfelt gratitude to my adored parents, sisters and brothers for providing tremendous moral support and encouragement for completion of my work.

Nishi Gupta

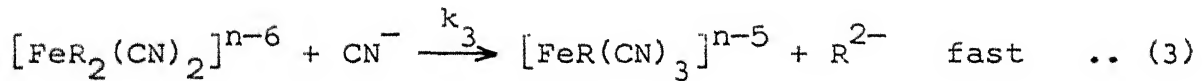
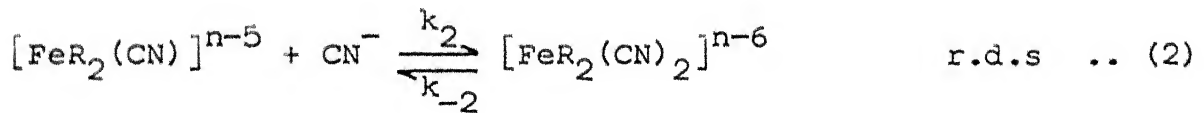
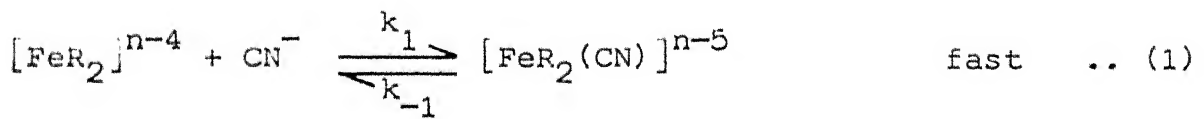
PREFACE

The work described in this thesis relates mainly to the kinetics and mechanisms of ligand substitution reactions on complexes of Fe(II), Fe(III), Pd(II) and Cd(II). Ligand substitution reactions of coordination compounds involving substitution of multidentate ligands by monodentate as well as multidentate ligands have been investigated. The thesis consists of seven chapters whose contents are described hereunder.

The first chapter is introductory and contains a brief survey of the earlier work reported in this area and the scope of present investigations.

The second chapter describes the kinetics and mechanism of formation of mixed-ligand complexes as the ultimate product from the reaction of $[\text{Fe}(\text{Par})_2]^{n-4}$ with cyanide ion (Par = 4-(2-pyridyl-azo)resorcinol and n = charge on Fe centre). The reactions have been studied spectrophotometrically for both Fe(II) and Fe(III) complexes at 720 nm which is the λ_{max} of $[\text{Fe}(\text{Par})_2]^{n-4}$ complexes. The reaction conditions for $[\text{Fe}(\text{Par})_2]^{2-} - \text{CN}^-$ reaction are: pH = 11.5 ± 0.02 , I = 0.1 M and temp. = $25 \pm 0.1^\circ\text{C}$ while for $[\text{Fe}(\text{Par})_2]^- - \text{CN}^-$ reaction are: pH = 10.0 ± 0.02 , I = 0.1 M, temp. = $25 \pm 0.1^\circ\text{C}$. The spectral scans of reaction mixture show that there is a continuous decrease in the peak height of 720 nm and 496 nm bands of $[\text{Fe}(\text{Par})_2]^{n-4}$ and formation of two new peaks at 490 and 460 nm in the later part of reaction due to formation

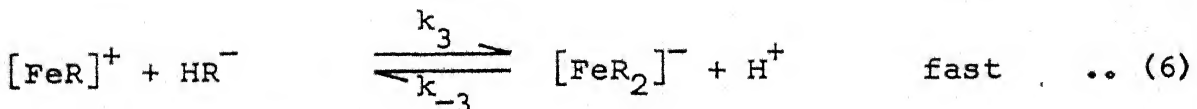
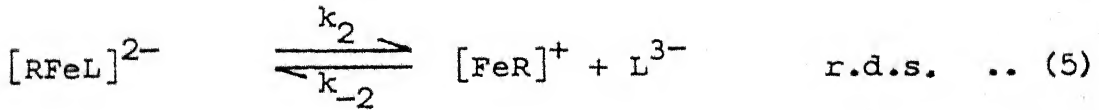
of mixed ligand complex, $[\text{FePar}(\text{CN})_3]^{n-5}$. The stoichiometry of these mixed ligand complexes was found to be 1:1:3 by the mole-ratio method for both Fe(II) and Fe(III) systems. The order with respect to cyanide varies from two at low cyanide concentration to one at high cyanide concentration respectively. The rates of formation of $[\text{FePar}(\text{CN})_3]^{n-5}$ increase with increase of pH between 7.5 to 11.5. These experimental observations lead one to propose a mechanism as given in equations (1) - (3). Now onward Par is further abbreviated as R.



The dependence of rate on ionic strength confirms the second step as the rate determining one. No reverse reaction has been observed even in the presence of large excess of Par. In the forward reaction a complete displacement of Par from the iron centre does not appear to take place even when cyanide concentration is high.

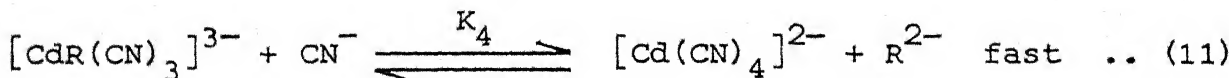
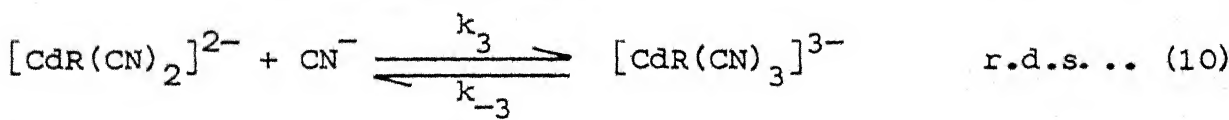
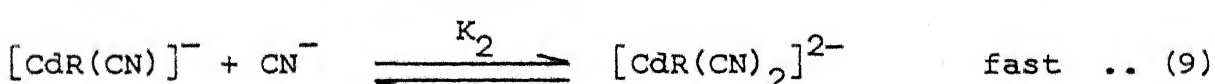
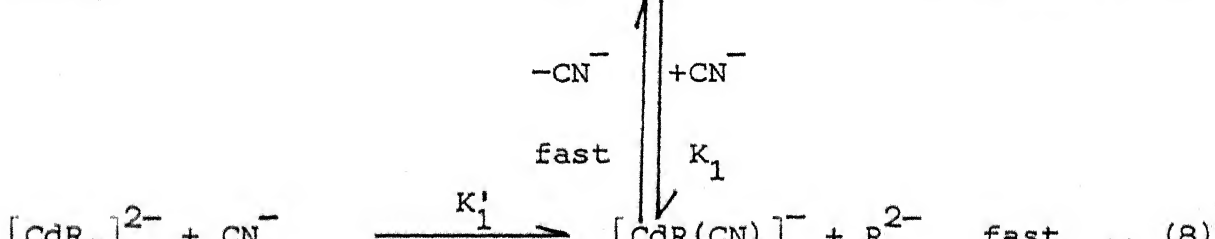
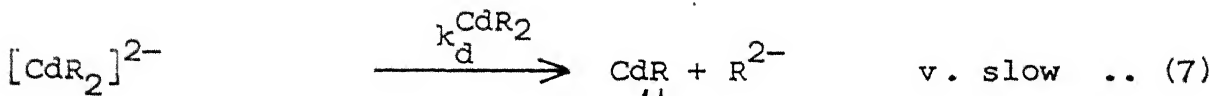
The third chapter is concerned with the kinetics and mechanism of two multidentate ligand exchange reactions on Fe(III) centre. The replacement of NTA (Nitrilotriacetic acid) and HEDTA (N-(2-Hydroxyethyl)ethylenediaminetriacetic acid) from Fe(III) ion

by Par occurs in steps. The forward reactions i.e. $[\text{FeNTA}]\text{-Par}$ and $[\text{FeHEDTA}]\text{-Par}$ exchanges exhibit first order dependence in each reactant and overall second order. The rate of reaction is found to be highly pH-dependent. In the case of $[\text{FeNTA}]^-$ -Par reaction, the rate increases upto pH 8.0 and then levels off, while in the case of $[\text{FeHEDTA}]\text{-Par}$ reaction, the rate increases with increase of pH in the range 9.0-11.25. There is no levelling of at higher pH but at lower pH levelling off occurs. This type of behaviour is explained on the basis of the reactivities of hydroxy forms of $[\text{FeNTA}]$ and $[\text{FeHEDTA}]$ as well as protonated forms of Par. It has been found that the reverse reactions between $[\text{Fe}(\text{Par})_2]^-$ and NTA or HEDTA follow first order dependence in each reactant and an inverse first order dependence in Par if the reverse reaction was carried out in presence of large excess of ligand i.e. NTA or HEDTA, however, The dependence in ligand concentration was found to be zero and first order at low and high concentrations of ligand. On the basis of above findings, a three steps mechanism can be proposed (eqns. 4 to 6).



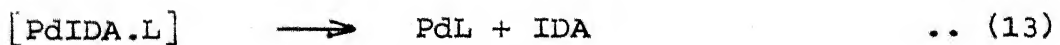
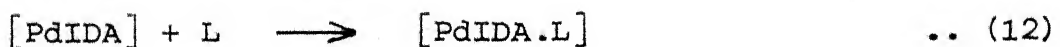
The magnitudes of activation parameters support the proposed mechanism.

The fourth chapter deals with the kinetic behaviour of $[\text{CdR}_2]^{2-}$ and $[\text{PdR(OH)}]^-$ in their reactions with cyanide ions. The bis complex is not converted directly to cyano complex but first loses one Par molecule and cyanide ion assists this loss. The reaction conditions used for this reaction are: $\text{pH} = 11.0 \pm 0.02$, $I = 0.1 \text{ M}$ and $\text{temp.} = 25 \pm 0.1^\circ\text{C}$. The forward reactions were carried out in presence of large excess of cyanide ions. A plot of \log (rate constant) versus $\log [\text{CN}^-]_T$ showed a zero order dependence in cyanide at very low concentrations while a first order dependence at higher concentration of cyanide. The observed zero order in $[\text{CN}^-]$ indicates the release of one Par from $[\text{Cd(Par)}_2]^{2-}$ in a very slow step (eqn. 7). The overall mechanistic scheme, for the reaction can be represented as



However, in the reaction of $[\text{PdR(OH)}]^-$ with cyanide, the order with respect to cyanide concentration is found to be zero and first order at low and high cyanide concentrations respectively. This is interpreted to mean that OH^- is lost in the first step followed by steps similar to eqns. 9-11 given in the scheme above. The activation parameters and effect of pH have also been investigated. The former has been used to support the proposed mechanism.

The fifth chapter contains the results of investigations on the multidentate ligand exchange reactions of square planar $[\text{PdIDA}]$ with EDTA and TTHA. In these reactions, there is fast formation of a mixed ligand intermediate $[\text{PdIDA} \cdot \text{L}]$ ($\text{L} = \text{EDTA}$ or TTHA) which decomposes slowly to give the respective products. The reaction conditions for these reactions are: $\text{pH} = 8.5 \pm 0.02$, $\text{I} = 0.2 \text{ M}$, $\text{temp.} = 30 \pm 0.1^\circ\text{C}$ for EDTA, while $\text{pH} = 8.0 \pm 0.02$, $\text{I} = 0.1 \text{ M}$, and $\text{temp.} = 30 \pm 0.1^\circ\text{C}$ for TTHA reaction. Spectral scans confirm that the reaction takes place in two stages. The first fast step of the reaction was followed under pseudo-first-order conditions taking EDTA or TTHA in large excess. The second step was not influenced by the addition of EDTA or TTHA. Thus a two step mechanism consistent with these observations can be written:



In both cases the rate of reaction decreases with increase of pH.

The sixth chapter is divided in two parts. The first part describes the kinetics and mechanism of the decomposition of hydrogen peroxide by the complex $[(\text{trien})\text{Fe}(\text{OH})_2]^+$, which possesses a 'catalase-like' activity, though of a lesser order than catalase itself. The reaction follows Michaelis-Menten type of behaviour. In presence of moderately high concentration of H_2O_2 and at specified conditions the initial rate is linearly related to $[(\text{trien})\text{Fe}(\text{OH})_2]^+$ concentration. The reaction has been used for trace determination of Fe(III) in presence of many cations and anions by a catalytic kinetic method. Only Mn(II) interferes to an appreciable extent.

In the second part the kinetics of oxidation of DTPA (diethylenetriaminepentaacetic acid) by hexacyanoferrate(III) has been investigated at $\text{pH} = 10.5$, $I = 0.25 \text{ M}$ and $\text{temp.} = 35 \pm 0.1^\circ\text{C}$. The reaction exhibits first order dependence each in hexacyanoferrate(III) and DTPA, over all second order. The effect of pH, ionic strength and temperature on the rate have been investigated.

The seventh and last chapter gives a summary of the whole work and suggestions for further investigations. The thesis contains figures and tables wherever needed. Relevant references have been cited at the end of each chapter.

LIST OF ABBREVIATIONS

acac	Acetylacetone
BEDA	N,N'-biscarboxymethylethylenedi-iminobis (ethylenenitrilo)-N'',N''-diacetic acid
bipy	2,2'-bipyridyl
CH ₃ CN	Acetonitril
CH ₃ OH	Methanol
C ₂ H ₅ OH	Ethanol
i-C ₃ H ₇ OH	Iso-butanol
Cit	Citric acid
3-CN-Py	3-Cyanopyridine
CyDTA	Cyclohexanediaminetetraacetic acid
diamper	1,3-diamino-2-methylenepropane
DMF	Dimethyl formamide
DMSO/Me ₂ SO ₄	Dimethyl sulphoxide
DTPA	Diethylenetriaminepentaacetic acid
EDDA	Ethylenediaminediacetic acid
EDTA	Ethylenediaminetetraacetic acid
EDTPA	Ethylenediaminetetrapropionic acid
EGTA	(Ethylenedioxy)diethylenedinitrilotetraacetic acid
en	Ethylenediamine
ENTMP	Ethylenediaminetetrakis(methylphosphonic) acid
Et ₄ Dien	N,N,N',N''-tetraethyl diethylenetriamine
HEDTA	N-(2-Hydroxyethyl)ethylenediaminetetraacetic acid

HF	Hydroflouric acid
HPDTA	1,3-diamino-2-hydroxypropanetetraacetic acid
IDA	Iminodiacetic acid
MeEt ₄ Dien	4-methyl-1,1,7,7-tetraethyldiethylenetriamine
4,7-Me ₂ -phen	4,7-dimethylphenanthroline
3,5-Me ₂ py	3,5-dimethylpyridine
NH ₃	Ammonia
NO	Nitric oxide
5-NO ₂ phen	5-nitrophenanthroline
NTA	Nitrilotriacetic acid
NN'-Me ₂ diamper	NN'-dimethyl 1,3-diamino-2-methylene propane
3-NHpd	3-azapentane-1,5-diamine
PADA	Pyridine-2-azo-p-dimethylaniline
PAR/R	4-(2-pyridylazo) resorcinol
PDTA	1,2-diaminopropanetetraacetic acid
Phen	Phenanthroline
pma	N-(2-pyridylidene)p-methoxyaniline
ppm	Parts per milion
py	Pyridine
SO ₃	Sulphite
Tart	Tartaric acid
Terpy	Terpyridyl
Tet/Tetren	Tetraethylenepentamine

TMDTA	Tetramethylenediaminetetraacetic acid
TPTZ	2,4,6-triptyridyl-s-triazine
TTMA	Triethylenetetraminehexaacetic acid
Trien	Triethylenetetramine

CONTENTS

		<u>page</u>
STATEMENT	...	i
CERTIFICATE I	...	ii
CERTIFICATE II	...	iii
ACKNOWLEDGEMENTS	...	iv
PREFACE	...	vi
LIST OF ABBREVIATIONS	...	xii
CHAPTER I : Introduction	...	1
CHAPTER II : Kinetics and Mechanism of the Reactions of Bis 4-(2-pyridylazo)resorcinol complexes of Iron(II) and Iron(III) with Cyanide Ions	...	55
CHAPTER III : Multidentate Ligand Exchange Kinetics: Substitution Reactions of Aminocarboxylatoferrate(III) Complexes with 4-(2-pyridylazo)-resorcinol	...	80
CHAPTER IV : The Study of Kinetics and Mechanism of Ligand Substitution Reactions of $[\text{PdPar}(\text{OH})]^-$ and $[\text{Cd}(\text{Par})_2]^{2-}$ with Cyanide Ions by Stopped Flow Technique	...	117
CHAPTER V : Multidentate Ligand Exchange Kinetics: Substitution Reactions of Ethylenediaminetetraacetate and Triethylenetetraamine-hexaacetate Anions with Imino-diacetatopalladium(II)	...	157

...contd.

CHAPTER VI : A. Kinetics and Mechanism of Catalytic Decomposition of Hydrogenperoxide in presence of $[FeTrien]^{3+}$ Complex and Trace Determination of Iron(III) by a Kinetic Method	...	198
B. Kinetics and Mechanism of Oxidation of Diethylenetriamine-pentaacetic acid by Hexacyano-ferrate(III)	...	220
CHAPTER VII : Summary of Work and Suggestions for further Investigations	...	241
LIST OF PUBLICATIONS	...	245

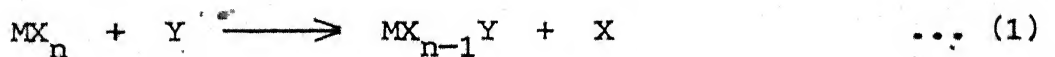
•••••

CHAPTER - I

INTRODUCTION

I.1 GENERAL

Ligand substitution reactions of coordination compounds have been studied as intensively as any class of inorganic reactions. Substitution reactions involving replacement of a ligand in a complex by another ligand constitute an important class of reactions of metal complexes which are of great utility in synthetic and analytical procedures. A considerable number of rate studies have been reported during the last forty years which have led to valuable clues for understanding of the mechanisms of such processes. These are the reactions for which a generalized equation (1) may be written as



In this equation, M is a metal atom and X and Y are any two ligands. The substitution process not only involves ligand substitution but

also the replacement of a coordinated metal ion by another free metal ion in solution. In general, no change of oxidation state of the metal occurs during a substitution process.

Although the kinetics of substitution processes have been studied with all the important stereo-chemistries but the most intensely investigated research relates to octahedral and square planar complexes. A very wide span of rates is found ranging from the extremely slow exchange of NH_3 in aqueous ammonia solution with the $[\text{Co}(\text{NH}_3)_6]^{3+}$ complex ion (no change in 162 days)¹ to the almost diffusion controlled exchange of H_2O between $[\text{Cu}(\text{H}_2\text{O})_6]^{2+}$ and solvent water ($t_{1/2} \sim 10^{-8}$ sec).² An understanding of the kinetics of substitution can be important for defining the best conditions for a preparative or analytical procedure in coordination chemistry.³ The process is undoubtedly important in the reactions of metal or metal activated enzymes, for example, in the inhibition of the catalytic function of metalloenzymes⁴ by ligands and the transport of metal ions through cell membranes.⁵

A whole armoury of techniques which are too well known to need mention, must be used to measure the substitution rate constants. Metal ions or complexes that generally react rapidly (within matter of seconds) are termed labile, whereas if they substitute slowly taking minutes or longer for completion, they are called inert.⁶

The substitution process permeates the whole realm of coordination chemistry. It is not infrequently the first step in a redox

process⁷⁻⁹ or in a dimerization or a polymerization reaction.¹⁰ In the past two decades several excellent monographs¹¹⁻²¹ have appeared on the mechanisms of inorganic reactions and a significant drive has been made towards visualising the nature of a variety of intermediates and transition states in their pathways. In not too distant past, reactions of coordination compounds have been investigated to test various theories of chemical reactivity. Most of the early kinetic studies on substitution were concerned with the inert Co(II) complexes which Werner had so well characterized and which undergo reactions at conveniently measurable rates.

An earlier review by Taube⁶ on labile octahedral complexes of transition metals and other reviews on their square planar complexes have appeared before. The collection of quantitative data for a large number of rapidly reacting bivalent and tetravalent transition metal complexes of the Vanadium-Zinc group had to await the development of flow methods as well as the invention of relaxation techniques.²² The conclusions were based mostly on the qualitative observations taken from the literature. Nevertheless, important deductions relating to reactivity vis-a-vis electronic configurations of the complexed ions were made.²³ For example, the base hydrolysis of pentaamine Co(III) ion has been used to study the effect of hydrostatic pressure²⁴, ionic strength²⁵ and ion-pairing²⁶ on the reaction rates.

The problem of demonstrating the involvement of a metal ion in a biological reaction has always been a very difficult one, since the most important metals (such as the alkali metals, alkaline earth

metals, and zinc) possess very few convenient 'handles'. It is well known that all living systems have a requirement for the so called 'trace elements', many of which are metals. It has been estimated that as many as 27 of enzymic reactions either require or are greatly enhanced by the presence of one or more metal ions.

The study of many ligand substitution reactions provides the basis for understanding and utilization of reactions of analytical interest.²⁷⁻³⁵ The concentration of Cd(II) has been determined kinetically by the ligand substitution reaction between 1-(2-thiazolylazo)-2-naphthol complexes and EDTA.³⁶ Similarly the concentration of Hg²⁺ has been determined upto a lower limit of 10⁻⁷ M level by its catalytic effect on the substitution rate of cyanide in hexacyanoferrate(II) by p-nitrosodiphenylamine.³⁷ Determination of metal ions^{36,38-43} or ligands present in closely related mixtures has become possible by making use of the differences in the rates of ligand substitution reactions of metal ions coordinated with appropriate ligands. Many metal ions have also been determined by a catalytic decomposition of some suitable compound. Such examples are the determination of Fe³⁺ at ppm level in mixtures by the decomposition of H₂O₂ catalysed by the Fe(III)trien,^{44,45} and Fe(III)Entmp²⁵¹ (Entmp = Ethylenediaminetetrakis(methylphosphonic) acid).

A well accepted method for elucidating the mechanism of ligand substitution on a metal ion is to compare the solvent exchange rate with the ligand substitution rate. After correction for ion-pair formation it has been found, at least for Co(II) and Ni(II), that

the dissociative mechanism suggested by Eigen and Wilkins⁴⁶ is most consistent with the results. Grant and Jordan⁴⁷ have suggested the same mechanism for water exchange rate of Fe(III). For a solvent molecule in the coordination sphere of some of the most labile transition metal ions such as Zn^{2+} and Cu^{2+} , these exchange rates can be measured by relaxation techniques, particularly NMR and ultrasonics, and may be distinguished from even shorter residence times of solvent molecules in the bulk of solvent. The solvent exchange rate studies have played a key role in enhancing our understanding of substitution mechanisms. The hexa-coordinated structure for $[Al(H_2O)_6]^{3+}$ and $[Cr(H_2O)_6]^{3+}$ in water^{48,49} as well as for $[Co(NH_3)_6]^{3+}$ in liquid ammonia⁵⁰ have been deduced from solvent exchange kinetics.

The kinetics and mechanism of the ligand substitution reactions have been studied extensively as mentioned before, for octahedral complexes and to a lesser extent for square-planar complexes. An excellent review on the octahedral substitution of Ni(II)⁵¹ and Fe(III)⁵² complexes have been attempted recently and, therefore, only a brief description is presented here. The kinetics and mechanisms of reactions involving displacement of polyamines^{53,54} and polyaminocarboxylates⁵⁵⁻⁶⁴ coordinated to Ni(II) by the monodentate cyanide ions have been studied extensively. The kinetics of exchange of mono, bis and binuclear complexes of Ni(II)⁶⁵⁻⁶⁷ and Fe(III)⁶⁸⁻⁷⁵ by the cyanide ions have been studied in our laboratory during the past few years.

Recently, a review has been presented by Cross²⁰ on ligand substitution reactions of square-planar complexes. Metals, with low spin d⁸ configuration, form four coordinated square-planar complexes. Of these, the Pt(II) complexes have received maximum attention. They also serve as representatives of this geometry. Investigations on square-planar complexes of Rh(I), Ir(I), Pd(II), Ni(II), Cu(II) and Au(II) have been rather limited, and the measurement of their reaction rates usually requires flow methods. Recently, we have also contributed to the understanding of the kinetics and mechanism of substitution reactions of polyaminocarboxylato complexes of Pd(II).^{76,77}

I.2 CLASSIFICATION OF SUBSTITUTION MECHANISMS

If a systematic classification is to be developed, some categories must be imposed. A mechanistic analysis is based on the study of reaction rates. It is convenient, therefore, to divide the task into two distinct phases. The first is the discovery of the sequence of elementary steps by which a complicated overall reaction is accomplished and the second is the determination and rationalisation of the rate constants for the individual steps in terms of the rearrangements of electrons, atoms and bonds occurring during the course of reactions. The most natural division in mechanistic study is that between stoichiometric and intimate mechanism, and it is perhaps equally natural to attempt categorizing from each of these points of view separately. The classical categories of substitution mechanism

introduced in organic chemistry by Hughes and Ingold⁷⁸ and later applied to ligand substitution processes were originally based on a feature of stoichiometric mechanism, viz., the molecularity of the rate-determining step of the reaction.

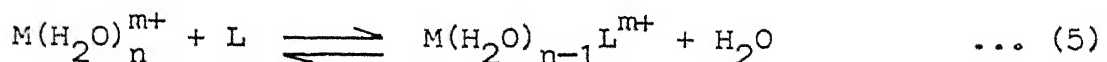
According to Langford and Gray⁷⁹ substitution mechanism are classified into three categories: a dissociative path (D) or S_N^1 reaction (Hughes and Ingold) in which the leaving ligand is lost in the first step, producing an intermediate of reduced coordination number, an associative path (A) or S_N^2 reaction in which the entering ligand adds in the first step, producing an intermediate of increased coordination number, and lastly the concerted path called interchange (I). During interchange the leaving group is moving from the inner to the outer coordination sphere while the entering group is moving from outer to the inner sphere. An interchange process can be further subclassified as Associative interchange process (I_a) and Dissociative interchange process (I_d).

I.3 LITERATURE SURVEY

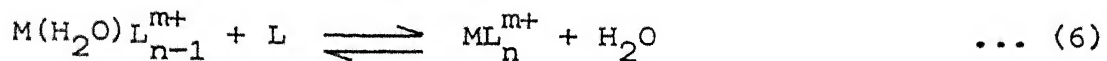
The kinetics and mechanisms of ligand substitution reactions of octahedral and square-planar complexes have been investigated mostly in the last forty years. The present survey covers mechanistic features of substitution reactions mainly of Fe(II), Fe(III), Cd(II) and Pd(II) complexes. Occasional mention of complexes of other metals has been made for the sake of comparison.

I.3.1 Ligand Exchange Reactions

The solvent molecules in a solvated ion can be replaced by other ligands, which may occupy one (unidentate) or more (multidentate) of the solvent positions; for example, in the simple case of a neutral unidentate ligand L replacing H_2O ,



leading eventually to



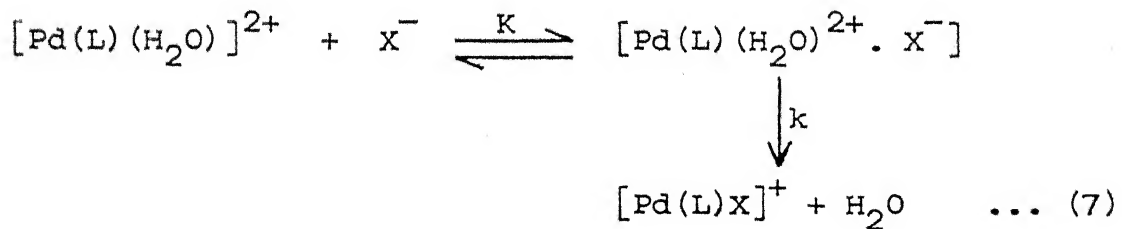
Information on solvent exchange rates and their comparison with ligand substitution rates have been used for elucidation of mechanism of substitution reactions.⁸⁰

Solvent-ligand exchange rates on iron(III)⁸¹⁻⁹⁷ complexes have been studied in some detail. The complexes $[Fe(H_2O)_6]^{3+}$ and $[Fe(dmsO)_6]^{3+}$ undergo labile solvent exchange and anation reactions with various ligands. Recently, the rate of ligand substitution of tris(acetylacetonato)iron(III) with 2-thenoyltrifluoroacetone has been reported in organic solvents such as carbon tetrachloride and benzene, but a definite mechanism has not been proposed⁹⁶ so far. The kinetic parameters of the solvent exchange reactions of FeS_6^{+3} type complexes (S = solvent) are compiled in Table I.1. The reactions listed therein exhibit a common trend in the values of activation parameters.

TABLE-I.1. Activation parameters of the solvent exchange reactions of Fe(III) complexes at 25°C.

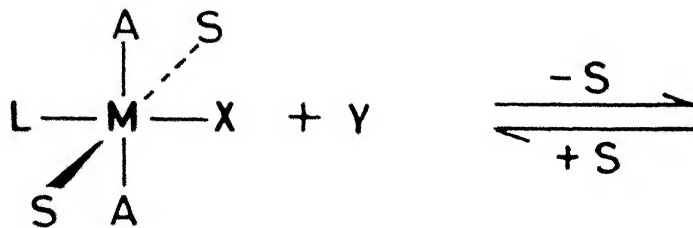
Complex	Solvent	k_1 s^{-1}	ΔH^\ddagger $k \text{ cal mol}^{-1}$	ΔS^\ddagger $\text{cal K}^{-1} \text{ mol}^{-1}$	Ref.
$[\text{Fe}(\text{acac})_3]$	Hacac	0.0033	14.4 \pm 0.9	-22 \pm 3	99
$[\text{Fe}(\text{H}_2\text{O})_6]^{3+}$	H_2O	150	-	-	81
$[\text{Fe}(\text{dmf})_6]^{3+}$	DMF	33	12.5 \pm 1.5	-10 \pm 5	81
		61	10.1 \pm 1	-16.5 \pm 3.0	87
$[\text{Fe}(\text{dmsO})_3]^{3+}$	DMSO	50	10 \pm 2	-11 \pm 4	87

There is considerable evidence to infer that the solvent path for planar substitution involves a direct displacement by the solvent¹⁰⁰ and it is to be expected that the contribution made by this path to the overall rate of reaction would increase with an increase in the coordinating ability of the solvent. Fig.I.1 shows a plausible reaction sequence involving square pyramidal intermediates. Both, a solvent reaction (path I) and a nucleophilic reaction (path II), are shown. It can be seen that there is necessary formation of the aquo complex in the nucleophilic path before the nucleophile can enter the final product. General mechanism for the solvent exchange of Pd(II) complexes involving ion-pairing,¹⁰¹ is given in equation (7).

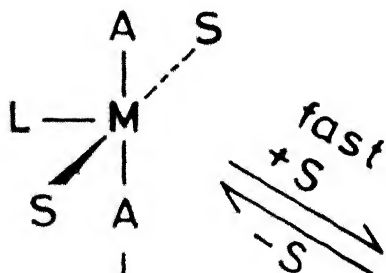
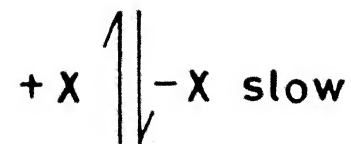
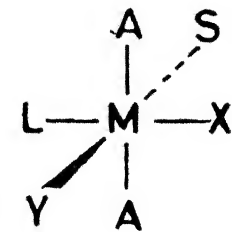
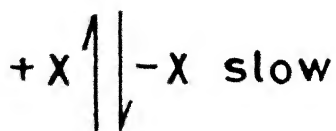
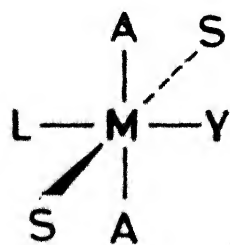


Solvent exchange reactions of Pd(II) complexes have been studied by many authors.¹⁰²⁻¹⁰⁹ The rates and activation parameters for the substitution reactions of $\text{Pd}(\text{Et}_4\text{dien})\text{x}^+$ with halide ions in various solvents are summarized in Table I.2.¹¹⁰ In protic solvents the reactivity of $\text{Pd}(\text{Et}_4\text{dien})\text{x}^+$ decreases as x is varied in the order $\text{Cl} > \text{Br} > \text{I}$. This reactivity order is due to a corresponding increase in ΔH^\neq along the halo series. The ΔS^\neq values in aqueous and alcoholic solutions suggest an associative mechanism for the

Path I



(starting materials)

 $+Y \text{ fast}$ 

(Product)

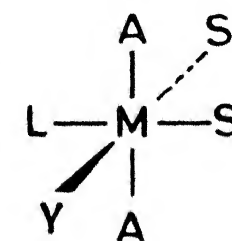
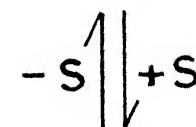
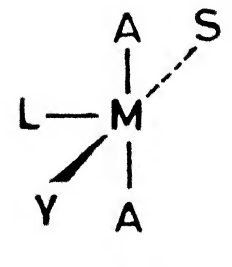
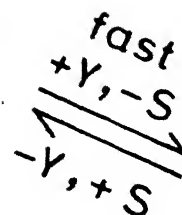
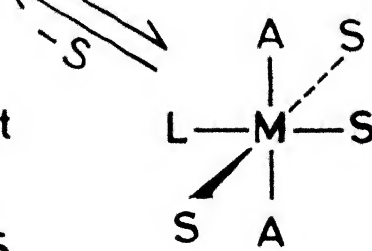


Fig. I.1 Reaction mechanism of substitution on a square planar complex.
Where S = solvent, Y = a monodentate ligand.

TABLE-I.2. Rates and activation parameters for substitution reactions of $\text{Pd}(\text{Et}_4\text{dien})\text{X}^+$ in different solvents.¹¹⁰

Substrate	Solvent	Entering group	$10^5 k_1/\text{s}^{-1}$	$k \text{ cal mol}^{-1}$	ΔH^\ddagger	ΔS^\ddagger e.u.
$\text{Pd}(\text{Et}_4\text{dien})\text{Cl}^+$	H_2O	I^-	420	16.5 \pm 0.5	-16 \pm 2	
		Br^-	430	16.5 \pm 0.5	-16 \pm 2	
	$\text{C}_2\text{H}_5\text{OH}$	I^-	8.0	18.0 \pm 0.5	-21 \pm 2	
		Br^-	8.1	18.6 \pm 1.0	-19 \pm 3	
$\text{i-C}_3\text{H}_7\text{OH}$		I^-	6.4	18.9 \pm 1.0	-18 \pm 3	
	H_2O	I^-	550	17.6 \pm 0.5	-13 \pm 2	
	DMSO	Cl^-	43	20.4 \pm 1.0	-7 \pm 2	
	CH_3OH	I^-	14.8	19.2 \pm 1.0	-16 \pm 2	
$\text{Pd}(\text{Et}_4\text{dien})\text{Br}^+$	$\text{C}_2\text{H}_5\text{OH}$	I^-	7.9	19.6 \pm 0.5	-16 \pm 2	
	$\text{i-C}_3\text{H}_7\text{OH}$	I^-	4.4	19.8 \pm 0.5	-18 \pm 2	
	H_2O	Br^-	140	18.4 \pm 0.5	-13 \pm 2	
	DMSO	Cl^-	96	19.6 \pm 0.5	-10 \pm 2	
$\text{Pd}(\text{Et}_4\text{dien})\text{I}^+$	DMF	Cl^-	89	19.4 \pm 0.5	-11 \pm 2	
	CH_3OH	Br^-	7.2	19.9 \pm 0.5	-15 \pm 2	
	$\text{C}_2\text{H}_5\text{OH}$	Br^-	5.5	20.4 \pm 0.5	-16 \pm 2	

solvent substitution path. An associative mechanism is assumed to operate in the aquations of $\text{trans-}[\text{Pd}(\text{NH}_3)_2\text{Cl}_2]$, $\text{trans-}[\text{Pd}(\text{NH}_3)_2(\text{OH})_2\text{Cl}]^+$, and $\text{trans-}[\text{Pd}(\text{NH}_3)_2(\text{OH}_2)(\text{NO}_2)]^+$. It may be observed that in different solvents the activation entropies are negative ¹¹¹ which is consistent with associative processes. Similarly, kinetics of the aquation of *cis*-Dichloro(ethylenediamine)palladium, *trans*-Dichlorobis(pyridine)palladium and *trans*-Dinitroamminepalladium in different solvents have been studied. ^{112,113}

Despite the wide distribution and importance of iron(II) there has been relatively little work on the substitution reactions of this ion especially when compared to other bivalent ions viz. cobalt(II), nickel(II) and manganese(II). ¹¹⁴ The water exchange rate on $\text{Fe}(\text{OH}_2)_6^{2+}$ was studied by Swift and Connick² and the results indicate that iron(II) and cobalt(II) are of comparable lability. More recently, solvent-exchange rates have been reported for iron(II) in methanol, ¹¹⁵ *N,N*-dimethylformamide, ¹¹⁶ acetonitrile, ¹¹⁷ and dimethylsulfoxide. ¹¹⁸

A comparison of the kinetic parameters for ligand substitution and solvent exchange ¹¹⁹⁻¹²² is being used increasingly to diagnose the dissociative ligand substitution mechanisms ¹²³ for first row dipoisitive transition metal ions. It is hoped that the present study will provide further understanding of substitution processes.

Solvent exchange kinetics of Fe(II) solutions of DMF and DMSO have been studied by NMR technique and the data are given in

Table I.3. The earlier studies by some workers^{117,119} in DMF and Me_2SO_4 seem to give unusually small activation enthalpies and very negative activation entropies. The results obtained in the study by Funahashi and Jordan¹²⁴ appear to be more in line with previous work on methanol, acetonitrile and water, but some questions must remain as to which values, if either, are correct. Although details of the earlier work¹¹⁶ in DMF have not been published, it is interesting to note that the deviation of about 6 k cal mol^{-1} from the ΔH^\neq reported in their paper is similar to the deviation reported with more recent studies on cobalt(II)¹²⁵ and nickel(II).^{125,126}

I.3.2 Formation Reactions of Complexes of Fe(II), Fe(III), Cd(II) and Pd(II)

An excellent review on the formation reactions of iron(III) complexes has been attempted⁵² recently and, therefore, only a brief description is presented here. A generally accepted mechanism for these complexes was proposed by Eigen and Tamm.¹²⁷⁻¹²⁹ For complexes of unidentate ligands it involves the formation of an outer sphere complex between a solvated metal ion and the incoming ligand followed by loss of a solvent molecule from this outer sphere complex to give the desired complex. The mechanism can be extended to formation of complexes of bidentate ligands with the modification that ring closure may constitute the rate determining step. Some values of the observed rate constants (k_{obsd}) for some bidentate and

TABLE I.3. Summary of solvent exchange rate kinetics for Fe(II)

Solvent	k s^{-1}	ΔH^\neq $k \text{ cal mol}^{-1}$	ΔS^\neq $\text{cal mol}^{-1} K^{-1}$	Ref.
DMF	$(1.7 \pm 0.3) \times 10^6$	11.7 ± 0.6	9.2 ± 2	124
DMF	5.3×10^5	5.3	-15	116
Me ₂ SO	$(1.0 \pm 0.2) \times 10^6$	11.3 ± 0.6	6.9 ± 2	124
Me ₂ SO	1.0×10^4	4.16	-28.8	118
CH ₃ OH	5.0×10^4	12.0	3.0	115
CH ₃ CN	5.5×10^5	9.7 ± 0.7	0.3 ± 2.2	117
H ₂ O	3.2×10^6	7.7	-3.0	2

polydentate ligands are summarized in Table I.4. Rate constants have been reported for the formation of several other complexes of iron(III);¹³³⁻¹³⁵ the results are given in Table I.5. In general, the hydroxo form of the metal seems to be the more important under the conditions used, but in the case of pyridoxal the major pathway is thought¹³⁵ to involve $\text{Fe}_{\text{aq}}^{3+}$ itself. The rate constants for the formation of a series of iron(III) complexes lie in the range $1-10 \text{ M}^{-1} \text{s}^{-1}$, whereas the rate constants for $\text{Fe}(\text{OH})^{2+}$ ion are larger, and lie in the range $1 \times 10^2 - 1 \times 10^5 \text{ M}^{-1} \text{s}^{-1}$.

Kinetic and mechanistic studies of substitution reactions of square planar metal complexes have been confined largely to those substrates containing Pt(II) as the central metal ion, and enough data has been accumulated so that the essential features of such substitutions are thought to be understood. In general, the square planar complexes of Pd(II) and Ni(II) are much more labile than analogous Pt(II) complexes. The relative reactivities of analogous Ni(II), Pd(II) and Pt(II) complexes are approximately $10^{7-8}:10^{5-6}$.¹³⁶ One type of reaction, where a Pd(II)-Pt(II) reactivity comparison is not possible, is that of substitution at $[\text{Pd}(\text{OH}_2)_4]^{2+}$.¹³⁷ Substitution reactions of this cation indeed provide a uniquely interesting example of complex formation from a square-planar aquo-cation.

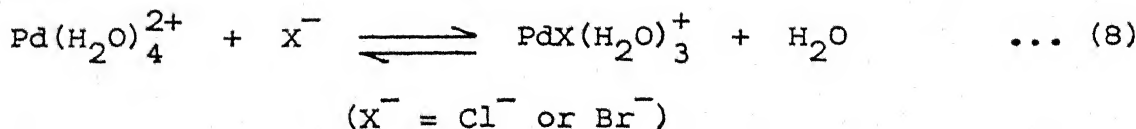


TABLE I.4. Rate constants and Activation parameters for the reaction of $\text{Fe(OH)}_{\text{aq}}^{2+}$ with some bidentate and multidentate ligands in aqueous solution at 25°C.

Reaction	k_1 $\text{M}^{-1}\text{s}^{-1}$	ΔH^\neq k cal mol^{-1}	ΔS^\neq $\text{cal K}^{-1}\text{mol}^{-1}$	R
$\text{Fe(OH)}^{2+} + \text{H}_2\text{IDA}$	$(2.5 \pm 0.3) \times 10^3$	6.1 ± 1.0	-23 ± 3	1
$\text{Fe(OH)}^{2+} + \text{HIDA}^-$	$(8.8 \pm 0.9) \times 10^3$	4.9 ± 1.0	-22 ± 3	1
$\text{Fe(OH)}^{2+} + \text{H}_3\text{NTA}$	$(1.5 \pm 0.2) \times 10^4$	9.9 ± 1.0	-5 ± 3	1
$\text{Fe(OH)}^{2+} + \text{H}_2\text{NTA}^-$	$(5.6 \pm 0.6) \times 10^4$	6.3 ± 1.0	-16 ± 3	1
$\text{Fe(OH)}^{2+} + \text{H}_4\text{EDTA}$	$(3.0 \pm 0.3) \times 10^4$	7.3 ± 1.0	-15 ± 3	1
$\text{Fe(OH)}^{2+} + \text{H}_3\text{EDTA}^-$	$(1.1 \pm 0.1) \times 10^5$	5.7 ± 1.0	-15 ± 3	1
$\text{Fe(OH)}^{2+} + \text{H}_5\text{DTPA}$	$(5.3 \pm 0.6) \times 10^4$	-	-	1
$\text{Fe(OH)}^{2+} + \text{H}_4\text{DTPA}^-$	$(1.6 \pm 0.2) \times 10^5$	-	-	1
$\text{Fe(OH)}^{2+} + \text{H}_4\text{Tart}$	$(5.1 \times 10^3)^a$ $(2.8 \times 10^3)^b$	7.6	-16	1
$\text{Fe(OH)}^{2+} + \text{H}_3\text{Tart}$	$(2.2 \times 10^4)^a$ $(0.7 \times 10^4)^b$	15.1	13	1
$\text{Fe(OH)}^{2+} + \text{H}_4\text{Cit}$	$(3.1 \times 10^3)^a$ $(2.0 \times 10^3)^b$	5.4	-24	1
$\text{Fe(OH)}^{2+} + \text{H}_3\text{Cit}$	$(2.6 \times 10^4)^a$ $(1.5 \times 10^4)^b$	5.4	-24	1

= Data at 20°C, b = Data at 8°C, Fe(OH)^{2+} represents $\text{Fe(OH)}_{\text{aq}}^{2+}$.

TABLE I.5. Rate constants^a for formation of iron(III) complexes.

Ligand (H_2L or HL)	$k_F, M^{-1}s^{-1}$ $HL + FeOH^{2+}$	$k_F, M^{-1}s^{-1}$ $H_2L + FeOH^{2+}$	$k_F, M^{-1}s^{-1}$ $HL + Fe^{3+}$	Ref.
Dimethylmalonic acid	1.6×10^5	2.2×10^3	—	133
Diethylmalonic acid	2.2×10^4	1.8×10^3	—	133
Cyclopropane-1,1-dicarboxylic acid	3.3×10^4	5.2×10^3	—	133
Cyclopentane-1,1-di-carboxylic acid	2.2×10^5	4.2×10^3	—	133
Salicylamide	2.9×10^3	—	14.5	134
Salicylaldehyde	1.37×10^3	—	2.6	134
2-Hydroxyacetophenone	1.84×10^3	—	3.0	134

^a conditions are: 25°C and I = 0.5 M (ref. 133) or 1.0 M (ref. 134).

The activation enthalpies and entropies for these reactions are given in Table I.6. The activation entropies are negative, indicating an associative reaction mechanism. An associative mechanism is also proposed for the reaction of $[\text{Pd}(\text{OH}_2)_4]^{2+}$ with aromatic amines.¹³⁸ The formation reactions of a series of monodentate carbonato complexes of Pd(II) were investigated by Mahal and Eldik.¹³⁹ The kinetic data clearly indicate that these complexes are not formed by the CO_2 uptake mechanism (as expected in octahedral complexes) but via anation of the aquo complex.

The rapid substitution of ligands into the inner hydration sphere of metal ions has recently been the subject of intensive investigation. For the divalent transition metal ions especially, a variety of techniques have been used leading to self consistent results in regard to the mechanism of substitution. Studies on $\text{Fe}(\text{II})$ ion have, however, been relatively few in number. Table I.7 presents available data for the formation kinetics of complexes of monodentate or multidentate ligands with $\text{Fe}(\text{II})$ ion. Formation of the Ferrous-Nitric Oxide complex¹⁴⁰ by the reaction between $\text{Fe}(\text{II})$ and NO leads to a value of rate constant $k_o = 3.3 \times 10^6 \text{ s}^{-1}$ (k_o = water substitution rate constant). By using nmr line-broadening techniques, Connick and Swift² were able to measure k_o for Fe^{2+} directly. Their value is in good agreement with the value calculated by Taube et al.¹⁴⁰ The results are, therefore, consistent with a substitution reaction of iron(II). The formation reactions of $\text{Fe}(\text{II})$ with many multidentate ligands^{142,143} have been studied extensively. Wilkins et al.¹⁴²

TABLE I.6. Rate constants, activation enthalpies and activation entropies at 25°C for substitution reactions of palladium(II) complexes. (Aqua ligands excluded)

Process	$k, M^{-1} s^{-1}$	$\Delta H^\ddagger k \text{ cal mol}^{-1}$	$\Delta S^\ddagger \text{ cal K}^{-1} \text{ mol}^{-1}$
$\text{Pd}^{2+} + \text{Cl}^- \rightarrow \text{PdCl}^+$	1.83×10^4	10 ± 2	-6 ± 6
$\text{Pd}^{2+} + \text{Br}^- \rightarrow \text{PdBr}^+$	9.2×10^4	10 ± 1	-3 ± 3
$\text{PdCl}_3^- + \text{Cl}^- \rightarrow \text{PdCl}_4^{2-}$	1.8×10^2	10 ± 1	-15 ± 3
$\text{PdBr}_3^- + \text{Br}^- \rightarrow \text{PdBr}_4^{2-}$	3.0×10^3	8 ± 1	-17 ± 3

TABLE I.7. Formation rate constants of Fe(II) aquo ion with monodentate and multidentate ligands at 25°C.

Ligand	$k_f, M^{-1}s^{-1}$	Ref.
NO	6.2×10^5	140
HF	9.3×10^5	141
F ⁻	1.4×10^6	141
Phen	5.6×10^4	142
Bipy	1.6×10^5	142
Terpy	8×10^4	142
TPTZ	1.3×10^5	143

have discussed the idea that the addition of any of these ligands to the metal ion is controlled by the first attachment and that this is followed by rapid complexation of the chelate. Further, it is clear that the rate of the first step mainly depends upon the water exchange rate of the metal ion.¹⁴⁴ The values of second order rate constants for the replacement of H_2O by a variety of unidentate and multidentate ligands for the reactions of cadmium(II) ion are given in Table I.8. These reactions also follow same mechanism commonly proposed for the reaction of an aquated metal ion with a ligand to form a metal complex.¹⁴⁴

I.3.3 Dissociation Reactions

The dissociation reactions of complexes are generally much slower than the formation reactions. Their mechanism also is accounted for by the mechanisms proposed for the formation reactions. In case of complexes of bidentate ligands, the rate constant will depend upon opening of the chelate ring or sometimes rupture of the second metal-ligand bond. Both these situations have been encountered with outgoing bidentate or multidentate ligand groups in literature. The presence of an acid generally enhances the dissociation rate because protonation of released ligand stabilises the intermediate relative to the fully coordinated form.¹⁵⁹⁻¹⁶⁷

The kinetics and mechanism of dissociation reactions of Fe(II) have been studied in some detail.^{34,162-168} The rate of dissociation of tris-(1,10 phenanthroline)iron(II) complex has been studied

TABLE I.8. Rate constants for monodentate and multidentate ligands reacting with Cd(II) ion at 25°C.

Ligand	$k_f, M^{-1} s^{-1}$	Ref.
Br ⁻	1.4 x 10 ⁹	145
Murexide (10°C)	1.1 x 10 ⁸	146
HNTA ²⁻	2.1 x 10 ⁵	147
	4 x 10 ⁶	46
	8 x 10 ⁵	148
Phen (12°C)	5 x 10 ⁶	142
Terpy	3.2 x 10 ⁶	142
PADA (15°C)	1.3 x 10 ⁷	149
H ₂ EGTA ²⁻	1.5 x 10 ⁶	150
NTA ³⁻	2 x 10 ¹⁰	148
	4 x 10 ⁹	151
	2.5 x 10 ⁹	147
HEDTA ³⁻	4 x 10 ⁹	152
	2.6 x 10 ⁸	153
	8 x 10 ⁸	154
	6.4 x 10 ⁹	155
HEGTA ³⁻	1 x 10 ⁹	150
HCyDTA ³⁻	1.1 x 10 ⁹	156
	1.4 x 10 ⁹	157
H(1,3-PDTA) ³⁻	4.1 x 10 ⁹	158
HEDDA ³⁻		158

by a number of investigators¹⁶² in acidic solutions. As might be expected, the mechanistic theme is that these reactions proceed via a dissociative rather than an associative process.¹⁶³ However, reactions of tris-(α,α' -diimine) complexes such as $[\text{Fe}(\text{bipy})_3]^{2+}$ and $[\text{Fe}(\text{phen})_3]^{2+}$ with strong nucleophiles such as OH^- and CN^- involve second order reaction path.¹⁶³⁻¹⁶⁵ This dependence on the incoming nucleophile could be due to a bimolecular associative attack on the iron centre, a process involving ion-pair formation or initial attack on the coordinated ligand.

Lucie and Stranks¹⁶⁶ determined volumes of activation for the dissociation of tris(1,10-phenanthroline)iron(II) and its derivatives. The high values for the activation enthalpies, the positive activation entropies as well as activation volumes (Table I.9) support the idea of a dissociative mechanism rather than an associative one for these iron(II) complexes. It has been demonstrated that reactions of Cd(II) complexes of polydentate ligands are ¹⁷⁶ proton assisted and that the rates of dissociation of these complexes are greatly enhanced as the hydrogen ion concentration is increased. This is evident from the data presented in Table I.10. The decrease in rate for the case of $[\text{Cd}(\text{NTA})_2]^{4-} - \text{H}^+$ reaction has been explained.¹⁴⁷ is being due to the slow rate of proton migration from the nitrogen atom in a partially bonded reaction intermediate. The acid dissociation kinetics for doubly deprotonated triglycine palladium(II) complex, $[\text{Pd}(\text{H}_2\text{GGG})]^-$, takes place via four sequential bond-¹⁷⁷ dissociation steps.

TABLE I.9. Kinetic parameters for dissociation of some Fe(II) complexes.

Complex	k s^{-1}	ΔH^\ddagger cal mol^{-1}	ΔS^\ddagger $\text{cal K}^{-1} \text{mol}^{-1}$	ΔV^\ddagger $\text{cm}^3 \text{mol}^{-1}$	Ref.
$[\text{Fe}(\text{phen})_3]^{2+}$	7.3×10^{-5}	29.4 ± 0.2	$+21.1 \pm 0.6$	$+15.4 \pm 0.4$	166
$[\text{Fe}(\text{5-NO}_2\text{phen})_3]^{2+}$	4.9×10^{-4}	28.0 ± 0.2	$+21 \pm 0.7$	$+17.9 \pm 0.3$	166
$[\text{Fe}(\text{4,7-Me}_2\text{-phen})_3]^{2+}$	2.2×10^{-5}	27.8 ± 0.2	$+13 \pm 0.7$	$+11.6 \pm 0.6$	166
$[\text{Fe}(\text{bipy})_3]^{2+}$	7.8×10^{-4}	26.1 ± 0.1	$+14.8 \pm 0.3$	-	169
$[\text{Fe}(\text{terpy})_2]^{2+}$	5.2×10^{-3}	24.2 ± 0.2	$+12.3 \pm 0.6$	-	167
$[\text{Fe}(\text{pma})_3]^{2+}$	9.3×10^{-2}	22.1 ± 0.6	$+10.7 \pm 2.0$	-	170

TABLE I.10. Rate constants for reactions involving complexes of Cd(II) and aminopolycarboxy acids at 25°C.

	Reaction	Rate constant		Ref.
		Forward reaction	Reverse reaction	
1				
(i)	$[\text{Cd(NTA)}]^- \rightleftharpoons \text{Cd}^{2+} + \text{NTA}^{2-}$	$1.03 \pm 0.27 \text{ s}^{-1}$	$8.7 \times 10^9 \text{ M}^{-1} \text{ s}^{-1}$	171
(ii)	$[\text{Cd(NTA)}]^- + \text{H}^+ \rightleftharpoons \text{Cd}^{2+} + \text{HNTA}^{2-}$	$(2.9 \pm 0.5) \times 10^5 \text{ M}^{-1} \text{ s}^{-1}$	$(2.1 \pm 0.4) \times 10^5 \text{ M}^{-1} \text{ s}^{-1}$	147
(iii)	$[\text{Cd(NTA)}_2]^{4-} \rightleftharpoons [\text{Cd(NTA)}]^- + \text{NTA}^{3-}$	$(2.2 \pm 0.4) \times 10^2 \text{ s}^{-1}$	$(1.8 \pm 0.3) \times 10^7 \text{ M}^{-1} \text{ s}^{-1}$	147
(iv)	$[\text{Cd(NTA)}_2]^{4-} + \text{H}^+ \rightleftharpoons [\text{Cd(NTA)}]^- + \text{HNTA}^{2-}$	$(1.3 \pm 0.4) \times 10^7 \text{ M}^{-1} \text{ s}^{-1}$	$(2.9 \pm 1.0) \times 10^2 \text{ M}^{-1} \text{ s}^{-1}$	147
(v)	$[\text{Cd(HEDTA)}]^- \rightleftharpoons \text{Cd}^{2+} + \text{HEDTA}^{3-}$	12 s^{-1}	$1 \times 10^9 \text{ M}^{-1} \text{ s}^{-1}$	172
		2.0 s^{-1}		
		10.8 s^{-1}	$3.7 \times 10^9 \text{ M}^{-1} \text{ s}^{-1}$	152
			$8.5 \times 10^8 \text{ M}^{-1} \text{ s}^{-1}$	154
(vi)	$[\text{Cd(EDTA)}]^{2-} + \text{H}^+ \rightleftharpoons [\text{Cd(HEDTA)}]^-$	$4.3 \times 10^4 \text{ M}^{-1} \text{ s}^{-1}$	$(5.3-64) \times 10^8 \text{ M}^{-1} \text{ s}^{-1}$	155
		54 s^{-1}		173

••• contd.

TABLE I.10 (contd.)

		1	2	3	4
(vii)	$[\text{Cd}(\text{HEGTA})]^- \rightleftharpoons \text{Cd}^{2+} + \text{HEGTA}^{3-}$	$\leq 5 \times 10^{-2} \text{ s}^{-1}$	$\leq 1 \times 10^9 \text{ M}^{-1} \text{s}^{-1}$		150
(viii)	$[\text{Cd}(\text{HEGTA})]^- + \text{H}^+ \rightleftharpoons \text{Cd}^{2+} + \text{H}_2\text{EGTA}^{2-}$	$(2 \pm 1) \times 10^4 \text{ M}^{-1} \text{s}^{-1}$	$1.5 \times 10^6 \text{ M}^{-1} \text{s}^{-1}$		150
(ix)	$[\text{Cd}(\text{HEDTA})]^- + \text{H}^+ \rightleftharpoons \text{Cd}^{2+} + \text{HEDTA}^{2-}$	$3 \times 10^5 \text{ M}^{-1} \text{s}^{-1}$	$2 \times 10^9 \text{ M}^{-1} \text{s}^{-1}$		174
(x)	$[\text{Cd}(\text{HBEDA})]^{2-} + \text{H}^+ \rightleftharpoons \text{Cd}^{2+} + \text{H}_2\text{BEDA}^{4-}$	98 s^{-1}	$2.3 \times 10^8 \text{ M}^{-1} \text{s}^{-1}$		175
(xi)	$[\text{Cd}(\text{H}_2\text{BEDA})]^{2-} + \text{H}^+ \rightleftharpoons \text{Cd}^{2+} + \text{H}_3\text{BEDA}^{3-}$	$2.9 \times 10^4 \text{ M}^{-1} \text{s}^{-1}$	$6.9 \times 10^8 \text{ M}^{-1} \text{s}^{-1}$		175

I.3.4 Ligand Displacement Reactions

Generally, four types of displacement reactions can take place:

- (a) Monodentate ligand exchange reactions (excess ligand).
- (b) Multidentate ligand exchange reactions (excess ligand).
- (c) Metal exchange between ligands (excess metal).
- (d) Double exchange reactions.

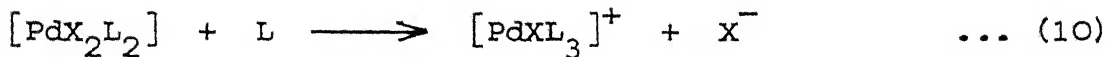
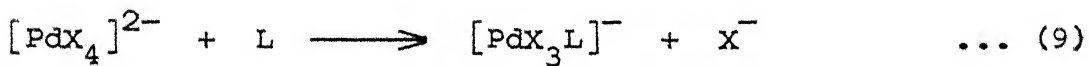
The above exchange reactions are often sluggish in nature because the reactions involve the breaking of a series of coordination bonds in succession. In case of displacement of the multidentate ligand EDTA, for example, six bonds must be broken during exchange process.

I.3.4a Monodentate ligand exchange reactions

This section is concerned with the kinetics and mechanisms of substitution in complexes in which monodentate ligands exchange with monodentate or multidentate ligands. Reactions in which water is the monodentate ligand as well as the solvent, have been considered before (I.3.1). Few examples involving other monodentate ligands, mainly cyanide, are now examined. The replacement of one monodentate ligand by another is the simplest situation to envisage and has been used extensively for investigating the mechanisms of substitution in many octahedral and square-planar complexes. The kinetics of substitution reactions of $[\text{Fe}(\text{CN})_5\text{L}]^{3-}$ ($\text{L} = \text{NO}$,

3-5-Me₂-Py, -ONPh, -SO₃, Py and 3-CN-Py etc) have recently been studied and they normally follow a dissociative path. The rate data for the formation and dissociation of these reactions have been compiled from literature by Phull.³⁴ However, the number of reports on the replacement of unidentate ligands coordinated to Fe(III) by other unidentate ligands¹⁷⁸ is rather limited.

Elding¹⁷⁹ has carried out a comprehensive study on Pd(II) halides and aquo halides. Rate constants and activation parameters have been reported for reactions of [PdCl₄]²⁻ and [PdBr₄]²⁻ with thiourea and selenourea (Table I.11). Two reactions were monitored,



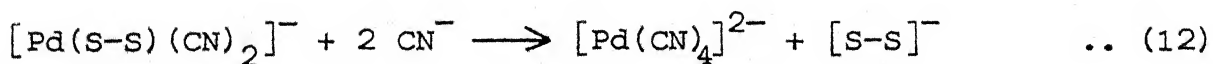
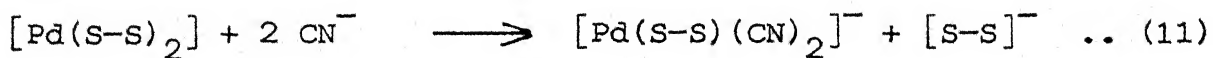
Reactions of [PdX₃L]⁻ and of [PdXL₃]⁺ were too fast even for stopped-flow monitoring owing to the very high trans effect of thiourea and selenourea.¹⁸⁰ Bromide substitution in the sterically hindered complexes [Pd(Et₄dien)XCN]⁺ and [Pd(MeEt₄dien)XCN]⁺ (X = S or Se) follows the usual two term rate law.¹⁸¹ One has a first-order rate constant for a solvolytic path and another has a second-order rate constant for a direct bimolecular substitution path. The influence of non-reacting chelate ligands terpy and 3-azapentane-1,5-diamine(3-NHpd) on the reactivity of square-planar palladium complexes has been studied by Cusumano et al.¹⁸³ The kinetics for substitution reaction of [Pd(terpy)X]⁺ (X = I⁻ > Br⁻ > Cl⁻ > N₃⁻ > NO₂⁻)

TABLE I.11. Kinetic parameters for associative nucleophilic attack
at $[PdX_4]^{2-}$ halogenoanions.

Nucleophile	k_2 $M^{-1} s^{-1}$	ΔH^\neq $k \text{ cal mol}^{-1}$	ΔS^\neq $\text{cal K}^{-1} \text{mol}^{-1}$	Ref.
<u>$[PdCl_4]^{2-}$</u>				
Ammonia	33	-	-	185
Thiourea	9.1×10^3	6.0	-19.5	180
Selenourea	4.5×10^3	4.4	-26.0	180
diamper	4.9×10^{-3}	20	+14	186
NN'-Me ₂ diamper	0.55×10^{-3}	23	+20	186
enH ⁺	296	-	-	187
Me ₂ enH ⁺	153	-	-	187
Me ₄ enH ⁺	14	-	-	187
<u>$PdBr_4]^{2-}$</u>				
Thiourea	2.1×10^4	7.3	-19.0	180
Selenourea	9.1×10^4	10.7	- 0.5	180

with Y^- ($Y = \text{thiourea} > I^- > Br^- > N_3^- > Cl^-$), have been studied¹⁸² and compared with those of the previously investigated $[\text{Pd}(3-\text{NHpd})_3]^+$ complexes.¹⁸³ The terpy complexes are both more reactive and more discriminating between various entering ligands. The higher reactivity of the terpy complexes may be explained by the possibility of extensive π -interaction between the metal atom and the coplanar nitrogen atoms of the ligand which enhances the electrophilicity of the reaction centre.¹⁸²

Some qualitative nmr studies on exchange reactions of tertiary phosphine complexes of palladium(II) have been reported.¹⁸⁴ Exchange between the complexes $[\text{PdL}_2X_2]$ and $[\text{PdL}_3X]^+$ ($L = \text{a tertiary phosphine, } X = \text{Cl, Br, or I}$) is fast on the nmr time scale at room temperature but slow at -50°C in CDCl_3 solvent. The line broadenings observed can be explained if the exchange is assumed to take place in a pathway in which a halide of $[\text{PdX}_2L_2]$ is exchanged directly with the phosphine trans to the X of $[\text{PdXL}_3]^+$ via a halide-bridged intermediate. Exchange between the cationic complex $[\text{PdXL}_3]^+$ and free phosphine has also been observed.¹⁸⁴ Two reaction steps were identified when methanolic solutions of the dithiophosphate and dithiocarbamate complexes of palladium(II) were treated with cyanide ion.²⁵² The two steps were assigned as in reactions (11) and (12) where $[\text{s-s}]^-$ represents the bidentate sulphur ligand



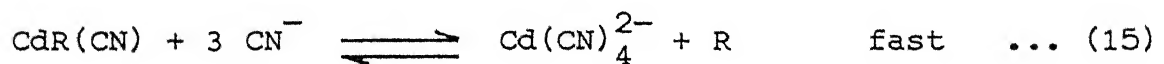
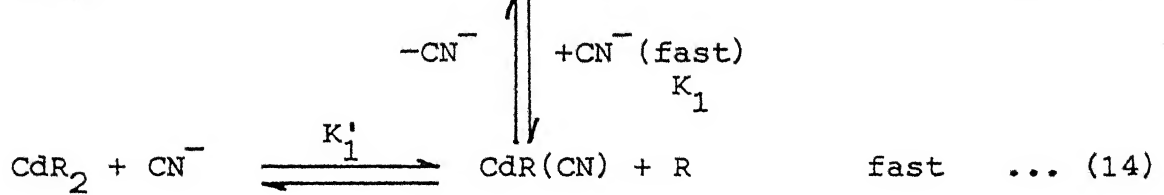
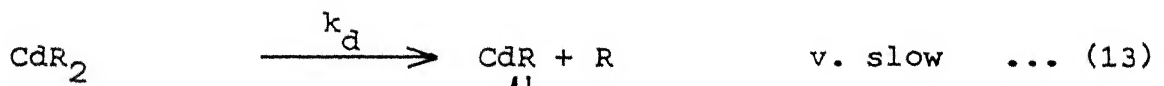
Other substitution reactions for which kinetic data have been reported include those of $\text{cis-}[\text{PdCl}_2(\text{NH}_3)_2]$ with ammonia,¹⁸⁸ of $[\text{PdX}_2\{\text{P}(\text{OMe})_3\}_2]$ with thiourea,¹⁸⁹ and of $[\text{PdCl}_4]^{2-}$ and $[\text{PdCl}_2(\text{en})_2]$ with protonated diamines.¹⁸⁷

The cyanide ion is a potential unidentate ligand having the capability of displacing multidentate ligands like polyaminocarboxylates,⁵⁴⁻⁶⁶ polyamines^{53,54} and macrocyclic ligands¹⁹⁰⁻¹⁹⁴ from their octahedral complexes of Ni(II) ions. Recently, Nigam et al. have investigated the kinetics and mechanism of replacement of amino-carboxylates from mono(aminocarboxylato)hydroxoferrate(III) complexes by cyanide ions.⁶⁸⁻⁷⁵ The general mechanistic scheme for $[\text{NiL}]^{2-n}-\text{CN}^-$ reaction system requires three cyanides to be bonded to nickel(II) while four cyanides are required in $[\text{FeL(OH)}]^{2-n}-\text{CN}^-$ systems ($n =$ charge on the ligand) in their respective rate determining steps. The last cyanide adds rapidly forming $[\text{Ni}(\text{CN})_4]^{2-}$ or $[\text{Fe}(\text{CN})_5\text{OH}]^{3-}$ respectively. A multistep mechanism via successive formation of mixed-ligand intermediates has been proposed for both reaction systems.

Stara and Kopanica⁶⁴ have studied the kinetics and mechanism of the reaction of the binuclear complex (Ni_2TTHA) with cyanide ion. Their mechanism was, however, refuted by Nigam et al.⁶⁵ and a plausible mechanism proposed. More recently, Nigam et al. have investigated for the first time, the kinetics and mechanism of reactions of binuclear $[\text{Fe}_2\text{TTHA(OH)}_2]^{2-}$ and $[\text{Fe}_2\text{HPDTA(OH)}_2]$ with cyanide ions. The essential feature of this mechanism is a slow cyanide-independent dissociation and a rapid cyanide-assisted dissociation of the

binuclear complex followed by a sequence of steps similar to reactions of 1:1 complex with cyanide.

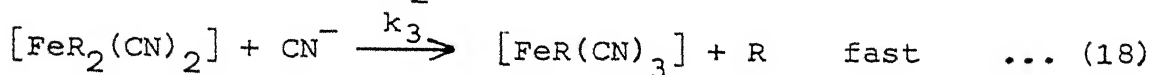
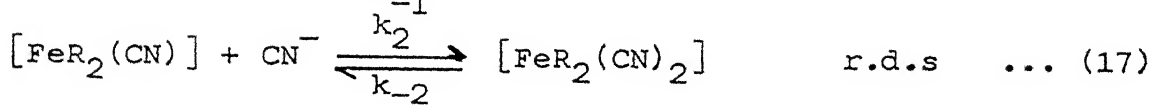
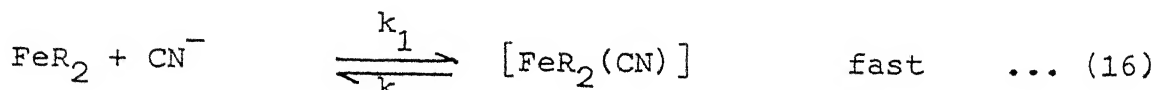
Very little is known, so far, on the exchange reactions of bis complexes of Pd(II) and Cd(II). The kinetics and mechanism of reactions of some bis complexes of Ni(II)^{53,196} and Zn(II)³³ with cyanide ions have been studied. The Cd(Par)₂-CN⁻ reaction follow a scheme given from eqns. (13)-(15). Here the bis complexes of multi-dentate ligands react with cyanide ion by a cyanide independent dissociative path (eqn. 13) and cyanide dependent associative path (eqns. 14,15).



(in three steps, Here R represents Par)

The formation of [Ni(CN)₄]²⁻ from reactions of cyanide ions with square-planar bis complexes of Ni(II) through the formation of very stable mixed-ligand complexes has been demonstrated by Billot et al.^{54,197} The reaction of cyanide ion with bis complexes of iron(II) and iron(III) with Par have been studied by Nigam et al.^{198,199} The reaction scheme is given in eqns. (16)-(18). In these reactions, formation of mixed-ligand complexes does not follow a cyanide independent dissociative path as in equation 13 followed by equations

14 and 15. Instead, release of only one multidentate ligand takes place in the last step of the reaction sequence (eqns. 16-18).

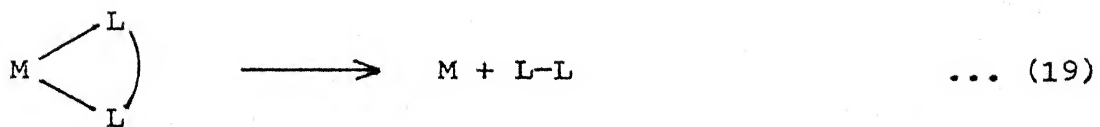


The reactions of cyanide ion with the cationic complex $\text{Fe}(\text{L-L})_3^{2+}$ where L-L is 1,10 phen²⁰⁰ or a substituted phen,^{165,201} Schiff's base,²⁰² bipy,²⁰³⁻²⁰⁷ substituted bipy²⁰⁸ or terpy^{209,169} or diimine²¹⁰ proceed in the same way forming mixed ligand complexes of the type $\text{Fe}(\text{L-L})_2(\text{CN})_2$.

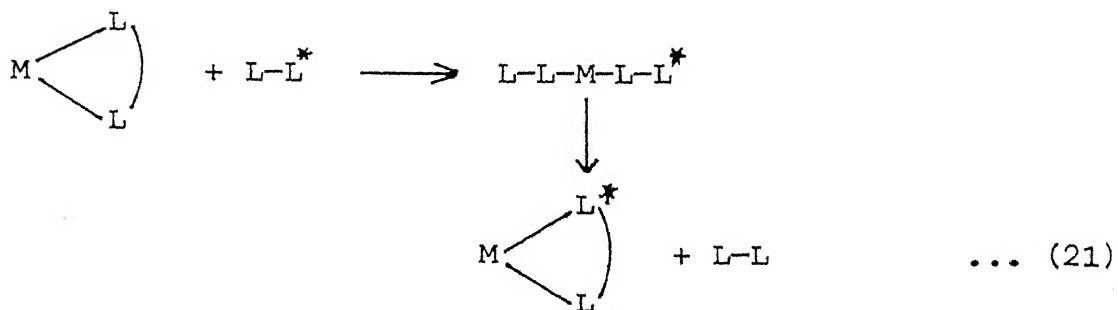
I.3.4b Multidentate ligand displacement reactions

The mechanism by which one multidentate ligand displaces another from a metal ion depends upon the ability of both ligands to coordinate with the metal ion simultaneously. There are four accepted mechanisms for this type of reactions.

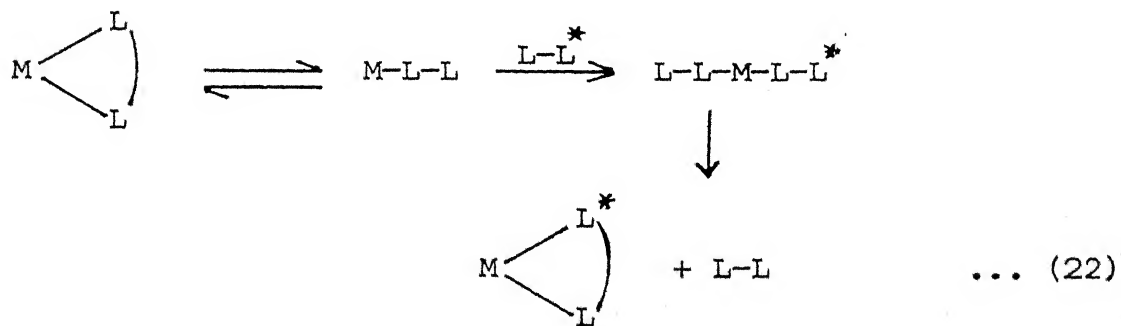
(i) The outgoing ligand (L-L) is completely dissociated from the metal cation (M) before association between M and the incoming ligand (L-L)^{*} starts.



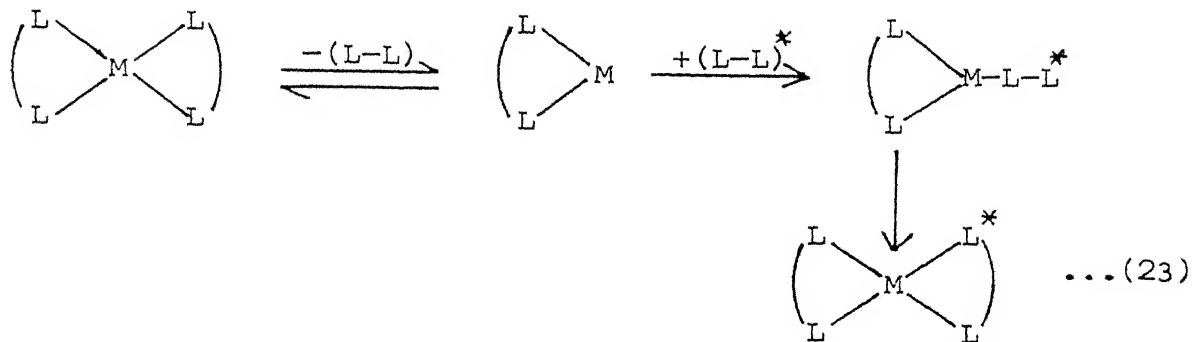
(ii) The association of the metal cation with the incoming ligand may begin before dissociation of the outgoing ligand is complete. In this mechanism there will thus be an intermediate in which both ligands are bonded to the same cation.



(iii) A variation on the above mechanism is the case of pre-equilibrium partial dissociation of the starting complex.



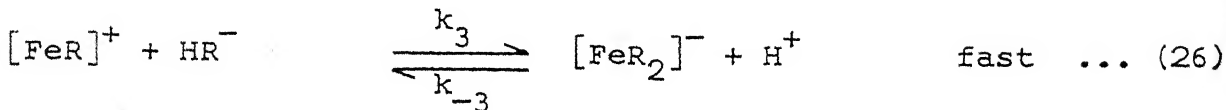
(iv) In the last scheme, there is a modification of the scheme (iii), one which can apply when two multi e.g., terdentate ligands are replaced by another multi e.g. quinqui or hexadentate ligand.



The rate determining step of the overall reaction is the cleavage of any one of the several bonds between metal and the leaving group which must be broken in the course of reaction. As examples, NiTet²⁺ reacts with EDTA,²¹¹ TMDTA,²¹² PDTA or DTPA²¹³ and NiTrien²⁺ reacts rapidly with EDTA,²¹¹ HEDTA²¹⁴ or DTPA²¹⁵ forming mixed ligand intermediates and give respective products by unwrapping of Tet or Trien.

A review of multidentate ligand exchange reactions and their applications to analytical chemistry has appeared for systems involving EGTA and 4-(2-pyridylazo)resorcinol.²¹⁶ Other multidentate ligand exchange reactions of metal ions such as Cu(II),²¹⁷⁻²¹⁹ Mn(II),²²⁰ Hg(II),²²¹ Cd(II)²²²⁻²²⁵ and Ni(II)²²⁶⁻²³⁰ have been investigated by many workers. Not much is known, so far, on the exchange of multidentate ligands on Fe(III) and Pd(II). A review²³¹ on substitution reactions of square-planar complexes involving polydentate ligands had appeared some years ago. Recently Nigam et al. have investigated, for the first time, the kinetics and mechanism of FeL with Par²³² and PdIDA with L (where L = EDTA or TTHA).⁷⁶ The reaction between FeL and Par renders products through a reaction

scheme given below (equations 24-26):



Similar multidentate ligand exchange reactions between EDTA complex of Fe(III)^{233} and salicylic acid or 1,2 dihydroxy-3,5 benzenedisulfonic acid have also been studied.

Multidentate ligand exchange reactions of Pd(II) followed a scheme different from Fe(III) . These reaction are of consecutive type in which fast formation of mixed ligand complex occurs which in turn dissociates into respective products as given below (equations 27,28).

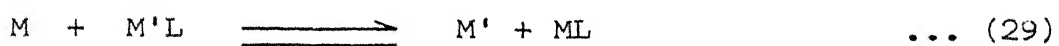


In many multidentate ligand replacement reactions the rate expression contains terms in various powers of the hydrogen ion concentration, which arise from the possible ways of protonating the ligands both free and in complexed form. It has been possible to resolve the rate constants due to various protonated reactants

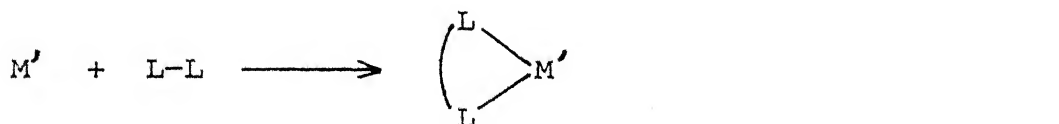
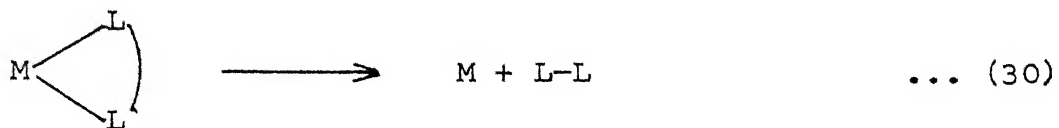
by algebraic manipulation and mathematical analysis of reaction rates measured over a wide pH range and resorting to some simplifying assumptions about species distribution.

I.3.4c Metal exchange and displacement reactions

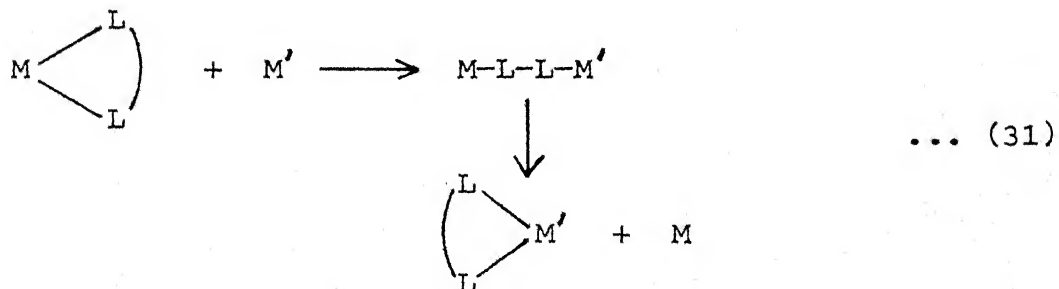
The displacement of one metal cation from its complex with a multidentate ligand by another metal ion (or the exchange with an identical labelled metal ion) is represented by equation (29).



Mechanism of metal displacement can be either dissociative:



or associative in nature



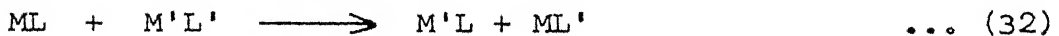
The mechanisms of some metal cation displacement reactions are indicated in Table I.12. Reactions following equation (30) are represented by D and equation (31) by DA.

TABLE I.12. Mechanisms of cation displacement from multidentate ligand complexes.

Complex	Replacing cation	Type of Mechanism	Ref.
Cd(II)-TTHA	Co(II)	DA	234
Cd(II)-TTHA	Ni(II)	DA	234
Cd(II)-TTHA	Cu(II)	DA	234
Cd(II)-TTHA	Zn(II)	DA	234
Cd(II)-CYDTA	Cu(II)	D	235
Cd(II)-EDTA	Cu(II)	DA	236
$[\text{Cd(II)}-(\text{EDTA})_H]^-$	Cu(II)	DA	236
Cu(II)-EDTA	Cd(II)	D	237
Fe(III)-HEDTA,-DTPA	Ga(III)	D	238
Fe(III)-HEDTA,-EGTA,-DTPA	In(III)	D	239
$[\text{Fe(III)}(\text{EDTA})_{H_2O}]^-$	In(III)	-	240
$[\text{MEDTA}]^-$ (M=Ga or In)	Fe(III)	D	241
Bi(III)EDTA	Fe(III)	D	242
Fe(III)CYDTA	In(III)	-	243

I.3.4d Double exchange reactions

An interesting situation exists when two multidentate complexes are mixed and thermodynamics dictates a double exchange.²⁴⁴ The exchange of ligands of the type given in equation (32) between two metal ion chelates has been studied²⁴⁵⁻²⁴⁷ and was found to be a slow process if the reaction goes via a dissociation sequence.



No evidence for the formation of a dicomplex intermediate has been given so far; but the rates of such coordination chain reactions were found to increase enormously if small amounts of either ligand or metal ion is added²⁴⁸⁻²⁵⁰ to the reaction mixture. This increase is the consequence of a coordination chain mechanism.

REFERENCES

1. D.R. Llewellyn, C.J. O'Conor and A.L. Odell, J. Chem. Soc., 1964, 196.
2. T.J. Swift and R.E. Connick, J. Chem. Phys., 1962, 37, 307; 1964, 41, 2553.
3. J.L. Burmeister and F. Basolo, Prep. Chem. React., 1968, 5, 1.
4. A.S. Mildvan, "Metals in Enzyme Catalysis", In the Enzymes, Ed. P.D. Boyer, Academic Press, New York, 1970, Vol. 2, 3rd edn., Chapter 9.
5. H. Diebler, M. Eigen, G. Ilgenfritz, G. Maass and R. Winkler, Pure. Appl. Chem., 1969, 20, 93.
6. H. Taube, Chem. Rev., 1952, 50, 69.
7. W. Kruse and D. Thusius, Inorg. Chem., 1968, 7, 464.
8. E. Chaffee and J.O. Edwards, "Progress in Inorganic Chemistry", Interscience Publ., John Wiley and Sons, New York, 1970, 13, p. 205.
9. J. Halpern and L.E. Orgel, Disc. Faraday Soc., 1960, 29, 32.
0. H. Wendt, Inorg. Chem., 1969, 8, 1527.
1. R.G. Wilkins, Acc. Chem. Research, 1970, 3, 408.
2. R.G. Wilkins, Pure and Appl. Chem., 1973, 33, 583.
3. A. Peloso, Coord. Chem. Rev., 1973, 10, 123.
4. T.W. Swaddle, Coord. Chem. Rev., 1974, 14, 217.
5. D. Banerjea, J. Ind. Chem. Soc., 1977, 54, 37.
6. D.W. Margerum, G.R. Cayley, D.C. Wetherburn and G.K. Pagenkopf, Adv. Coord. Chem., Vol. II, Ed. A.E. Martell, Published by Am. Chem. Soc., 1978, 1-220.

17. A Specialist Periodical Report, Inorg. Reaction Mechanisms, Vol. I to VII, Published by Chemical Society, London.
18. S. Kazuo, S. Yoichi, Kido H. Nagazawa, Akira Ogino Kazuko, Chem. Abstr., 1981, 95, 161122t.
19. L.I. Elding, Inorg. React. Mech., 1981, 7, 135; 1981, 7, 159.
20. R.J. Cross, Chem. Soc. Rev., 1985, 14, 197.
21. H. Elias, Chem. Abstr., 1983, 99, 77564p; Proc. Conf. Coord. Chem., 1983, 9th, 79.
22. M. Eigen and L. Demaeyer in, "Techniques of Organic Chemistry", S.L. Friess, E.S. Lewis and A. Weissberger, Ed., Vol. VIII, Part II, Interscience, New York, N.Y., 1963, p.895; E.F. Caldin Fast Reactions in Solution", Blackwell Scientific Publications, Oxford, 1964.
23. J. Bjerrum and K.G. Poulsen, Nature, 1952, 169, 463.
24. C.J. Burris and K.J. Laidler, Trans. Faraday Soc., 1955, 51, 1497.
25. J.N. Bronsted and R. Livingston, J. Amer. Chem. Soc., 1927, 49, 435.
26. C.W. Davies and I.W. Williams, Trans. Faraday Soc., 1958, 54, 1547.
27. R.G. Gamon and C.N. Reilley, Anal. Chem., 1962, 34, 600.
28. D.W. Margerum and T.J. Bydalek, Inorg. Chem., 1962, 1, 852 and J. Amer. Chem. Soc., 1961, 83, 4326.
29. H.B. Mark, Jr. and G.A. Rechnitz, "Kinetics in Analytical Chemistry", Interscience Publishers, New York (1968).
30. G.K. Pagenkopf and D.W. Margerum, J. Amer. Chem. Soc., 1968, 90, 502.
31. G.R. Dukes, G.K. Pagenkopf and D.W. Margerum, Inorg. Chem., 1971, 10, 2419.

32. L.C. Coombs and J. Vasiliades and D.W. Margerum, Anal. Chem., 1972, 44, 2325.
33. H.A. Mottola and H.B. Mark Jr., Anal. Chem., 1980, 52, 31R and references contained therein.
34. Ms. Madhu Phull, Ph.D. Thesis, I.I.T. Kanpur, India (1983).
35. H.A. Mottola, Anal. Chem. Rev., 1984, 56, 96R.
36. S. Ito, K. Haraguchi and K. Nakagawa, Bunseki Kagaku, 1978, 27(6), 334.
37. Ms. Madhu Phull, H.C. Bajaj and P.C. Nigam, Talanta, 1981, 28, 610
38. M. Tanaka, S. Funahashi and K. Shirai, Anal. Chim. Acta, 1967, 39, 437.
39. G.M. Ridder and D.W. Margerum in "Essays on Analytical Chemistry, (in memory of Prof. Anders Ringbom)", Wannien E., Ed . Pergamon Press, Oxford, 1977, pp. 529-36.
40. S. Ito, K. Haraguchi, K. Nakagawa and K. Yamada, Bunseki Kagaku, 1977, 26, 554; Chem. Abstr., 1978, 88, 163250n.
41. (Ms) Madhu Phull and P.C. Nigam (unpublished).
42. E. Mentasti, Anal. Chim. Acta, 1979, 111(1), 177.
43. K. Nakagawa, T. Ogata, K. Haraguchi and S. Ito, Bunseki Kagaku, 1981, 30(3), 149.
44. Demetrius, G. Themelis and George S. Vasilikiotis, Analyst, 1987, 112(6), 791 and 797.
5. (Ms) Nishi Gupta and P.C. Nigam, Indian J. Chem., 1988 (In press).
6. M. Eigen and R.G. Wilkins, Adv. Chem. Ser., 1965, 49, 55.
7. M. Grant and R.B. Jordan, Inorg. Chem., 1981, 20, 55.
8. H.W. Baldwin and H. Taube, J. Chem. Phys., 1960, 33, 206.
9. J.P. Hunt and H. Taube, J. Chem. Phys., 1951, 19, 602.

50. Hans U.D. Weisendanger, W.H. Jones and C.S. Garner, J. Chem. Phys., 1957, 27, 668.
51. H.C. Bajaj, Ph.D. Thesis, I.I.T. Kanpur, India (1982).
52. R.M. Naik, Ph.D. Thesis, I.I.T. Kanpur, India (1986).
53. H.C. Bajaj, (Ms) Madhu Phull and P.C. Nigam, Bull. Chem. Soc. Japan, 1984, 57, 564.
54. J.C. Pleskowicz and E.J. Billo, Inorg. Chim. Acta., 1985, 99, 149 and references contained therein.
55. K. Kumar, P.C. Nigam and G.S. Pandey, J. Phys. Chem., 1978, 82, 1955.
56. K. Kumar and P.C. Nigam, J. Phys. Chem., 1979, 83, 2090.
57. K. Kumar and P.C. Nigam, J. Phys. Chem., 1980, 84, 140.
58. K. Kumar and P.C. Nigam, J. Coord. Chem., 1979, 9, 139.
59. D.W. Margerum, T.J. Bydalek and J.J. Bishop, J. Amer. Chem. Soc., 1961, 83, 1791.
60. L.C. Coombs, D.W. Margerum and P.C. Nigam, Inorg. Chem., 1970, 9, 2081.
61. D.W. Margerum and L.I. Simandi, Proceedings of 9th International Conference on Coordination Chem., W. Scheider, Ed., Verlag Helvetica Chimica Acta, Basel (1966).
2. L.C. Coombs and D.W. Margerum, Inorg. Chem., 1970, 9, 1711.
3. G.K. Pagenkopf, J. Coord. Chem., 1972, 2, 129.
4. V. Stara and M. Kopanica, Coll. Czech. Chem. Comm., 1972, 37, 2882.
5. K. Kumar, H.C. Bajaj and P.C. Nigam, J. Phys. Chem., 1980, 84, 2351.
6. H.C. Bajaj, (Ms) Madhu Phull and P.C. Nigam, J. Coord. Chem., 1983, 13, 41.
7. R.M. Naik and P.C. Nigam, Trans. Met. Chem., 1986, 11, 11.

68. H.C. Bajaj and P.C. Nigam, Trans. Met. Chem., 1982, 7, 190.
69. H.C. Bajaj and P.C. Nigam, Trans. Met. Chem., 1983, 8, 109.
70. R.M. Naik and P.C. Nigam, Trans. Met. Chem., 1985, 10, 227.
71. R.M. Naik and P.C. Nigam, Trans. Met. Chem., 1986, 11, 337.
72. R.M. Naik and P.C. Nigam, Trans. Met. Chem., 1985, 10, 220.
73. R.M. Naik and P.C. Nigam, Inorg. Chim. Acta., 1986, 114, 55.
74. (Ms) Pratima Mishra, R.M. Naik and P.C. Nigam, Inorg. Chim. Acta, 1987, 127, 71.
75. (Ms) Pratima Mishra and P.C. Nigam, Trans. Met. Chem., 1987 (In Press).
76. (Ms) Nishi Gupta and P.C. Nigam, Trans. Met. Chem. 1988 (communicated).
77. (Ms) Nishi Gupta, R.M. Naik and P.C. Nigam, Inorg. Chim. Acta. 1988 (communicated).
78. E.D. Hughes and C.K. Ingold in "Structure and Mechanism of Organic Chemistry", Ed. C.K. Ingold, Cornell Univ. Press, Ithaca, N.Y., 1953, Chapter V.
79. C.H. Langford and H.B. Gray, "Ligand Substitution Process", Benjamin, New York, 1965, p.7.
80. R.G. Wilkins, "The study of Kinetics and Mechanism of Reactions of Transition Metal Complexes", Allyn and Bacon: Boston, 1974; Chapter 4.
81. F.W. Breivogel Jr., J. Phys. Chem., 1969, 73, 4203.
82. J.F. Below Jr., R.E. Connick and C.P. Coppel, J. Amer. Chem. Soc., 1958, 80, 2961.
83. D. Seawald and N. Sutin, Inorg. Chem., 1963, 2, 643.
84. R.E. Bauer and W.M. Smith, Can. J. Chem., 1965, 43, 2763.
85. E.G. Moorhead and N. Sutin, Inorg. Chem., 1966, 5, 1866.

86. M.R. Judkins, Ph.D. Thesis, Univ. of Calf., May 1967.
87. C.H. Langford and F.M. Chung, J. Amer. Chem. Soc., 1968, 90, 4485.
88. F.P. Cavasino and E. Didio, J. Chem. Soc., Sect. A, 1971, 3176.
89. J. Hodgkinson and R.B. Jordan, J. Amer. Chem. Soc., 1973, 95, 763.
90. E. Mentasti and E. Pellizzetti, J. Chem. Soc. Dalton, 1973, 2605
91. D.H. Devia and D.W. Watts, Inorg. Chim. Acta., 1973, 7, 691.
92. K. Nakamura, T. Tsuchida, A. Yamagishi and M. Fujimoto, Bull. Chem. Soc. Jpn., 1973, 46, 456.
93. S. Funahashi, S. Adachi and M. Tanaka, Bull. Chem. Soc. Jpn., 1973, 46, 479.
94. G. Wada and Y. Kobayashi, Bull. Chem. Soc. Jpn., 1975, 48, 2451
95. S. Gouger and J. Stuehr, Inorg. Chem., 1974, 13, 379.
96. A. Jost and B. Bunsenges, J. Phys. Chem., 1976, 80, 316.
97. B.B. Hasinoff, Can. J. Chem., 1976, 54, 1820.
98. T. Sekine, H. Honda, M. Kokiso and T. Tosaka, Bull. Chem. Soc. Jpn., 1979, 52, 1046.
99. H. Kido and K. Saito, Bull. Chem. Soc. Jpn., 1980, 53, 424.
100. F. Basolo and R.G. Pearson, "Mechanism of Inorganic Reactions" 2nd Ed., John Wiley and Sons, Inc., New York, London, Sydney, 1967, Chapter V.
101. J.B. Goddard and F. Basolo, Inorg. Chem., 1968, 7, 936.
102. W.H. Baddley and F. Basolo, J. Am. Chem. Soc., 1966, 88, 2944.
103. M. Kotowski, D.A. Palmer and H. Kelm, Inorg. Chim. Acta., 1980, 44, L113.

104. W. Rindermann, D.A. Palmer and H. Kelm, Inorg. Chim. Acta, 1980, 40, 179.
105. R. Van Eldik, D.A. Palmer, R. Schmidt and H. Kelm, Inorg. Chim. Acta, 1981, 50, 131.
106. E.L.J. Breet, R. Van Eldik and H. Kelm, Polyhedron, 1983, 2, 118.
107. D.A. Palmer, R. Schmidt, R. Van Eldik and H. Kelm, Inorg. Chim. Acta, 1978, 29, 261.
108. E.L.J. Breet, R. Van Eldik and H. Kelm, Inorg. Chim. Acta, 1984, 85, 151.
109. G. Mahal and R. Van Eldik, Inorg. Chem., 1985, 24, 4165.
110. R. Roulet and H.B. Gray, Inorg. Chem., 1972, 11, 2101.
111. V.D. Panasyuk and T.I. Denisova, Russ. J. Inorg. Chem., 1970, 15, 377.
112. V.D. Panasyuk and T.I. Denisova, Russ. J. Inorg. Chem., 1971, 16, 1342.
113. V.D. Panasyuk, T.I. Denisova and S.K. Rybak, Russ. J. Inorg. Chem., 1972, 17, 874.
114. D.J. Hewkin and R.H. Prince, Coord. Chem. Rev., 1970, 5, 45.
115. F.W. Breivogel, Jr., J. Chem. Phys., 1969, 51, 445.
116. J. Babiec, Thesis, University of Massachusetts, 1966; Diss. Abstr., B, 1967, 27, 4336.
117. R.J. West and S.F. Lincoln, Aust. J. Chem., 1971, 24, 1189.
118. G.S. Vigee and P. Ng, J. Inorg. Nucl. Chem., 1971, 33, 2477.
119. H. Hoffmann, Pure Appl. Chem., 1975, 41, 327.
120. J.F. Coetzee and E. Hsu, J. Solution Chem., 1975, 4, 45.
121. H.P. Bennetto and Z.S. Imani, J. Chem. Soc. Faraday, 1975, 1, 1143.
122. D.M.W. Buck and P. Moore, J. Chem. Soc. Dalton, 1975, 409.
123. M. Eige and R.G. Wilkins, Adv. Chem. Ser., 1865, No.49.

124. S. Funahashi and J.B. Jordan, Inorg. Chem., 1977, 16, 1301.
125. N.A. Matwyoff, Inorg. Chem., 1966, 5, 788.
126. L.S. Frankel, Inorg. Chem., 1971, 10, 2360.
127. M. Eigen, Z. Elektrochem., 1960, 64, 115.
128. M. Eigen and K. Tamm, Z. Elektrochem., 1962, 66, 93.
129. M. Eigen and K. Tamm, Z. Elektrochem., 1966, 66, 107.
130. E. Mentasti, E. Pellizzetti and G. Saini, Gazzetta, 1974, 104, 201.
131. F.P. Cavasino and E. Dido, J. Chem. Soc., A, 1970, 1151.
132. E. Mentasti and C. Baiocchi, J. Coord. Chem., 1980, 10, 229.
133. G. Calvaruso, F.P. Cavasino, E. Didio and R. Triolo, Inorg. Chim. Acta, 1977, 22, 61.
134. V.D. Gomwalk, A.G. Lappin, J.P. McCann and A. McAuley, Inorg. Chim. Acta., 1977, 24, 39.
135. M.S. El-Ezaly, A.I. Abu-Shady, N. Gayed and F.R. El-Eziri, J. Inorg. Nucl. Chem., 1977, 39, 169.
136. C.H. Langford and H.B. Gray, "Ligand Substitution Process", Benjamin, New York, 1965, p.49.
137. L.I. Elding, Inorg. Chim. Acta., 1972, 6, 683.
138. M.N. Vargaftik, E.D. German, R.R. Dogonadze and Ya.K. Syrkin, Doklady Akad. Nauk S.S.R., 1972, 206, 370 (Chem. Abstr., 1973, 78, 8494v).
139. G. Mahal and R. Van Eldik, Inorg. Chem., 1985, 24, 4165.
140. K. Kusin, I.A. Taub and E. Weinstock, Inorg. Chem., 1966, 5, 1079.
141. M. Eisenstadt, J. Chem. Phys., 1969, 51, 4421.
142. R.H. Holyer, C.D. Hubbard, S.F.A. Kettle and R.G. Wilkins, Inorg. Chem., 1965, 4, 929; 1966, 5, 622.

143. G.K. Pagenkopf and D.W. Margerum, Inorg. Chem., 1968, 7, 2514.
144. M. Eigen and R.G. Wilkins, "The Kinetics and Mechanism of formation of Metal Complexes", Advances in Chemistry Series, No. 29, American Chemical Society, Washington, D.C., 1965, p.55.
145. H.G.Z. Hertz, Elektrochem., 1961, 65, 36.
146. G. Geier, Helv. Chim. Acta, 1968, 51, 94.
147. D.L. Rabenstein and R.J. Kula, J. Am. Chem. Soc., 1969, 91, 2492.
148. J.Z. Koryta, Elektrochem., 1960, 64, 196.
149. R.G. Wilkins, Inorg. Chem., 1964, 3, 520.
150. G.H. Reed and R.J. Kula, Inorg. Chem., 1971, 10, 2050.
151. M. Kodama, K. Namekawa and T. Horiuchi, Bull. Chem. Soc. Jpn., 1974, 47, 2011.
152. N. Tanaka, R. Tamamushi and M. Kodama, Z. Phys. Chem., 1958, 14, 141.
153. J.R. Kuempel and W.B. Schaap, Inorg. Chem., 1968, 7, 2435.
154. J. Koryta and Z. Zabransky, Collect. Czech. Chem. Commun., 1960, 25, 3153.
155. G.H. Aylward and J.W. Hayes, Anal. Chem., 1965, 37, 195.
156. M. Kimura, Nippon Kagaku Zasshi, 1969, 90, 1246.
157. G.F. Smith and D.W. Margerum, Inorg. Chem., 1969, 8, 135.
158. B.J. Fuhr and D.L. Rabenstein, Inorg. Chem., 1973, 12, 1868.
159. R.A. Read and D.W. Margerum, Inorg. Chem., 1981, 20, 3143.
160. C.E. Bannister and D.W. Margerum, Inorg. Chem., 1981, 20, 3149.
161. J.M.T. Raychebra and D.W. Margerum, Inorg. Chem., 1980, 19, 497.

162. D.W. Margerum, J. Am. Chem. Soc., 1957, 79, 2728 and references contained therein.
163. J. Burgess, "Inorg. React. Mech.", Chem. Soc. Specialist Periodical Report, London, 1971, 1, 176; 1972, 2, 168.
164. D.W. Margerum and L.P. Morgenthaler, J. Am. Chem. Soc., 1962, 84, 706.
165. J. Burgess, Inorg. Chim. Acta, 1971, 5, 133.
166. J.M. Lucie and D.R. Stranks, J. Chem. Soc. Dalton, 1975, 245.
167. J. Burgess, J. Chem. Soc. Dalton, 1974, 2032.
168. G.A. Lawrence, D.R. Stranks and S. Suvachittanont, Inorg. Chem. 1979, 18, 82.
169. M.V. Twigg, Inorg. Chim. Acta, 1974, 10, 17.
170. J. Burgess and R.H. Prince, J. Chem. Soc. A, 1967, 434.
171. C.V. D'Alkaine and J. Koryta, Coll. Czech. Chem. Comm., 1969, 34, 2138.
172. J.L. Sudmeier and C.N. Reilley, Inorg. Chem., 1966, 5, 1047.
173. R.W. Schmid and C.N. Reilley, J. Amer. Chem. Soc., 1958, 80, 2101.
174. Y. Koike and H. Hamaguchi, J. Inorg. Nucl. Chem., 1967, 29, 473.
175. G. Conradi, M. Kopanica and J. Koryta, Coll. Czech. Chem. Comm. 1965, 30, 2029.
176. P. Letkeman and J.B. Westmore, J. Chem. Soc. Dalton, 1975, 480.
177. J.C. Cooper, L.F. Wong and D.W. Margerum, Inorg. Chem., 1978, 17, 261.
178. J.H. Espenson and S.G. Wolenuk, Inorg. Chem., 1972, 11, 2035.
179. L.I. Elding, Inorg. Chim. Acta, 1973, 7, 581.

180. P.V.Z. Bekker and W. Robb, Internat. J. Chem. Kinetics, 1975, 7, 87.

181. M. Cusumano, G. Guglielmo and P. Marricchi, Inorg. Chim. Acta, 1978, 30, 29.

182. M. Cusumano and G. Guglielmo, Inorg. Chim. Acta, 1976, 27, 197.

183. L. Cattalini, M. Cusumano, V. Ricevuto and M. Trozzi, J. Chem. Soc. Dalton, 1975, 771.

184. W.J. Louch and D.R. Eaton, Inorg. Chim. Acta, 1978, 30, 243.

185. R.A. Reinhardt and W.W. Monk, Inorg. Chem., 1970, 9, 2026.

186. H. Hennig, K. Schulze, M. Muhlstadt, E. Hoyer, R. Kirmse and L.S. Emeljanowa, Z. anorg. Chem., 1975, 413, 10.

187. R. Ernst and R. Roulet, Chimia (Switzerland), 1974, 28, 347.

188. R.G. Hibler, Chem. Abs., 1975, 83, 85574.

189. A.D. Troitskaya, I.A. Orlova and G.P. Sadakova, Chem. Abstr., 1976, 84, 129854.

190. L. Hertle and T.A. Kaden, Chimia (Switzerland), 1975, 29, 304.

191. M.J. D'Amiello, M.T. Mocella, E.K. Barefield and J.C. Paul, J. Amer. Chem. Soc., 1975, 97, 192.

192. W. Steinman and T.A. Kaden, Helv. Chim. Acta, 1975, 58, 1358.

193. E.K. Barefield and M.T. Mocella, J. Amer. Chem. Soc., 1975, 97, 4238.

194. E.P. Hintz and D.W. Margerum, Inorg. Chem., 1974, 13, 2941.

195. G.B. Kolski and D.W. Margerum, Inorg. Chem., 1969, 8, 1125.

196. K. Kumar, Ph.D. Thesis, I.I.T. Kanpur, India (1978), Chap. 4.

197. R.G. Pearson and D.A. Swigart, Inorg. Chem., 1970, 9, 1167.

198. (Ms) Nishi Gupta and P.C. Nigam, Trans. Met. Chem., 1988 (in press).

CELESTE LIBRARY

106263

199. (Ms) Nishi Gupta and P.C. Nigam, Trans. Met. Chem., 1988 (In press).
200. D.W. Margerum and L.P. Morgenthaler, J. Amer. Chem. Soc., 1962, 84, 706.
201. J. Burgess and F.M. Mekhail, Trans. Met. Chem., 1978, 3, 162.
202. J. Burgess and G.M. Burton, Rev. Latimomer. Quim., 1980, 11, 107 and references contained therein.
203. J. Burgess, J. Chem. Soc. Dalton, 1972, 1061.
204. G. Nord, Acta Chim. Scand., 1973, 27, 743.
205. M.J. Blandamer, J. Burgess and J.G. Chambers, J. Chem. Soc. Dalton, 1976, 606.
206. M.J. Blandamer, J. Burgess, J.G. Chambers, R.I. Hains and H.E. Marshall, J. Chem. Soc. Dalton, 1977, 165.
207. D.D. Dollberg and R.D. Archer, Inorg. Chem., 1975, 14, 1888.
208. J. Burgess and R.H. Prince, J. Chem. Soc., 1965, 6061.
209. J. Burgess and M.V. Twigg, J. Chem. Soc. Dalton, 1974, 2032.
210. M.V. Blandamer, J. Burgess, P.P. Duee, K.S. Payne, R. Sherry and P. Wellings, Trans. Met. Chem., 1984, 9, 163 and references contained therein.
211. D.B. Rorabacher and D.W. Margerum, Inorg. Chem., 1964, 3, 382.
212. K. Kumar and P.C. Nigam, Inorg. Chem., 1981, 20, 1623.
213. R.M. Naik and P.C. Nigam, Ind. J. Chem., 1987, 26A, 205.
214. H.C. Bajaj and P.C. Nigam, Ind. J. Chem., 1981, 19A, 1070.
215. H.C. Bajaj and P.C. Nigam, Ind. J. Chem., 1984, 23A, 8.
216. S. Funahashi and M. Tanaka, Chem. Abs., 1974, 80, 33411g.
217. M. Tabata and M. Tanaka, Inorg. Chem., 1978, 17(10), 2779.
218. K. Hitoshi, Chem. Abstr., 1977, 87, 123307j.

219. J.D. Carr and V.K. Olson, Inorg. Chem., 1975, 14(9), 2168.
220. M. Kodama and K. Hagiya, Bull. Chem. Soc. Jpn., 1973, 46(10), 3151.
221. S. Funahashi, M. Tabata and M. Tanaka, Bull. Chem. Soc. Jpn., 1971, 44, 1586.
222. T. Fujisawa and M. Tanaka, Chem. Abstr., 1972, 76, 63982m.
223. M. Kodama and N. Oyama, Bull. Chem. Soc. Jpn., 1972, 45, 2169.
224. D.L. Rabenstein and B.J. Fuhr., Inorg. Chem., 1972, 11, 2430.
225. T. Katsuyama and T. Kumai, Bull. Chem. Soc. Jpn., 1978, 51, 1072.
226. M. Kodama, Chem. Abstr., 1970, 73, 18953e.
227. M. Kodama, Y. Fujii and T. Ueda, Bull. Chem. Soc. Jpn., 1970, 43, 2085.
228. S. Funahashi and M. Tanaka, Inorg. Chem., 1970, 9, 2092.
229. M. Kodama, S. Karasawa and T. Watanabe, Bull. Chem. Soc. Jpn., 1971, 44, 1815.
230. R.K. Steinhaus, Inorg. Chim. Acta, 1982, 63, 1.
231. R.J. Murenik, Rev. Inorg. Chem., 1979, 1(1), 1 (Chem. Abs., 91, 101204d).
232. (Ms) Nishi Gupta and P.C. Nigam, J. Coord. Chem., 1988 (communicated).
233. E. Mentasti and E. Pelizzetti, Talanta, 1975, 22, 930.
234. L. Neubauer and M. Kopanica, Coll. Czech. Chem. Comm., 1971, 36, 1121.
235. M. Kimura, Bull. Chem. Soc. Jpn., 1970, 43, 1594.
236. N. Tanaka and M. Kanada, Bull. Chem. Soc. Jpn., 1962, 35, 1596.
237. J.R. Kuempel and W. Schaap, Inorg. Chem., 1968, 7, 2435.

238. T. Nozaki and K. Kasuga, Chem. Abstr., 1973, 80, 41267n.

239. T. Nozaki, K. Kasagu and K. Koshiba, Nippon Kagaku Kaishi, 1972, 568 (Chem. Abs. 1972, 76, 145394k).

240. R.F. Lumu and P. Gougerh, Chem. Abs., 1976, 85, 100071x.

241. R.R. Das, J. Ind. Chem. Soc., 1974, 51, 1024.

242. N. Ana, P. Ecaterina and B. Agenta, Rev. Roum. Chim., 1981, 26(7), 967.

243. V.I. Kornev and V.A. Valyaeva, Koord. Khim., 1981, 7(12), 1866.

244. D.W. Margerum, Rec. Chem. Prog., 1963, 24, 237.

245. D.C. Olson and D.W. Margerum, J. Amer. Chem. Soc., 1963, 85, 297.

246. V. Stara and M. Kopanica, Coll. Czech. Chem. Comm., 1973, 38, 2581.

247. E. Mentasti, J. Chem. Soc. Dalton, 1980, 958.

248. D.W. Margerum and J.D. Carr, J. Amer. Chem. Soc., 1966, 88, 1639; 1645.

249. D.W. Margerum and R.K. Steinhaus, Anal. Chem., 1965, 37, 222.

250. R.H. Stehl, D.W. Margerum and J.L. Latterell, Anal. Chem., 1967, 39, 1346.

251. E.N. Rizkalla, S.S. Anis and M.N. Ramsis, J. Coord. Chem., 1987, 15, 307.

252. M.J. Hynes and P.F. Brannick, J. Chem. Soc. Dalton, 1977, 2281.

CHAPTER - II

KINETICS AND MECHANISM OF THE REACTIONS OF BIS 4-(2-PYRIDYLATO)RESORCINOL COMPLEXES OF IRON(II) AND IRON(III) WITH CYANIDE IONS

ABSTRACT

Cyanide ions react with $[\text{Fe}(\text{Par})_2]^{n-4}$ complexes (where Par represents 4-(2-pyridylazo)resorcinol) to form 1:1:3 mixed cyano-complexes. The reactions have been studied spectrophotometrically at 720 nm (λ_{max} of $[\text{Fe}(\text{Par})_2]^{n-4}$). The reaction conditions for Fe(II) system are: pH = 11.5 \pm 0.02, temperature = 25 \pm 0.1°C and I = 0.1 M (NaClO₄) while for Fe(III) system the pH is 10.0 \pm 0.02. The order with respect to cyanide varies from one to two at high and low cyanide concentrations respectively. The reverse reaction does not occur at a measurable extent even in presence of large excess of Par. These observations suggest that $[\text{FeR}_2]^{n-4}$ (R = Par) forms a mixed complex $[\text{FeR}(\text{CN})_3]^{n-5}$ in presence of excess cyanide ions. A three step mechanism consistent with these results is proposed in which the second step is rate determining one. The

activation parameters for the reaction have been calculated and used to support the proposed mechanism. The effect of ionic strength lends further support to the same. The pH dependence of rate has been investigated for both reactions.

III.1 INTRODUCTION

The kinetics of formation of some mixed ligand complexes of iron(II)¹ and iron(III)² have been investigated. Mixed ligand complexes of iron(II) with monodentate ligands have also been reported.³ A majority of iron(II) complexes are high spin ($t_{2g}^4 e_g^2$) but the complexes containing ligands which produce a large crystal field effect are low spin and kinetically inert. The reactions of cyanide ion with the cationic complex $Fe(L-L)_3^{2+}$, where L-L is 1,10 Phen⁴ or a substituted Phen,^{5,6} Schiff's base,⁷ bipy,⁸⁻¹² substituted bipy¹³ or terpy^{14,15} produce mixed ligand complexes of the type $Fe(L-L)_2(CN)_2$. The kinetics of complexation of other metal ions like Ni(II)¹⁶ and Cu(II)¹⁷ have been extensively studied using a variety of slow and fast reaction techniques. The substitution of multidentate ligands in their complexes of metal ions by monodentate ligands has been a subject of interest for many workers. The formation of tetracyanonickelate(II) and hexacyanoferrate(III) from the reaction of polyaminocarboxylato complexes of Ni(II)¹⁸⁻²³ and Fe(III)²⁴⁻²⁸ respectively with cyanide ion has been studied extensively. In recent years exchange reactions of polyaminocarboxylato complexes of Co(II)²⁹⁻³⁰ and Mn(II)³¹⁻³² with cyanide ion have also attracted some attention.

In the present study, kinetics and mechanism of formation of $[\text{Fe}(\text{Par})(\text{CN})_3]^{n-5}$ from the reactions of $[\text{Fe}(\text{Par})_2]^{n-4}$ and cyanide ions has been reported.³³⁻³⁴ The complete displacement of Par from this mixed complex has not been successful even in presence of sufficiently large excess of cyanide: n is charge on Fe(II)/Fe(III).

II.3 EXPERIMENTAL

Chemicals

Aqueous stock solution of Ferrous Ammonium Sulphate was prepared and acidified with concentrated H_2SO_4 (in order to prevent hydrolysis) and standardized by KMnO_4 .³⁵ $\text{Fe}(\text{ClO}_4)_3$ was prepared by dissolution of a precipitate of $\text{Fe}(\text{OH})_3$ in calculated amount of HClO_4 and standardized complexometrically using sulphosalicyclic acid as an indicator.³⁶ These solutions of Ferrous Ammonium Sulphate and Perchlorate were used for the preparation of $[\text{Fe}(\text{Par})_2]^{2-}$ and $[\text{Fe}(\text{Par})_2]^-$ respectively. The monosodium salt of Par (Reidel, Germany) was used after recrystallization from aqueous ethanol. A stock solution of sodium cyanide (M and B Ltd., England) was prepared fresh and standardized argentometrically.³⁷

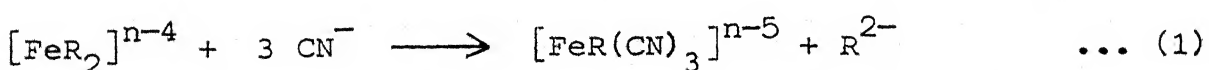
Sodium tetraborate (AR, BDH) and sodium hydroxide (AR, BDH) were used to prepare buffers of desired pH values. Sodium perchlorate (AR, E. Merck, Germany) was used to maintain ionic strength.

Apparatus

A Shimadzu double beam spectrophotometer model UV 240, with a circulatory arrangement for thermostating the cell compartment, was used for kinetic study. The temperature of the reaction mixture was maintained at $25 \pm 0.1^\circ\text{C}$ by an ultracryostat model 2 NBE (VEB Kombinat Medizin and Labortechnik Kombinatsbetrieb, GDR). All pH measurements were made on an Elico digital pH meter model LI-120 using BDH standard buffers for standardization.

III.4 KINETIC MEASUREMENTS

The formation of mixed ligand complex from the reaction of bis 4-(2-pyridylazo)resorcinolferrate(II) and with cyanide ions was followed at 720 nm (λ_{max} of $\text{Fe}^{\text{II}}(\text{Par})_2$, $\epsilon = 19,880 \text{ M}^{-1}\text{cm}^{-1}$) at $\text{pH} = 11.5 \pm 0.02$, $\text{I} = 0.1 \text{ M} (\text{NaClO}_4)$ and temperature = $25^\circ \pm 0.1^\circ\text{C}$. The formation of mixed ligand complex from the reaction of bis 4-(2-pyridylazo)resorcinolferrate(III) and cyanide ions was also followed at 720 nm (λ_{max} of $\text{Fe}^{\text{III}}(\text{Par})_2$, $\epsilon = 9850 \text{ M}^{-1}\text{cm}^{-1}$) at $\text{pH} = 10.0 \pm 0.02$, $\text{I} = 0.1 \text{ M} \text{NaClO}_4$ and temperature = $25 \pm 0.1^\circ\text{C}$. No other species absorb at 720 nm to any appreciable extent. A corresponding increase in absorbances at 414 nm (λ_{max} of Par, $\epsilon = 3 \times 10^4 \text{ M}^{-1}\text{cm}^{-1}$) in both reactions is due to liberation of one molecule of Par complexed to iron in $[\text{FeR}_2]^{n-4}$ complex according to reaction (1)



where R is 4-(2-pyridylazo)resorcinol.

All reactions were run in presence of an adequately large excess of cyanide. The pseudo-first-order rate constants were calculated from the plots of $\log C$ versus t over at least 80% of the reaction. C is the concentration of $[\text{FeR}_2]^{n-4}$ at any time t and n is the charge on the metal ion under consideration.

The reverse reaction does not occur to a measurable extent even in presence of thousand fold excess of Par. The stoichiometry of the $[\text{FeR}(\text{CN})_3]^{n-5}$ complex was established by the mole ratio method.

II.5 RESULTS

II.5.1 Effect of concentration of reactants on the rate

The rate of decay of $[\text{FeR}_2]^{n-4}$ is first order in $[\text{FeR}_2]_T$, but has a variable order with respect to cyanide ion concentration. The observed pseudo-first-order rate constants at various cyanide concentration levels (always in excess) are compiled in Table II.1. Values of $\log k_{\text{obsd}}$ are plotted against $\log [\text{CN}^-]_T$ in Fig. II.1. The slope of above plots is found to change from two to one as the cyanide concentration is increased. A rate law for both the reactions is given as

$$\begin{aligned} \text{Rate} &= d[\text{Fe(Par)}(\text{CN})_3^{n-5}]/dt = k_f [\text{Fe(Par)}_2^{n-4}] [\text{CN}^-]^x \\ &= k_{\text{obsd}} [\text{Fe(Par)}_2^{n-4}] \quad \dots (2) \end{aligned}$$

where $k_{\text{obsd}} = k_f [\text{CN}^-]^x$, x being one or two.

TABLE II.1. Kinetics of formation of $[\text{FeR}(\text{CN})_3]^{n-5}$ from bis 4-(2-pyridylazo)resorcinolferrate(II) complexes in presence of excess cyanide. (A) $[\text{Fe}^{2+}] = 5.0 \times 10^{-5} \text{ M}$, $[\text{Par}] = 1.0 \times 10^{-4} \text{ M}$, $\text{pH} = 11.5 \pm 0.02$, $I = 0.1 \text{ M} (\text{NaClO}_4)$, temp. = $25 \pm 0.1^\circ\text{C}$.

$[\text{CN}^-]_T, \text{M}$	$k_{\text{obsd}}, \text{s}^{-1}$	$k_f^* = k_{\text{obsd}}/[\text{CN}^-]^x$
1	2	3
1.45×10^{-1}	8.6×10^{-3}	5.9×10^{-2}
6.0×10^{-2}	3.6×10^{-3}	6.0×10^{-2}
4.0×10^{-2}	2.65×10^{-3}	6.6×10^{-2}
2.0×10^{-2}	1.1×10^{-3}	5.6×10^{-2}
1.26×10^{-6}	7.6×10^{-4}	6.0×10^{-2}
8.30×10^{-3}	5.25×10^{-4}	6.3×10^{-2}
$\text{Av. } (6.1 \pm 0.3) \times 10^{-2}, \text{ M}^{-1} \text{s}^{-1}$		
3.98×10^{-3}	1.9×10^{-4}	12.0
2.0×10^{-3}	4.5×10^{-5}	11.3
1.0×10^{-3}	1.3×10^{-5}	13.1
5.3×10^{-4}	5.5×10^{-6}	13.8
$\text{Av. } (12.6 \pm 0.1), \text{ M}^{-2} \text{s}^{-1}$		

...contd.

TABLE II.1 (contd.)

(B) $[\text{Fe}^{3+}] = (5.0 - 6.0) \times 10^{-5} \text{M}$, $[\text{Par}] = (1.0 - 1.2) \times 10^{-4} \text{M}$,
 $\text{pH} = 10.0 \pm 0.02$, $I = 0.1 \text{M}$, temp. = $25 \pm 0.1^\circ \text{C}$.

1	2	3
9.0×10^{-2}	8.7×10^{-3}	9.7×10^{-2}
6.9×10^{-2}	7.2×10^{-3}	10.4×10^{-2}
5.85×10^{-2}	6.6×10^{-3}	11.3×10^{-2}
4.0×10^{-2}	4.4×10^{-3}	11.0×10^{-2}
3.0×10^{-2}	3.1×10^{-3}	10.3×10^{-2}
2.1×10^{-2}	2.4×10^{-3}	11.4×10^{-2}
1.45×10^{-2}	1.6×10^{-3}	11.0×10^{-2}
<hr/>		
$\text{Av } (10.8 \pm 0.6) \times 10^{-2}, \text{M}^{-1} \text{s}^{-1}$		
1.2×10^{-2}	1.2×10^{-3}	8.4
8.3×10^{-3}	4.8×10^{-4}	6.95
5.0×10^{-3}	1.9×10^{-4}	7.6
2.5×10^{-3}	4.8×10^{-5}	7.66
<hr/>		
$\text{Av } (7.7 \pm 0.5), \text{M}^{-2} \text{s}^{-1}$		
<hr/>		

* $x = 1$ or 2 .

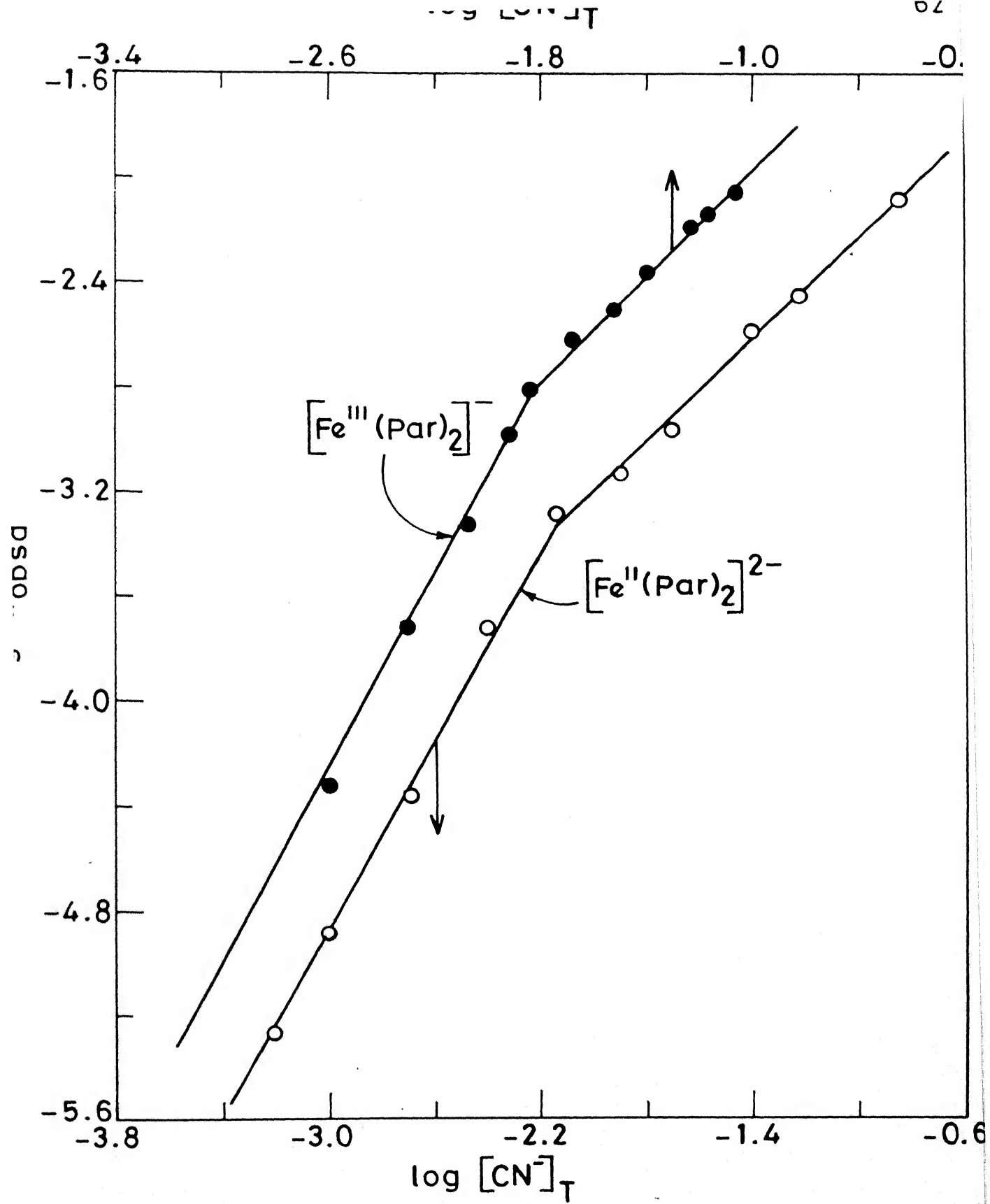


Fig.II.1 The cyanide dependence of observed pseudo-first order rate constants for $[\text{FeR}_2]^{n-4} - \text{CN}^-$ (The conditions as given in Table II.1)

III.5.2 Effect of ionic strength on the reaction rate

The rate of reaction was found to increase with increase of ionic strength of the medium, varied by adding calculated amounts of sodium perchlorate before mixing the reactants. The pH, temperature and concentrations of reactants were kept constant during these measurements. The observed rate constants obeyed the Bronsted-Bjerrum Equation³⁸ (Equation 3).

$$\log k_f = \log k_o + 1.018 z_A z_B \frac{\sqrt{I}}{(1 + \sqrt{I})} \quad \dots (3)$$

where k_f is the specific rate constant, k_o is the specific rate constant at zero ionic strength, and z_A and z_B are the charges on the two reactant species. The plots of $\log k_f$ versus $\sqrt{I}/(1 + \sqrt{I})$ is given in Fig. II.2. The values of k_{obsd} and k_f at different ionic strengths are listed in Table II.2. The values of $z_A z_B$ calculated from the slopes of these plots agree very well with the values expected according to the rate determining step envisaged in the kinetic scheme (vide supra).

III.5.3 Effect of Temperature on Rate

Activation parameters for these reactions have been calculated from the Arrhenius plots. The reactions were carried out at different temperatures in 20°C - 35°C range. Arrhenius equation, may be written in the logarithmic form (Equation 4)

$$\ln k_f = - \frac{E_a}{RT} + \ln A \quad \dots (4)$$

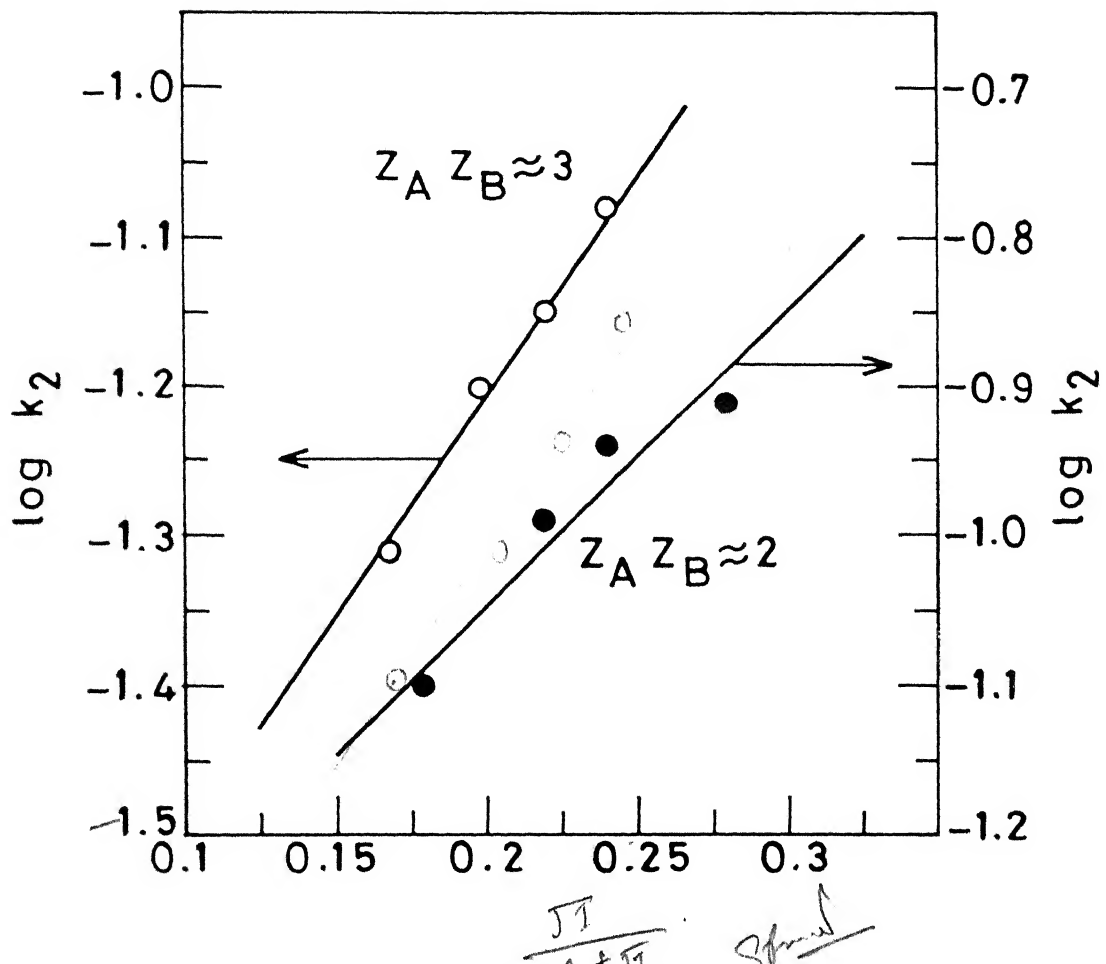


Fig.II.2 Dependence of rate constants on ionic strength for $[\text{FeR}_2]^{n-4} + \text{CN}^-$ reaction (The conditions are given in Table II.2).

TABLE II.2. Effect of ionic strength on the formation rate of
 $[\text{FeR}(\text{CN})_3]^{n-5}$.

$I, \text{ M (NaClO}_4\text{)}$	$k_{\text{obsd}}, \text{s}^{-1}$	$k_f, \text{ M}^{-1} \text{s}^{-1}$
(A) $[\text{Fe}^{2+}] = 5.0 \times 10^{-5} \text{ M}$, $[\text{Par}] = 1.0 \times 10^{-4} \text{ M}$, $[\text{CN}^-] = 4.0 \times 10^{-2} \text{ M}$, $\text{pH} = 11.5 \pm 0.02$, temp. = $25 \pm 0.1^\circ\text{C}$.		
0.04	1.96×10^{-3}	4.9×10^{-2}
0.06	2.52×10^{-3}	6.3×10^{-2}
0.08	2.83×10^{-3}	7.1×10^{-2}
0.10	3.33×10^{-3}	8.3×10^{-2}
(B) $[\text{Fe}^{3+}] = 5.0 \times 10^{-5} \text{ M}$, $[\text{Par}] = 1.0 \times 10^{-4} \text{ M}$, $[\text{CN}^-] = 4.0 \times 10^{-2} \text{ M}$, $\text{pH} = 10.0 \pm 0.02$, temp. = $25 \pm 0.1^\circ\text{C}$.		
0.05	3.09×10^{-3}	7.9×10^{-2}
0.08	4.0×10^{-3}	1.0×10^{-1}
0.10	4.4×10^{-3}	1.1×10^{-1}
0.15	4.84×10^{-3}	1.2×10^{-1}

The activation energy can be calculated by plotting $\ln k_f$ versus $1/T$ and other activation parameters like ΔH°_f , ΔS°_f and p_z can be calculated by the Eyring equation (6) making use of relation $\Delta H^\circ_f = E_a - RT$.

$$k_f = \frac{k_B \cdot T}{h} e^{-\Delta G^\circ_f/RT} = \frac{k_B \cdot T}{h} e^{\Delta S^\circ_f/R} e^{-\Delta H^\circ_f/RT} \dots (5)$$

where all terms have their usual meanings. The above equation can be simplified to equation (6).

$$k_f = p_z \cdot e^{-\Delta H^\circ_f/RT} \dots (6)$$

where p_z is the probability factor defined in equation (7)

$$p_z = \frac{k_B \cdot T}{h} e^{\Delta S^\circ_f/R} \dots (7)$$

The values of activation parameters are given in Table II.3. These values of activation parameters are consistent with our proposed mechanism (vide supra).

II.5.4 Dependence of Reaction rate on pH

In case of Fe(II) system the rate was varied from 8.5 to 11.5 in presence of excess of cyanide and it was observed that the rate increases with an increase of pH upto 11.5 (Table II.4), while in case of Fe(III) system the rate was studied in pH range 7.5-10.5 and it was found that rate increases upto pH 9.5 and then levels

TABLE II.3. Activation parameters

(A) $[\text{Fe}^{2+}] = 5.0 \times 10^{-5} \text{M}$, $[\text{Par}] = 1.0 \times 10^{-4} \text{M}$, $[\text{CN}^-] = 4.0 \times 10^{-2} \text{M}$,
 $\text{pH} = 11.5 \pm 0.02$, $I = 0.1 \text{M}$ (NaClO_4).

$$E_a = 27.4 \pm 0.3 \text{ kJ mol}^{-1}$$

$$\Delta H^{\circ\neq} = 25.0 \pm 0.3 \text{ kJ mol}^{-1}$$

$$\Delta S^{\circ\neq} = -185 \pm 1 \text{ JK}^{-1} \text{ mol}^{-1}$$

$$p_z = 1.2 \times 10^3 \text{ cm}^{-1}$$

(B) $[\text{Fe}^{3+}] = 5.0 \times 10^{-5} \text{M}$, $[\text{Par}] = 1.0 \times 10^{-4} \text{M}$, $[\text{CN}^-] = 4.0 \times 10^{-2} \text{M}$,
 $\text{pH} = 10.5 \pm 0.02$, $I = 0.1 \text{M}$ (NaClO_4).

$$E_a = 48.8 \pm 2.5 \text{ kJ mol}^{-1}$$

$$\Delta H^{\circ\neq} = 46.3 \pm 2.5 \text{ kJ mol}^{-1}$$

$$\Delta S^{\circ\neq} = -110.6 \pm 8.5 \text{ JK}^{-1} \text{ mol}^{-1}$$

$$p_z = 1.1 \times 10^7 \text{ cm}^{-1}$$

TABLE II.4. Effect of pH on the formation of $[\text{FeR}(\text{CN})_3]^{n-5}$

pH	$k_{\text{obsd}}, \text{s}^{-1}$	$k_f, \text{M}^{-1} \text{s}^{-1}$
(A) $[\text{Fe}^{2+}] = 5.0 \times 10^{-5} \text{M}$, $[\text{Par}] = 1.0 \times 10^{-4} \text{M}$, $[\text{CN}^-] = 4.0 \times 10^{-2} \text{M}$, temp. = $25 \pm 0.1^\circ \text{C}$, $I = 0.1 \text{M}$ (NaClO_4).		
8.5	1.3×10^{-5}	3.2×10^{-4}
9.5	5.5×10^{-5}	1.4×10^{-3}
10.17	2.8×10^{-4}	7.0×10^{-3}
10.75	1.3×10^{-3}	3.2×10^{-2}
11.5	3.3×10^{-3}	8.3×10^{-2}
(B) $[\text{Fe}^{3+}] = 5.0 \times 10^{-5} \text{M}$, $[\text{Par}] = 1.0 \times 10^{-4} \text{M}$, $[\text{CN}^-] = 5.6 \times 10^{-2} \text{M}$, temp. = $25 \pm 0.1^\circ \text{C}$, $I = 0.1 \text{M}$ (NaClO_4).		
7.0	4.5×10^{-5}	8.7×10^{-4}
7.9	1.8×10^{-4}	3.5×10^{-3}
8.5	5.0×10^{-4}	9.6×10^{-3}
9.35	1.4×10^{-3}	2.7×10^{-2}
10.0	5.6×10^{-3}	1.0×10^{-1}
10.5	5.4×10^{-3}	1.04×10^{-1}

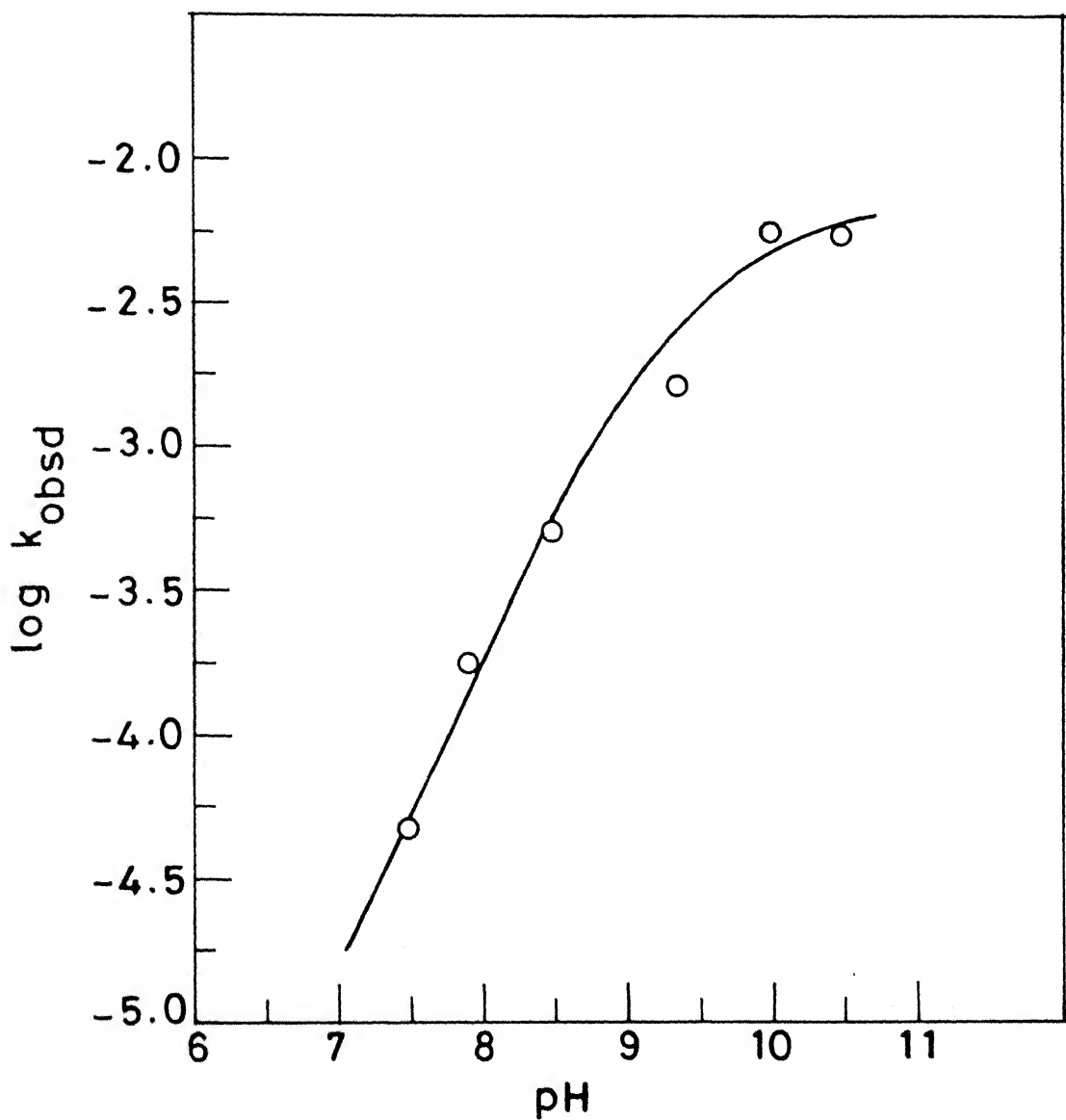
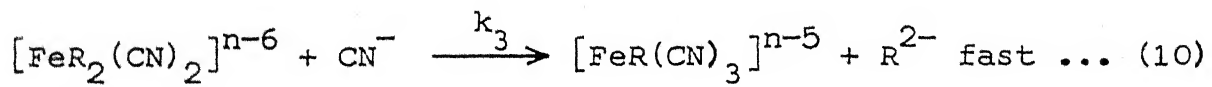
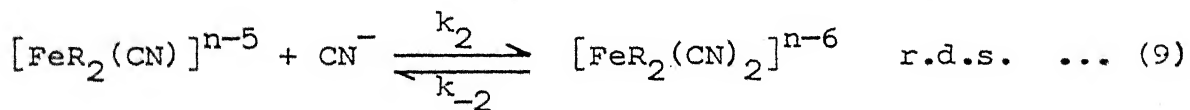


Fig.II.3 Effect of pH on the reaction of $[\text{FeR}_2]^-$ with cyanide.

off (Fig. II.3). In both cases the rate has been studied in a concentration range where order with respect to cyanide is one. The increase in the rate constants in the above pH ranges are due to different reactivities of the protonated and unprotonated forms of $[\text{Fe}(\text{Par})_2]^{n-4}$ and also HCN and CN^- ($\text{pK}_{\text{HCN}} = 9.18$).³⁹ Attempts at resolving the rate constants were not successful in absence of information on the protonation constant(s) of $[\text{Fe}(\text{Par})_2]^{n-4}$ complexes.

II.6 DISCUSSION

These experimental observations on the rates of formation of the mixed complex $[\text{FeR}(\text{CN})_3]^{n-5}$ from bis 4-(2-pyridylazo)-resorcinol ferrate(II) and ferrate(III) complexes and cyanide ions lead one to propose a mechanism as given in equation (8)-(10).



There is no evidence for the existence of FeR complex even when metal ligand ratio is 1:1 or less, also there is no indication that the intermediates in reactions (8) and (9) are produced in any appreciable concentration.

This mechanism assumes that two cyanides react in steps with $[\text{FeR}_2]^{n-4}$ (Equation 8 and 9) to produce $[\text{FeR}_2(\text{CN})_2]^{n-6}$ upto the rate determining step, which gives rise to the observed first and second order dependences at high and low cyanide concentrations respectively. The positive salt effect and values of $Z_A Z_B$ calculated from the slopes of the ionic strength plots (Fig. II.2) show that the assumption made about the rate determining step (Equation 9) is reasonable. The low activation energy and highly negative entropy of activation (Table II.3) for the reaction is also in accord with the rate determining step where bond formation is taking place. The mechanism is an associative one.

The application of steady state treatment on the intermediate species produced in the rate determining step gives,

$$\begin{aligned} \frac{d[\text{FeR}_2(\text{CN})^{n-5}]}{dt} &= k_1 [\text{FeR}_2^{n-4}] [\text{CN}^-] - k_{-1} [\text{FeR}_2(\text{CN})^{n-5}] \\ &\quad - k_2 [\text{FeR}_2(\text{CN})^{n-5}] [\text{CN}^-] + k_{-2} [\text{FeR}_2(\text{CN})_2^{n-6}] = 0 \quad \dots (11) \end{aligned}$$

$$\text{Thus, } [\text{FeR}_2(\text{CN})^{n-5}] = \frac{k_1 [\text{FeR}_2^{n-4}] [\text{CN}^-] + k_{-2} [\text{FeR}_2(\text{CN})_2^{n-6}]}{k_{-1} + k_2 [\text{CN}^-]} \quad \dots (12)$$

Substituting for $[\text{FeR}_2(\text{CN})^{n-5}]$ in the rate expression (Equation 9) and ignoring the last term in numerator, we get

$$\text{Rate} = k_2 [\text{FeR}_2(\text{CN})^{n-5}] [\text{CN}^-] \quad \dots (13)$$

$$= \frac{k_2 k_1 [\text{FeR}_2^{n-4}] [\text{CN}^-]^2}{k_{-1} + k_2 [\text{CN}^-]} \quad \dots (14)$$

This expression shows that when $[CN^-]$ is small, the second term in the denominator can be neglected in comparison to unity and a second order dependence in cyanide would be observed.

$$\text{Rate} = k_1 k_2 [FeR_2^{n-4}] [CN^-]^2, \quad k_1 = k_1/k_{-1}$$

On the other hand when $[CN^-]$ is high, we may neglect unity in comparison to the $k_2 [CN^-]$ and first order dependence in cyanide would be observed.

$$\text{Rate} = k_1 [FeR_2^{n-4}] [CN^-]$$

These conclusions agree with our experimental observation that a variable order dependence in cyanide changing from two to one is actually found (Equation 2, Table II.1).

It has been stated in the reaction on the effect of pH that it has not been possible to resolve the rates arising out of different reactivities of protonated and unprotonated forms of reactants. It has been shown that in the reaction of aminocarboxylato and polyamino- complexes of $Ni(II)^{40}$ and $Fe(III)^{28}$ with cyanide, the cyanide ion is a better nucleophile than HCN ($pK_a = 9.18$). The rate of substitution by cyanide in these reactions generally increases with increase of pH between pH = 7.5-9.5 and then levels off. The same may hold good in the present reaction system also but the levelling off occurs at higher pH in case of $Fe(II)$. This could be attributed to the different reactivities of protonated and unprotonated forms of $[FeR_2]^{2-}$ complex itself.

However, a mathematical resolution of rates has not been possible because protonation constants of $[\text{Fe}^{\text{II}}(\text{Par})_2]^{2-}$ and $[\text{Fe}^{\text{III}}(\text{Par})_2]^-$ complexes are not known. The linear portion of the plot of $\log k_{\text{obsd}}$ versus $[\text{H}^+]$ has a slope equal to unity (Fig. II.3). It is concluded that one HCN molecule is involved in addition to one cyanide upto the rate determining step below pH 9.2.

The spectral changes occurring during a typical kinetic run have been recorded in Fig. II.4 and II.5. It was observed that the spectra of the iron(II) and iron(III) complexes of Par differ from each other in matter of detail. The absorption spectra display two maxima at 496 nm and 720 nm, the latter being better defined in the iron(II)-Par complex. During the course of reaction, there is continuous decrease in the peak heights at 720 nm and 496 nm and a new peak formation at 490 nm due to formation of $[\text{FeR}(\text{CN})_3]^{n-5}$. There is continuous increase in the peak height at 490 nm in $\text{Fe}^{\text{II}}(\text{Par})_2-\text{CN}^-$ reaction, while in $\text{Fe}^{\text{III}}(\text{Par})_2-\text{CN}^-$ reaction this peak height does not increase. This behaviour is probably due to the different reactivities of Fe(II) and Fe(III) complexes. There is also a continuous increase of absorbance at 414 nm (λ_{max} of Par) due to gradual release of Par during the course of reaction. The absorbance change at this peak shows that the complete displacement of Par from this mixed complex does not occur. The appearance of a new absorption band at 460 nm is also due to formation of the mixed complex in the later part of reaction. The appearance of isosbestic points at 630, 580, 495

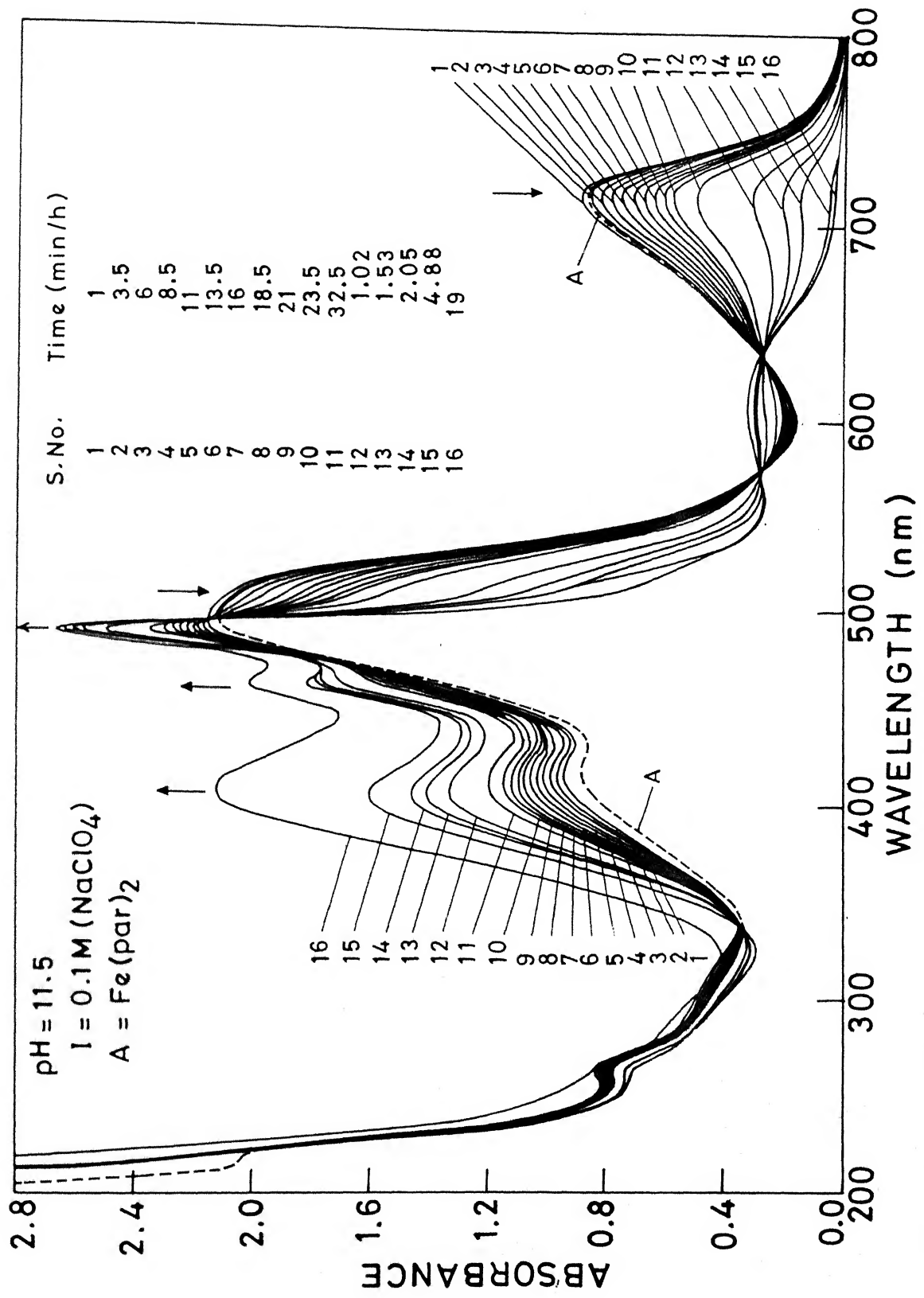


Fig.II.4 Repetitive scan of the reaction mixture during a typical kinetic run at temp. = 35°C , $[\text{Fe}^{2+}] = 5.0 \times 10^{-5} \text{ M}$, $[\text{par}] = 1.0 \times 10^{-4} \text{ M}$, $[\text{CN}^-] = 1.0 \times 10^{-2} \text{ M}$.

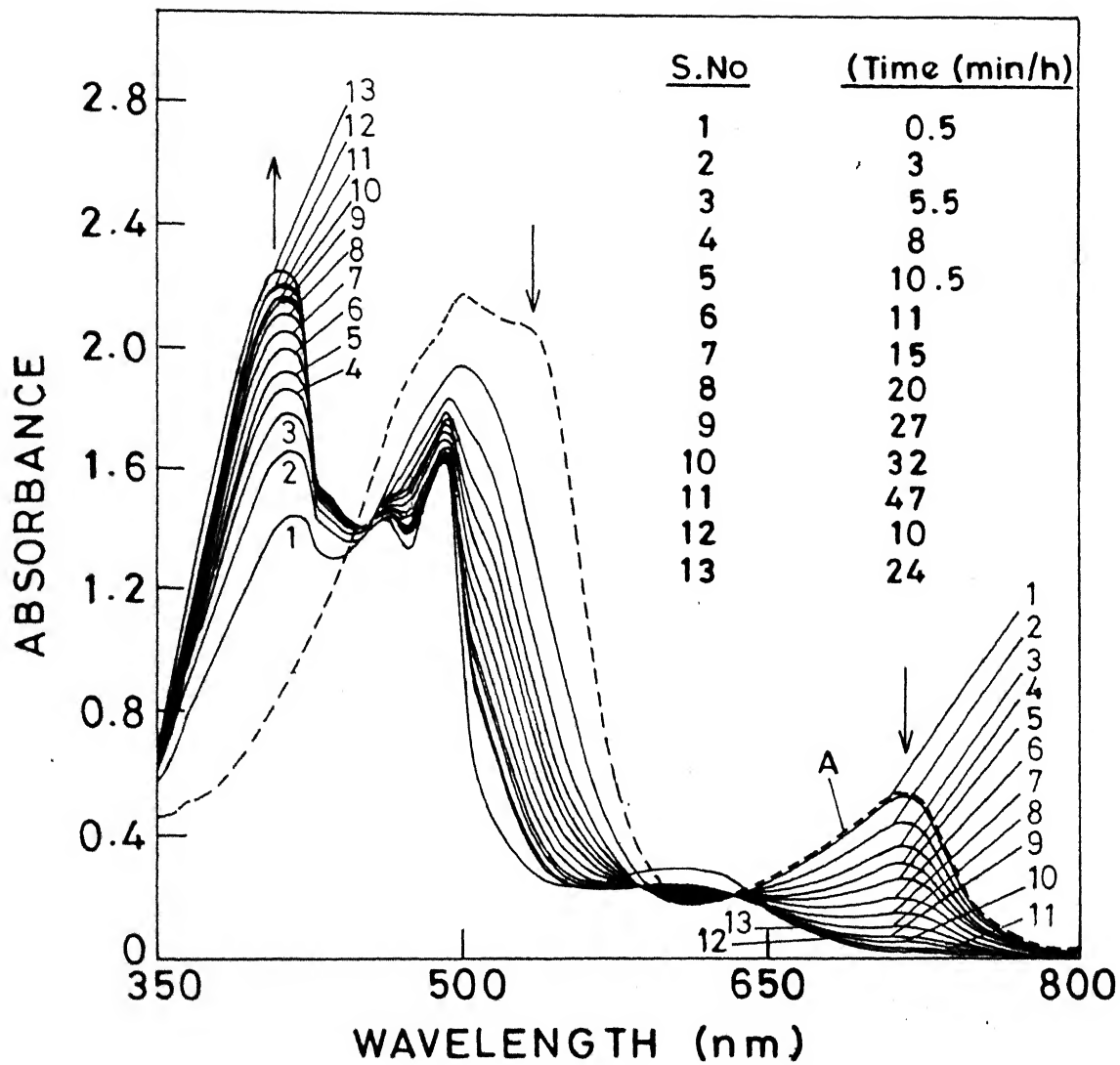


Fig.II.5 Repetitive scan of the reaction mixture during a typical kinetic run at temp. = 16°C $[\text{Fe}^{3+}] = 5.7 \times 10^{-5} \text{ M}$, $[\text{Par}] = 1.14 \times 10^{-4} \text{ M}$, $[\text{CN}^-] = 3.9 \times 10^{-2} \text{ M}$, $\text{pH} = 10$, $I = 0.1 \text{ M} (\text{NaClO}_4)$.
 $A = \text{Fe}(\text{Par})_2$.

and 340 nm suggest that the species $[\text{FeR}_2]^{n-4}$ and $[\text{FeR}(\text{CN})_3]^{n-5}$ coexist during the course of reaction. The spectral scan in case of Fe(III) system has been not be recorded below 350 nm (Fig. II.5).

In the case of $\text{Ni}(\text{Par})_2$ -cyanide exchange,⁴¹ a cyanide independent path was observed at low cyanide concentrations, which indicates a slow dissociation of the bis complex in addition to the cyanide assisted rapid dissociation of $\text{Ni}(\text{Par})_2$ and formation of mixed ligand complexes of the type $[\text{Ni}(\text{Par})(\text{CN})_x]$ and finally $[\text{Ni}(\text{CN})_4]^{2-}$. However, this type of behaviour was not observed in the case of FeR_2 complex even over a wide range of cyanide concentration (Fig. II.1). If this were so, there should have been a sudden increase in the peak height at 414 nm (λ_{max} of Par) due to dissociation of the bis complex into Par and the mixed complex immediately after mixing. This would be followed by further reaction with cyanide to give the end products.

In brief, the reactions of $[\text{Fe}(\text{Par})_2]^{n-4}$ with cyanide ions take place in three steps, the addition of second cyanide being the rate determining one (Equation 9). The stoichiometry of the ternary complexes is found to be 1:1:3 $[\text{Fe}(\text{Par})(\text{CN})_3]^{n-5}$. The complete displacement of Par from the iron centre does not take place even in presence of large excess of cyanide. The reverse reaction does not appear to take place to any appreciable extent.

REFERENCES

1. J. Blandamer, J. Burgess and P. Wellings, *Trans. Met. Chem.*, 1981, 6, 129.
2. M.A. El. Dersouky, M.S. El.Ezaly and M.M. Shuaib, *Inorg. Chim. Acta*, 1980, 46, 7.
3. J. Burgess and G.M. Burton, *Rev. Latinomer. Quim.*, 1980, 11, 107.
4. D.W. Margerum and L.P. Morgenthaler, *J. Amer. Chem. Soc.*, 1962, 84, 706.
5. J. Burgess, *Inorg. Chim. Acta*, 1971, 5, 133.
6. J. Burgess and F.M. Mekhail, *Trans. Met. Chem.*, 1978, 3, 162.
7. J. Burgess, G.E. Ellis, D.J. Evans, A. Porter and R.D. Wyvill, *J. Chem. Soc. A*, 1971, 44.
8. J. Burgess, *J. Chem. Soc. Dalton*, 1972, 1061.
9. G. Nord, *Acta Chim Scand.*, 1973, 27, 743.
10. M.J. Blandamer, J. Burgess and J.G. Chambers, *J. Chem. Soc. Dalton*, 1976, 606.
11. M.J. Blandamer, J. Burgess, J.G. Chambers, R.I. Hains and H.E. Marshall, *J. Chem. Soc. Dalton*, 1977, 165.
12. D.D. Dollberg and R.D. Archer, *Inorg. Chem.*, 1975, 14, 1888.
13. J. Burgess and R.H. Prince, *J. Chem. Soc.*, 1965, 6061.
14. J. Burgess and M.V. Twigg, *J. Chem. Soc. Dalton.*, 1974, 2032.
15. M.V. Twigg, *Inorg. Chem.*, 1974, 10, 17.
16. H.C. Bajaj, *Ph.D. Thesis, I.I.T. Kanpur, India*, 1982.
17. Y. Fukuda and K. Sone, *Bull. Chem. Soc. Jpn.*, 1972, 45, 465.

18. L.C. Coombs, D.W. Margerum and P.C. Nigam, Inorg. Chem., 1970, 9, 2081.
19. L.C. Coombs and D.W. Margerum, Inorg. Chem., 1970, 9, 1711.
20. D.W. Margerum, T.J. Bydalek and J.J. Bishop, J. Amer. Chem. Soc., 1961, 83, 1791.
21. D.W. Margerum and L.I. Simandi, Proc. of 9th Int. Conf. on Coordination Chemistry, W. Schneider Ed., Verlag Helv. Chim. Acta, Basel, Switzerland (1966), p. 371.
22. G.K. Pagenkopf, J. Coord. Chem., 1972, 2, 129.
23. V. Stara and M. Kopanica, Coll. Czech. Chem. Comm., 1972, 37, 2882.
24. H.C. Bajaj and P.C. Nigam, Trans. Met. Chem., 1982, 7, 190.
25. H.C. Bajaj and P.C. Nigam, Trans. Met. Chem., 1983, 8, 109.
26. R.M. Naik and P.C. Nigam, Trans. Met. Chem., 1985, 10, 227.
27. R.M. Naik and P.C. Nigam, Inorg. Chim. Acta, 1986, 114, 55.
28. P. Mishra, R.M. Naik and P.C. Nigam, Inorg. Chim. Acta, 1986, 127, 71.
29. S. Nakamura, Ph.D. Thesis, Univ. of Chicago, 1964.
30. J.P. Jones and D.W. Margerum, Inorg. Chem., 1969, 8, 1486.
31. R.E. Hamm and J.P. Tompleton, Inorg. Chem., 1973, 12, 755.
32. R.M. Naik, P. Mishra and P.C. Nigam, Trans. Met. Chem., 1987 (In press).
33. (Miss) Nishi Gupta and P.C. Nigam, Trans. Met. Chem., 1988 (in press).
34. (Miss) Nishi Gupta and P.C. Nigam, Trans. Met. Chem., 1988 (In press).
35. A.I. Vogel, Text book of Quantitative Inorganic Analysis, 3rd Ed., Longman Green, London, 1962, p. 286.

36. G. Schwarzenbach, Complexometric Titrations, Int. Sci. Pub., N.Y., 1955, p. 77.
37. A.I. Vogel, Text book of Quantitative Analysis, 3rd Ed., Longman Green, London, 1962, p. 270.
38. F. Basolo and R.G. Pearson, Mechanism of Inorganic Reactions, 2nd Ed., John Wiley and Sons, New York, London and Sydney, 1967, p. 34.
39. L.G. Sillen and A.E. Martell, "Stability Constants of Metal Ion Complexes", Suppl. No. 1, The Chem. Soc. London, 1971, p. 768.
40. H.C. Bajaj, M. Phull and P.C. Nigam, J. Coord. Chem., 1983, 13, 41.

CHAPTER - III

MULTIDENTATE LIGAND EXCHANGE KINETICS: SUBSTITUTION REACTIONS OF AMINOCARBOXYLATOIRON(III) COMPLEXES WITH 4-(2-PYRIDYLATO)RESORCINOL

ABSTRACT

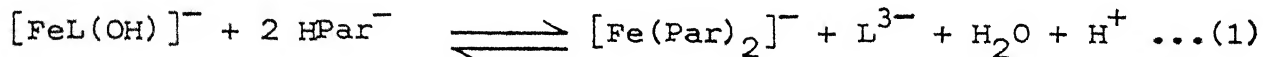
The kinetics and mechanism of ligand substitution reactions of nitrilotriacetatoiron(III), $[\text{Fe}(\text{NTA})]$, and N-(2-hydroxyethyl)-ethylenediaminetriacetatoiron(III), $[\text{Fe}(\text{HEDTA})]$, complexes with 4-(2-pyridylazo)resorcinol (abbreviated Par) have been investigated at $\text{pH} = 9.0 \pm 0.02$, $I = 0.1\text{M}$ (NaClO_4) and $\text{temperature} = 25 \pm 0.1^\circ\text{C}$ and $30 \pm 0.1^\circ\text{C}$ respectively. The reaction has been studied spectrophotometrically at 496 nm the λ_{max} of $[\text{Fe}(\text{Par})_2]^-$ which is the final product of both reactions. The values of second order rate constants for NTA and HEDTA exchange were studied in the pH range 6-9.5 and 7-10.85 respectively. The rate of reaction of $[\text{Fe}(\text{NTA})]$ with Par^{2-} first increases with pH and then levels off. However, in the case of $[\text{Fe}(\text{HEDTA})]$ reaction, the rate increases monotonically with increase of pH between 9 to 11 but levels down at $\text{pH} < 9$.

The reverse reactions, that is the reactions between $[\text{Fe}(\text{Par})_2]^-$ and L^{3-} ($\text{L} = \text{HEDTA}$ or NTA), have been studied in the presence of large excess of L^{3-} . The reactions are pseudo-first-order and zero order at high and low ligand (L^{3-}) concentrations respectively and inverse first order in Par concentration. Activation parameters for the forward and reverse reactions have been calculated and support the proposed mechanism.

III.1 INTRODUCTION

Ligand substitution reactions of metal complexes containing multidentate ligands have been studied by many authors.¹⁻¹⁰ A ligand substitution reaction often proceeds through the formation of mixed ligand complex intermediate(s) in which the central metal ion is simultaneously bonded to both leaving and entering ligands. In general, the rate determining step of the reaction is the cleavage of a bond between metal ion and the leaving ligand. $[\text{Ni}(\text{EDDA})]$ and $[\text{Ni}(\text{NTA})]^-$ react with Par to give mixed-ligand complex intermediates viz. $[\text{Ni}(\text{EDDA})\text{Par}]^{2-}$ and $[\text{Ni}(\text{NTA})\text{Par}]^{3-}$ respectively⁹ ($\text{EDDA}^{2-} = \text{Oxylenediamine N,N'-diacetate ion}$, $\text{NTA}^{3-} = \text{Nitrilotriacetate ion}$) followed by further reaction to give $[\text{Ni}(\text{Par})_2]^{2-}$. Tanaka et al.¹¹ have studied the substitution reactions of $[\text{Cu}(\text{EGTA})]^{2-}$ and $[\text{Cu}(\text{NTA})]^-$ with Par ($\text{EGTA}^{4-} = (\text{Ethylene glycol})\text{bis}(2\text{-aminoethyl ether})-\text{N,N,N',N'-tetraacetate}$). Similar results are noticed also in these reactions.

It seemed worthwhile to extend this study to the substitution reactions involving other metal ions e.g. the ligand substitution reactions of $[\text{Fe}^{\text{III}}(\text{NTA})]$ and $[\text{Fe}^{\text{III}}(\text{HEDTA})]$ complexes with Par in alkaline medium. In the specified conditions the reactions represented by equation (1) were undertaken in order to obtain a better understanding and insight into multidentate exchange processes. The kinetics of reverse reactions have also been investigated to provide support for the proposed mechanism.



III.2 EXPERIMENTAL

reagents

Purified and recrystallized varieties of NTA (Hopkin and Williams, England), HEDTA (Sigma, U.S.A.). Par (Reidel, Germany), ferric nitrate (Thomas and Baker, U.K.) and sodium perchlorate (E. Merck, F.R.G.) were used in this study.

A stock solution of $\text{Fe}(\text{ClO}_4)_3$ was prepared by dissolution of a precipitate of $\text{Fe}(\text{OH})_3$ in calculated amount of HClO_4 and standardized complexometrically using sulfosalicylic acid as an indicator.¹²

Equipment

A Shimadzu double beam spectrophotometer model UV-240, with circulatory arrangement for thermostating the cell compartment

was used for all kinetic studies and for obtaining repetitive scans of the reaction mixtures. The temperature of the reaction mixtures was maintained by an ultracryostat model 2 NBE (VEB Kombinat Medizin and Labortechnik Kombinatsbetrieb, GDR). All pH measurements were made on an Elico digital pH meter model LI-120 using BDH standard buffers for standardization.

III.3 RESULTS

III.3.1 Kinetic Measurements

The rate of formation of $[\text{Fe}(\text{Par})_2]^-$ was measured at 496 nm (λ_{max} of $[\text{Fe}(\text{Par})_2]^-$, $\epsilon = 51,800 \text{ M}^{-1}\text{cm}^{-1}$) at $\text{pH} = 9.0 \pm 0.02$ and $I = 0.1\text{M}$ (NaClO_4). A correction was applied for the absorbance of Par at 496 nm. It can be derived that

$$c_A = (A_t - \epsilon_B c_B^0) / (\epsilon_A - 2\epsilon_B) \quad \dots (2)$$

where c_A represents the concentration of $[\text{Fe}(\text{Par})_2]^-$ at $t = t$ and c_B^0 is the concentration of Par at $t = 0$, while ϵ_A and ϵ_B are the molar extinction coefficients of A and B in order. In the following text the aminocarboxylato complexes will be represented by $\text{FeL}]$ while Par will be further abbreviated as R.

The reverse reactions were also studied at 496 nm by the decay of $[\text{Fe}(\text{Par})_2]^-$. An expression with a suitable absorption correction is given as

$$C_A = (A_t - 2\epsilon_B \cdot C_A^0) / (\epsilon_A - 2\epsilon_B) \quad \dots (3)$$

where C_A^0 represents the concentration of $[\text{Fe(Par)}_2^-]$ at $t = 0$.

III.3.2 Kinetics of Forward Reaction

The forward reaction is favoured thermodynamically,

$K_{\text{FeNTA}} = 10^{16.26}$, $K_{\text{FeHEDTA}} = 10^{19.06^{13}}$ and β_2 of $[\text{Fe(Par)}_2^-] = 10^{34.2^{14}}$. In both systems the forward reaction is first order in each reactant. The observed second order rate constants for both systems are given in Table III.1.

A rate law for both reactions is given as

$$\text{Rate} = d[\text{Fe(Par)}_2^-]/dt = k[\text{FeL(OH)}^-][\text{HR}^-] \quad \dots (4)$$

$[\text{FeL(OH)}^-]$ and $[\text{HR}^-]$ are the principal reactive species of iron complexes and Par respectively at the pH of medium. Integration of equation (4) yields

$$\log \frac{C_R - 2[\text{FeR}_2^-]}{C_{\text{Fe}} - [\text{FeR}_2^-]} = \frac{C_R - 2 C_{\text{Fe}}}{2.303} kt + \log \frac{C_R}{C_{\text{Fe}}} \quad \dots (5)$$

here C_R and C_{Fe} are the initial concentration of Par and FeL.

plots of $\log C_R - 2[\text{FeR}_2^-] / (C_{\text{Fe}} - [\text{FeR}_2^-])$ versus t give straight lines according to equation (5). The second order rate constants, k , are calculated from the slopes of these straight lines (Table III.1).

TABLE III.1. Rate constants for the reactions of $[\text{Fe(NTA)}]$ and $[\text{Fe(HEDTA)}]$ with Par. Temperature = $25 \pm 0.1^\circ\text{C}$, $I = 0.1\text{M} (\text{NaClO}_4)$, $\text{pH} = 9.0 \pm 0.02$ for NTA reaction. Temperature = $30 \pm 0.1^\circ\text{C}$, $I = 0.1\text{M} (\text{NaClO}_4)$, $\text{pH} = 9.0 \pm 0.02$ for HEDTA reaction.

Fe(NTA)-Par System

$[\text{Fe(NTA)}], \text{M}$	$[\text{Par}], \text{M}$	$10^{-1} \times k, \text{M}^{-1} \text{s}^{-1}$
5.0×10^{-6}	1.21×10^{-5}	9.8
5.0×10^{-6}	1.81×10^{-5}	9.2
5.0×10^{-6}	2.54×10^{-5}	9.6
5.0×10^{-6}	3.13×10^{-5}	9.9
5.0×10^{-6}	4.17×10^{-5}	11.7
2.88×10^{-5}	1.2×10^{-5}	9.2
3.6×10^{-5}	1.2×10^{-5}	10.1
6.0×10^{-5}	1.2×10^{-5}	10.7

$$k(\text{av}) = (10.03 \pm 0.8) \times 10^{-1} \text{ M}^{-1} \text{s}^{-1}$$

Fe(HEDTA)-Par System

$[\text{Fe(HEDTA)}], \text{M}$	$[\text{Par}], \text{M}$	$10^1 \times k, \text{M}^{-1} \text{s}^{-1}$
1.0×10^{-5}	2.43×10^{-5}	2.9
1.0×10^{-5}	4.14×10^{-5}	2.6
1.0×10^{-5}	6.87×10^{-5}	2.6
1.0×10^{-5}	8.24×10^{-5}	2.6
1.0×10^{-5}	1.0×10^{-4}	2.5
5.76×10^{-5}	2.4×10^{-5}	2.9
8.4×10^{-5}	2.4×10^{-5}	2.7
1.2×10^{-4}	2.4×10^{-5}	2.8
1.92×10^{-4}	2.4×10^{-5}	2.6

$$k(\text{av}) = (2.7 \pm 0.14) \times 10^{-1} \text{ M}^{-1} \text{s}^{-1}$$

III.3.3 Kinetics of Reverse Reaction

The reverse of reaction (1) is thermodynamically not favoured and it becomes possible to force the reverse reactions only by adding a relatively large excess of NTA or HEDTA compared to $[\text{Fe(Par)}_2]^-$. The disappearance of $[\text{Fe(Par)}_2]^-$ was used to follow the reverse rates.

It has been found that the reverse rate exhibits an inverse first order dependence in Par concentration and a first order dependence each in $[\text{Fe(Par)}_2]^-$ and the ligands NTA/HEDTA. A rate expression formulated on the basis of above findings is

$$-\frac{d[\text{Fe(Par)}_2^-]}{dt} = \frac{k_r [\text{Fe(Par)}_2^-][\text{L}^{3-}]}{[\text{HR}^-]} \quad \dots (6)$$

The integrated form of equation (6) is written as

$$(A_o - A'_t) + A_o \ln \frac{A'_t}{A_o} = -\frac{\epsilon \cdot l}{2} \cdot k'_{\text{obsd}} \cdot t \quad \dots (7)$$

where A_o is the initial absorbance due to $[\text{Fe(Par)}_2]^-$, A'_t is the corrected absorbance for $[\text{Fe(Par)}_2]^-$ at time t , and ϵ is the molar extinction coefficient of $[\text{Fe(Par)}_2]^-$ at 496 nm. Plots of left hand side of equation (7) versus time give straight lines (Fig. III.1). The rate constants k'_{obsd} and hence k_r ($k_r = k'_{\text{obsd}} / [\text{L}^{3-}]$) are calculated from the slopes of these plots and are given in Table III.2. Values of $\log k'_{\text{obsd}}$ are plotted against $\log [\text{L}^{3-}]_T$ in Fig. III.2. The slope of the above plots is found to be one at higher ligand concentration and tends to zero at low ligand

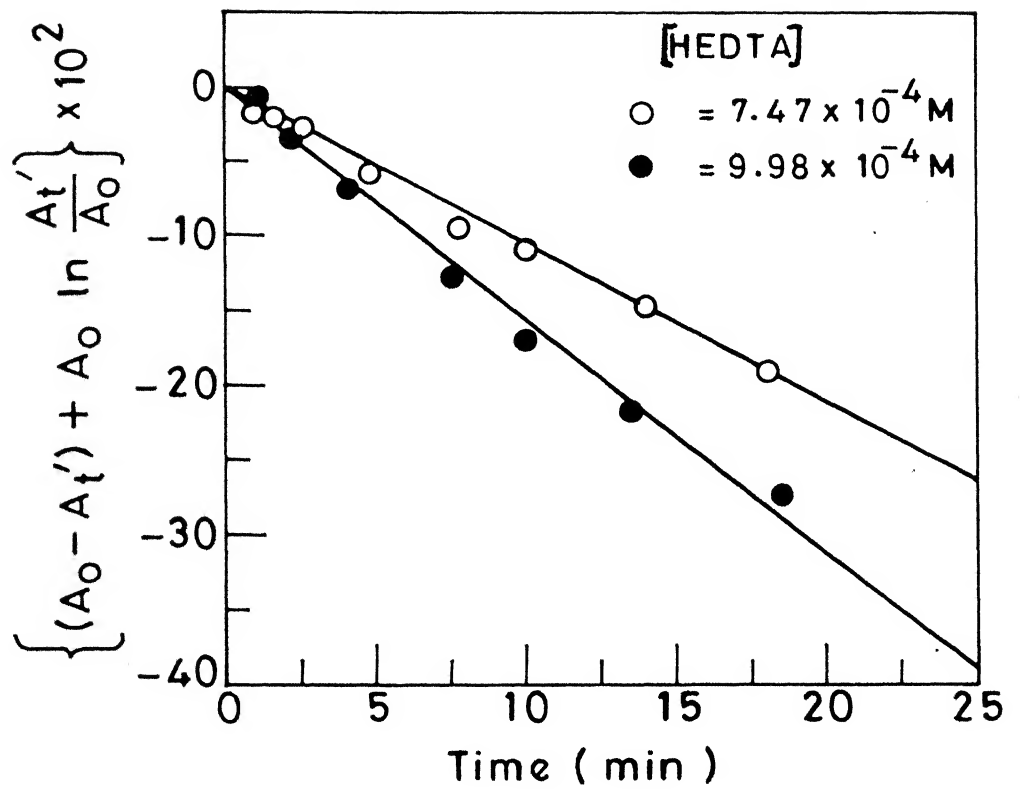


Fig. III.1 Inverse first order plots for reaction of $[\text{Fe(Par)}_2]^-$ and HEDTA at temp. = 30°C , $\text{pH} = 9.0$, $I = 0.1 \text{ M}$ (NaClO_4).

TABLE III.2. Kinetics of decomposition of $[\text{Fe}(\text{Par})_2]^-$ by L^{3-} .For NTA reaction, $[\text{Fe}^{3+}] = (1.5-2.0) \times 10^{-5} \text{ M}$, $[\text{Par}] = (3.0-4.0) \times 10^{-5} \text{ M}$, Temperature = $25 \pm 0.1^\circ\text{C}$, $I = 0.1 \text{ M}(\text{NaClO}_4)$, pH = 9.0 ± 0.02 . For FeHEDTAreaction $[\text{Fe}^{3+}] = (0.5-1.0) \times 10^{-5} \text{ M}$, $[\text{Par}] =$ $(1.0-2.0) \times 10^{-5} \text{ M}$, Temperature = $30 \pm 0.1^\circ\text{C}$, $I = 0.1 \text{ M}(\text{NaClO}_4)$, pH = 9.0 ± 0.02 . $\text{Fe}(\text{Par})_2$ -NTA System

$[\text{NTA}], \text{M}$	$10^9 \times k'_{\text{obsd}} \text{ Ms}^{-1}$	$10^6 \times k_r \text{ s}^{-1}$
2.0×10^{-2}	25.5	1.3
1.0×10^{-2}	15.9	1.6
8.0×10^{-3}	9.1	1.1
6.0×10^{-3}	8.0	1.3
5.0×10^{-3}	5.4	1.1
		$\text{Av.} = (1.3 \pm 0.2) \times 10^{-6} \text{ s}^{-1}$
2.5×10^{-3}	4.7	
2.19×10^{-3}	3.9*	
1.25×10^{-3}	3.7*	
1.0×10^{-3}	3.8*	

 $\text{Fe}(\text{Par})_2$ -HEDTA System

$[\text{HEDTA}], \text{M}$	$10^9 \times k'_{\text{obsd}} \text{ Ms}^{-1}$	$10^5 \times k_r \text{ s}^{-1}$
1.92×10^{-3}	24.2	1.3
9.98×10^{-4}	10.0	1.0
7.47×10^{-4}	7.8	1.1
4.97×10^{-4}	5.4	1.1
2.88×10^{-4}	3.2	1.1
1.96×10^{-4}	2.0	1.0
		$\text{Av.} = (1.1 \pm 0.1) \times 10^{-5} \text{ s}^{-1}$
1.25×10^{-4}	1.3*	
8.0×10^{-5}	1.2*	
6.0×10^{-5}	1.2*	

*Zero Order dependence in $[\text{L}^{3-}]$, $k_r = k'_{\text{obsd}} / [\text{L}^{3-}]$

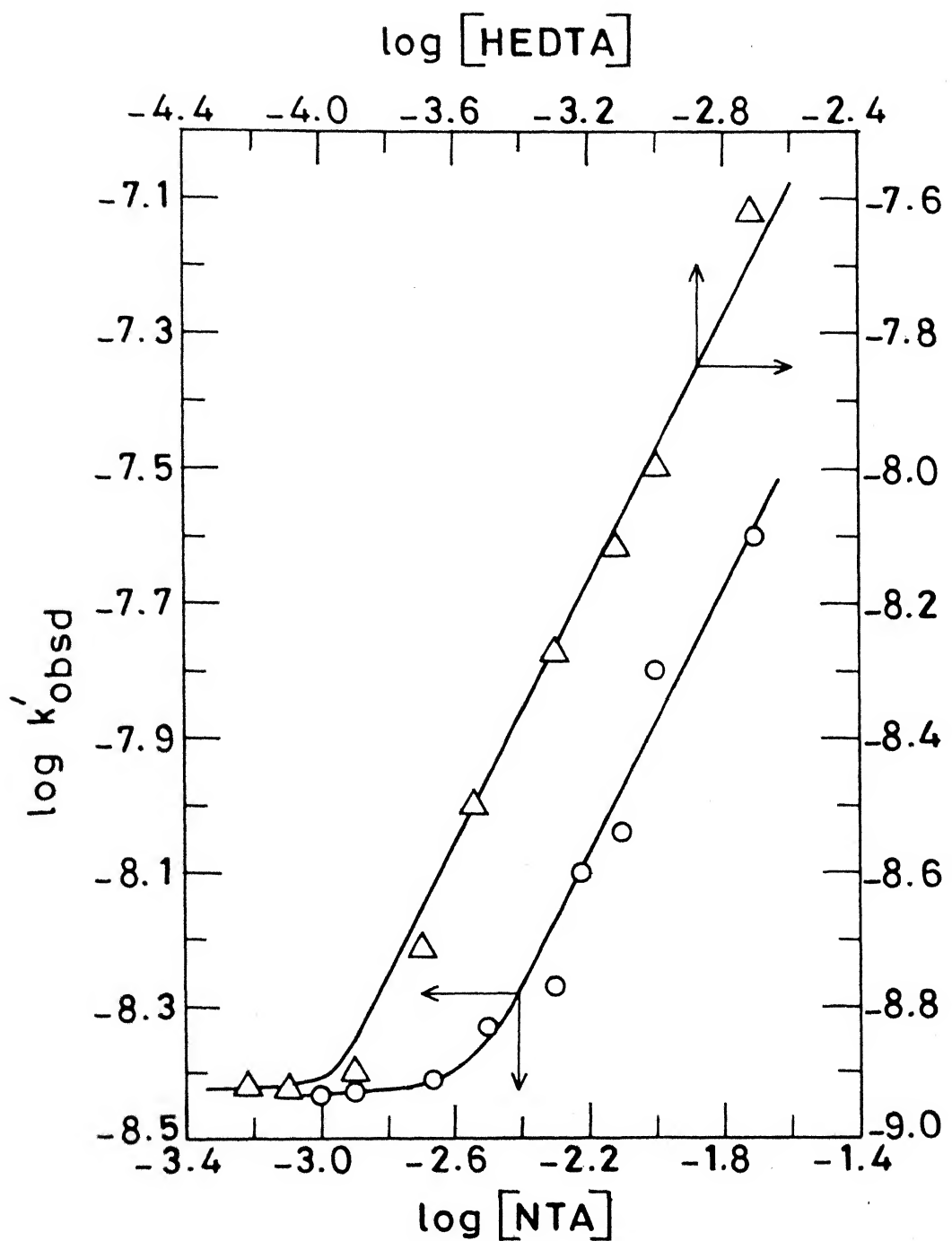


Fig.III.2 Ligand dependence of the observed rate constants for the reactions of $[Fe(Par)_2]^-$ with NTA (○) and HEDTA (△). (The reaction conditions are given in Table III.2)

concentration. This zero order dependence in $[L^{3-}]$ indicates a slow dissociation of the $[FeR_2]^-$ complex to $[FeR]^+$ and Par, followed by further reaction of $[FeR]^+$ (formed in situ) with L^{3-} to give $[FeL(OH)]^-$ and $HPar^-$ (vide supra).

The observed rate constant, k'_{obsd} , can be written as

$$k'_{obsd} = k_d^{FeR_2} + k' [L^{3-}] \quad \dots (8)$$

The values of the two constants on right hand side of equation (8) are $1.0 \times 10^{-9} \text{ Ms}^{-1}$ and $1.2 \times 10^{-6} \text{ s}^{-1}$ for NTA reaction and $5.0 \times 10^{-10} \text{ Ms}^{-1}$ and $1.1 \times 10^{-5} \text{ s}^{-1}$ for HEDTA reaction respectively. A similar observation has been made by previous workers while studying reactions of cyanide with some bis complexes of nickel(II).^{15,16}

III.3.4 pH dependence of the forward rate

The pH profiles ($pH = -\log [H^+]$ for dilute solutions) for both reactions over the range of interest are shown in Fig. III.3 (Table III.3). In the case of $[Fe(NTA)]$, the rate was found to increase in the pH range 6-8.5 and then level off. In the case of $[Fe(HEDTA)]$, however, the rate was found to remain unchanged between pH 7 to 9 and then increase with increase of pH above 9.

The concentration of different complex species viz., FeL , $FeL(OH)$, $FeL(OH)_2$ and Par as a function of pH can be determined by using a computer programme given by Perrin and Sayce¹⁷ after

TABLE III.3. Dependence of the rate constants on pH for the reactions of $[\text{Fe(NTA)}]$ and $[\text{Fe(HEDTA)}]$ with Par at temp. = $25 \pm 0.1^\circ\text{C}$, $I = 0.1\text{M}(\text{NaClO}_4)$.

pH	$k, \text{M}^{-1}\text{s}^{-1}$
$[\text{Fe(NTA)}] = (0.5-3.6) \times 10^{-5} \text{M}$, $[\text{Par}] = (2.54-1.2) \times 10^{-5} \text{M}$.	
6.0	4.2×10^1
6.6	5.5×10^1
7.25	7.4×10^1
7.95	8.5×10^1
8.45	9.4×10^1
9.0	9.8×10^1
9.45	10.6×10^1
$[\text{Fe(HEDTA)}] = 1.0 \times 10^{-5} \text{M}$, $[\text{Par}] = 2.4 \times 10^{-5} \text{M}$.	
7.0	1.8×10^{-1}
7.5	1.8×10^{-1}
8.0	1.8×10^{-1}
8.75	2.0×10^{-1}
9.0	2.9×10^{-1}
9.25	4.2×10^{-1}
9.5	8.5×10^{-1}
10.0	2.0
10.25	4.1
10.5	5.3
10.85	13.9

inserting the pK_a 's of complexes and ligands. The values of stability constants of Fe(NTA) , Fe(HEDTA) and Fe(Par)_2 and protonation constants of ligands viz., Par, NTA, and HEDTA are compiled in Table III.4. The species distribution of Par, Fe(NTA) and Fe(HEDTA) are shown in Figs. III.4, III.5 and III.6 respectively. These are used to resolve the rate constants due to different protonated, unprotonated and hydroxy forms of the metal complexes as well as different protonated forms of ligands.

III.3.5 Resolution of rate constants for the forward reactions

The pH dependence of the observed rates can be used for evaluating the rate constants due to reactant species present in different pH ranges. In the pH range 6-10 the complex $[\text{Fe(NTA)}]$ exists as $[\text{FeL(OH)}]^-$ and $[\text{FeL(OH)}_2]^{2-}$ while the Par as HR^- only. The observed rate can be resolved by an algebraic procedure outlined below:

$$\begin{aligned} \text{Rate} &= k[\text{FeL}]_T[\text{R}]_T \\ &= k_{\text{HR}}^{\text{FeL(OH)}} [\text{FeL(OH)}^-] + k_{\text{HR}}^{\text{FeL(OH)}_2} [\text{FeL(OH)}_2^{2-}] [\text{HR}^-] \end{aligned} \quad \dots (9)$$

The subscript T in the above expression indicates the total concentration of both species in all their forms. Algebraic manipulation yields an expression suitable for graphical treatment given below:

TABLE III.4. Protonation Constants of aminocarboxylates and stability constants of aminocarboxylatoiron(III) complexes.

Temp. = 25°C, I = 0.1M(NaClO₄) unless stated otherwise.

A. Protonation constants of Par and aminocarboxylates ($\log K_{H_n L}$)

L^{n-}	K_{HL}	$K_{H_2 L}$	$K_{H_3 L}$	$K_{H_4 L}$
Par ^a	12.5	5.83	2.3 ^b	-
NTA	9.65	2.48	1.8	0.8 ^c
HEDTA	9.81	5.37	2.6	-

B. Stability constants of aminocarboxylatoiron(III) complexes ($\log K$)

L^{n-}	K_{FeL}	$K_{FeL(OH)}$	$K_{FeL(OH)}_2$
NTA	15.9	9.9	6.2
HEDTA	19.8	10.12	4.98

(a) I = 0.1M(KNO₃); (b) I = 0.005M (50% dioxan); (c) temp.=20°C.

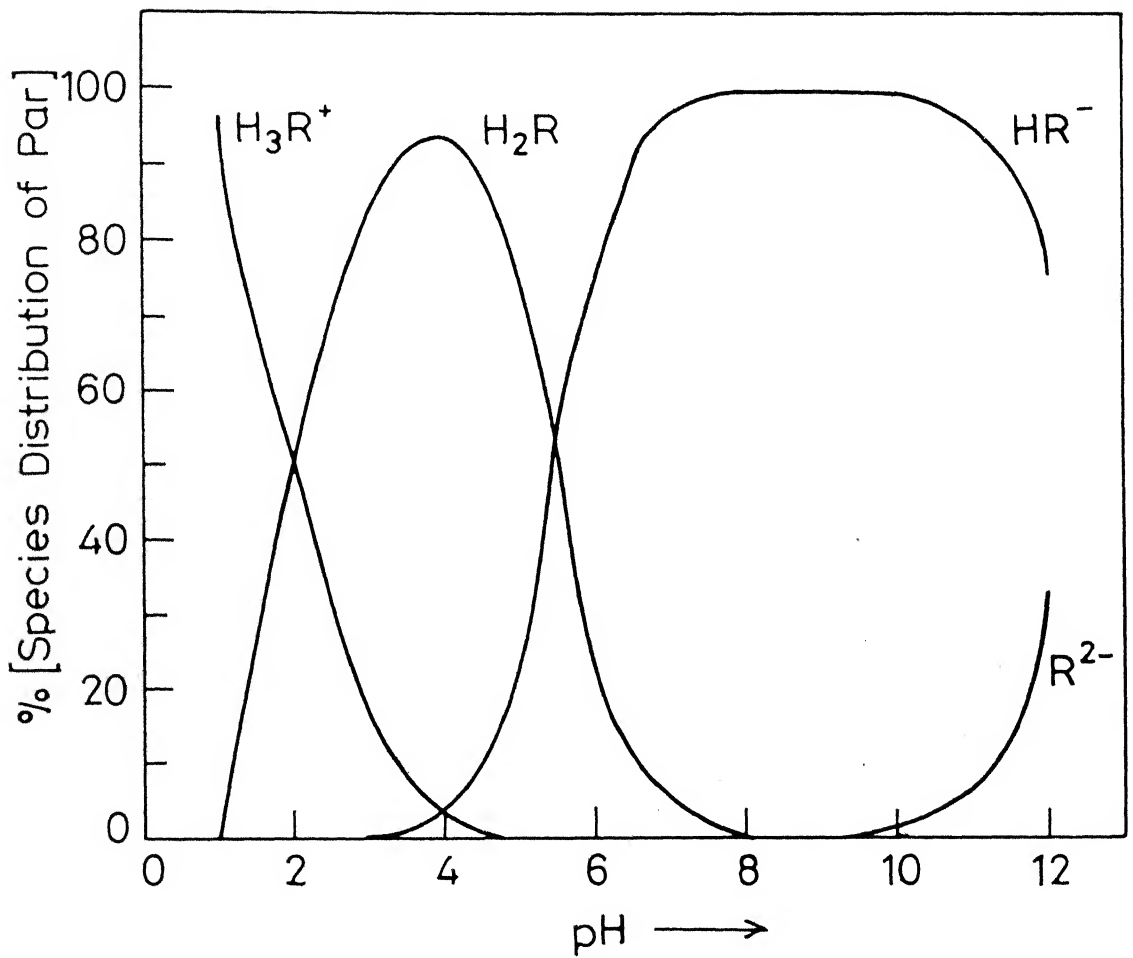


Fig.III.4 Species distribution of Par as a function of pH; $[\text{Par}] = 5.0 \times 10^{-5} \text{ M.}$

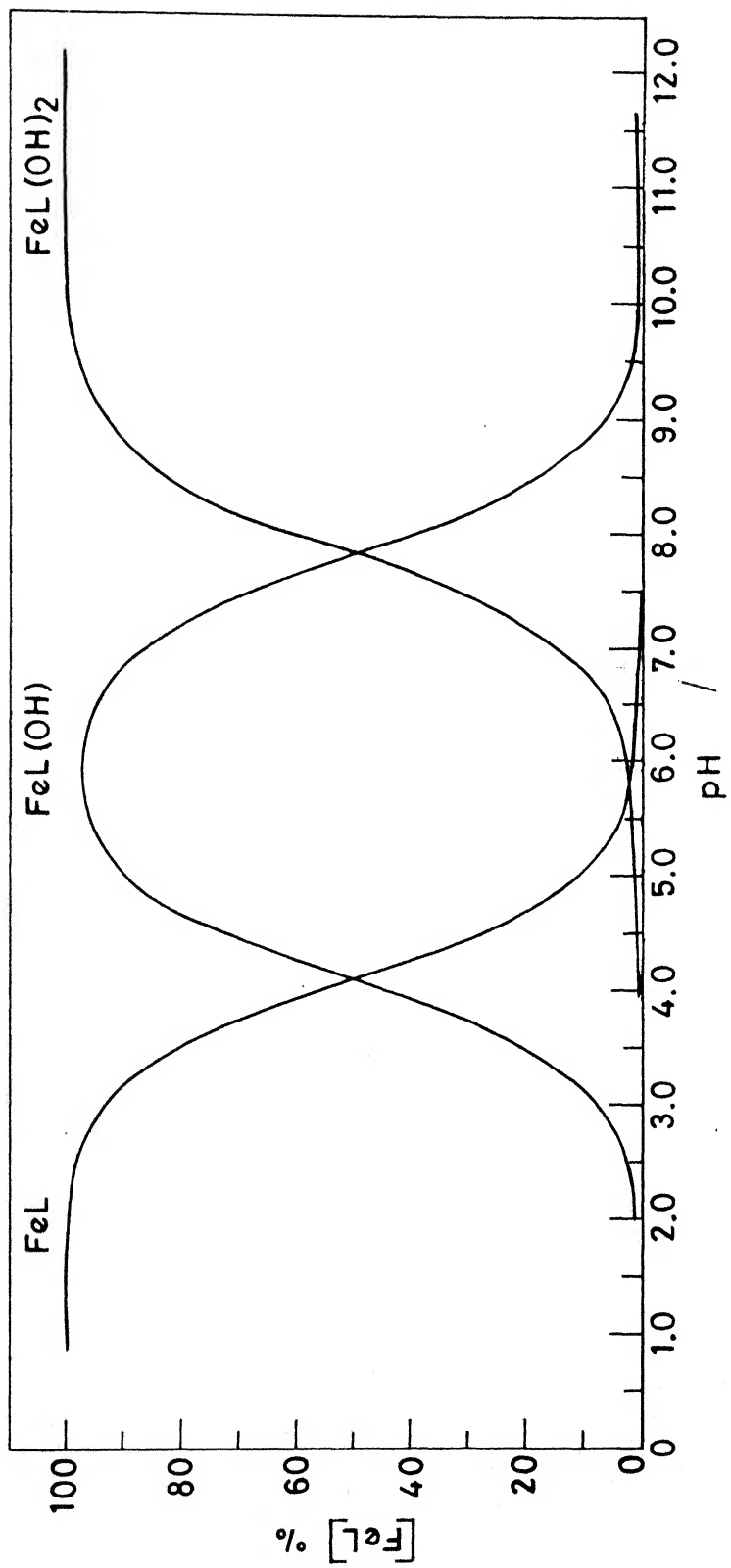


Fig. III.5 Species distribution of $[\text{Fe(NTA)}]$ system as a function of pH $[\text{Fe(NTA)}] = 2.5 \times 10^{-4} \text{ M}$ temp. = 25°C .

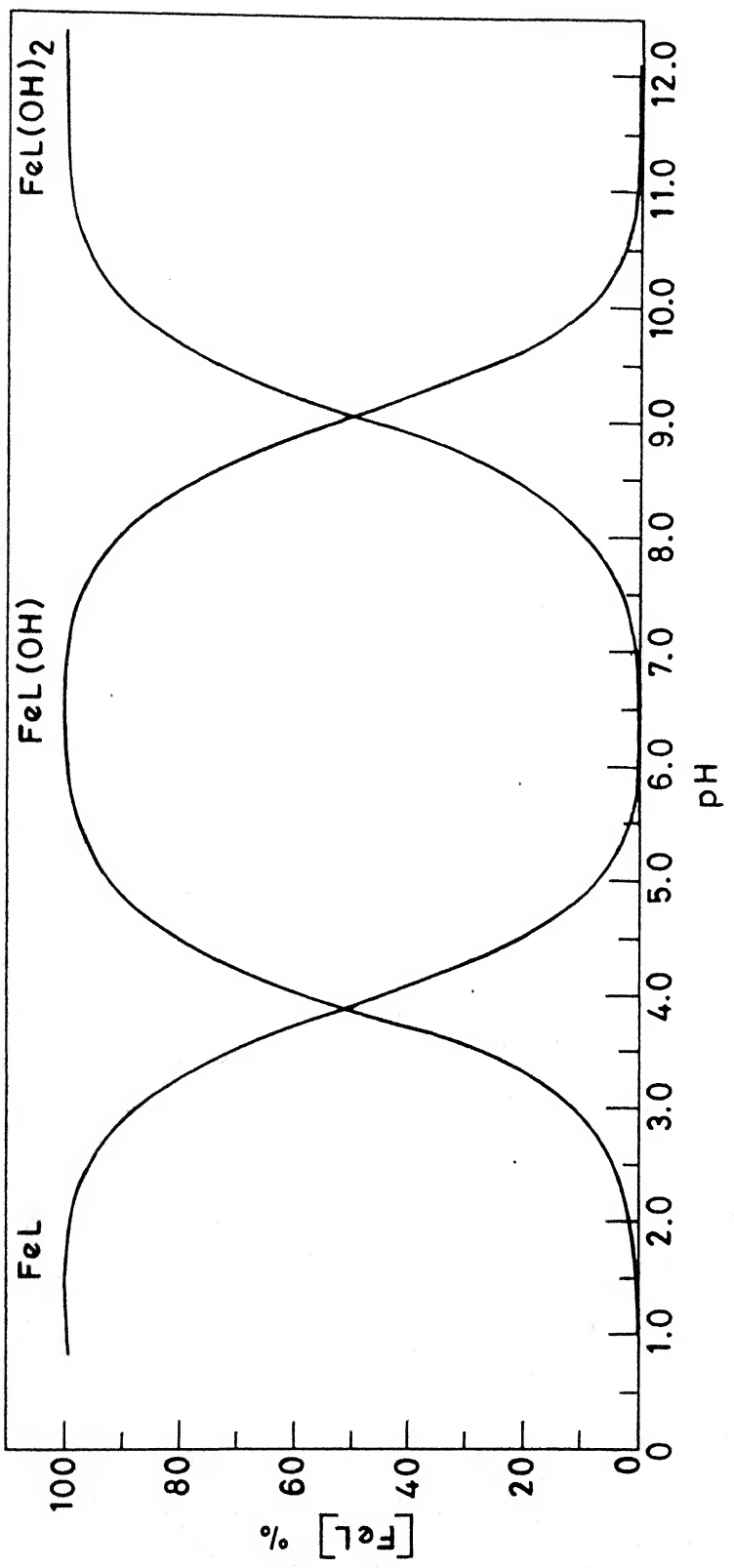


Fig.III.6 Species distribution of $[\text{Fe}(\text{HEDTA})]$ system as a function of pH
 $[\text{Fe}(\text{HEDTA})] = 2.5 \times 10^{-4} \text{ M}$ temp = 25°C .

$$k \cdot \frac{[FeL]_T}{[FeL(OH)^-]} \cdot \frac{[R]_T}{[R^{2-}]} = k_{HR}^{FeL(OH)} \cdot K_{HR} \cdot [H^+] \\ + k_{HR}^{FeL(OH)} \cdot K_{FeL(OH)}^2 \cdot K_{HR} \cdot K_w \dots \quad (10)$$

$$\text{where } [FeL]_T = [FeL(OH)^-] + [FeL(OH)_2^{2-}] \\ = [FeL(OH)^-] (1 + K_1 K_w / [H^+])$$

$$[FeL]_T / [FeL(OH)^-] = (1 + K_1 K_w / [H^+])$$

$$\text{and } [R]_T / [R^{2-}] = 1 + K_{HR} [H^+] + K_{H_2R} K_{HR} [H^+]^2 + \dots$$

In the above expressions

$$K_1 = [FeL(OH)_2^{2-}] / [FeL(OH)^-] [OH^-] = 10^{6.2^{18}} \text{ for Fe(NTA) complex and} \\ K_w \text{ is the ionization constant of water at } 25^\circ\text{C}.$$

By inserting the values of $[FeL]_T / [FeL(OH)^-]$ and $[R]_T / [R^{2-}]$ equation (10) transforms to equation (11)

$$k \cdot ([FeL]_T / [FeL(OH)^-]) \cdot ([R]_T / [R^{2-}]) = k \{1 + K_1 K_w / [H^+]\} \{1 + K_{HR} [H^+]\} \\ = \{k_{HR}^{FeL(OH)} K_{HR} [H^+] \\ + k_{HR}^{FeL(OH)} \cdot K_{FeL(OH)}^2 \cdot K_{HR} \cdot K_w\} \dots \quad (11)$$

A plot of left hand side of equation (11) versus $[H^+]$ gives a straight line (Fig. III.7) and the rate constants due to $[FeL(OH)^-]$ and $[FeL(OH)_2^{2-}]$ are calculated from the slope and the intercept respectively (Table III.5).

The treatment for the reaction of $[Fe(HEDTA)]$ and Par is a little more involved. In the pH range 7-11, $[Fe(HEDTA)]$ exists as

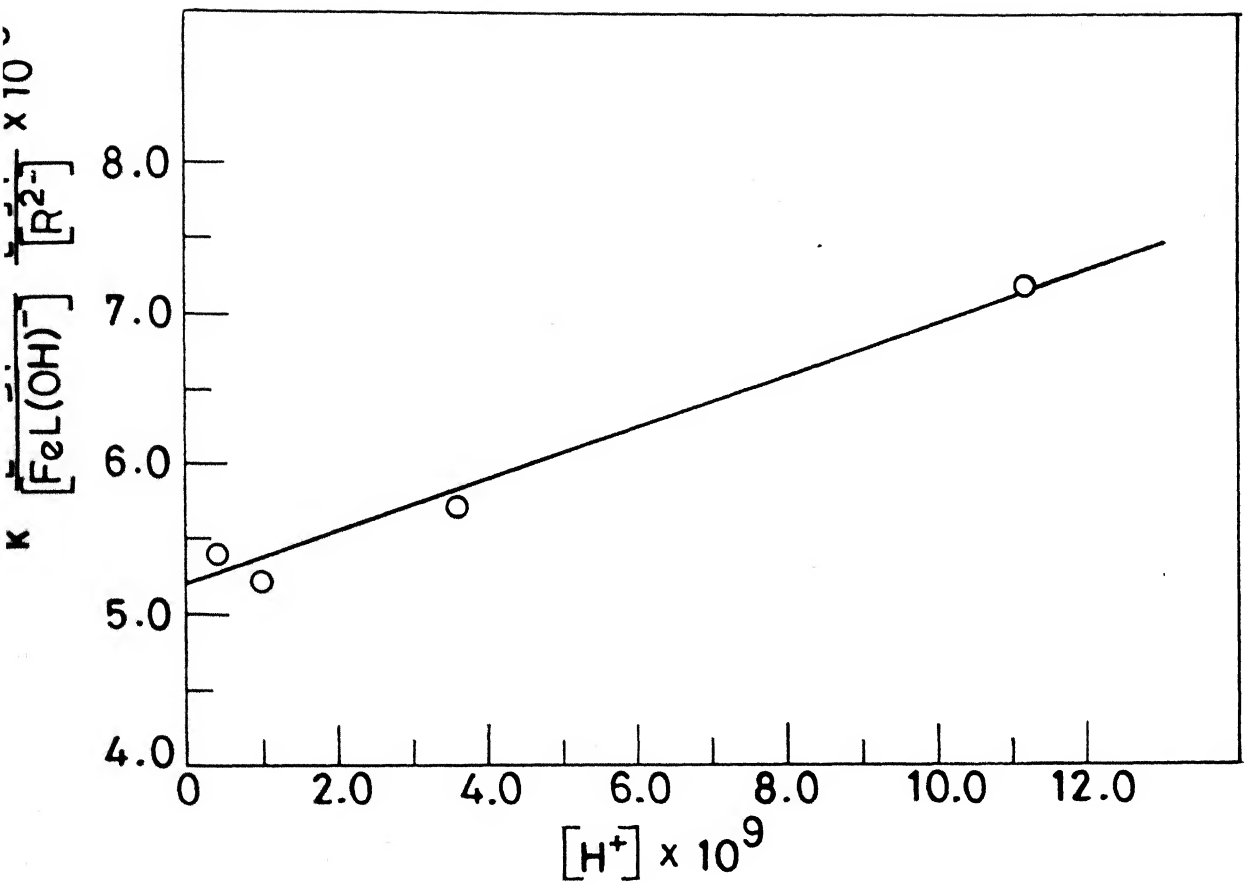


Fig. III.7 Resolution of the rate constants for the reactions of $[\text{FeNTA(OH)}]^-$ and $[\text{FeNTA(OH)}]^{2-}$ with HR^- .

$[\text{FeL(OH)}]^-$ and $[\text{FeL(OH)}_2]^{2-}$ and Par as HR^- and R^{2-} . As in the case of $[\text{Fe(NTA)}]$, the rate can be resolved again using the algebraic procedure outlined above, by making use of protonation constants of Par and stability constants of $[\text{FeL(OH)}]^-$ and $[\text{FeL(OH)}_2]^{2-}$.

The rate can be then written as

$$\begin{aligned}
 k[\text{FeL}]_T[\text{R}]_T &= \{ k_{\text{HR}}^{\text{FeL(OH)}} [\text{HR}^-] [\text{FeL(OH)}^-] \\
 &+ k_{\text{R}}^{\text{FeL(OH)}} [\text{R}^{2-}] [\text{FeL(OH)}] + k_{\text{HR}}^{\text{FeL(OH)}} {}^2[\text{HR}^-] [\text{FeL(OH)}_2^{2-}] \\
 &+ k_{\text{R}}^{\text{FeL(OH)}} {}^2[\text{R}^{2-}] [\text{FeL(OH)}_2^{2-}] \} \quad \dots (12)
 \end{aligned}$$

In the pH range 7-8.75, the term containing $[\text{R}^{2-}]$ and $[\text{FeL(OH)}_2^{2-}]$ can be neglected and equation (12) reduces to equation (13).

$$k(1 + K_1 K_w / [\text{H}^+])(1 + K_{\text{HR}} [\text{H}^+]) = k_{\text{HR}}^{\text{FeL(OH)}} \cdot K_{\text{HR}} [\text{H}^+] \quad \dots (13)$$

Left hand side of this equation is defined in the resolution of rate constants of $[\text{Fe(NTA)}]$ -Par reaction first discussed. K_1 is for $[\text{Fe(HEDTA)}]$ is equal to the $10^{4.98}$.

By plotting left hand side of equation (13) versus $[\text{H}^+]$, we get, as expected, a straight line with an intercept equal to zero and slope = $k_{\text{HR}}^{\text{FeL(OH)}} \cdot K_{\text{HR}}$ (Fig. III.8). $k_{\text{HR}}^{\text{FeL(OH)}}$ can be evaluated from the slope.

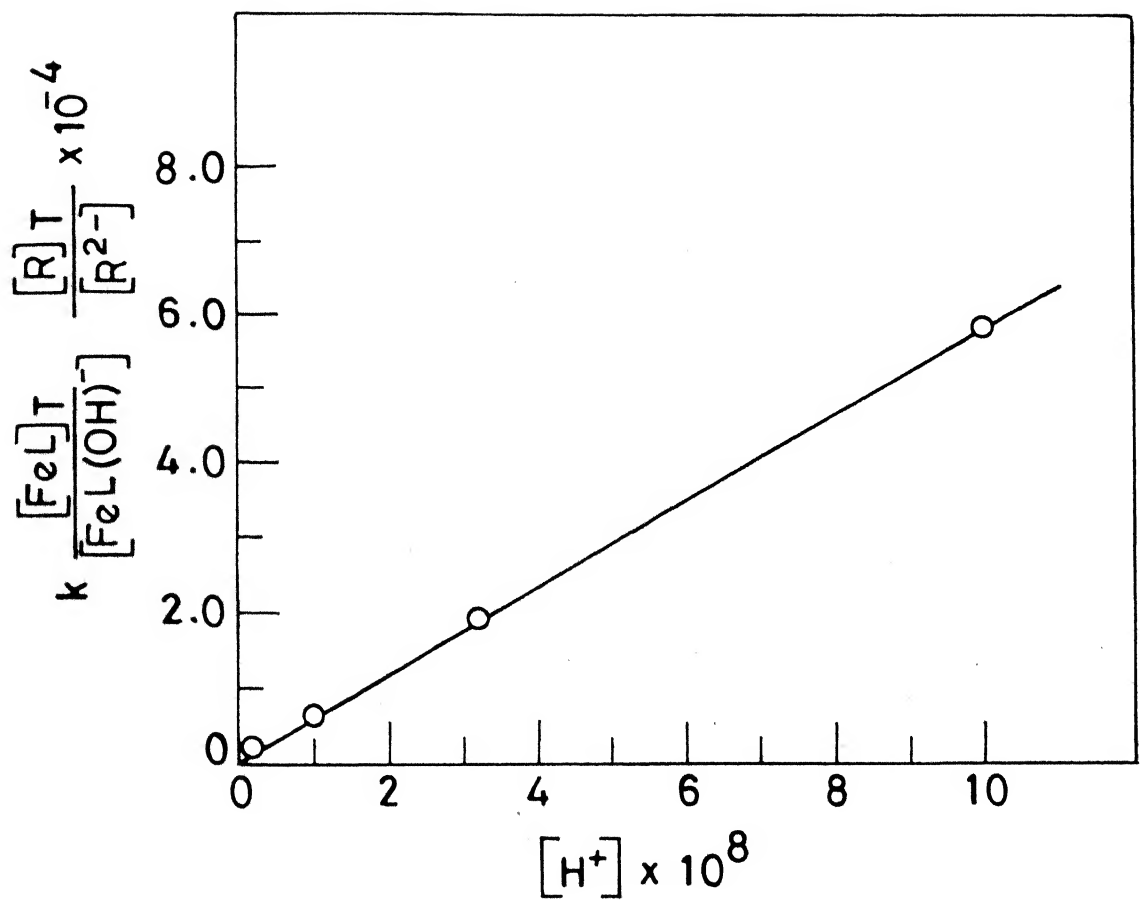


Fig.III.8 Resolution of rate constant due to the reaction of $[\text{FeHEDTA(OH)}]^-$ and HR^-

In the pH range 8.75-9.25, however, the term containing $[R^{2-}]$ can be neglected and equation (12) transforms to equation (14).

$$\begin{aligned} & k(1 + K_1 K_w / [H^+])(1 + K_{HR} [H^+]) - k_{HR}^{FeL(OH)} \cdot K_{HR} [H^+] \\ & = k_{HR}^{FeL(OH)} \cdot K_{FeL(OH)}^2 \cdot K_{HR} \cdot K_w \quad \dots (14) \end{aligned}$$

Dividing by $[H^+]$ throughout.

$$\begin{aligned} & k(1 + K_1 K_w / [H^+])(1 + K_{HR} [H^+]) \cdot \frac{1}{[H^+]} - k_{HR}^{FeL(OH)} \cdot K_{HR} \\ & = k_{HR}^{FeL(OH)} \cdot K_{FeL(OH)}^2 \cdot K_{HR} \cdot K_w \cdot \frac{1}{[H^+]} \quad \dots (15) \end{aligned}$$

For simplification we may set

$$A = k(1 + K_1 K_w / [H^+])(1 + K_{HR} [H^+]) \cdot \frac{1}{[H^+]} - k_{HR}^{FeL(OH)} \cdot K_{HR} \quad \dots (16)$$

A plot of 'A' versus $1/[H^+]$ yields a straight line passing through the origin (Fig. III.9) with a slope equal to $k_{HR}^{FeL(OH)} \cdot K_{FeL(OH)}^2 \cdot K_{HR} \cdot K_w$ from which $k_{HR}^{FeL(OH)} \cdot K_{HR} \cdot K_w$ can be obtained.

Above pH 9.5, on the other hand, the term containing $[FeL(OH)^-]$ can be neglected, and equation (12) transforms to equation (17).

$$\begin{aligned} & k(1 + K_1 K_w / [H^+])(1 + K_{HR} [H^+]) - k_{HR}^{FeL(OH)} \cdot K_{HR} \cdot K_{FeL(OH)}^2 \cdot K_w \\ & = k_R^{FeL(OH)} \cdot K_{FeL(OH)}^2 \cdot K_w \cdot \frac{1}{[H^+]} \quad \dots (17) \end{aligned}$$

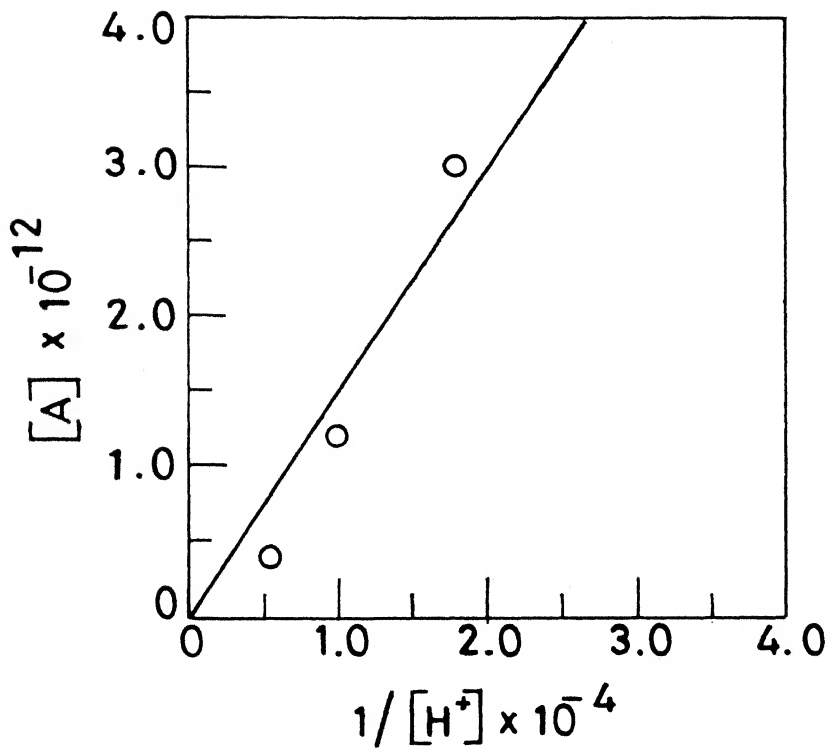


Fig. III.9 Resolution of rate constant
viz. $k_{HR^-}^{FeHEDTA(OH)_2}$

For simplification we may set

$$B = k(1 + K_1 K_w / [H^+])(1 + K_{HR} [H^+]) - k_{HR}^{FeL(OH)_2^2} \cdot K_{HR} \cdot K_{FeL(OH)_2} \cdot K_w$$

... (18)

A plot of left hand side of equation (17) versus $1/[H^+]$, again yields a straight line (Fig. III.10) passing through the origin with a slope equal to $k_R^{FeL(OH)_2^2} \cdot K_{FeL(OH)_2} \cdot K_w$, which enables us to obtain $k_R^{FeL(OH)_2^2}$. It is not possible to calculate the fourth rate constant $k_R^{FeL(OH)_2^2}$, because the species $[FeL(OH)_2^-]$ exists only upto pH 10 (Fig. III.6) and $[R^{2-}]$ exists above pH 10.5 (Fig. III.5). The concentration of any one in the presence of other is negligibly small and the rate is, therefore, very slow. All the resolved rate constants are listed in Table III.5.

III.3.6 Temperature dependence of forward and reverse rate

Activation parameters for the forward and the reverse reactions were obtained from the Arrhenius plots drawn in the temperature range 25-45°C. These are given in Table III.6.

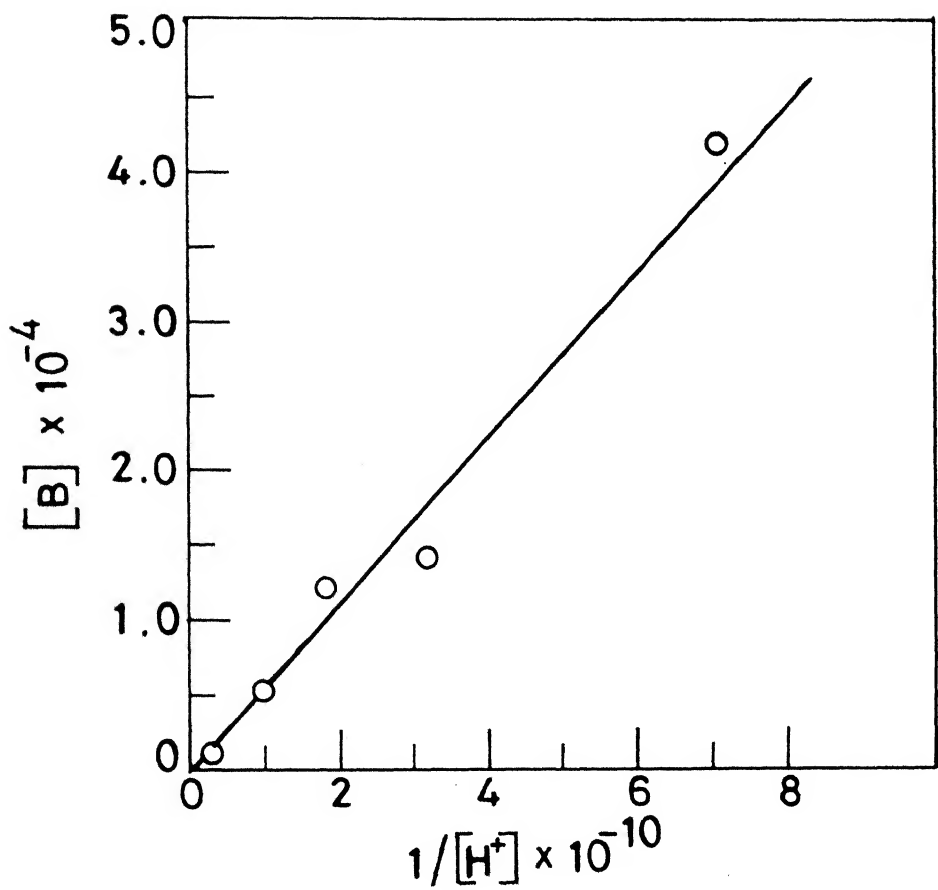


Fig. III.10 Resolution of rate constant for the reaction of $[\text{FeHEDTA(OH)}_2]^{2-}$ and R^{2-} .

TABLE III.5. Resolved rate constants for the reaction of Fe(NTA) and Fe(HEDTA) with Par.

<u>Fe(NTA)-Par System</u>	<u>Fe(HEDTA)-Par System</u>
$k_{HR}^{FeL(OH)} = 5.6 \times 10^1 \text{ M}^{-1} \text{s}^{-1}$	$k_{HR}^{FeL(OH)} = 1.8 \times 10^{-1} \text{ M}^{-1} \text{s}^{-1}$
$k_{HR}^{FeL(OH)_2} = 1.04 \times 10^2 \text{ M}^{-1} \text{s}^{-1}$	$k_{HR}^{FeL(OH)_2} = 5.0 \times 10^{-1} \text{ M}^{-1} \text{s}^{-1}$
	$k_R^{FeL(OH)_2} = 5.9 \times 10^2 \text{ M}^{-1} \text{s}^{-1}$

TABLE III.6. Activation Parameters

Forward Reaction

(a) Fe(NTA) + 2 Par Reaction (b) Fe(HEDTA) + 2 Par Reaction

$$pH = 9.0 \pm 0.02$$

$$pH = 10.0 \pm 0.02$$

$$\Delta H^{\circ\neq} = 62.6 \pm 0.7 \text{ kJ mol}^{-1}$$

$$\Delta H^{\circ\neq} = 86.1 \pm 2.1 \text{ kJ mol}^{-1}$$

$$\Delta S^{\circ\neq} = 3 \pm 1 \text{ JK}^{-1}\text{mol}^{-1}$$

$$\Delta S^{\circ\neq} = 46 \pm 7 \text{ JK}^{-1}\text{mol}^{-1}$$

Reverse Reaction

Zero order dependence in [Par] First order dependence in [Par]

(c) Fe(Par)₂ + NTA Reaction

$$pH = 9.0 \pm 0.02$$

$$\Delta H^{\circ\neq} = 41.8 \pm 0.4 \text{ kJ mol}^{-1}$$

$$\Delta H^{\circ\neq} = 34.5 \pm 0.4 \text{ kJ mol}^{-1}$$

$$\Delta S^{\circ\neq} = -254 \pm 4 \text{ JK}^{-1}\text{mol}^{-1}$$

$$\Delta S^{\circ\neq} = -237 \pm 1.3 \text{ JK}^{-1}\text{mol}^{-1}$$

(d) Fe(Par)₂ + HEDTA Reaction

$$pH = 10.0 \pm 0.02$$

$$\Delta H^{\circ\neq} = 72.3 \pm 2.0 \text{ kJ mol}^{-1}$$

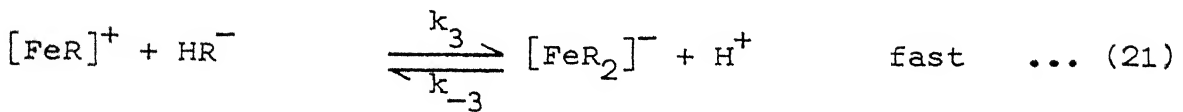
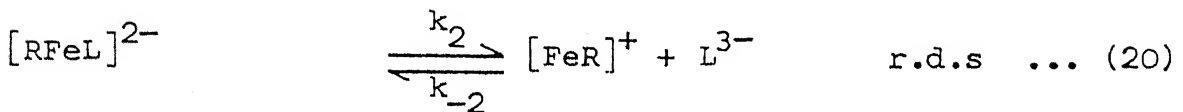
$$\Delta H^{\circ\neq} = 53.2 \pm 2.1 \text{ kJ mol}^{-1}$$

$$\Delta S^{\circ\neq} = -171 \pm 6 \text{ JK}^{-1}\text{mol}^{-1}$$

$$\Delta S^{\circ\neq} = -160 \pm 7 \text{ JK}^{-1}\text{mol}^{-1}$$

III.4 DISCUSSION

The results of studies on the forward and reverse reactions of $[\text{FeL}]$ and $[\text{Par}]$ suggest a mechanism given in equations (19)–(21).



According to the proposed mechanism the rate of forward reaction is given by

$$\text{Rate} = k_2 [\text{RFeL}]^{2-} \quad \dots \quad (22)$$

and from equilibrium of equation (19)

$$\begin{aligned} [\text{RFeL}]^{2-} &= K_1 [\text{FeL(OH)}^-][\text{HR}^-]/[\text{H}_2\text{O}] \quad (K_1 = k_1/k_{-1}) \\ &= \frac{K_1}{[\text{H}_2\text{O}]} [\text{FeL(OH)}^-][\text{HR}^-] \quad \dots \quad (23) \end{aligned}$$

By putting the value of $[\text{RFeL}]^{2-}$ from equation (23) into equation (22),

$$\begin{aligned} \text{Rate} &= \frac{k_2 K_1}{[\text{H}_2\text{O}]} [\text{FeL(OH)}^-][\text{HR}^-] \\ &= k [\text{FeL(OH)}^-][\text{HR}^-] \quad \dots \quad (24) \end{aligned}$$

$k = k_2 K_1 / [\text{H}_2\text{O}]$, concentration of water is large enough to be

considered constant. This is consistent with the experimental forward rate equation (4).

The reverse reaction between $[\text{FeR}_2]^-$ and L^{3-} is zero order at low ligand concentration. This shows a dissociation of the bis complex to the monocomplex $[\text{FeR}]^+$ and the free ligand R^{2-} , according to equation (21). The rate law for the reverse reaction may also be derived as for the forward reaction.

$$\text{Rate} = k_{-2} [\text{FeR}^+] [\text{L}^{3-}] \quad \dots (25)$$

Considering the equilibrium shown in equation (21)

$$[\text{FeR}^+] = \frac{k_3^{-1} [\text{FeR}_2^-] [\text{H}^+]}{[\text{HR}^-]} \quad \dots (26)$$

$$= \frac{k_3^{-1} [\text{FeR}_2^-]}{K_{\text{HR}} [\text{R}^{2-}]} \quad \dots (27)$$

$$\text{So Rate} = \left(\frac{k_{-2} K_3^{-1}}{K_{\text{HR}}} \right) \cdot \frac{[\text{FeR}_2^-] [\text{L}^{3-}]}{[\text{R}^{2-}]} \quad \dots (28)$$

This is also consistent with the experimental observation that the reverse reaction is first order in each $[\text{FeR}_2]^-$ and L^{3-} and inverse first order in R^{2-} (equation 6). By comparing equation (6) and equation (28) we get

$$k_r = \frac{k_{-2} K_3^{-1}}{K_{\text{HR}}} \quad \text{where} \quad K_3^{-1} = \frac{k_{-3}}{k_3}$$

The observed orders for the forward and the reverse reaction lead to the preposition that the first step is very fast and that a stable 1:1:1 intermediate $[RFeL]^{2-}$ forms instantaneously in each case. This type of intermediate formation has been reported by many authors in the case of Ni^{II}^9 , Cu^{II}^{11} , Hg^{II}^{10} , Zn^{II}^4 etc. This mixed ligand intermediate gives $[FeR]^+$ and $[L]^{3-}$ (equation 20). It is presumed that Par is not as flexible as aliphatic polyamines. It is unlikely, therefore, that NTA or HEDTA would react with Par complexes via a stepwise removal of the donor atoms of Par from the coordination sphere of the central metal as postulated previously in the substitution of polyamine complexes of nickel by EDTA²⁻, DTPA,¹⁹ PDTA,²⁰ TMDTA²¹ and HEDTA.²² As soon as one donor atom of Par is removed from the central metal ion of the intermediate $[RFeL]$ in the reverse reaction, the other two also get detached. The ligand attack on FeR^+ should, therefore, be the rate-determining one.

The moderately high activation enthalpies and positive entropies of activation (Table III.6) for the forward reactions compared to the reverse reaction are also in accord with the proposed rate determining step. In the forward reactions a bond dissociation is taking place. Thus, the mechanism is a dissociative one rather than associative. A comparison of activation parameters of the reverse reactions in conditions of first and zero order dependences in $[HPar^-]$ indicates that the ligand dependent pathway is associated with lower activation enthalpy

than the ligand independent path. The entropies of activation for the reverse reaction (when order is one in ligand) is large and negative as expected for the reverse reaction of the second and rate determining step (equation 20). However, the entropies of activation for the dissociation of $\text{Fe}(\text{Par})_2$ complex (equation 21, when order is zero in ligand) is not easily rationalized. It would be necessary to give a detailed consideration to the solvation of the reactants and the transition state species in the dissociation step and this is not easily done. We are, therefore, content with reporting the experimental values without comment.

Evidence for these reactions is provided by repetitive spectral scans of the reaction mixtures at suitable intervals. Repetitive scans for the forward and reverse reactions of $[\text{Fe}(\text{HEDTA})]-\text{Par}$ reaction system are given in Fig. III.11 and III.12. These scans show the formation and decay of the product and the reactant species respectively. The growth of peaks at 720 and 496 nm (Fig. III.11) is due to formation of $[\text{Fe}(\text{Par})_2]^-$. There is also a continuous decrease of absorbance at 414 nm due to consumption of Par during the course of reaction. The shift of peak at 210 nm to 225 nm also shows the formation of $[\text{Fe}(\text{Par})_2]^-$ and release of HEDTA. The appearance of isosbestic points at 450 and 335 nm suggests that $[\text{Fe}(\text{Par})_2]^-$ and Par coexist during the course of reaction. The spectral changes occurring during a kinetic run of the reverse reaction (Fig. III.12) also support these conclusions. There is a continuous decrease in the height of the 720 and 496 nm peaks and increase in the peak height at 414 nm due to release of

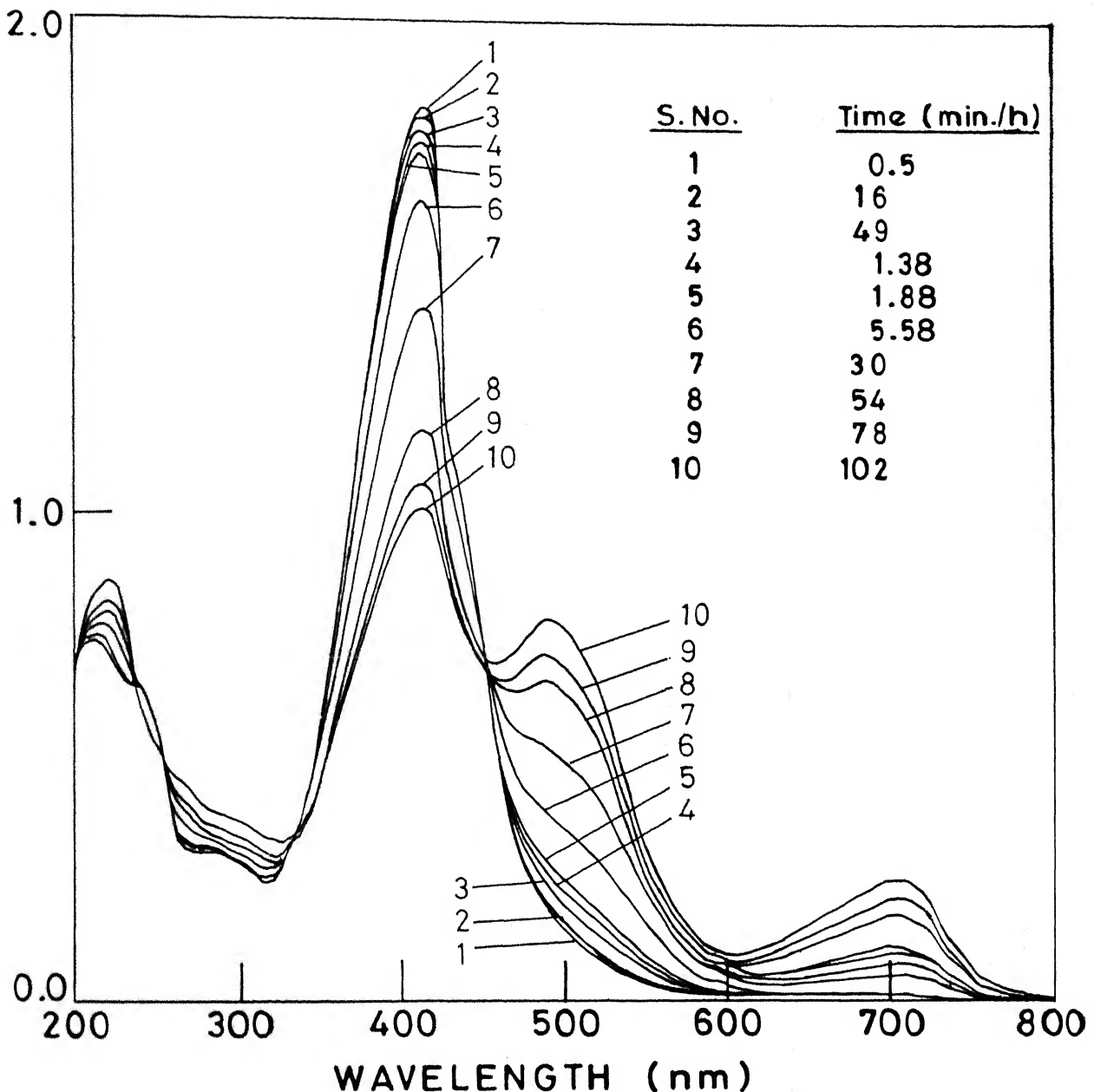


Fig. III.11 Spectral scan of the reaction mixture of $[\text{Fe}(\text{HEDTA})]$ and Par. $[\text{Fe}(\text{HEDTA})] = 5.0 \times 10^{-6} \text{ M}$, $[\text{Par}] = 5.0 \times 10^{-5} \text{ M}$, $\text{pH} = 9.0 \pm 0.02$, $I = 0.1 \text{ M}$ (NaClO_4), temp. = $25 \pm 0.1^\circ \text{C}$.

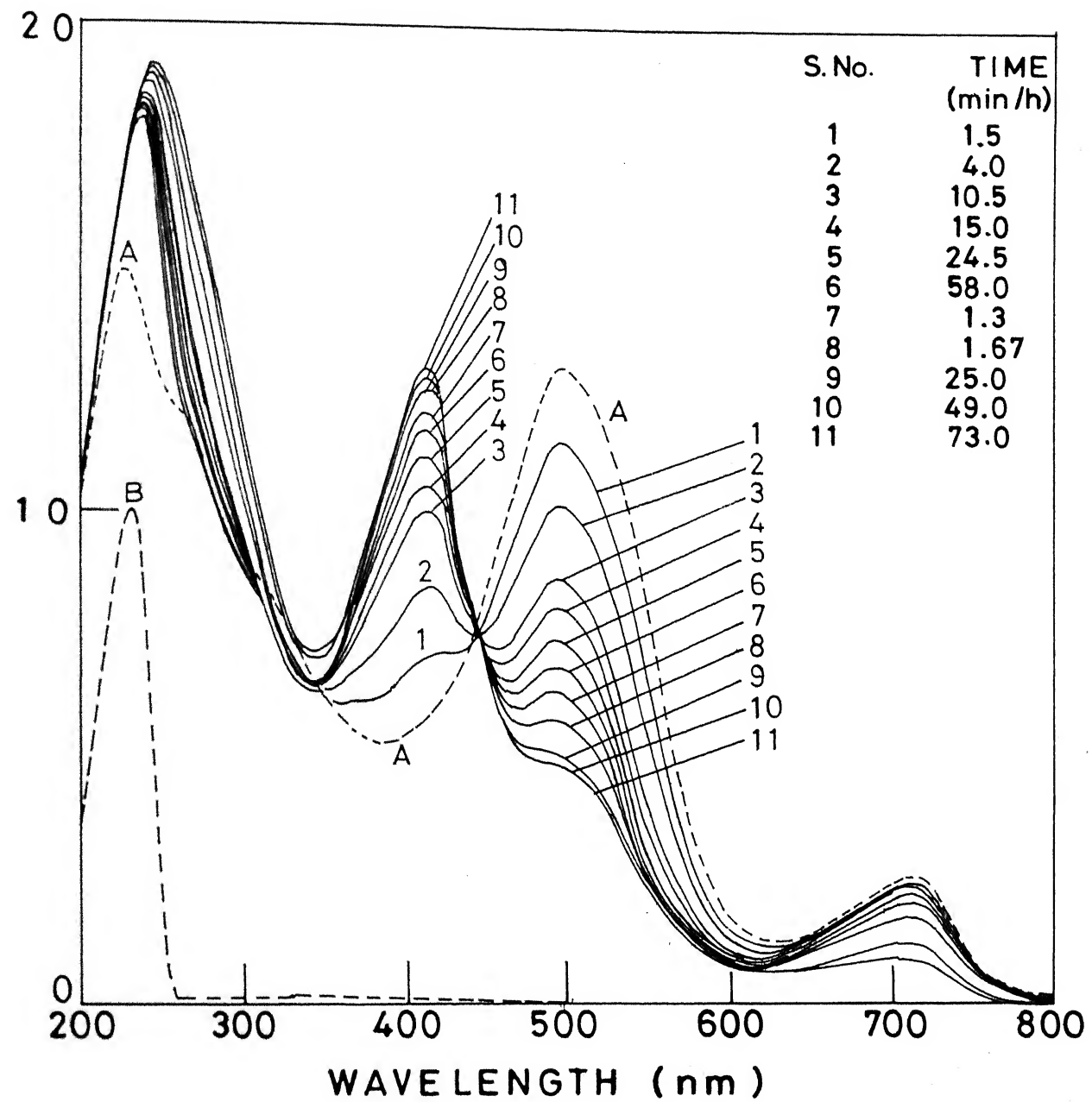


Fig. III.12 Repetitive scan of reaction mixture of reverse reaction during a typical kinetic run. $[\text{Fe}^{3+}] = 2.5 \times 10^{-5} \text{ M}$, $[\text{Par}] = 5.0 \times 10^{-5} \text{ M}$, $[\text{HEDTA}] = 5 \times 10^{-5} \text{ M}$, $\text{pH} = 9.0$, $I = 0.1 \text{ M}$, temp = 25°C ; A = $[\text{Fe}(\text{Par})_2]$; B = HEDTA.

Par. Isosbestic points at 450 and 335 nm confirm the conclusions. Appreciable concentration of neither $[RFeL]^{2-}$ nor $[FeR]^+$ are produced during the course of reaction.

To summarise, the substitution of $[FeL]$ complexes by Par takes place in three steps (equations 19-21) through the formation of a mixed ligand intermediate $[RFeL]^{2-}$. The dissociation of this intermediate to $[FeR]^+$ and L^{3-} constitutes the rate determining step. The addition of second molecule of Par is fast resulting in the formation of $[FeR_2]^-$ finally.

REFERENCES

1. D.W. Rogers, D.A. Aikens and C.N. Reilley, *J. Phys. Chem.*, 1962, 66, 1582.
2. D.B. Rorabacher and D.W. Margerum, *Inorg. Chem.*, 1964, 3, 382.
3. W.H. Baddley and F. Basolo, *J. Amer. Chem. Soc.*, 1966, 88, 2944.
4. M. Tanaka, S. Funahashi and K. Shirai, *Inorg. Chem.*, 1968, 7, 573.
5. D.L. Rabenstein and R.J. Kula, *J. Amer. Chem. Soc.*, 1969, 91, 2492.
6. S. Funahashi, S. Yamada and M. Tanaka, *Bull. Chem. Soc. Jpn.*, 1970, 43, 769.
7. S. Funahashi and M. Tanaka, *Inorg. Chem.*, 1969, 8, 2159.
8. A.G. Desai, H.W. Dodgen and J.P. Hunt, *J. Amer. Chem. Soc.*, 1970, 92, 798 and references contained therein.
9. S. Funahashi and M. Tanaka, *Inorg. Chem.*, 1970, 9, 2092.
10. S. Funahashi, M. Tabata and M. Tanaka, *Bull. Chem. Soc. Jpn.*, 1971, 44, 1586.
11. S. Funahashi, S. Yamada and M. Tanaka, *Inorg. Chem.*, 1971, 10, 257.
12. G. Schwarzenbach, *Complexometric Titrations*, Int. Sci. Pub., N.Y., 1985, p. 77.
13. A.E. Martell "Stability Constants of Metal Ion Complexes", Alden Press, Oxford, 1971, No. 25.
14. H. Hoshino and T. Yotsuyanagi, *Talanta*, 1984, 37, 525.
15. L.C. Coombs and D.W. Margerum, *Inorg. Chem.*, 1970, 9, 1711.

16. H.C. Bajaj, (Ms) Madhu Phull and P.C. Nigam, Bull. Chem. Soc. Jpn., 1984, 57, 564.
17. D.D. Perrin and I.G. Sayce, Talanta, 1967, 14, 833.
18. A.E. Martell, "Critical Stability Constants", Plenum Press, New York and London, 1974, Vol. 1.
19. H.C. Bajaj and P.C. Nigam, Ind. J. Chem., 1984, 23A, 8.
20. R.M. Naik and P.C. Nigam, Ind. J. Chem., 1987, 26A, 205.
21. K. Kumar and P.C. Nigam, Inorg. Chem., 1981, 20, 1623.
22. H.C. Bajaj, K. Kumar and P.C. Nigam, Ind. J. Chem., 1981, 19A, 1070.

CHAPTER - IV

THE STUDY OF KINETICS AND MECHANISM OF LIGAND SUBSTITUTION REACTIONS OF $[PdPar(OH)]^-$ AND $[Cd(Par)_2]^{2-}$ WITH CYANIDE IONS BY STOPPED FLOW TECHNIQUE

ABSTRACT

The reaction of $[PdPar(OH)]^-$ with cyanide ion has been followed at 510 nm (λ_{max} of $[PdPar(OH)]^-$) while the reactions of $[Cd(Par)]$ and $[Cd(Par)_2]^{2-}$ with cyanide ions have been followed at 495 nm (λ_{max} of $[Cd(Par)]$ or $[Cd(Par)_2]^{2-}$) by stopped flow technique at $pH = 11.0 \pm 0.02$, $I = 0.1M(NaClO_4)$ and temperature = $25 \pm 0.1^\circ C$ under pseudo-first-order conditions taking cyanide in large excess (Par = 4-(2-pyridylazo)resorcinol). The reaction between $[PdPar(OH)]^-$ and cyanide ion followed first order kinetics each in $[CN^-]$ and $[PdPar(OH)]^-$. The reactions of $[Cd(Par)]$ and $[Cd(Par)_2]^{2-}$ with cyanide ions also followed first order kinetics in each reactant at higher cyanide concentrations. However, the reactions of $[PdPar(OH)]^-$ and $[Cd(Par)_2]^{2-}$ with cyanide ions

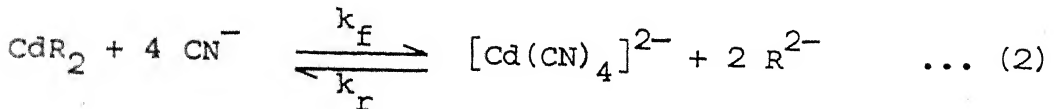
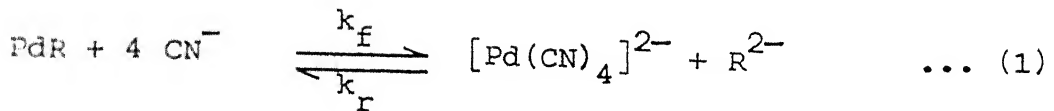
followed zero order dependences in $[CN^-]$ at extremely low cyanide concentration.

The reverse reaction between $[Pd(CN)_4]^{2-}$ and $[Cd(CN)_4]^{2-}$ with Par followed first order kinetics in each reactant and an inverse first order dependence in cyanide ion. It is inferred that the fourth step is the rate determining one in the proposed five step mechanistic scheme. Other studies viz. effect of ionic strength, pH dependence and temperature dependence are also conducted and support the proposed mechanism.

IV.1 INTRODUCTION

The kinetics of formation and dissociation reactions of mono- and bis- complexes of metal ions in aqueous solutions have been widely studied since the development of techniques for the study of fast reactions.¹ Kinetic investigations of the reactions of Ni(II) complexes have been undertaken by many workers. The formation of $[Ni(CN)_4]^{2-}$ from the reactions of $Ni(en)_2$, $Ni(dien)_2$ and $Ni(Par)_2$ with cyanide ion has been studied by Nigam et al.² Recently we have been investigating the kinetics and mechanism of reactions involving the exchange of polyaminocarboxylate ligands complexed to Ni(II)³ and Fe(III)⁴ by a monodentate ligand viz. cyanide ion. There are many studies on the substitution reactions of bis and binuclear complexes of Ni(II)^{2,5} and Fe(III).^{6,7} Relatively much less is known, so far, on the exchange reactions of Pd(II) and Cd(II).⁸

In the present investigation we report the kinetics of the reactions of PdR and CdR_2 with CN^- represented grossly by equations (1) and (2). Par is further abbreviated to R in the following narration.



k_f and k_r are the overall rate constants for the forward and reverse reactions. The reaction of CdR with cyanide is also investigated to provide further support for the mechanism proposed for the bis- complex reaction with cyanide.

IV.2 EXPERIMENTAL

The reagents were of AR(BDH) grade unless stated otherwise. The stock solution of $[\text{PdCl}_4]^{2-}$ was prepared by using a method given in literature⁹ and standardized gravimetrically by using dimethylglyoxime.¹⁰ Tetracyanopalladate(II) was prepared by using palladous chloride and potassium cyanide as starting materials.¹¹ A solution of tetracyanocadmate(II) was prepared according to the method of Brauer.¹² The mono complex PdR and CdR and the bis complex CdR_2 were prepared by mixing solutions containing stoichiometric amounts of $[\text{PdCl}_4]^{2-}$ or CdSO_4 with recrystallized sodium salt of Par (Reidel, Germany) respectively. Sodium cyanide was standardized argentometrically.¹³ Sodium

tetraborate, Boric acid and Sodium hydroxide were used to maintain desired pH wherever needed. NaClO_4 (E. Merck) was used to maintain the ionic strength.

A stopped flow spectrophotometer model SF-3A from Hitech (England) equipped with a storage oscilloscope model OS-768S of ECIL (India) was used for the study of both forward and reverse reactions. A polaroid camera was used to record the kinetic traces. All pH measurements were made on a digital pH meter model LI-120 from Elico (India) using BDH standard buffers for standardization. A Shimadzu double beam spectrophotometer model UV-240, with a circulatory arrangement for thermostating the cell compartment, was used for kinetic study. An ultracryostat model 2 NBE (VEB Kombinat Medizin and Labortechnik Kombinatsbetrieb) was used to maintain temperature of the reactants.

IV.3 KINETIC MEASUREMENTS

The ligand exchange reactions of $[\text{PdR(OH)}]^-$ with cyanide ions were followed at 510 nm (λ_{max} of $[\text{PdR(OH)}]^-$, $\epsilon = 3.34 \times 10^4 \text{ M}^{-1} \text{cm}^{-1}$) by monitoring the disappearance of $[\text{PdR(OH)}]^-$, over a pH range of 8.5-11.25. The reactions of $[\text{CdR}]$ and $[\text{CdR}_2]^{2-}$ with cyanide ions were followed at 495 nm (λ_{max} of $[\text{CdR}]$ or $[\text{CdR}_2]^{2-}$, $\epsilon_{\text{CdR}} = 3.2 \times 10^4 \text{ M}^{-1} \text{cm}^{-1}$, $\epsilon_{\text{CdR}_2} = 9.08 \times 10^4 \text{ M}^{-1} \text{cm}^{-1}$) by monitoring the disappearance of $[\text{CdR}_2]^{2-}$, over a pH range of 9.0-11.25. The forward reactions were run in the presence of a large excess of CN^- and all gave pseudo-first-order plots. At

these wavelengths, Par also absorbs appreciably, so corrections were applied to the absorbances of $[\text{PdR(OH)}]^-$ or $[\text{CdR}_2]^{2-}$ at this wavelength. A formula has been derived for calculation of the concentration of respective species (C_A) as given in equation (3).

$$C_A = \frac{A_t - C_A^0 \cdot \epsilon_B}{\epsilon_A - \epsilon_B} \quad \dots (3)$$

where A_t is the total absorbance, ϵ_A and ϵ_B are the respective molar extinction coefficients of the complex and Par respectively at that wavelength. C_A^0 is the initial concentration of respective complex species. The reverse reactions, that is the formations of $[\text{PdR(OH)}]^-$ and $[\text{CdR}_2]^{2-}$ from tetracyanopalladate(II) and tetracyanocadmide(II) with Par were also followed at 510 nm and 495 nm respectively because the spectra of $[\text{Pd}(\text{CN})_4]^{2-}$ and $[\text{Cd}(\text{CN})_4]^{2-}$ are almost featureless in visible region.

IV.4 RESULTS

IV.4.1 Reaction of $[\text{PdR(OH)}]^-$ with cyanide

The rate of formation of $[\text{Pd}(\text{CN})_4]^{2-}$ is first order each in $[\text{PdR(OH)}]^-$ and CN^- at $\text{pH} = 11.0$ and at relatively high cyanide concentration. The effect of concentration of cyanide can be seen in Fig. IV.1, where the slope of a plot of $\log k_{\text{obsd}}$ versus $\log [\text{CN}^-]_T$ gives the order of reaction in cyanide. $[\text{CN}^-]_T$ represents the total concentration present as HCN and CN^- .

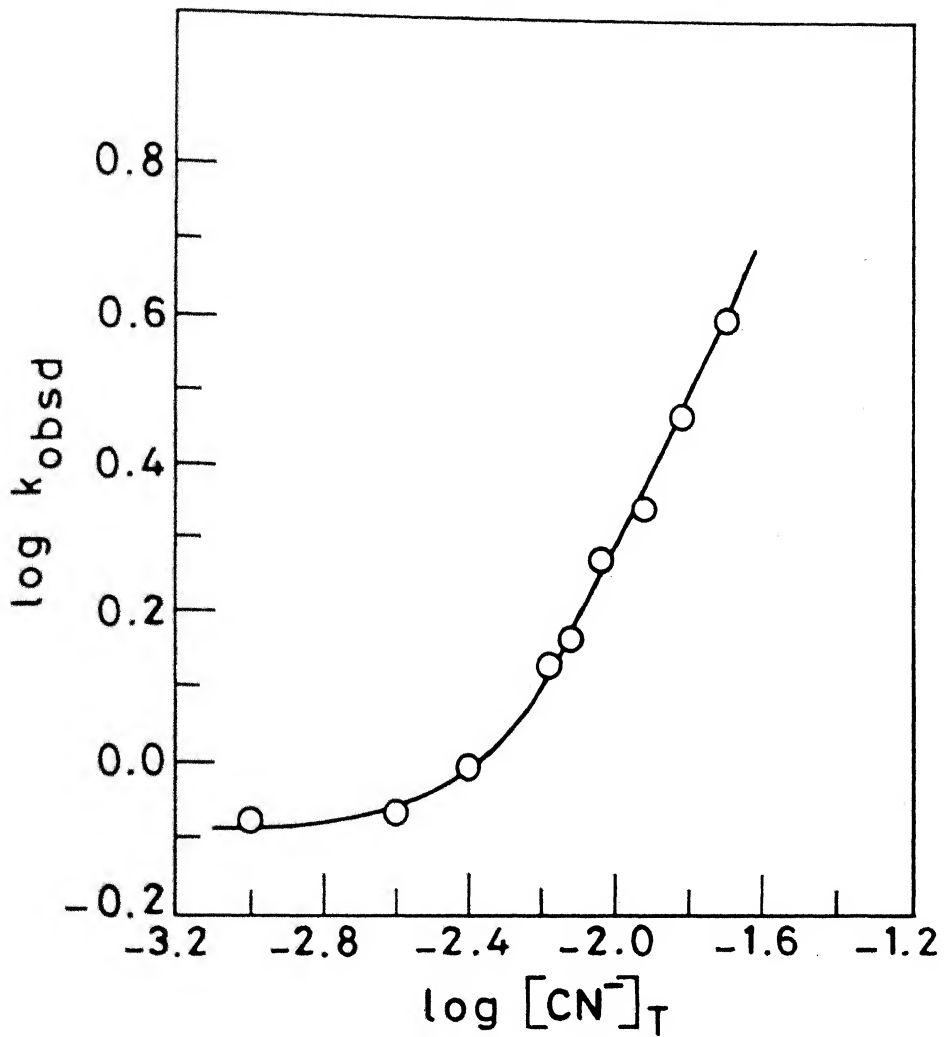
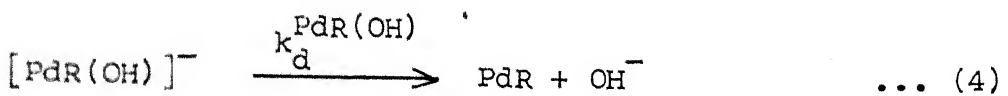


Fig. IV.1 Effect of cyanide concentration on the reaction of $[\text{PdR(OH)}]^-$ with cyanide ion. The reaction conditions as in Table IV.1.

Various rate constants are given in Table IV.1. The order in cyanide varies from zero at low cyanide concentration to one at higher cyanide concentration. The zero order dependence indicates a slow release of hydroxyl ions from the $[\text{PdR(OH)}]^-$ according to equation (4). This is followed by further reaction of $[\text{PdR}]$ with cyanide to give $[\text{Pd}(\text{CN})_4]^{2-}$. A similar dissociation of hydroxyl ion has been demonstrated in the case of $[\text{FeTTHA(OH)}_2]^{5-}$ cyanide reaction⁶ also.



Thus the rate expression has the form

$$\text{Rate} = \left\{ k_d^{\text{PdR(OH)}} + k'[\text{CN}^-] \right\} [\text{PdR(OH)}^-] \quad \dots (5)$$

and $k_{\text{obsd}} = k_d^{\text{PdR(OH)}} + k'[\text{CN}^-] \quad \dots (6)$

The values of the two constants on the right hand side of the equation (6) are $1.5 \times 10^{-1} \text{ s}^{-1}$ and $1.88 \times 10^2 \text{ M}^{-1} \text{s}^{-1}$ respectively at 25°C and $I = 0.1\text{M}(\text{NaClO}_4)$.

IV.4.2 Dependence of reaction rate of $[\text{PdR(OH)}]^-$ and CN^- on pH

An S-shaped curve is obtained when the reaction between $[\text{PdR(OH)}]^-$ and CN^- ion is followed in the pH range 8.5-11.25 (Fig. IV.2 and Table IV.2) with a levelling off at $\text{pH} \sim 11$. The pH profile in the lower range can be explained on the basis of

TABLE IV.1. Dependence of cyanide concentration on the reaction of $[\text{PdR(OH)}^-]$ and cyanide ion at $\text{pH} = 11.0 \pm 0.02$, temp. = $25 \pm 0.1^\circ\text{C}$ and $I = 0.1\text{M}(\text{NaClO}_4)$, $[\text{PdR(OH)}^-] = (1.0 - 4.0) \times 10^{-5}\text{M}$.

$[\text{CN}^-]_T, \text{M}$	$k_{\text{obsd}}, \text{s}^{-1}$	$10^{-2} \times k_f = k_{\text{obsd}} / [\text{CN}^-]_T, \text{M}^{-1} \text{s}^{-1}$
2.0×10^{-2}	3.98	1.99
1.5×10^{-2}	2.95	1.97
1.2×10^{-2}	2.19	1.83
9.12×10^{-3}	1.86	2.04
7.59×10^{-3}	1.45	1.91
6.61×10^{-3}	1.35	2.04
3.98×10^{-3}	0.99*	-
2.51×10^{-3}	0.74*	-
1.0×10^{-3}	0.76*	-

$$k_f(\text{av}) = (1.96 \pm 0.07) \times 10^2 \text{ M}^{-1} \text{s}^{-1}$$

*Zero order dependence in $[\text{CN}^-]$.

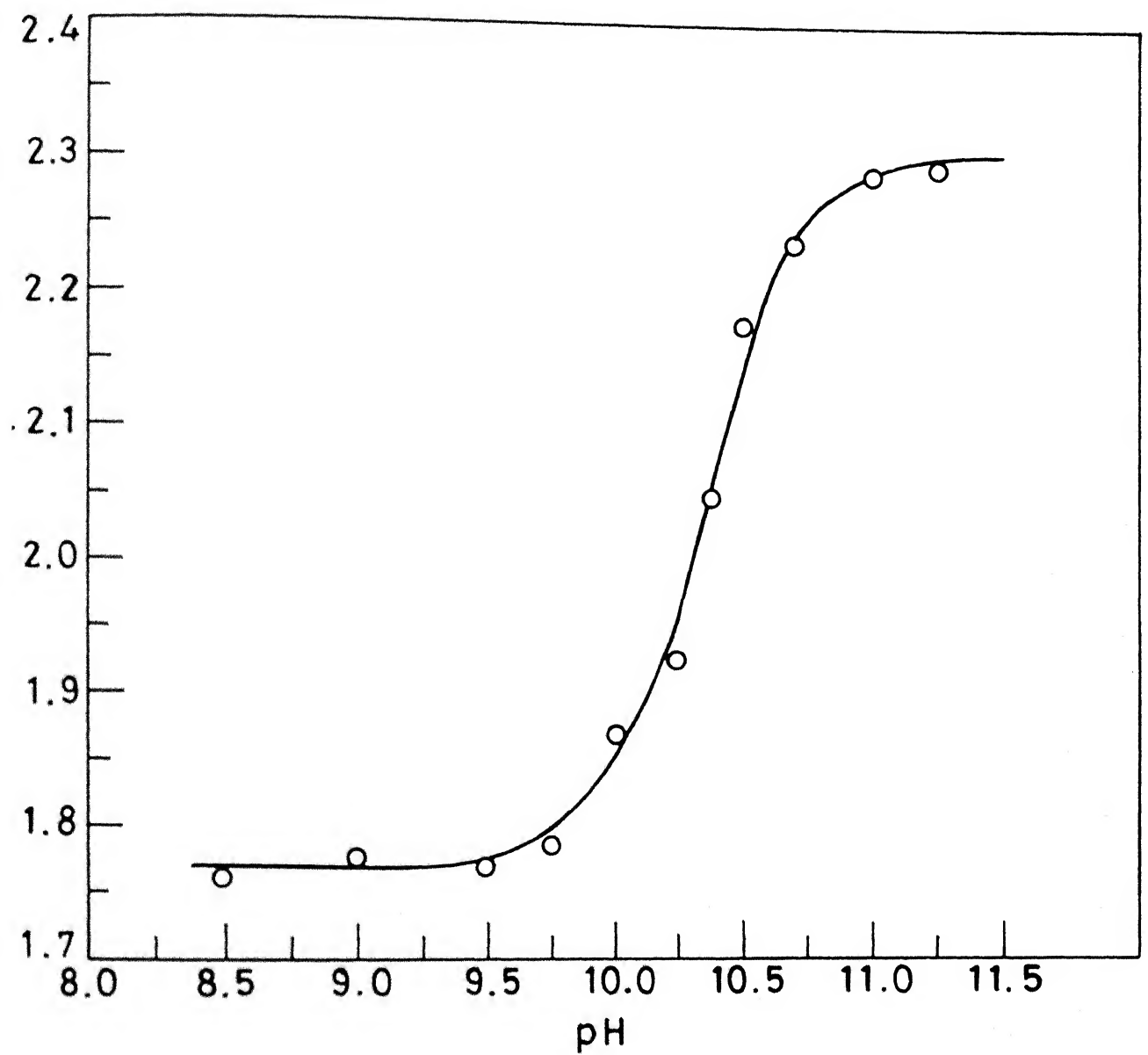


Fig. IV.2 Dependence of reaction rate of $[\text{PdR(OH)}^-]$ and cyanide ion on pH.

TABLE IV.2. Dependence of reaction rate of $[\text{PdR(OH)}^-]$ and CN^- on pH; $[\text{PdR(OH)}^-] = 4.0 \times 10^{-5} \text{M}$, $[\text{CN}^-] = 1.5 \times 10^{-2} \text{M}$, temp. = $25 \pm 0.1^\circ\text{C}$ and $I=0.1\text{M}(\text{NaClO}_4)$.

pH	$k_{\text{obsd}}, \text{s}^{-1}$	$k_f, \text{M}^{-1} \text{s}^{-1}$
8.5	8.63×10^{-1}	5.75×10^1
9.0	8.94×10^{-1}	5.96×10^1
9.5	8.84×10^{-1}	5.89×10^1
9.75	9.15×10^{-1}	6.1×10^1
10.0	1.11	7.41×10^1
10.25	1.26	8.41×10^1
10.38	1.68	1.12×10^2
10.5	2.27	1.51×10^2
10.7	2.61	1.74×10^2
11.0	2.95	1.97×10^2
11.25	2.96	1.97×10^2

different reactivities of HCN and CN^- . The levelling off of rate at pH above 10.75 appears to be due to polymerization of $[\text{PdR(OH)}]^-$ species¹⁴ at high pH.

A rate expression consistent with these observations can be written in the form of equation (7).

$$k_f [\text{CN}]_T / [\text{CN}^-] = k_{\text{CN}} + k_{\text{HCN}} K_{\text{HCN}} [\text{H}^+] \quad \dots (7)$$

where $[\text{CN}]_T / [\text{CN}^-] = 1 + K_{\text{HCN}} [\text{H}^+]$ and K_{HCN} is the protonation constant of cyanide ($\log K_{\text{HCN}} = 9.2$ at 25°C and $I = 0.1\text{M}$).¹⁵ By plotting left hand side of equation (7) versus $[\text{H}^+]$, one gets a straight line. One can calculate k_{CN} and k_{HCN} from the intercept and the slope respectively (Fig. IV.3). Their respective values are $7.0 \times 10^1 \text{ M}^{-1}\text{s}^{-1}$ and $5.5 \times 10^1 \text{ M}^{-1}\text{s}^{-1}$.

IV.4.3 Reaction of $[\text{CdR}_2]^{2-}$ with cyanide

The exchange reaction of $[\text{CdR}_2]^{2-}$ with cyanide ions and vice versa were followed at 495 nm. The rate of decay of CdR_2 is first order each in $[\text{CdR}_2]^{2-}$ and $[\text{CN}]^-$ over a wide range of cyanide concentration always present in excess. The effect of variation of cyanide can be seen in Fig. IV.4, where the slope of a plot of $\log k_{\text{obsd}}$ versus $\log [\text{CN}^-]$ gives the order with respect to cyanide ion. A significant feature of this curve is that at low cyanide concentration the plot tends towards zero order dependence in cyanide. This observation indicates the slow dissociation of the bis- complex according to equation (8).

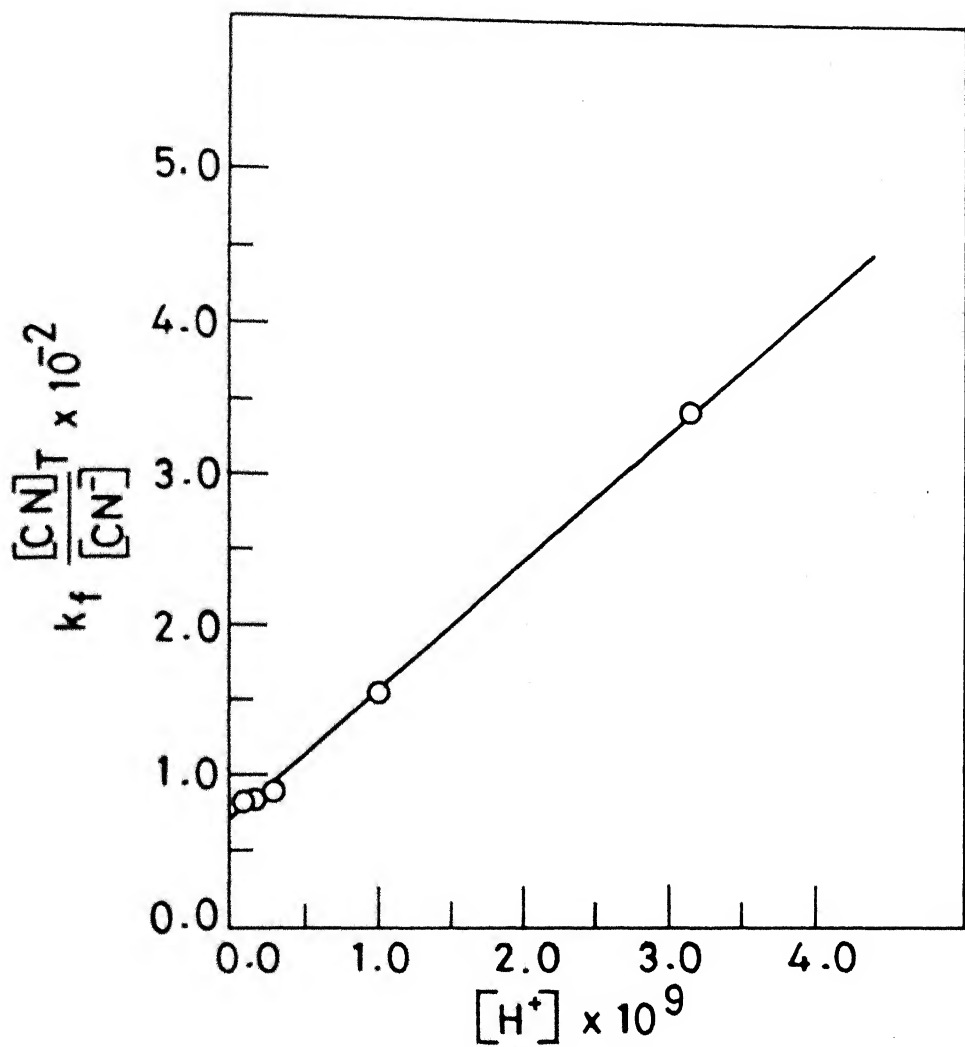
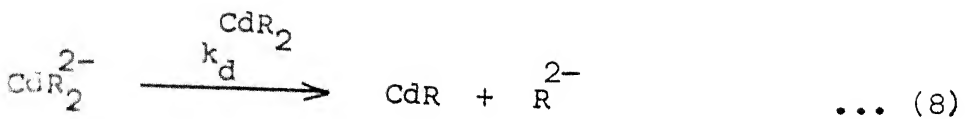
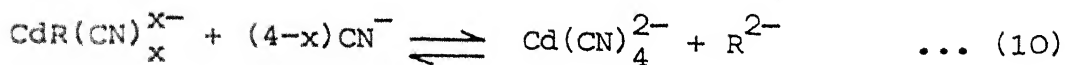
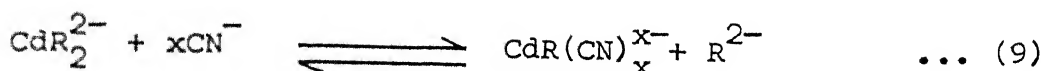


Fig. IV.3 Resolution of rate constants k_{CN} and k_{HCN} for the reaction of $[PdR(OH)]^-$ with cyanide ion.



At higher concentration of cyanides however, a first order dependence in cyanide has been observed (Table IV.3, Fig. IV.4). This points to a faster cyanide assisted dissociation of CdR_2 according to equation (9)



The observed rate constant, k_{obsd} , can be written as

$$k_{\text{obsd}} = k_d \text{CdR}_2^{2-} + k'[\text{CN}^-] \dots (11)$$

The monocomplex $[\text{CdR}]$ also reacts with excess cyanide following first order kinetics with respect to cyanide. The rate constants are comparable with those of substitution reaction of the bis complex (Fig. IV.4) in the same concentration range. This leads to the conclusion that the rate determining step is the same in both reactions. The observed rate constants are given in Table IV.3.

IV.4.4 Dependence of reaction rate on pH

The reaction rates of $[\text{CdR}_2]^{2-}$ and $[\text{CdR}]$ with CN^- ion are found to decrease with increase of pH from 9.0 to 10.5 and

TABLE IV.3. Cyanide dependence for (a) $[CdR_2]^{2-} - CN^-$ and (b) $[CdR] - CN^-$ reactions.

(a) $[Cd^{2+}] = 5 \times 10^{-6} M$, $[Par] = 1 \times 10^{-5} M$
 (b) $[Cd^{2+}] = 1 \times 10^{-5} M$, $[Par] = 1 \times 10^{-5} M$

pH = 11.0 \pm 0.02, temp. = 25 \pm 0.1°C, I = 0.1M(NaClO₄).

$[CN^-]_T, M$	Cd(Par) 2			Cd(Par)		
	$10^1 \times k_{obsd}, s^{-1}$	$10^{-2} \times k_F, M^{-1} s^{-1}$	$10^1 \times k_{obsd}, s^{-1}$	$10^{-2} \times k_F, M^{-1} s^{-1}$	$10^1 \times k_{obsd}, s^{-1}$	$10^{-2} \times k_F, M^{-1} s^{-1}$
1.5×10^{-2}	25	1.7	16	1.0	—	—
1.12×10^{-2}	19	1.7	—	—	—	—
9.0×10^{-3}	16	1.8	9.9	1.1	—	—
7.5×10^{-3}	14	1.9	8.0	1.1	—	—
5.0×10^{-3}	8.9	1.8	5.1	1.0	—	—
4.0×10^{-3}	7.4	1.9	—	—	—	—
2.5×10^{-3}	—	—	2.7	1.1	—	—
2.0×10^{-3}	—	—	—	—	—	—
8.0×10^{-4}	—	—	—	—	—	—
5.0×10^{-4}	—	—	—	—	—	—
2.0×10^{-4}	—	—	—	—	—	—
	$3 \cdot 8 \cdot k_F^{(av)} = (1.8 \pm 0.1) \times 10^2 M^{-1} s^{-1}$	—	$k_F^{(av)} = (1.06 \pm 0.05) \times 10^2 M^{-1} s^{-1}$	—	—	—

* Zero order dependence in $[CN^-]$.

the remain almost constant (Fig. IV.5, Table IV.4). The reactions were studied in presence of excess cyanide where order in cyanide is unity. Using rate data between pH 9 and 10 and adopting a procedure similar to that described in section IV.4.2, it has been possible to resolve the rates due to reaction of protonated form of cadmium complex with CN^- and HCN. The graphical resolution is given in Fig. IV.6. The values of k_{CN} and k_{HCN} are found to be $2.0 \times 10^2 \text{ M}^{-1} \text{s}^{-1}$ and $4.9 \times 10^2 \text{ M}^{-1} \text{s}^{-1}$ respectively. The rate data above pH 10 is analysed in the following manner. At pH > 10 cyanide is present mainly as CN^- ($\text{pK}_a = 9.2$) while the cadmium complex is present as CdHR and CdR ($\text{pK}_a = 10.5$)¹⁹

$$\text{Rate} = k_f [\text{CdR}]_T [\text{CN}^-].$$

$$= \{ [k_{\text{CdR}} [\text{CdR}] + k_{\text{CdHR}} [\text{CdHR}] \} [\text{CN}^-] \quad \dots (12)$$

$$\text{where } [\text{CdR}]_T = [\text{CdR}] + [\text{CdHR}]$$

$$= [\text{CdR}] \{ 1 + k_{\text{CdHR}} [\text{H}^+] \}$$

$$\text{Therefore, } [\text{CdR}]_T / [\text{CdR}] = \{ 1 + k_{\text{CdHR}} [\text{H}^+] \}$$

Thus equation (12) is transformed to equation (13)

$$k_f [\text{CdR}]_T / [\text{CdR}] = \{ k_{\text{CN}}^{\text{CdR}} + k_{\text{CN}}^{\text{CdHR}} \cdot k_{\text{CdHR}} \cdot [\text{H}^+] \} \quad \dots (13)$$

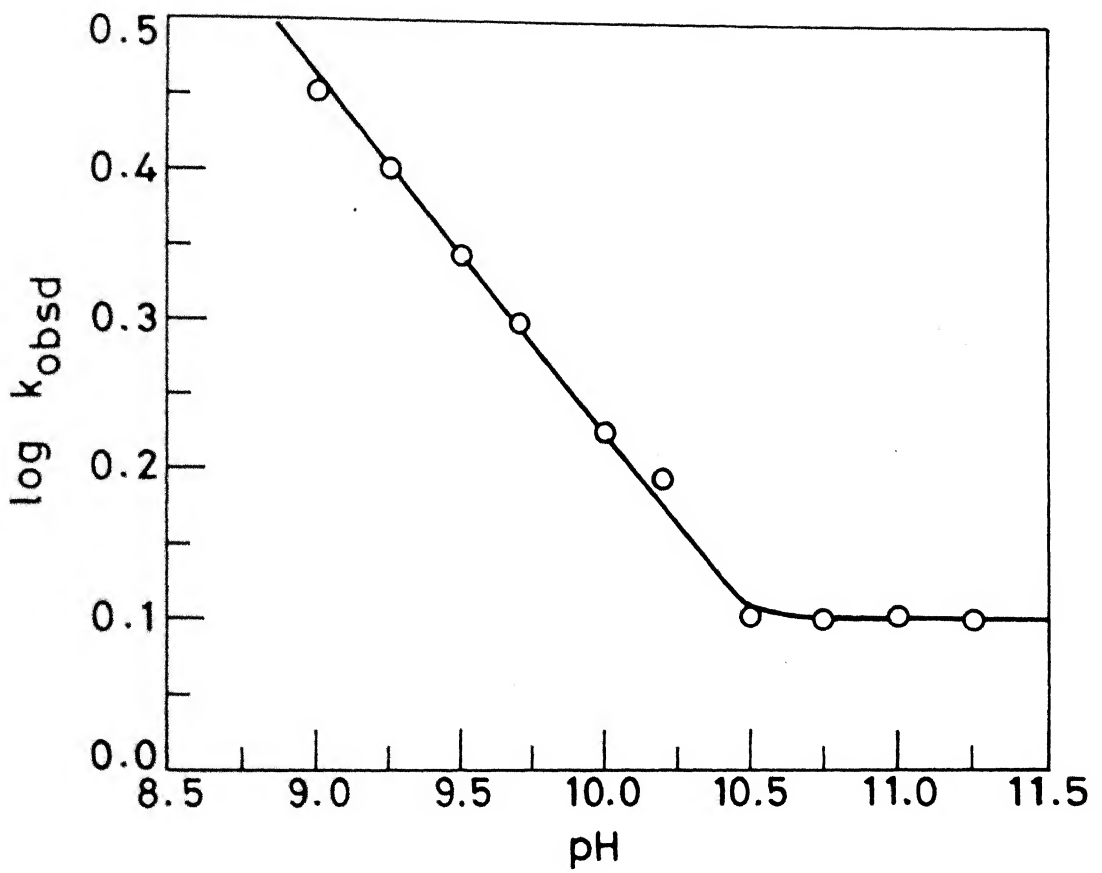


Fig. IV.5 Effect of pH on the reaction of $[\text{CdR}_2]^{2-}$ with cyanide.

TABLE IV.4. Effect of pH on the rate constants of $[\text{CdR}_2]^{2-}-\text{CN}^-$ and $[\text{CdR}]-\text{CN}^-$ reaction at temp. = $25 \pm 0.1^\circ\text{C}$ and I = 0.1M(NaClO_4).

pH	CdR_2-CN^- System		$\text{CdR}-\text{CN}^-$ System	
	$k_{\text{obsd}} \text{ s}^{-1}$	$10^2 \times k_f \text{ M}^{-1} \text{s}^{-1}$	$k_{\text{obsd}} \text{ s}^{-1}$	$10^2 \times k_f \text{ M}^{-1} \text{s}^{-1}$
8.5	-	-	1.4	1.9
9.0	2.8	3.8	1.2	1.6
9.25	2.5	3.4	1.1	1.4
9.5	2.2	3.0	-	-
9.7	2.0	2.7	-	-
10.0	1.7	2.2	9.7×10^{-1}	1.3
10.2	1.6	2.1	-	-
10.5	1.3	1.7	8.7×10^{-1}	1.2
10.75	1.3	1.7	8.4×10^{-1}	1.1
11.0	1.3	1.7	8.3×10^{-1}	1.1
11.25	1.3	1.7	-	-

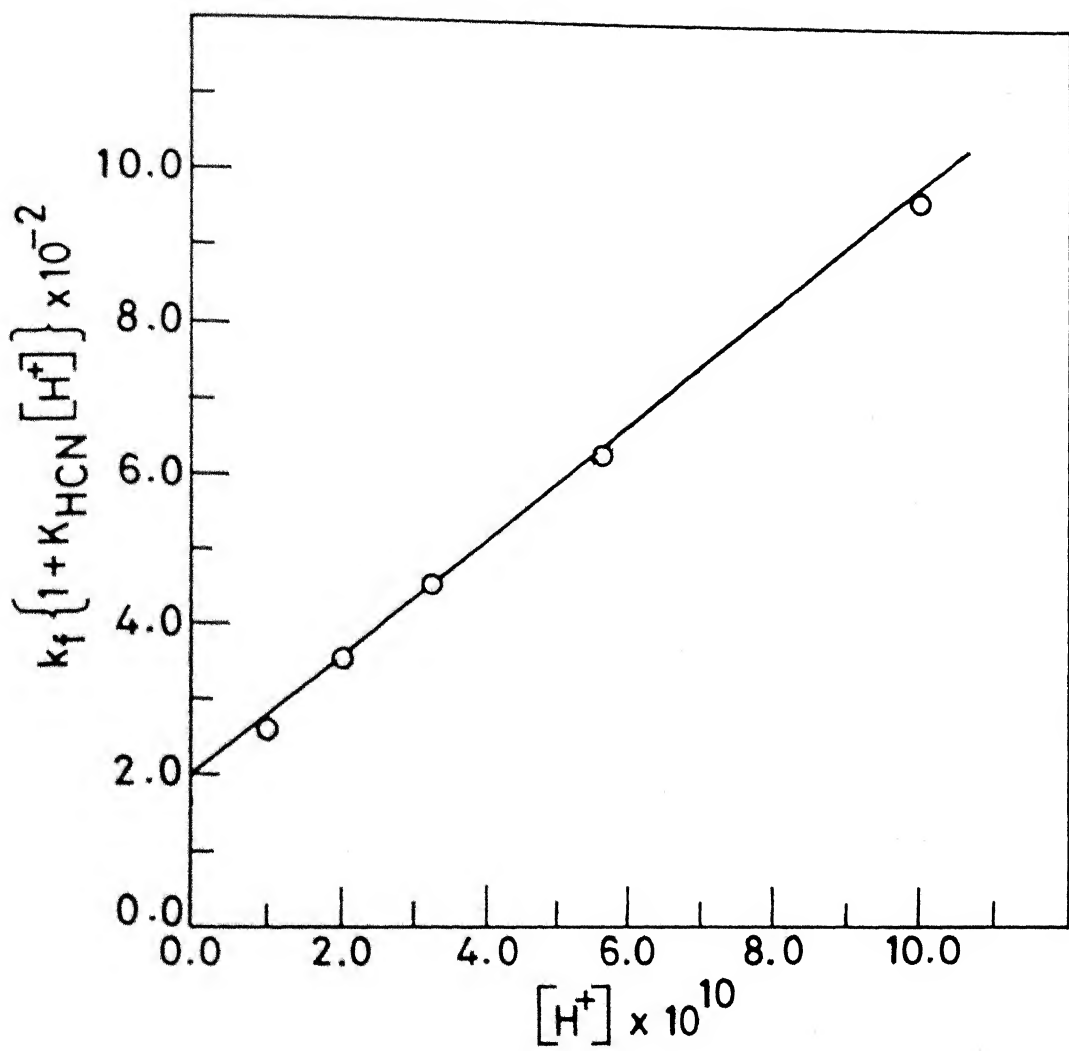


Fig. IV.6 Resolution of rate constants for the reaction of $[\text{CdR}_2]^{2-}$ with cyanide.

Transposing and dividing throughout by $[H^+]$, one obtains

$$k_f \left\{ 1 + K_{CdHR} [H^+] \right\} \frac{1}{[H^+]} - k_{CN}^{CdHR} \cdot K_{CdHR} = k_{CN}^{CdR} \cdot \frac{1}{[H^+]} \quad \dots (14)$$

By plotting left hand side of equation (14) versus $1/[H^+]$, one gets a straight line passing through the origin (Fig. IV.7). A slope of this line gives the value of k_{CN}^{CdR} as $1.6 \times 10^2 \text{ M}^{-1} \text{s}^{-1}$. All the three constants are included in Table IV.8.

It is interesting to note that the reactivity of HCN is greater than CN^- towards Par complexes of Cd(II) as in the case of $NiPar_2 - CN^-$ reaction while in case of $NiL_2 - CN^-$ reaction (L = polyaminocarboxylates) the reactivity order is reversed. It may also be mentioned that the reactivities of CdHPar is slightly higher than that of CdPar complex.

IV.4.5 Kinetics of reverse reaction

The stability constant of $[Pd(CN)_4]^{2-}$ and $[Cd(CN)_4]^{2-}$ are much greater than those of $[PdR(OH)]^-$, $[CdR]$ and $[CdR_2]^{2-}$ complexes ($\log \beta_4$ of $[Pd(CN)_4]^{2-} = 42^{16}$ and $\log \beta_4$ of $[Cd(CN)_4]^{2-} = 19^{17}$, $\log K_{PdR} = 4.9^{18}$ and $\log \beta_2$ of $CdR_2 = 17.5^{19}$). It becomes possible to force the reverse reactions only by using a sufficiently high concentration of Par. As Par does not obey Lambert-Beer's law at concentration higher than 10^{-4} M , low concentration of $[Pd(CN)_4]^{2-}$ and $[Cd(CN)_4]^{2-}$ ($\sim 2 \times 10^{-6} \text{ M}$) were taken in order to maintain pseudo-first-order conditions. The rate law for reverse reaction has been written as rate of decay of $[Pd(CN)_4]^{2-}/[Cd(CN)_4]^{2-}$ as given in equation (15).

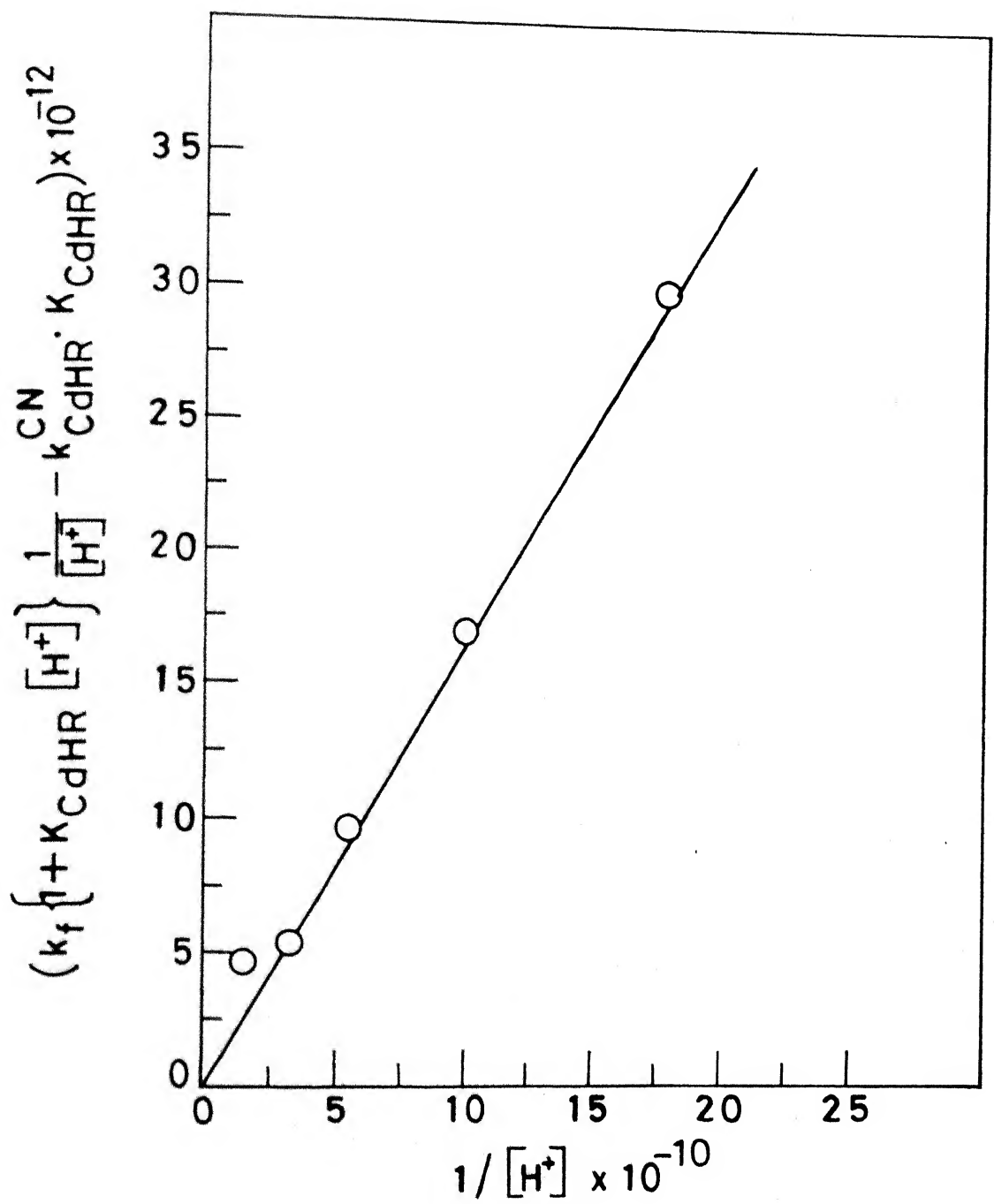
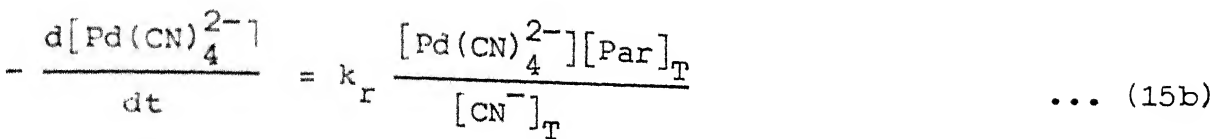
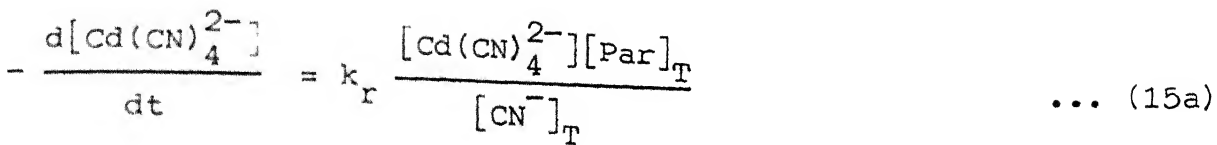


Fig. IV.7 Resolution of rate constant $k_{\text{CdR}}^{\text{CN}}$.



The integrated rate equation in terms of the absorbances of $[\text{CdR}_2]^{2-}$ or $[\text{PdR(OH)}]^-$ at their respective λ_{max} can be formulated as given in equation (16)

$$(A_t - A_0) + (A_\infty - A_0) \ln \frac{A_\infty - A_t}{A_\infty - A_0} = - \frac{\epsilon \cdot l}{4} \cdot k'_{\text{obsd}} \cdot t \dots (16)$$

where A_0 is the initial absorbance due to Par. A_t and A_∞ are the absorbances at time t and after completion of reaction respectively. ϵ is the molar extinction coefficient of $[\text{PdR(OH)}]^-$ or $[\text{CdR}_2]^{2-}$ and l is the path length. By plotting left hand side of equation (16) versus t , one gets a straight line (Fig. IV.8) by which one can calculate k'_{obsd} and hence k_r ($k_r = k'_{\text{obsd}} / [\text{Par}]_T$). The values are given in Table IV.5.

IV.4.6 Dependence of forward rate on ionic strength

The forward rates for both reactions have been studied at different ionic strengths by adding different amounts of sodium perchlorate. The Bronsted-Bjerrum equation was obeyed by these reactions. The value of the product $Z_A Z_B$ have been calculated for both reactions (Fig. IV.9; IV.10 and Table IV.6).

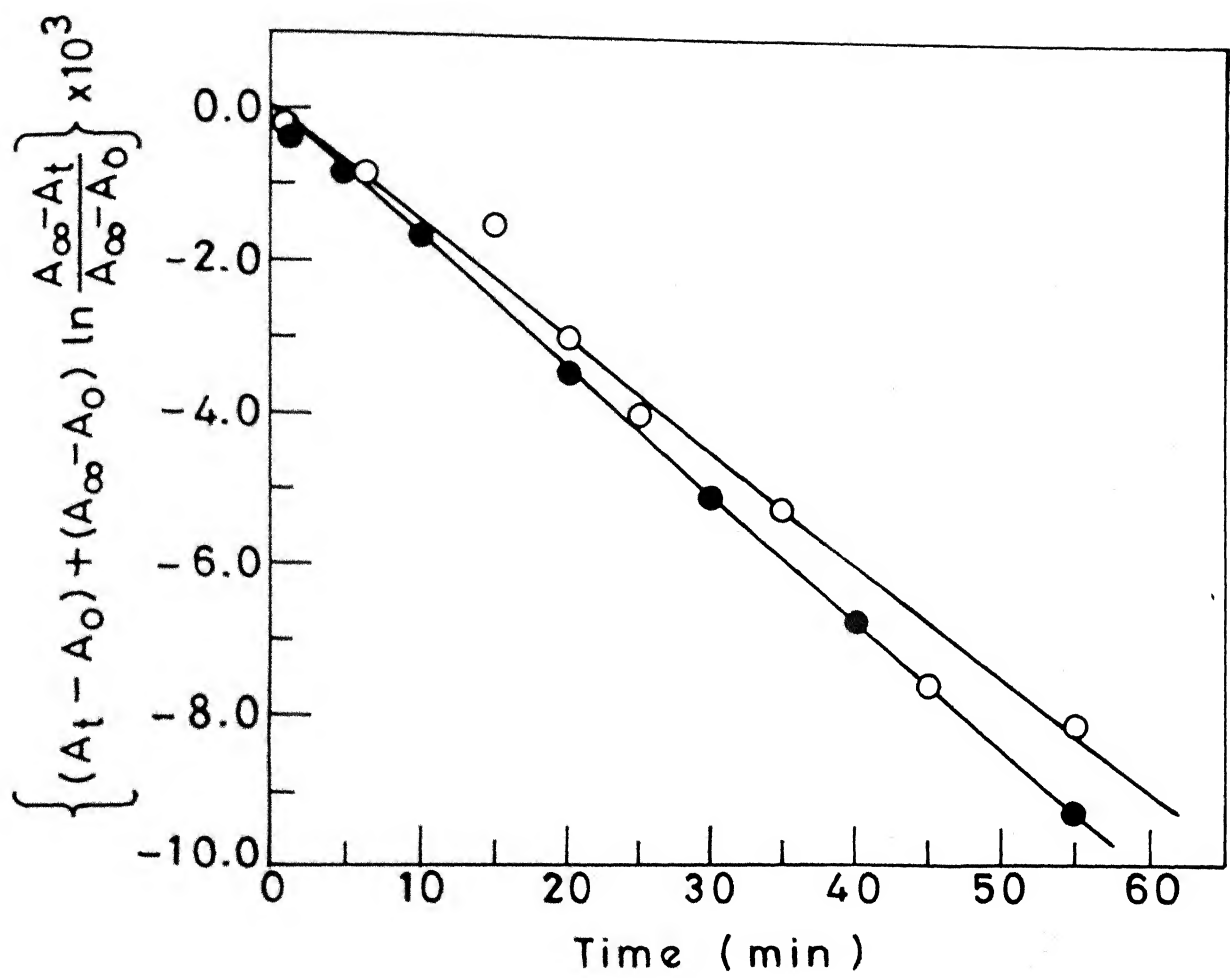


Fig. IV.8 Inverse first order plots for the reaction of $[\text{Pd}(\text{CN})_4]^{2-}$ (○) and $[\text{Cd}(\text{CN})_4]^{2-}$ (●) with par reaction conditions as in table IV.5.

TABLE IV.5. Kinetics of reverse reactions.

pH = 9.0 \pm 0.02, I = 0.1M(NaClO₄).

$10^5 \times [\text{Par}]_T, \text{M}$	$10^{10} \times k'_{\text{obsd}}, \text{Ms}^{-1}$	$10^6 \times k_r = k'_{\text{obsd}} / [\text{Par}]_T, \text{s}^{-1}$
--	---	--

(A) $[\text{Pd}(\text{CN})_4^{2-}] = 1.33 \times 10^{-6} \text{M}$, temp. = $40 \pm 0.1^\circ\text{C}$.

3.0	1.1	3.7
5.0	1.9	3.8
7.5	3.0	4.0
9.0	3.4	3.8

$$k_r(\text{av}) = (3.8 \pm 0.1) \times 10^{-6}, \text{s}^{-1}$$

(B) $[\text{Cd}(\text{CN})_4^{2-}] = 2.0 \times 10^{-6} \text{M}$, temp. = $30 \pm 0.1^\circ\text{C}$.

4.0	0.76	1.9
6.66	1.1	1.7
7.5	1.2	1.6
9.0	1.6	1.8

$$k_r(\text{av}) = (1.8 \pm 0.1) \times 10^{-6}, \text{s}^{-1}$$

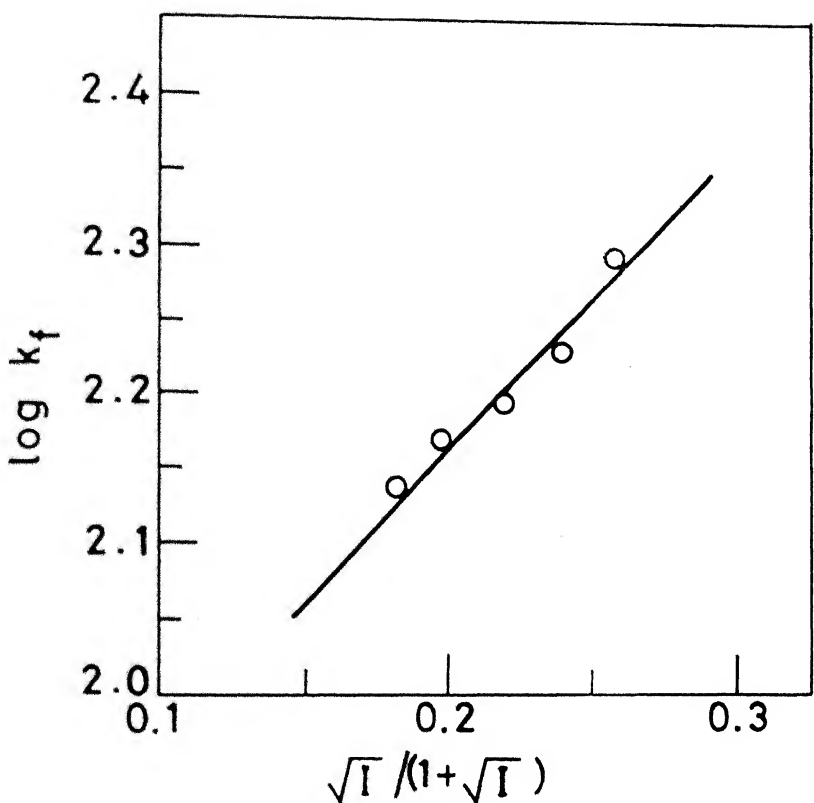


Fig. IV.9 Dependence of forward rate on ionic strength for the reaction of $[\text{CdR}_2]^{2-}-\text{CN}^-$. Reaction conditions as in Table IV.6.

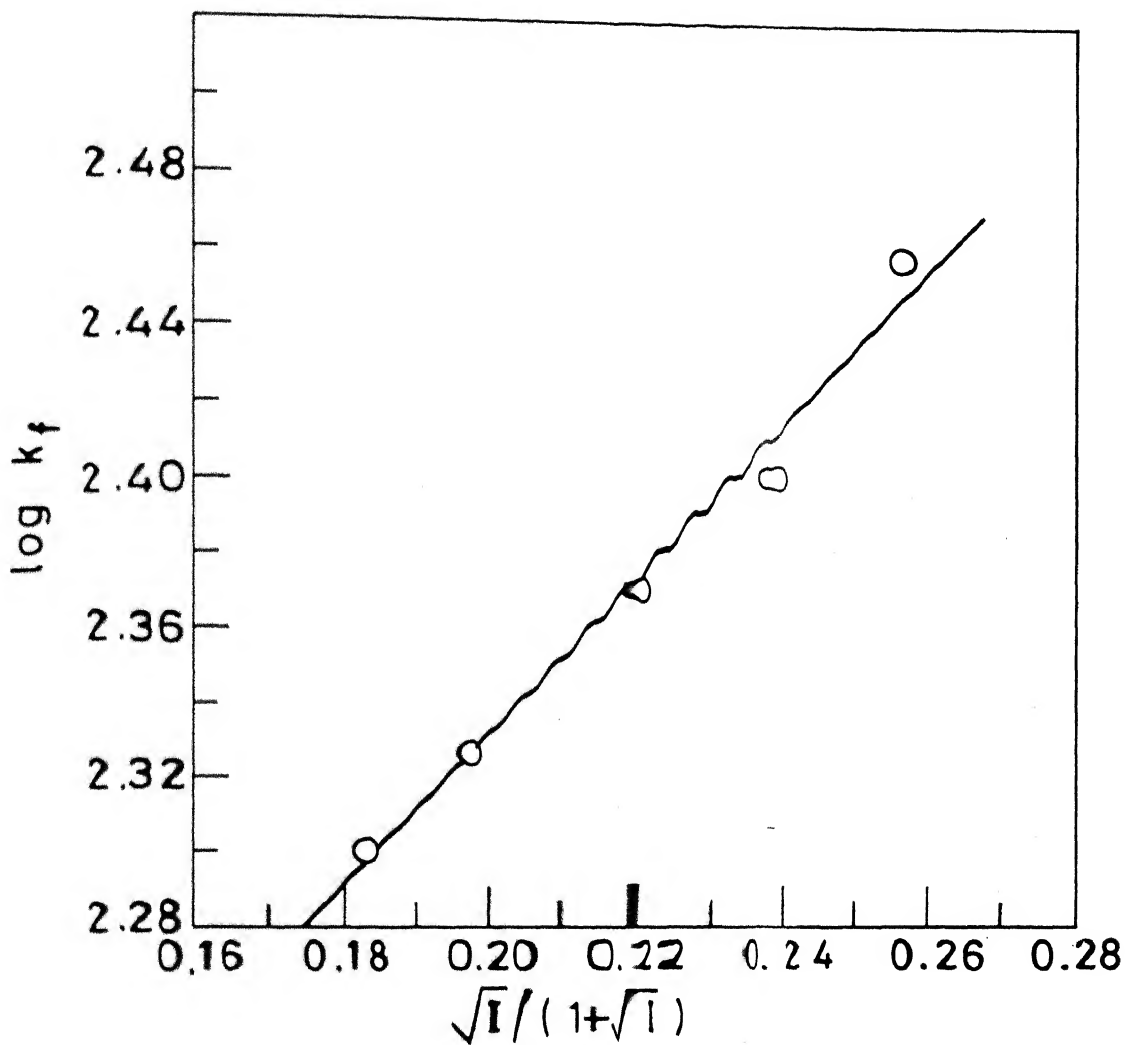


Fig. IV.10 Dependence of forward rate on ionic strength for the reaction of $[\text{PdR(OH)}]^- - \text{CN}$.

TABLE IV.6. Effect of ionic strength on the forward reaction rate.

I, M(NaClO ₄)	k_{obsd} , s ⁻¹	$10^{-2} \times k_f$, M ⁻¹ s ⁻¹
(i) [PdR(OH) ⁻] = 4.0×10^{-5} M, [CN ⁻] = 1.5×10^{-2} M, pH = 11.0 ± 0.02 , temp. = $30 \pm 0.1^\circ\text{C}$.		
0.05	3.0	2.0
0.06	3.2	2.1
0.08	3.5	2.4
0.1	3.7	2.5
0.12	4.3	2.9
(ii) [CdR ₂ ²⁻] = 5.0×10^{-6} M, [CN ⁻] = 7.5×10^{-3} M, pH = 11.0 ± 0.02 , temp. = $25 \pm 0.1^\circ\text{C}$.		
0.05	1.0	1.4
0.06	1.1	1.5
0.08	1.2	1.6
0.1	1.4	1.9
0.12	1.5	2.0

TABLE IV.7. Activation parameters.

A. $[\text{PdR(OH)}]^{2-}$ - CN^- System

Forward Reaction:

Zero order dependence

$$\Delta H^{\circ\ddagger} = 67.1 \pm 1.3 \text{ kJ mol}^{-1}$$

$$\Delta S^{\circ\ddagger} = -21.7 \pm 4.5 \text{ JK}^{-1} \text{mol}^{-1}$$

First order dependence

$$16.6 \pm 1.0 \text{ kJ mol}^{-1}$$

$$-146.0 \pm 3.4 \text{ JK}^{-1} \text{mol}^{-1}$$

Reverse Reaction:

$$\Delta H^{\circ\ddagger} = 37.7 \pm 1.1 \text{ kJ mol}^{-1}$$

$$\Delta S^{\circ\ddagger} = -224 \pm 4.0 \text{ JK}^{-1} \text{mol}^{-1}$$

B. $[\text{CdR}_2]^{2-}$ - CN^- System

Forward Reaction:

Zero order dependence

$$\Delta H^{\circ\ddagger} = 39.7 \pm 1.0 \text{ kJ mol}^{-1}$$

$$\Delta S^{\circ\ddagger} = -120.1 \pm 3.3 \text{ JK}^{-1} \text{mol}^{-1}$$

First order dependence

$$14.6 \pm 0.3 \text{ kJ mol}^{-1}$$

$$-153.3 \pm 0.9 \text{ JK}^{-1} \text{mol}^{-1}$$

Reverse Reaction:

$$\Delta H^{\circ\ddagger} = 13.1 \pm 1.0 \text{ kJ mol}^{-1}$$

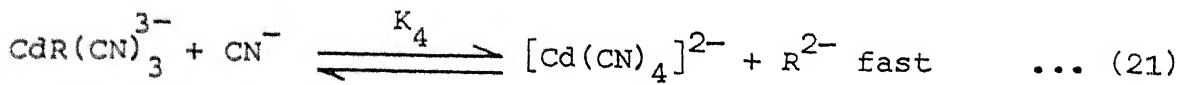
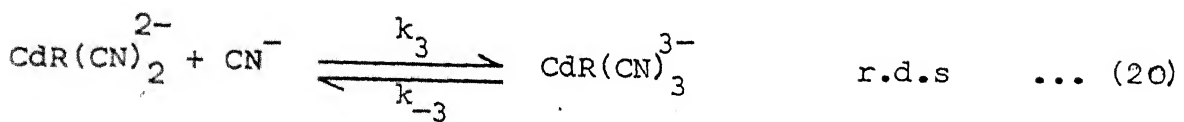
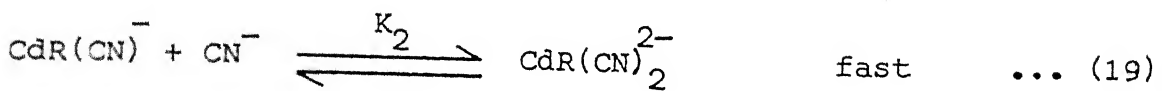
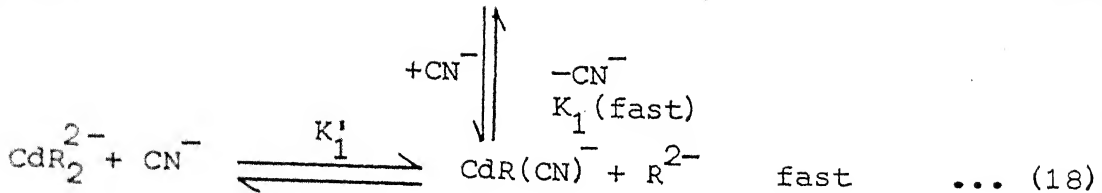
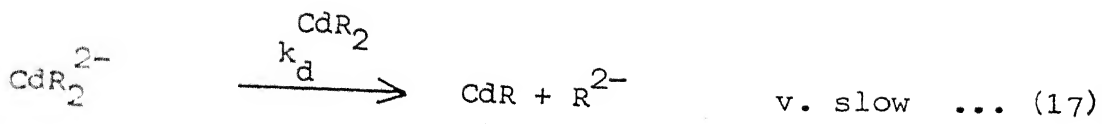
$$\Delta S^{\circ\ddagger} = -305.1 \pm 1.8 \text{ JK}^{-1} \text{mol}^{-1}$$

IV.4.7 Activation parameters of the forward and reverse reaction rates

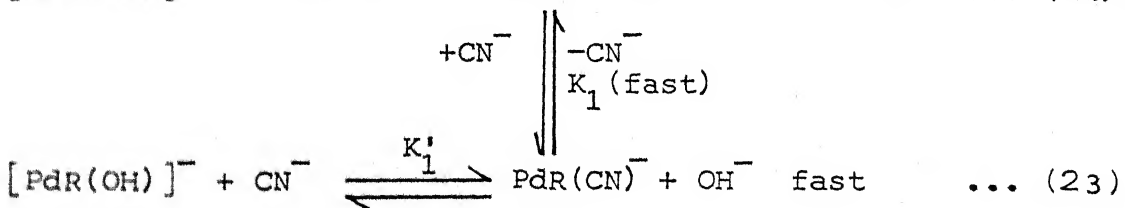
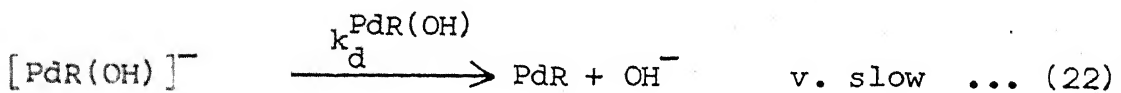
The forward and reverse reactions have been studied over a temperature range of 25-45°C. The Arrhenius equation was obeyed by both forward and reverse reactions. The activation parameters have been calculated for the situations where dependence on cyanide is zero and one respectively. These data are given in Table IV.7. The activation parameters for the reverse reaction are also included in the same table.

IV.5 DISCUSSION

It has been demonstrated (vide infra) that in the forward reactions of both $[\text{CdPar}_2]^{2-}$ and $[\text{PdPar}(\text{OH})]^-$, a zero order dependence in cyanide at low concentration and a first order dependence at high concentration has been observed. In the reverse reactions, first order dependence each in $[\text{Cd}(\text{CN})_4]^{2-}$ / $[\text{Pd}(\text{CN})_4]^{2-}$ and Par while an inverse first order dependence in cyanide have been exhibited. This inverse first order dependence shows that the penultimate step is rate determining. A combination of forward and reverse rates points to a stepwise mechanism, for the octahedral-tetrahedral transformation or vice versa, given from equations 17-21.



In the case of $[\text{PdR(OH)}]^-$ reaction, however, the first step constitutes the slow dissociation of hydroxyl group followed by second rapid step according to equations 22 and 23 respectively.



The evidence for release of OH^- is provided by a slight but definite increase in pH when the reaction is carried out in unbuffered medium. Reactions 22 and 23 are followed by three step similar to reactions 19-21 of $\text{CdPar}_2-\text{CN}^-$ reaction. An important feature of both reactions is the cyanide assisted fast dissociations of CdPar_2 and PdR(OH) according to equations 18 and 23.

Similar stepwise mechanisms, as proposed herein, have been proposed for the reactions of bis and binuclear complexes of NiL_2^2 and $\text{Ni}_2\text{L}^{5,20-22}$ (L = polyaminocarboxylates or polyamines), NiPar_2^2 (Par = 4-(2-pyridylazo)resorcinol) and $\text{Fe}_2\text{L}^{23,24}$ (L = polyaminocarboxylates) with cyanide ions. Though a variable order dependence in cyanide ranging from zero to three is expected, as in the case of reactions cited above, we could observe only a zero order and first order dependence in cyanide in both reactions. This may happen due to the immediate formation of the stable intermediates $\text{CdR}(\text{CN})_2$ or $\text{PdR}(\text{CN})_2$. The point will be discussed later.

A steady state treatment on intermediate species $[\text{CdR}(\text{CN})_3]^{3-}$, $[\text{CdR}(\text{CN})_2]^{2-}$, $[\text{CdR}(\text{CN})]^{1-}$ and $[\text{CdR}]$ and a consideration of dissociation of $[\text{CdR}_2]^{2-}$ gives a rate expression (24).

$$\text{Rate} = k_d^{\text{CdR}_2} [\text{CdR}_2^{2-}] + \frac{k_1^* k_2 k_3 [\text{CN}^-]^3 [\text{CdR}_2^{2-}]}{1 + k_1^* [\text{CN}^-] + k_1^* k_2 [\text{CN}^-]^2} \quad \dots (24)$$

This expression reduces to a third, second and first order dependence in cyanide concentration at low, medium and high cyanide concentrations respectively. The first term in equation (24) corresponds to $[\text{Cd}(\text{CN})_4^{2-}]$ formation from dissociation of CdR_2 according to equation (17). A rate expression for $[\text{PdR}(\text{OH})]^-$ reaction can also be derived in a similar manner.

One can proceed now to derive the experimental rate law for the reverse reaction also by applying steady state treatment to the

intermediate produced in the rate determining step, viz., $[CdR(CN)_3]^{3-}$. Rate of formation of this intermediate is given by equation (25), which may be set equal to zero. Thus,

$$\begin{aligned}
 -d[CdR(CN)_3^{3-}]/dt &= k_3[CdR(CN)_2^{2-}][CN^-] - k_{-3}[CdR(CN)_3^{3-}] \\
 &\quad + k_{-4}[Cd(CN)_4^{2-}][R^{2-}] - k_4[CdR(CN)_3^{3-}][CN^-] \\
 &= 0 \quad \dots (25)
 \end{aligned}$$

$$\text{so } [CdR(CN)_3^{3-}] = \frac{k_3[CdR(CN)_2^{2-}][CN^-] + k_{-4}[Cd(CN)_4^{2-}][R^{2-}]}{k_4[CN^-] + k_{-3}} \quad \dots (26)$$

$$\begin{aligned}
 -d[Cd(CN)_4^{2-}]/dt &= k_{-3}[CdR(CN)_3^{3-}] \\
 &= \frac{k_{-3}\{k_3[CdR(CN)_2^{2-}][CN^-] + k_{-4}[Cd(CN)_4^{2-}][R^{2-}]\}}{k_4[CN^-] + k_{-3}} \\
 & \quad \dots (27)
 \end{aligned}$$

In presence of excess Par, the first term in the numerator can be ignored. In the proposed kinetic scheme it has been assumed that the fifth step is fast compared to the fourth one and value of k_4 (also k_{-4}) must be quite large compared to k_{-3} . Thus even though $[CN^-]$ may be small, $k_4[CN^-]$ may still be quite large compared to k_{-3} which may be omitted in the denominator. With these assumptions equation (27) reduces to equation (28):

$$\begin{aligned}
 \text{Rate} = -d[\text{Cd}(\text{CN})_4^{2-}]/dt &= \frac{k_{-3} K_4^{-1} [\text{Cd}(\text{CN})_4^{2-}] [\text{R}^{2-}]}{[\text{CN}^-]} \\
 &= \frac{k_r [\text{Cd}(\text{CN})_4^{2-}] [\text{R}^{2-}]}{[\text{CN}^-]} \quad \dots (28)
 \end{aligned}$$

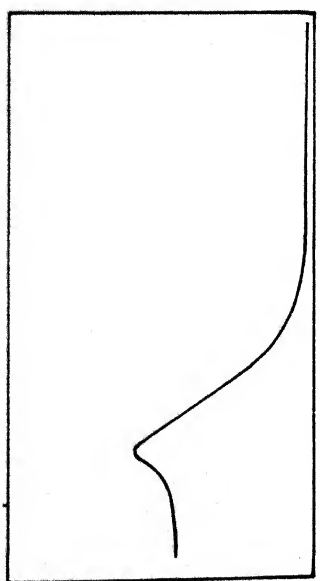
where $K_4^{-1} = k_{-4}/k_4$, and $k_r = k_{-3} K_4^{-1}$.

This rate expression is in confirmity with the observed rate law for the reverse reactions (equation 15a). The evidence for formation of an intermediate ($[\text{CdR}(\text{CN})_x]$) is provided by a sudden rise in absorbance immediately after the start of reaction in presence of high concentration of cyanide followed by the usual exponential decay. Three such traces are shown in Fig. IV.11 and IV.12.

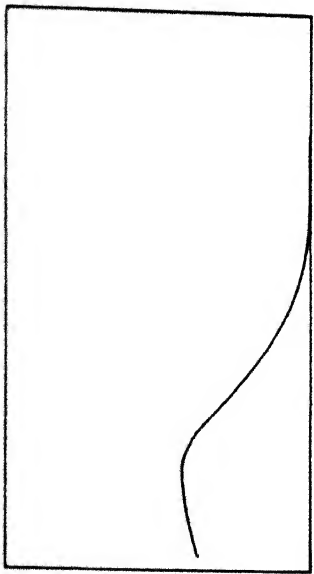
A combination of the forward and reverse reaction of $[\text{PdR(OH)}]$ with cyanide gives the values of $K_1 K_2$ (or β_2) for $[\text{PdR}(\text{CN})_2]^{2-}$ which is the reactive species for forward reaction in presence of moderate or high concentration of cyanide. The stability of this mixed ligand complex must be quite high. The value can be calculated by an expression similar to one given by Margerum et al.²² for $\text{Ni}(\text{CN})_4^{2-}$ formation reactions. For PdR reaction with cyanide, the expression takes the form (equation 29)

$$K_1 K_2 = \frac{K_4^{-1} k_{-3} \beta_4}{k_3 K_{\text{PdR}}} \quad \dots (29)$$

where β_4 is the overall formation constant of $[\text{Pd}(\text{CN})_4]^{2-}$, $k_r = K_4^{-1} k_{-3}$ and K_{PdR} is the stability constant of the mono complex.



(A)



(B)

Fig. IV.11 Typical kinetic traces showing the sudden increase in absorbance immediately after the start of a reaction of $[\text{Cd}(\text{par})_2]^{2-}$ with cyanide ion. (A) Time base = 10 m sec. (B) Time base = 5 m sec.

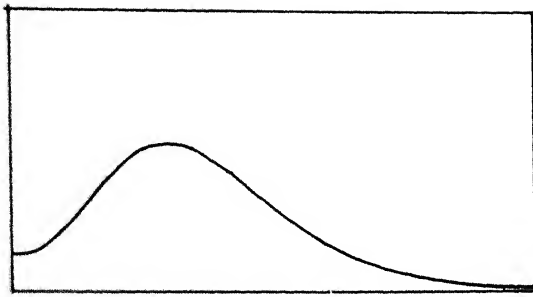


Fig. IV.12 Kinetic trace showing the sudden increase in absorbance immediately after the start of a reaction of $[\text{PdR(OH)}]^-$ with cyanide ion. Time base = 5 m sec.

The value of $K_1 K_2$ thus calculated for $[\text{PdR}(\text{CN})_2]^{2-}$ is 1.14×10^{29} . It is difficult to calculate the value of product $K_1 K_2$ for $\text{CdR}(\text{CN})_2$, because of lack of knowledge about the stability constant of CdR complex.

The observed positive salt effect giving $Z_A Z_B \approx 2$ and the observed first order dependence may indicate that equation (18) or equation (20) could be the rate determining step in case of CdR_2-CN^- system. The step involving k_{CN}^{2-} (equation 18) has been shown by Margerum et al.²⁵ to be the slow step while studying the reaction of $\text{Ni}(\text{MIDA})_2$ and $\text{Ni}(\text{IDA})_2$ with cyanide ion. Nigam et al.² have also arrived at a similar conclusion in the case of reaction of $\text{Ni}(\text{en})_2$ with cyanide ion. On the other hand, addition of the third cyanide has been reported to be rate determining in the case of exchange reactions of polyamino and aminocarboxylato chelates of Ni(II) by cyanide.^{3,26} Thus in the case of $\text{Ni}(\text{dien})_2-\text{CN}^-$ reaction, the value of k_{CN}^{2-} is higher than the value of k_3 at higher cyanide concentration which indicates that k_{CN}^{2-} is not the rate determining step.²

The high activation enthalpy at low cyanide concentration (i.e. for cyanide independent path) compared to that at high cyanide concentration (i.e. for cyanide dependent path) in $[\text{PdR}(\text{OH})]^--\text{CN}^-$ reaction indicates the rupture of metal-ligand bond in the former process. The much less negative entropy of activation provides further support for cyanide independent dissociation in the first step (equation 22) in the reaction

mechanism. The large and negative entropy change for the forward reaction at high cyanide concentration and also for reverse reaction indicates the formation of a highly ordered activated complex in these cases.

In the case of $\text{CdR}_2\text{-CN}^-$ system the activation parameters for the forward reaction (Table IV.7) indicates that the cyanide dependent dissociation (octahedral-tetrahedral transformation) is associated with low activation enthalpy but more negative entropy change than the cyanide independent path of higher enthalpy and less negative entropy change. For reverse reaction involving a tetrahedral to octahedral conversion, ΔH^\ddagger was found to be low and comparable to those reported by other workers²⁷ for some ligands.

In brief, the bis complex $[\text{CdR}_2]^{2-}$ and mono complex $[\text{PdR(OH)}]^-$ do not convert directly to cyano complexes of Cd(II) and Pd(II) respectively but lose one of the ligands viz. Par in case of Cd(II) and hydroxy group in the case of Pd(II) before the rate determining step (equations 17, 18 and 22, 23) and mixed ligand complexes of type $\text{MR}(\text{CN})_x^-$ (where M = Pd(II) or Cd(II) and $x = 1$ or 2) are formed rapidly. Addition of the third cyanide constitutes the rate determining step. Table IV.8 summarises the equilibrium and rate constant data obtained from these studies.

TABLE IV.8. Summary of the rate and equilibrium constants.

Constant	Pd(II)	Cd(II)
K	$10^{4.9}$	-
β_2	-	3.16×10^{17}
$k_d (s^{-1})$	1.5×10^{-1}	2.0×10^{-1}
$K_1 K_2 (M^{-2})$	1.14×10^{29}	-
$k_3 (M^{-1} s^{-1})$	$(1.96 \pm 0.07) \times 10^2$	$(1.8 \pm 0.04) \times 10^2$
$k_{CN} (M^{-1} s^{-1})$	7.0×10^1	2.0×10^2
$k_{HCN} (M^{-1} s^{-1})$	5.5×10^1	4.9×10^2
$K_4^{-1} k_{-3} (s^{-1})$	$(3.82 \pm 0.1) \times 10^{-6}$	$(1.75 \pm 0.12) \times 10^{-6}$

REFERENCES

1. M. Eigen and R.G. Wilkins, "Mech. Inorg. Reactions", R.F. Gould, Ed., Adv. Chem. Series No. 49 (Amer. Chem. Soc., Washington, 1965) p.55.
2. H.C. Bajaj, M. Phull and P.C. Nigam, Bull. Chem. Soc. Jpn., 1984, 57, 564.
3. K. Kumar and P.C. Nigam, J. Phys. Chem., 1980, 84, 140 and references contained therein.
4. R.M. Naik and P.C. Nigam, Inorg. Chim. Acta, 1986, 114, 55 and references contained therein.
5. R.M. Naik and P.C. Nigam, Trans. Met. Chem., 1986, 11, 11 and references therein.
6. P. Mishra, R.M. Naik and P.C. Nigam, Inorg. Chim. Acta, 1987, 127, 71 and references therein.
7. N. Gupta and P.C. Nigam, Trans. Met. Chem., 1987 (communicated).
8. N. Gupta and P.C. Nigam, Inorg. Chim. Acta, 1988 (communicated).
9. W.M. MacNevin and O.H. Kriege, J. Am. Chem. Soc., 1955, 77, 6149.
10. A.I. Vogel, "Text book of Quantitative Inorganic Analysis" 4th edn., Longman Green, London, 1978, p. 474.
11. J.H. Bigelow, Inorg. Synth. 1946, 2, 245.
12. G. Brauer, "Hand book of Preparative Inorganic Chemistry", Vol. 2, 2nd edn., Academic Press, New York, London, 1965, p. 1106.
13. A.I. Vogel, "Text book of Quantitative Inorganic Analysis", 4th edn., Longman Green, London, 1978, p. 345.

14. T. Yotsuyanagi, H. Hoshimo and K. Aomura, *Anal. Chim. Acta*, 1974, 71, 349.
15. L.G. Sillen and A.E. Martell, "Stability constants of Metal Ion Complexes", Suppl. No.1, The Chem. Soc. London, 1971, p. 768.
16. R.M. Izatt, G.D. Watt, D. Eatough and J.J. Christensen, *J. Chem. Soc. A*, 1967, 1304.
17. H. Pearson, *Acta Chem. Scand.*, 1971, 25, 543.
18. K.K. Saxena and R.S. Saxena, *J. Chem. Soc. Pak.*, 1983, 5, 267.
19. D. Nonova and S. Pavlova, *Anal. Chim. Acta*, 1981, 123, 289.
20. K. Kumar and P.C. Nigam, *J. Phys. Chem.*, 1979, 83, 2090.
21. H.C. Bajaj, M. Phull and P.C. Nigam, *J. Coord. Chem.*, 1983, 13, 41.
22. K. Kumar, H.C. Bajaj and P.C. Nigam, *J. Phys. Chem.*, 1980, 84, 2351.
23. R.M. Naik and P.C. Nigam, *Trans. Met. Chem.*, 1986, 11, 337.
24. R.M. Naik and P.C. Nigam, *Trans. Met. Chem.*, 1987, 12, 261.
25. L.C. Coombs and D.W. Margerum, *Inorg. Chem.*, 1981, 123, 289.
26. G.B. Kolski and D.W. Margerum, *Inorg. Chem.*, 1969, 8, 1125.
27. P. Holyer, C. Hubbard, S. Kettle and R.G. Wilkins, *Inorg. Chem.*, 1965, 4, 929; 1966, 5, 622.

CHAPTER - V

MULTIDENTATE LIGAND EXCHANGE KINETICS: SUBSTITUTION REACTIONS OF ETHYLENEDIAMINETETRAACETATE AND TRIETHYLENETETRAMINEHEXA- ACETATE ANIONS WITH IMINODIACETATOPALLADIUM(II)

ABSTRACT

The kinetics of formation of $[PdEDTA]^{2-}$ and $[PdTTHA]^{4-}$ from the reaction of $[PdIDA]$ with L^{n-} (L = Ethylenediaminetetraacetic acid or Triethylenetetraminehexaacetic acid abbreviated as EDTA and TTHA respectively) have been studied spectrophotometrically. Both reactions take place in two steps; the first step consists of the fast formation of mixed ligand complexes $[PdIDAL]^{n-}$, which slowly decompose to the $[PdL]^{2-n}$ complexes in the second step. The formation of mixed ligand complexes in presence of excess incoming ligand in both reactions is pseudo-first-order in $[PdIDA]$. The rates of reaction in the second step were not influenced by the addition of $EDTA^{4-}$ and $TTHA^{6-}$.

The rate constants decrease as the pH increases in both steps of either reaction, which has been explained. The activation

parameters for the reactions have been calculated and used to support the proposed mechanism. The effect of ionic strength on rate was negligible.

V.I INTRODUCTION

The mechanism by which one multidentate ligand displaces another from a metal ion centre depends on the ability of both ligands to coordinate with the metal simultaneously. It may be necessary to replace segments of the initially bound ligand by solvent before an incoming ligand can gain a coordination foothold. More the segments which must be unwrapped from the metal, the slower may be the reaction. Certain multidentate ligands can rapidly replace other multidentate ligands from their metal complexes and others slowly.¹⁻⁴ The kinetics of multidentate ligand substitution reactions on Cu(II) and Zn(II) have been studied extensively.⁵⁻⁸ The kinetics and mechanism of the exchange reactions of nickel(II)-polyamine complexes with some aminocarboxylates viz. TMDTA,⁹ NEDTA,¹⁰ DTPA¹¹ and PDTA¹² have been studied previously in this laboratory. Steinhaus et al.¹³ have studied the exchange of 1,10 phenanthroline or triethylenetetramine complex of nickel(II) and have demonstrated the formation of a mixed ligand intermediate viz. $[\text{Nitrien}.\text{Phen}]^{2+}$ in this reaction. The dissociation of this mixed complex gives $[\text{Ni}(\text{Phen})]^{2+}$ which reacts with excess phenanthroline to give $[\text{Ni}(\text{Phen})_3]^{2+}$ finally.

In the present chapter, we report the kinetics and mechanism of reactions (1) and (2) which have been investigated to obtain a better understanding of the ligand substitution processes involving multidentate ligands on the Pd(II) centre.



v.2 EXPERIMENTAL

v.2.1 Chemicals

Purified and recrystallized varieties of IDA (AR, BDH), EDTA (AR, BDH) and TTHA (AR, Fluka) were used. Palladous chloride was procured from John Baker (USA). NaClO_4 (E. Merck, F.R.G.) was used in this study for maintaining ionic strength. All other reagents were of AR grade. Sodium hydroxide or perchloric acid were used to maintain the pH of solutions.

One gram of palladous chloride was dissolved in 1 litre 0.1M hydrochloric acid. A complete solution required an hour of stirring. The presence of $[\text{PdCl}_4]^{2-}$ was verified spectrophotometrically by comparison with the data of Cohen and Davidson.¹⁴ The exact strength of the solution was established gravimetrically by precipitation with dimethylglyoxime.¹⁵ The complex PdIDA was prepared by mixing stoichiometric amount of $[\text{PdCl}_4]^{2-}$ and IDA.

V.2.2 Instrumentation

All kinetic runs were taken on a Toshniwal Spectrophotometer model RL-02. Shimadzu double beam spectrophotometer model UV-240 was used for scanning the reaction mixtures. Both spectrophotometers were equipped with a circulatory arrangement for thermostating the cell compartment. A stopped flow spectrophotometer model SF-3A from Hitech, England coupled with an ECIL storage oscilloscope model OS-768s was used to record kinetic traces for studying fast reactions. A polaroid camera was utilised to photograph these traces. The temperature was maintained by an ultracryostat model 2NBE (VEB Kombinat Medizin and Labortechnik Kombinatsbetrieb, GDR). An Elico digital pH meter model LI-120 was used for the measurement of pH.

V.2.3 Kinetic measurements

The substitution reactions of $[PdIDA]$ with $EDTA^{4-}$ and $TTHA^{6-}$ were followed spectrophotometrically at 325 nm (λ_{max} of $[PdIDA \cdot L]^{n-}$ for both complexes) at $30 \pm 0.1^\circ C$, $pH = 8.5 \pm 0.02$ and $I = 0.2M$ $NaClO_4$ in case of EDTA and $pH = 8.0 \pm 0.02$ and $I = 0.1M$ $NaClO_4$ in case of TTHA respectively.

V.3 RESULTS

V.3.1 Protonation and stability constants and species distributions

The protonation constants of IDA, EDTA and TTHA, and the stability constants of $[PdIDA]$, $[Pd(EDTA)]^{2-}$ and $[Pd(TTHA)]^{4-}$ are

listed in Table V.1. The species distribution of reactants, calculated by a procedure due to Perrin and Sayce,¹⁶ from the pK_a 's of the complex and the ligands are shown in Fig. V.1, V.2 and V.3.

V.3.2 Kinetics of formation of $[PdIDA \cdot L]^{n-}$

The first step of reaction was followed under pseudo-first-order conditions taking $EDTA^{4-}$ or $TTHA^{6-}$ in large excess. The rate constants were obtained from the plots of $\log C_B$ versus t where C_B is the concentration of $[PdIDA \cdot L]^{n-}$ at any time t and obtainable by expression (3).

$$C_B = (A_t - \epsilon_A \cdot C_A^0) / (\epsilon_B - \epsilon_A) \quad \dots (3)$$

ϵ_A and ϵ_B are the molar extinction coefficients of $[PdIDA]$ and $[PdIDA \cdot L]^{n-}$ respectively. A_t is the total absorbance at time t at 325 nm and C_A^0 is the initial concentration of $[PdIDA]$.

The reaction was found to be first order in both $[PdIDA]$ and L^{n-} . The values of the rate constants are given in Table V.2 and are also plotted as $\log k_{obsd}$ versus $\log [L^{n-}]$ in Fig. V.4. The experimental rate expression is formulated as

$$\begin{aligned} \text{Rate} &= d[PdIDA \cdot L]^{n-} / dt = k_1 [PdIDA] [L^{n-}] \\ &= k_{obsd} [PdIDA] \quad \dots (4) \end{aligned}$$

where $k_{obsd} = k_1 [L^{n-}]$.

TABLE V.1. Protonation constants of aminocarboxylates and stability constants of aminocarboxylatopalladate(II) complexes.

A. Protonation Constants of Aminocarboxylates at 25°C (log K):
 $I = 0.1M \text{ (NaClO}_4/\text{KNO}_3)$

L^{n-}	K_{HL}	K_{H_2L}	K_{H_3L}	K_{H_4L}	K_{H_5L}	K_{H_6L}	Ref. •
IDA ²⁻	9.34	2.61	1.82	—	—	—	17
EDTA ⁴⁻	10.34	6.24	2.75	2.07	—	—	18
TTHA ⁶⁻	10.19	9.40	6.16	4.16	2.95	2.42	19-22

B. Stability Constants of Aminocarboxylatopalladate(II) Complexes (log K) at 25°C,
 $I = 0.1M \text{ (NaClO}_4/\text{KNO}_3)$

L^{n-}	K_{PdL}	K_{PdHL}	K_{PdH_2L}	K_{PdH_3L}	K_{PdH_4L}	Ref. •
IDA ²⁻	9.62	0.75 ^a	—	—	17	23
EDTA ⁴⁻	18.5 ^b	3.1 ^c	0.9 ^c	—	—	24
TTHA ⁶⁻	18.73	6.92	2.9	2.5	2.45	25

a) $I = 1.0M$ and temp. = 20°C; b) $I = 0.2M$ and temp. = 25°C; c) $I = 1.0M$ and temp. = 20°C.

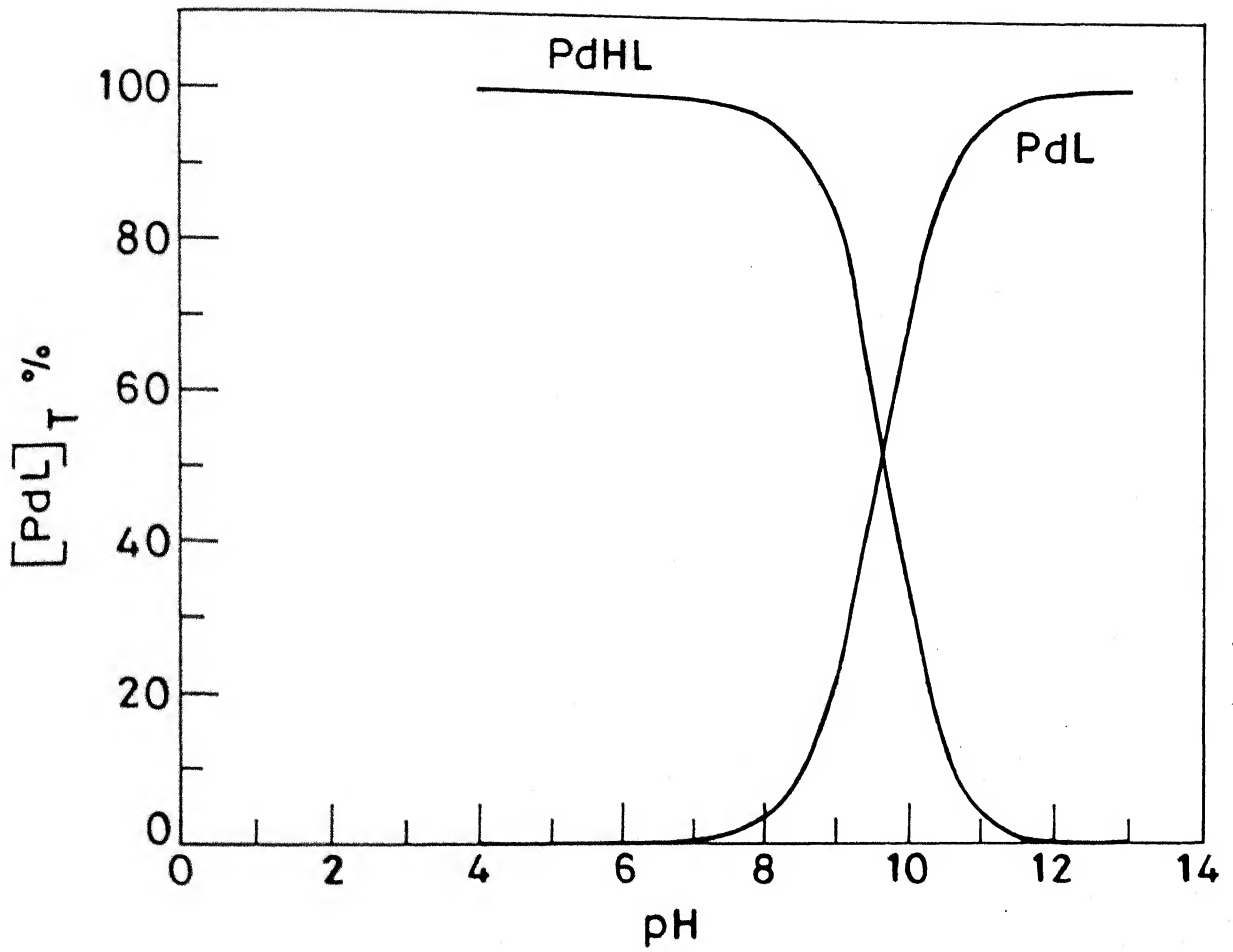


Fig. V.1 Species distribution of PdIDA as a function of pH. $[Pd^{2+}] = [IDA] = 1.0 \times 10^{-4} M$.

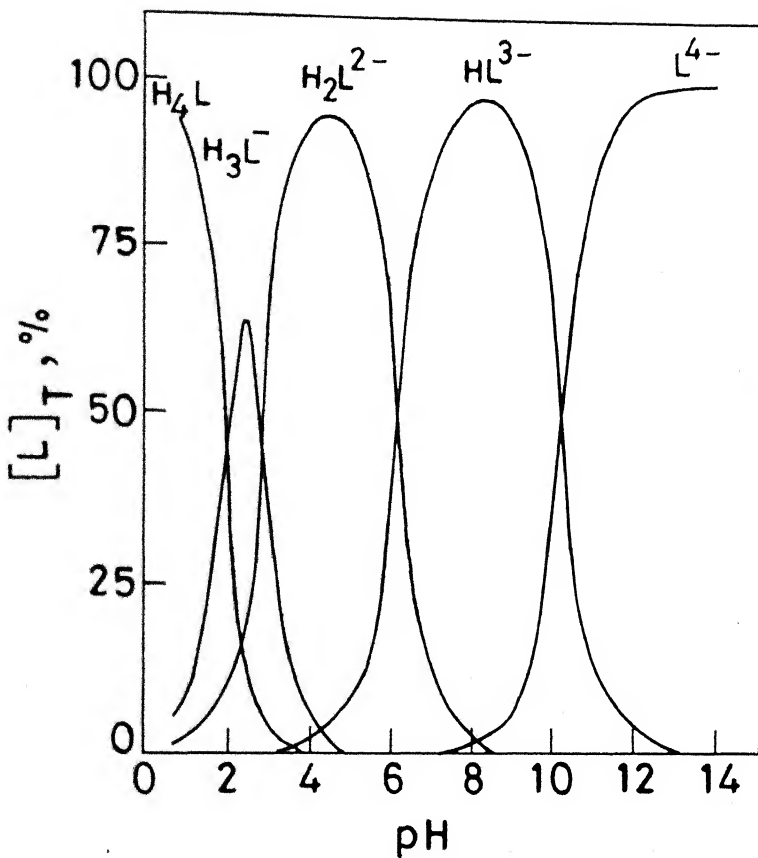


Fig.V.2 Species distribution of EDTA as a function of pH.

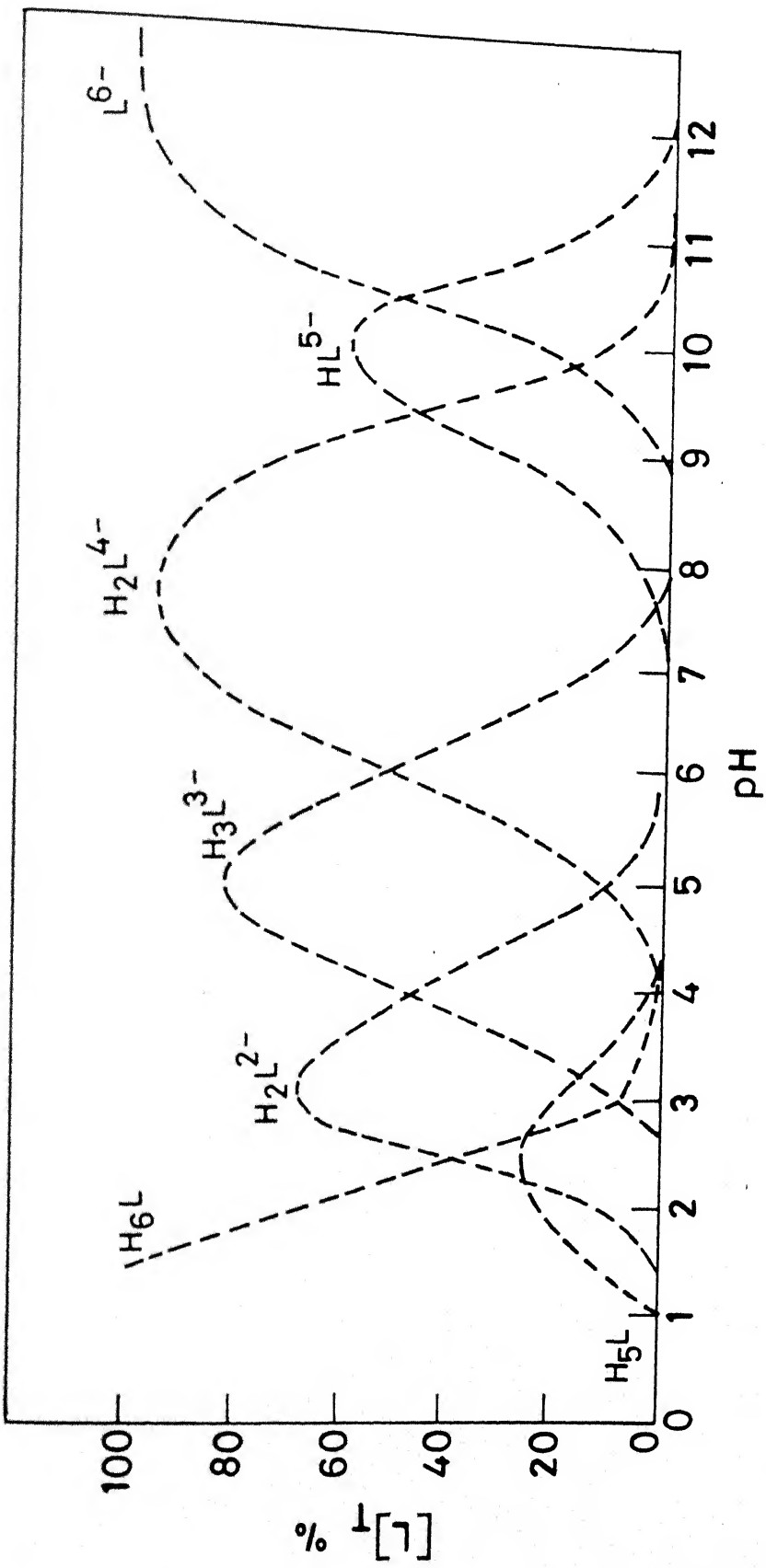


Fig. V.3 Species distribution of TTHA as a function of pH.
 $[TTHA] = 2.0 \times 10^{-4} M.$

TABLE V.2. Evaluation of pseudo-first-order rate constants and second order rate constants for the first stage of reactions.

[EDTA], M	$10^1 \times k_{\text{obsd}}, \text{s}^{-1}$	$10^{-1} \times k_1 = k_{\text{obsd}} / [\text{EDTA}], \text{M}^{-1} \text{s}^{-1}$
(A) $[\text{PdIDA}] = (1.7-3.7) \times 10^{-5} \text{M}$, $\text{pH} = 8.5 \pm 0.02$, $I = 0.1 \text{M}(\text{NaClO}_4)$, temp. = $25 \pm 0.1^\circ\text{C}$.		
2.0×10^{-2}	5.6	2.8
1.0×10^{-2}	2.9	2.9
9.0×10^{-3}	2.6	2.9
7.5×10^{-3}	2.3	3.0
5.0×10^{-3}	1.7	3.4
3.5×10^{-3}	1.1	3.1
2.5×10^{-3}	0.6	2.4
$\text{Av.} = (2.9 \pm 0.3) \times 10^1 \text{ M}^{-1} \text{s}^{-1}$		

[TTHA], M	$10^1 \times k_{\text{obsd}}, \text{s}^{-1}$	$10^{-1} \times k_1 = k_{\text{obsd}} / [\text{TTHA}], \text{M}^{-1} \text{s}^{-1}$
(B) $[\text{PdIDA}] = (0.42-3.4) \times 10^{-5} \text{M}$, $\text{pH} = 8.0 \pm 0.02$, $I = 0.1 \text{M}(\text{NaClO}_4)$, temp. = $30 \pm 0.1^\circ\text{C}$.		
1.0×10^{-2}	7.4	7.4
9.0×10^{-3}	6.6	7.3
7.5×10^{-3}	5.6	7.5
5.0×10^{-3}	3.7	7.4
2.5×10^{-3}	1.9	7.6
1.6×10^{-3}	1.2	7.5
1.0×10^{-3}	0.73	7.3
$\text{Av.} = (7.4 \pm 0.1) \times 10^1 \text{ M}^{-1} \text{s}^{-1}$		

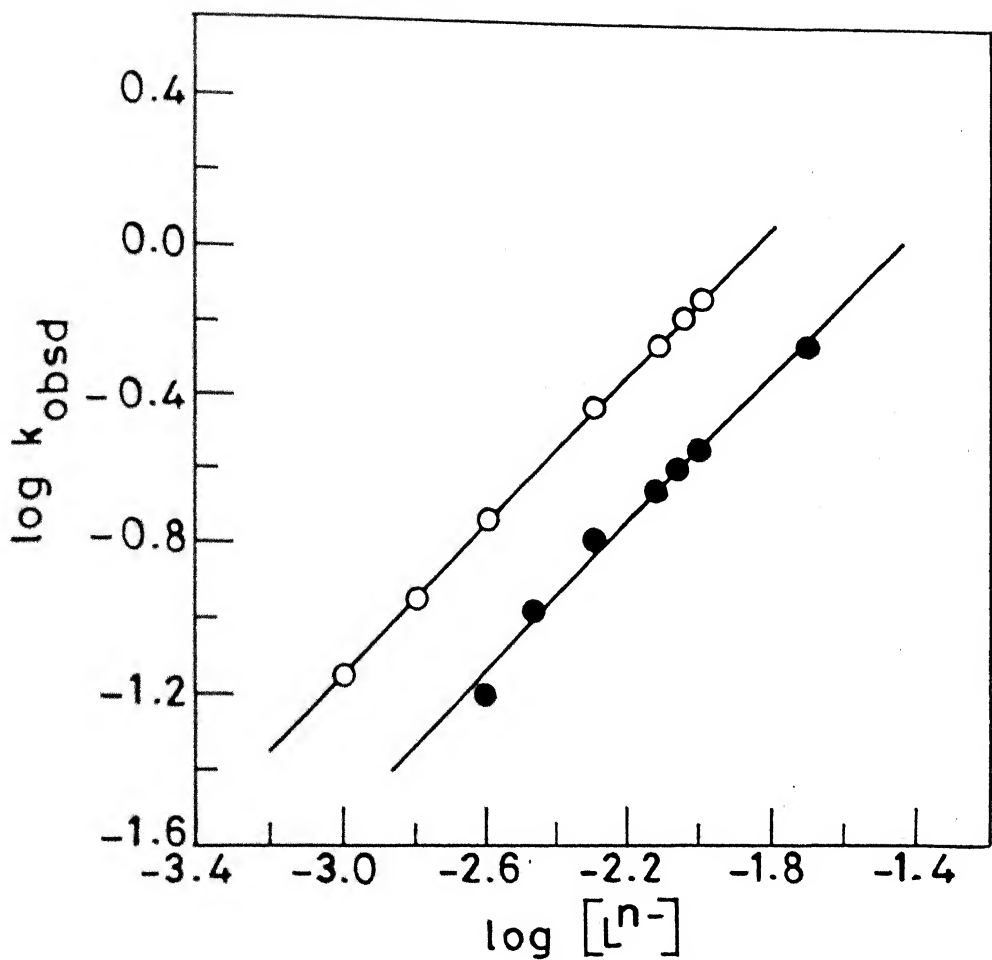


Fig. V.4 Ligand dependence of the observed pseudo first-order rate constants for the reaction of $[PdIDA]$ with EDTA (●) and TTHA (○). The reaction conditions are given in table V.2.

V.3.3 Effect of pH on the formation of $[PdIDA \cdot L]^{n-}$

Formation of the ternary complexes were studied at various hydrogen ion concentrations and it was observed that the rate increases with increase of hydrogen ion concentration. The reaction between $[PdIDA]$ and EDTA was studied in the pH range 7.25-9.5. The reaction was found to decrease upto pH 8.75 and then level off (Fig. V.5, Table V.3). This can be explained on the basis of reactivities of the different protonated and unprotonated forms of $[PdIDA]$ and EDTA. The resolution of rate constants has been carried out by a procedure described hereafter. The rate expression for the whole pH range is given by

$$\text{Rate} = k_{L_T}^{\text{PdIDA}T} [PdIDA]_T \cdot [L]_T \quad \dots (5)$$

where subscript T denotes the total concentration of reactants $[PdIDA]$ and EDTA in all the forms and $k_{L_T}^{\text{PdIDA}T}$ represents the observed rate constant of the fast step and is same as k_1 of equation (16) (vide supra).

Algebraic manipulation yields a suitable expression given by equation (6) for PdIDA-EDTA reaction.

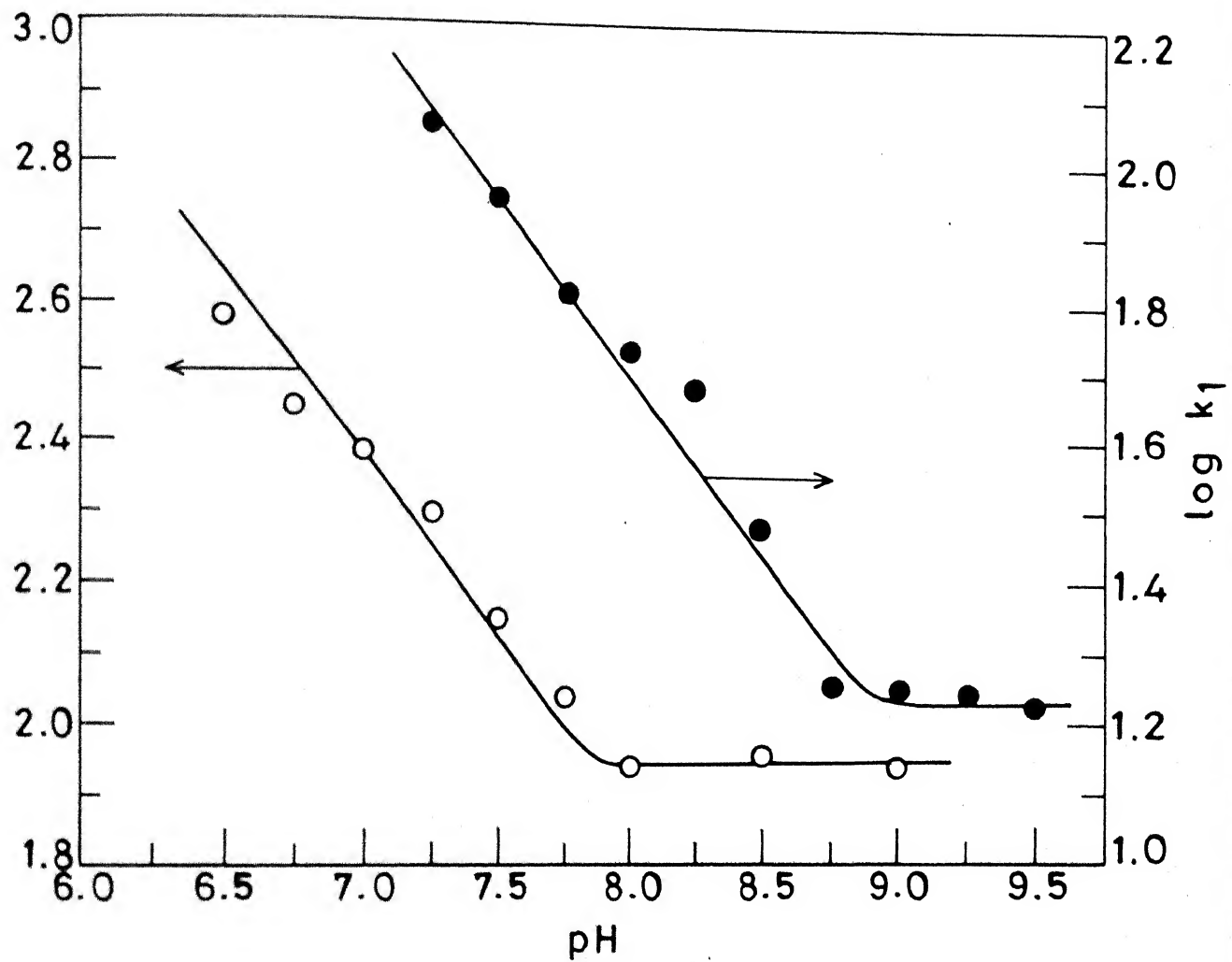


Fig. V.5 Effect of pH on the formation of $[\text{PdIDA}\cdot\text{L}]^{n-}$.
 For EDTA (●) For TTHA (○).

TABLE V.3. Effect of pH on the formation of mixed ligand complex $[PdIDA \cdot L]^{n-}$. $[PdIDA] = 1.7 \times 10^{-5} M$, $[L^{n-}] = 7.5 \times 10^{-3} M$, I = 0.1M(NaClO₄).

pH	k_{obsd}, s^{-1}	$k_1, M^{-1}s^{-1}$
(A) $[PdIDA] + EDTA$ reaction ; temp. = $25 \pm 0.1^\circ C$.		
7.25	8.5×10^{-1}	1.13×10^2
7.5	6.6×10^{-1}	8.8×10^1
8.0	4.04×10^{-1}	5.4×10^1
8.25	3.57×10^{-1}	4.76×10^1
8.5	2.25×10^{-1}	3.0×10^1
8.75	1.32×10^{-1}	1.76×10^1
9.0	1.33×10^{-1}	1.77×10^1
9.5	1.23×10^{-1}	1.64×10^1
(B) $[PdIDA] + TTHA$ reaction; temp. = $30 \pm 0.1^\circ C$.		
6.5	2.82	3.76×10^2
6.75	2.13	2.84×10^2
7.0	1.84	2.46×10^2
7.25	1.52	2.03×10^2
7.5	1.06	1.41×10^2
7.75	0.82	1.09×10^2
8.0	0.56	7.47×10^1
8.5	0.57	7.65×10^1
9.0	0.56	7.47×10^1

$$\begin{aligned}
 & k_{L_T}^{PdIDA_T} \cdot \frac{[PdIDA]_T}{[PdIDA]} \cdot \frac{[L]_T}{[L^{4-}]} \\
 & = k_{H_2L}^{PdIDA} \cdot K_{H_2L} \cdot K_{HL} \cdot [H^+]^2 + k_{HL}^{PdIDA} \cdot K_{HL} \cdot [H^+] + \\
 & k_{H_2L}^{PdHIDA} \cdot K_{PdHIDA} \cdot K_{H_2L} \cdot K_{HL} [H^+]^3 + k_{HL}^{PdHIDA} \cdot K_{PdHIDA} \cdot K_{HL} \cdot [H^+]^2 \\
 & \dots \quad (6)
 \end{aligned}$$

$$\text{where } \frac{[PdIDA]_T}{[PdIDA]} = 1 + K_{PdHIDA} [H^+]$$

$$\text{and } \frac{[L]_T}{[L^{4-}]} = 1 + K_{HL} [H^+] + K_{H_2L} \cdot K_{HL} [H^+]^2 + \dots$$

K_{PdHIDA} is the protonation constant of PdIDA and K_{HL} and K_{H_2L} are the first and second protonation constants of EDTA respectively (Table V.1). In the pH range 7.25-8.25, the rate terms involving PdIDA as reactant can be neglected (Fig. V.1) and equation (6) transforms to equation (7)

$$\begin{aligned}
 & k_{L_T}^{PdIDA_T} \cdot \frac{[PdIDA]_T}{[PdIDA]} \cdot \frac{[L]_T}{[L^{4-}]} \cdot \frac{1}{[H^+]^2} = k_{HL}^{PdHIDA} \cdot K_{PdHIDA} \cdot K_{HL} \\
 & + k_{H_2L}^{PdHIDA} \cdot K_{PdHIDA} \cdot K_{H_2L} \cdot K_{HL} \cdot [H^+] \quad \dots \quad (7)
 \end{aligned}$$

By plotting left hand side of equation (7) versus $[H^+]$ (Fig. V.6) one gets a straight line with an intercept and a slope from which one can calculate k_{HL}^{PdHIDA} and $k_{H_2L}^{PdHIDA}$ respectively (Table V.4).

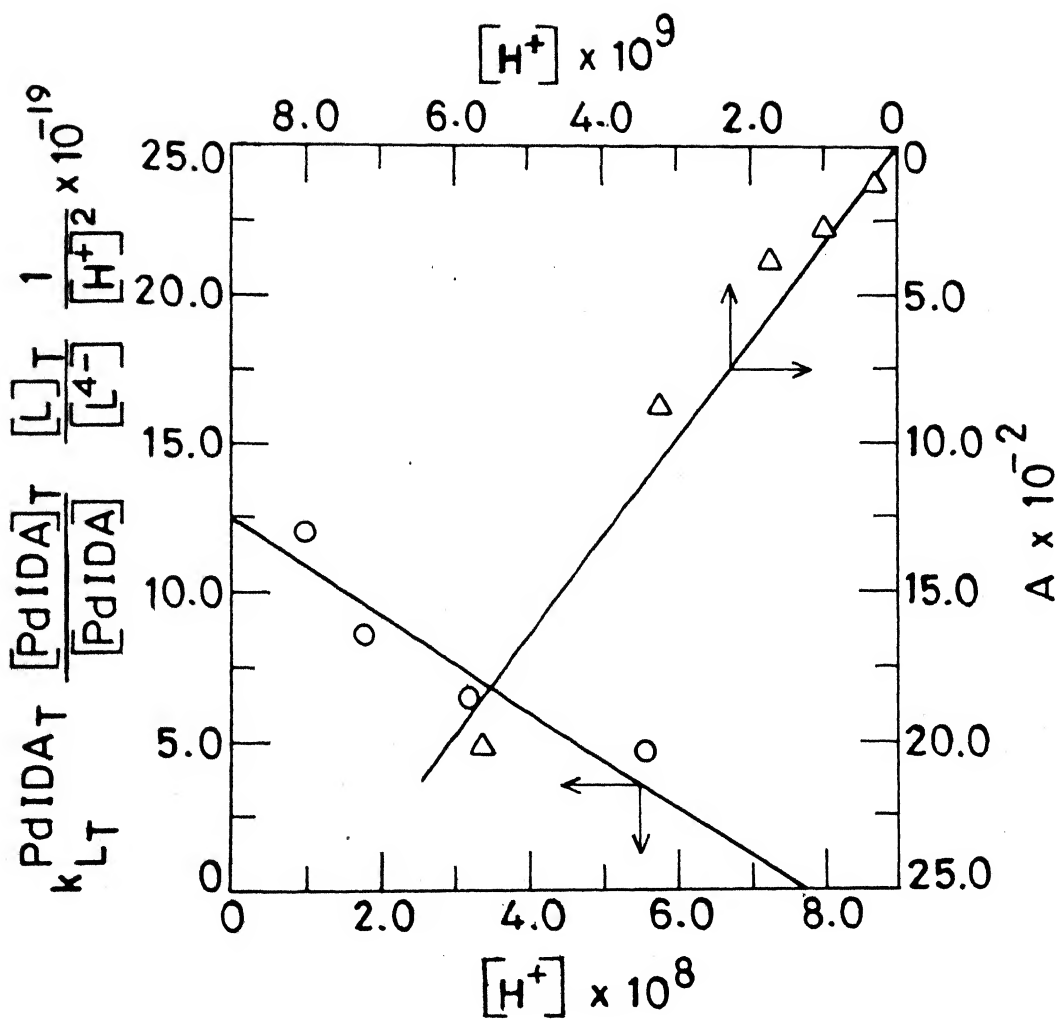


Fig. V.6 Resolution of rate constants
 k_{HL}^{PdIDA} , k_{HL}^{PdHIDA} , $k_{H_2L}^{PdHIDA}$ for
 the reaction of $[PdIDA]$ with EDTA
 (Temp. = $25^\circ C$ and $I = 0.1M$)

In the pH range 8.25-9.5, the term containing $[H_2L]$ can be neglected and equation (6) after transposition transforms to equation (8).

$$k_{L_T}^{PdIDA} \cdot \frac{[PdIDA]_T}{[PdIDA]} \cdot \frac{[L]_T}{[L^{4-}]} - k_{HL}^{PdIDA} \cdot K_{HL} \cdot [H^+]^2 \\ = k_{HL}^{PdIDA} \cdot K_{HL} [H^+] \quad \dots (8)$$

One may set left hand side of equation (8) as 'A' and by plotting 'A' versus $[H^+]$ (Fig. V.6) one again gets a straight line passing through origin. From the slope one can calculate k_{HL}^{PdIDA} (Table V.4).

It is not possible to calculate the fourth rate constant $k_{H_2L}^{PdIDA}$, because the species $[H_2L^{2-}]$ exists only upto pH 8 (Fig. V.2) and PdIDA exists above pH 8.5 (Fig. V.1). The concentration of anyone in presence of the other is negligibly small and the rate involving these species is, therefore, slow enough to be negligible.

Similarly, for the reaction of TTHA with $[PdIDA]$, the rate decreases with increase of pH (Table V.3) upto pH 8.0, and then remains constant at higher pH (Fig. V.5). This can be explained by resolution of rate constants as in the case of PdIDA and EDTA reaction. In the whole pH range the following rate expression is proposed.

$$\text{Rate} = k_{L_T}^{\text{PdIDA}_T} \cdot \frac{[\text{PdIDA}]_T}{[\text{PdIDA}]} \cdot \frac{[L]_T}{[L^{6-}]} \quad \dots \quad (9)$$

$$= k_{HL}^{\text{PdIDA}} \cdot K_{HL} \cdot [H^+] + k_{H_2L}^{\text{PdIDA}} \cdot K_{H_2L} \cdot K_{HL} \cdot [H^+]^2$$

$$+ k_{H_3L}^{\text{PdIDA}} \cdot K_{H_3L} \cdot K_{H_2L} \cdot K_{HL} \cdot [H^+]^3 + k_{HL}^{\text{PdHIDA}} \cdot K_{PdHIDA} \cdot K_{HL} \cdot [H^+]^2$$

$$+ k_{H_2L}^{\text{PdHIDA}} \cdot K_{PdHIDA} \cdot K_{H_2L} \cdot K_{HL} \cdot [H^+]^3$$

$$+ k_{H_3L}^{\text{PdHIDA}} \cdot K_{PdHIDA} \cdot K_{H_3L} \cdot K_{H_2L} \cdot K_{HL} \cdot [H^+]^4 \quad \dots \quad (10)$$

Using the protonation constants of TTHA (Table V.1) and $[\text{PdIDA}]$, in different pH ranges, the following three equations (11, 12 and 13) can be obtained by an algebraic manipulation similar to the one for EDTA reaction outlined above. In the pH range 7.5-8.5,

$$k_{L_T}^{\text{PdIDA}_T} \cdot \frac{[\text{PdIDA}]_T}{[\text{PdIDA}]} \cdot \frac{[L]_T}{[L^{6-}]} \cdot \frac{1}{[H^+]^2}$$

$$= k_{H_2L}^{\text{PdIDA}} \cdot K_{H_2L} \cdot K_{HL} + k_{H_2L}^{\text{PdHIDA}} \cdot K_{PdHIDA} \cdot K_{H_2L} \cdot K_{HL} \cdot [H^+] = B$$

$$\dots \quad (11)$$

and in pH range 6.5-7.0,

$$k_{L_T} \cdot \frac{[PdIDA]_T}{[PdIDA]} \cdot \frac{[L]_T}{[L^{6-}]} \cdot \frac{1}{[H^+]^3}$$

$$= k_{H_2L}^{PdHIDA} \cdot K_{PdHIDA} \cdot K_{H_2L} \cdot K_{HL}$$

$$+ k_{H_3L}^{PdHIDA} \cdot K_{PdHIDA} \cdot K_{H_3L} \cdot K_{H_2L} \cdot K_{HL} [H^+] = C \quad \dots (12)$$

and lastly above pH 8.5,

$$k_{L_T} \cdot \frac{[PdIDA]_T}{[PdIDA]} \cdot \frac{[L]_T}{[L^{6-}]} \cdot \frac{1}{[H^+]^2} - k_{H_2L}^{PdHIDA} \cdot K_{PdHIDA} \cdot K_{H_2L} \cdot K_{HL} [H^+]$$

$$- k_{H_2L}^{PdHIDA} \cdot K_{H_2L} \cdot K_{HL}$$

$$= k_{HL}^{PdHIDA} \cdot K_{PdHIDA} \cdot K_{HL} + k_{HL}^{PdHIDA} \cdot K_{HL} \cdot \frac{1}{[H^+]} = D \quad \dots (13)$$

where 'B', 'C', 'D', represent the left hand sides of equations (11), (12) and (13) respectively. The various rate constants can be resolved using the above three equations. For example, by plotting 'B' of equation (11) versus $[H^+]$ (Fig. V.7) one gets $k_{H_2L}^{PdHIDA}$ and $k_{H_2L}^{PdHIDA}$; by plotting 'C' of equation (12) versus $[H^+]$ (Fig. V.8) one gets $k_{H_2L}^{PdHIDA}$ and $k_{H_3L}^{PdHIDA}$ and from the plot of 'D' versus $1/[H^+]$ (Fig. V.8) one gets k_{HL}^{PdHIDA} and k_{HL}^{PdHIDA} .

The various resolved rate constants one listed in Table V.4. In the case of TTHA too it is not possible to resolve the rate constant between the species $[PdIDA]$ and $[H_3L^{3-}]$ (Fig. V.1 and V. due to reasons advanced in the case of EDTA reaction.

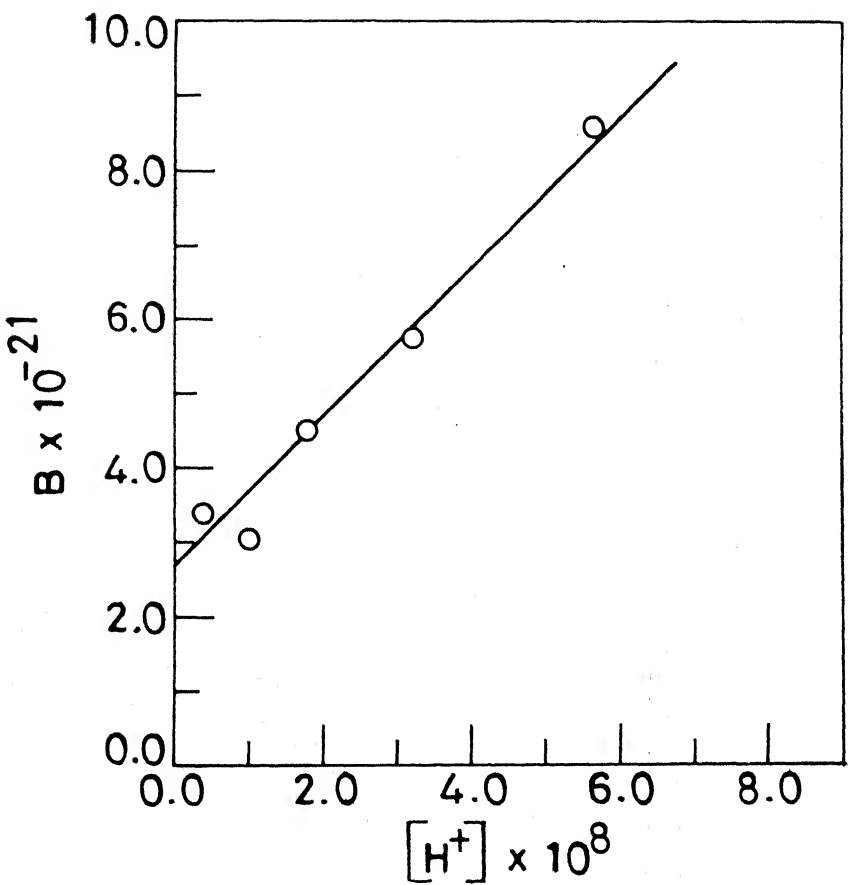


Fig.V.7 Resolution of rate constants for the reaction of PdIDA and TTHA. Reaction conditions as in Fig.V.6 .

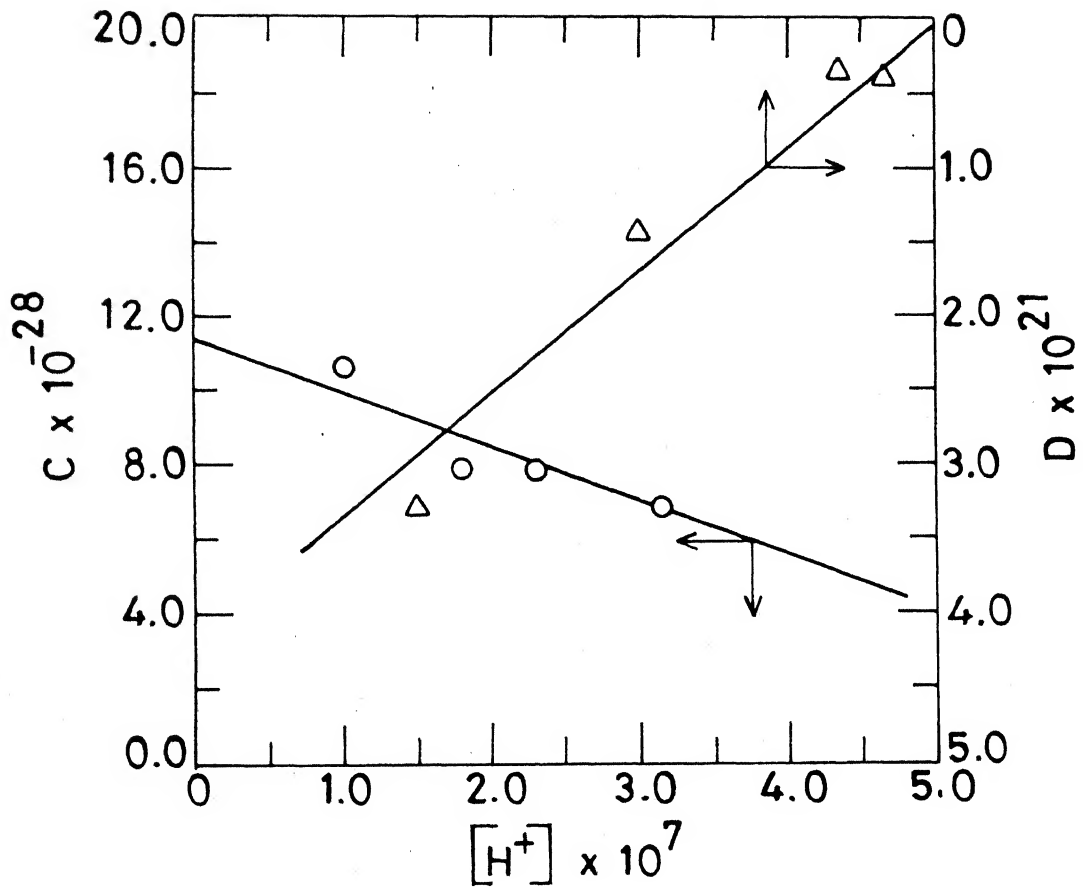


Fig.V.8 Resolution of rate constants k_{HL}^{PdHIDA} and k_{HL}^{PdIDA} for the reaction of PdIDA and TTHA. Reaction conditions as in figure V.6 .

TABLE V.4. Resolved rate constants

(A) $[PdIDA] + EDTA$ reaction

$$k_{HL}^{PdIDA} = 1.5 \times 10^1 \text{ M}^{-1}\text{s}^{-1} \quad k_{HL}^{PdHIDA} = 1.0 \times 10^9 \text{ M}^{-1}\text{s}^{-1}$$

$$k_{H_2L}^{PdHIDA} = 7.6 \times 10^9 \text{ M}^{-1}\text{s}^{-1}$$

(B) $[PdIDA] + TTHA$ reaction

$$k_{HL}^{PdIDA} = 1.1 \times 10^2 \text{ M}^{-1}\text{s}^{-1} \quad k_{H_2L}^{PdHIDA} = 4.6 \times 10^8 \text{ M}^{-1}\text{s}^{-1}$$

$$k_{H_2L}^{PdIDA} = 6.9 \times 10^1 \text{ M}^{-1}\text{s}^{-1} \quad k_{HL}^{PdHIDA} = 1.2 \times 10^{10} \text{ M}^{-1}\text{s}^{-1}$$

$$k_{H_3L}^{PdHIDA} = 4.7 \times 10^8 \text{ M}^{-1}\text{s}^{-1}$$

V.3.4 Effect of ionic strength on the formation of $[PdIDA \cdot L]^{n-}$

The rate of formation of mixed-ligand-intermediates was studied over a range of ionic strength. The rate of reaction was found to be independent of ionic strength of the medium. This provides additional support for the formation of the intermediate proposed. The ionic strength was maintained by adding calculated amounts of sodium perchlorate before mixing the reactants. The other conditions were kept constant during these measurements. The rate constants at different ionic strengths are given in Table V.5.

The effect of ionic strength on the formation of $[PdIDA \cdot TTHA]^{6-}$ has not been carried out because of nonavailability of sufficient quantity of TTHA. It is to be expected that similar results will be obtained in this case also as in the case of formation of $[PdIDA \cdot EDTA]^{4-}$.

V.3.5 Kinetics of decomposition of $[PdIDA \cdot L]^{n-}$

The slow decomposition reaction of $[PdIDA \cdot L]^{n-}$ complexes was studied in presence of different concentrations of L^{n-} and it was observed that the reaction rates were not influenced by addition of $EDTA^{4-}$ or $TTHA^{6-}$. The rate is first order in $[PdIDA \cdot L]^{n-}$ in accordance with rate equation (14).

$$\text{rate} = d[PdL]^{2-n}/dt = k_2 [PdIDA \cdot L]^{n-} \quad \dots (14)$$

TABLE V.5. Effect of ionic strength on the formation of $[\text{PdIDA} \cdot \text{EDTA}]^{4-}$ from the reaction of $[\text{PdIDA}]$ and EDTA^{4-} at temp. = $25 \pm 0.1^\circ\text{C}$, pH = 8.5 ± 0.02 , $[\text{PdIDA}] = 2.1 \times 10^{-5}\text{M}$, $[\text{EDTA}] = 7.5 \times 10^{-3}\text{M}$.

$I, \text{M}(\text{NaClO}_4)$	$k_{\text{obsd}}, \text{s}^{-1} \times 10^1$	$k_1, \text{M}^{-1}\text{s}^{-1} \times 10^1$
0.06	2.23	2.97
0.08	2.25	3.00
0.1	2.25	3.00
0.12	2.22	2.95

The rate constants were calculated from the plot of $\log C_B$ versus t where C_B is the concentration of $[PdIDA \cdot L]^{n-}$ at any time t and calculated by an expression given in equation (15).

$$C_B = (A_t - \epsilon_C \cdot C_B^0) / (\epsilon_B - \epsilon_C) \quad \dots \quad (15)$$

where ϵ_C is the molar extinction coefficient of $[PdL]^{2-n}$, A_t is the total absorbance at time t at 325 nm and C_B^0 is the initial concentration of $[PdIDA \cdot L]^{n-}$. The rate constants along with reaction conditions are given in Table V.6.

V.3.6 Dependence of decomposition rate of $[PdIDA \cdot L]^{n-}$ on pH

The rates of both reactions are highly pH dependent. The decomposition reaction of $[PdIDA \cdot EDTA]^{4-}$ was studied in the pH range 4.75-9.0 (Fig. V.9) whereas that of $[PdIDA \cdot TTHA]^{5-}$ was studied in the pH range 5.5-8.9 (Fig. V.10). It was observed that the rate increases with decrease of pH below 8 (Table V.7). This increase may be due to higher dissociation rate of the protonated form of $[PdIDA \cdot L]^{n-}$ compared to that of unprotonated one. This behaviour has been observed for dissociation reactions of many other metal complexes. Attempts at resolving the rate constants of the decomposition of $[PdIDA \cdot L]^{n-}$ were not successful because of lack of information on the protonation constants of these mixed ligand complexes. The plots of $\log k_2$ versus pH are given in Fig. V.11 and 12.

TABLE V.6. First order rate constants for the dissociation of $[PdIDA \cdot L]^{n-}$ to form $[PdL]^{2-n}$ and IDA^{2-} .

$10^5 \times [PdIDA], M$	$10^3 \times [EDTA], M$	$10^4 \times k_2, s^{-1}$
(A) temp. = $30 \pm 0.1^\circ C$, pH = 8.5 ± 0.02 and I = 0.2M(NaClO ₄).		
4.80	1.0	1.13
2.40	3.0	1.09
2.88	5.0	1.12
2.88	8.0	1.11
4.80	10.0	1.20
7.20	20.0	1.11
$Av. = (1.13 \pm 0.04) \times 10^{-4} s^{-1}$		

$10^4 \times [PdIDA], M$	$10^4 \times [TTHA], M$	$10^5 \times k_2, s^{-1}$
(B) temp. = $30 \pm 0.1^\circ C$, pH = 8.0 ± 0.02 and I = 0.1M(NaClO ₄).		
1.2	0.88	8.05
1.0	1.0	9.36
1.0	2.5	10.20
1.2	5.0	9.42
1.0	8.0	9.76
1.0	10.0	9.97
1.0	25.0	9.95
1.0	50.0	9.82
$Av. = (9.83 \pm 0.24) \times 10^{-5} s^{-1}$		

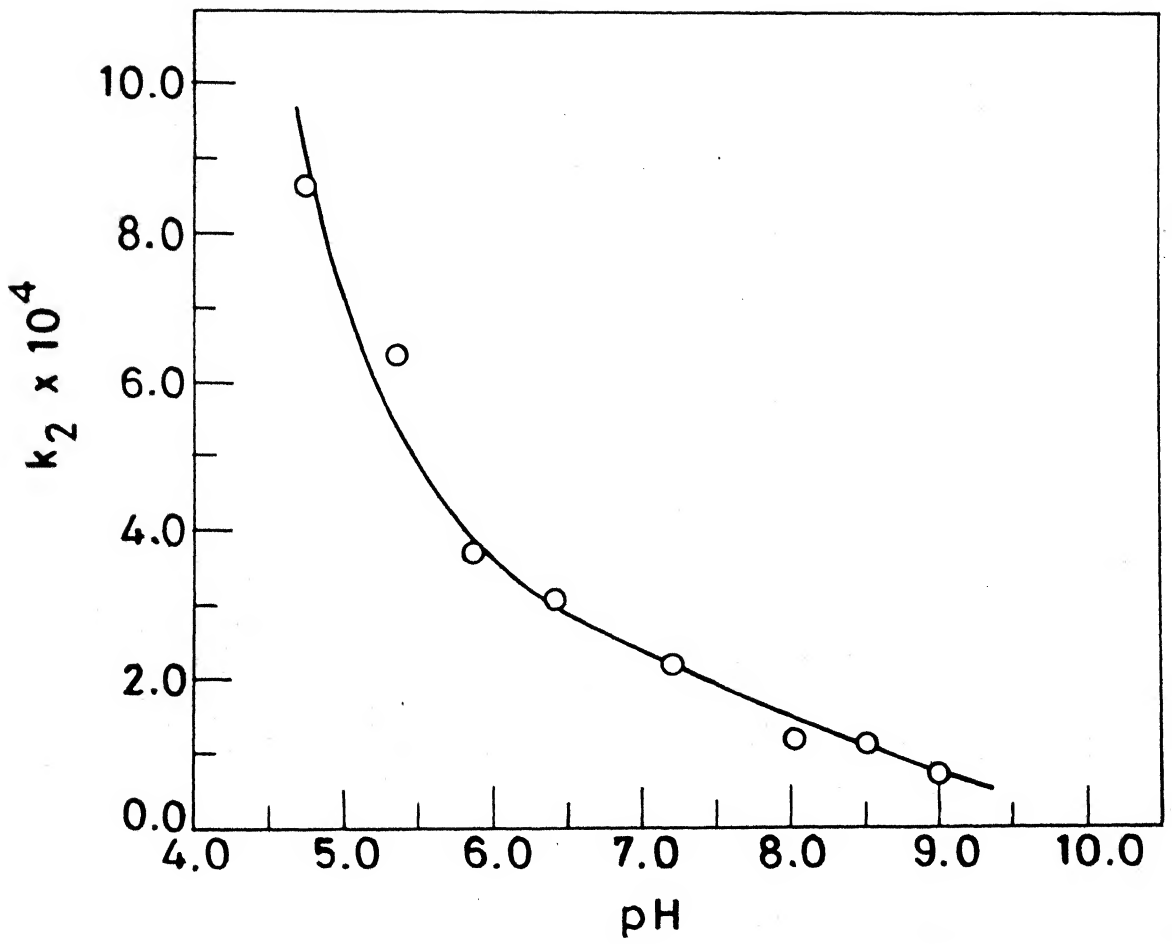


Fig. V.9 Effect of pH on the decomposition of $[\text{PdIDA} \cdot \text{EDTA}]^{2-}$.

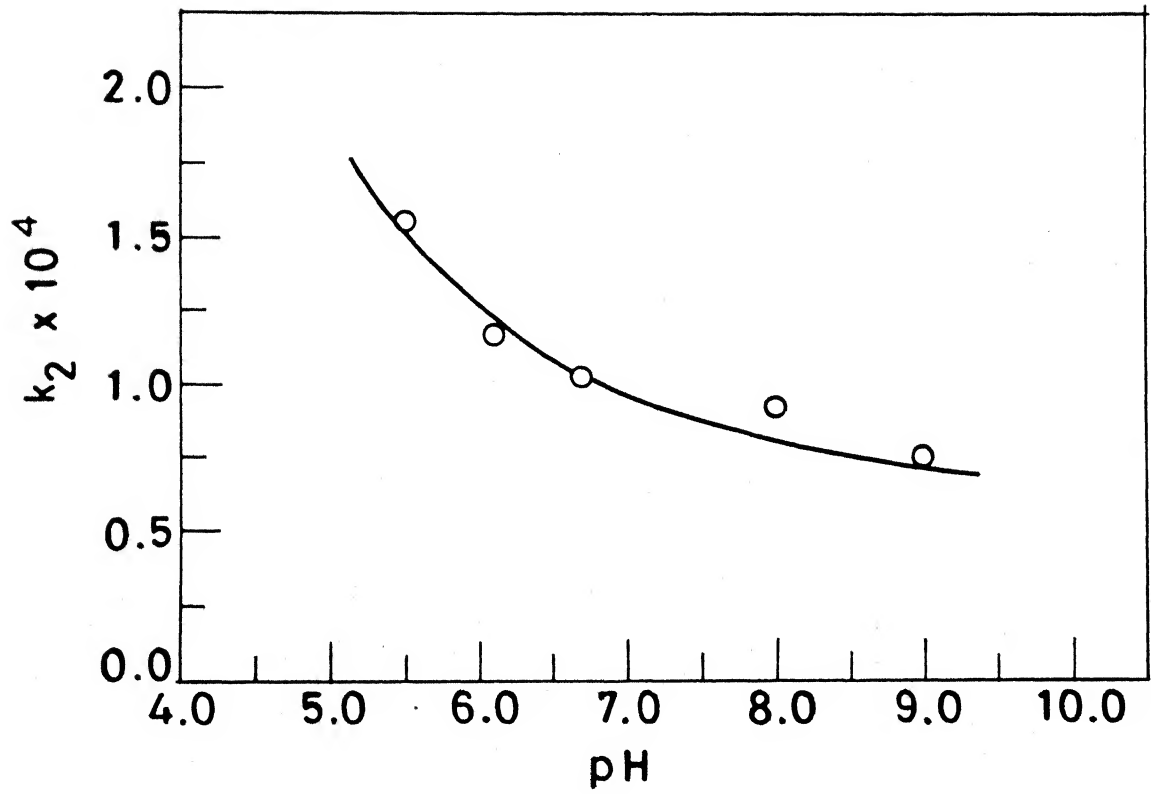


Fig.V.10 Effect of pH on the decomposition of $[\text{PdIDA. TTHA}]^{4-}$

TABLE V.7. Effect of pH on the decomposition rate of
 $[PdIDA \cdot L]^{n-}$

pH	k_2, s^{-1}
(A) $[PdIDA] = 2.88 \times 10^{-5} M, [EDTA] = 8.0 \times 10^{-3} M,$	
$I = 0.2M(NaClO_4)$, and temp. = $30 \pm 0.1^\circ C.$	
4.75	8.6×10^{-4}
5.35	6.4×10^{-4}
5.85	3.7×10^{-4}
6.4	3.1×10^{-4}
7.2	2.2×10^{-4}
8.0	1.2×10^{-4}
8.5	1.1×10^{-4}
9.0	7.0×10^{-5}
(B) $[PdIDA] = [TTHA] = 1.0 \times 10^{-4} M, I = 0.1M(NaClO_4),$	
and temp. = $30 \pm 0.1^\circ C.$	
5.5	1.55×10^{-4}
6.1	1.17×10^{-4}
6.7	1.03×10^{-4}
8.0	9.36×10^{-5}
9.05	7.53×10^{-5}

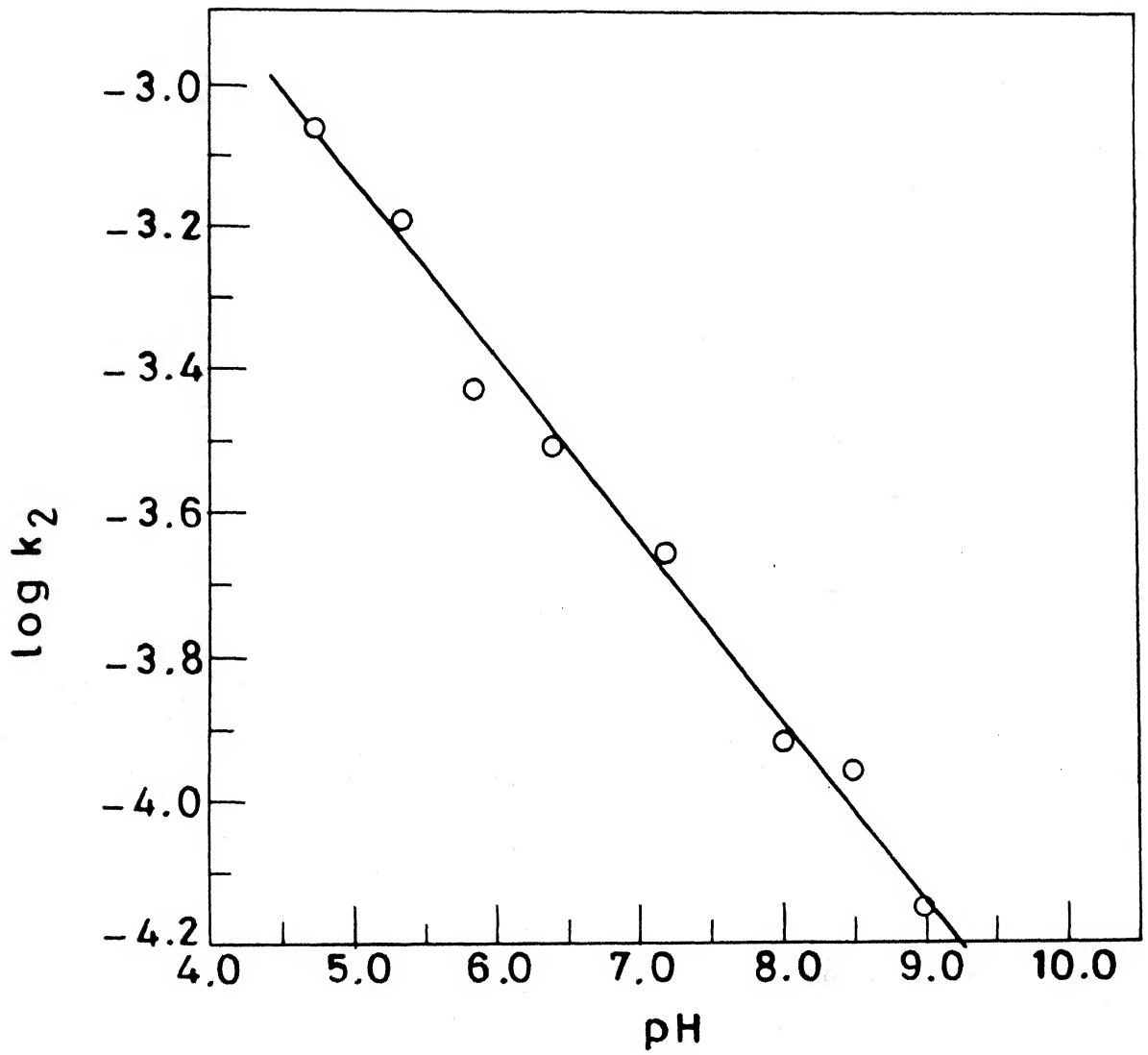


Fig. V.11 Plot of $\log k_2$ versus pH for the decomposition of $[\text{PdIDA} \cdot \text{EDTA}]$. Reaction conditions as in Fig. V.10.

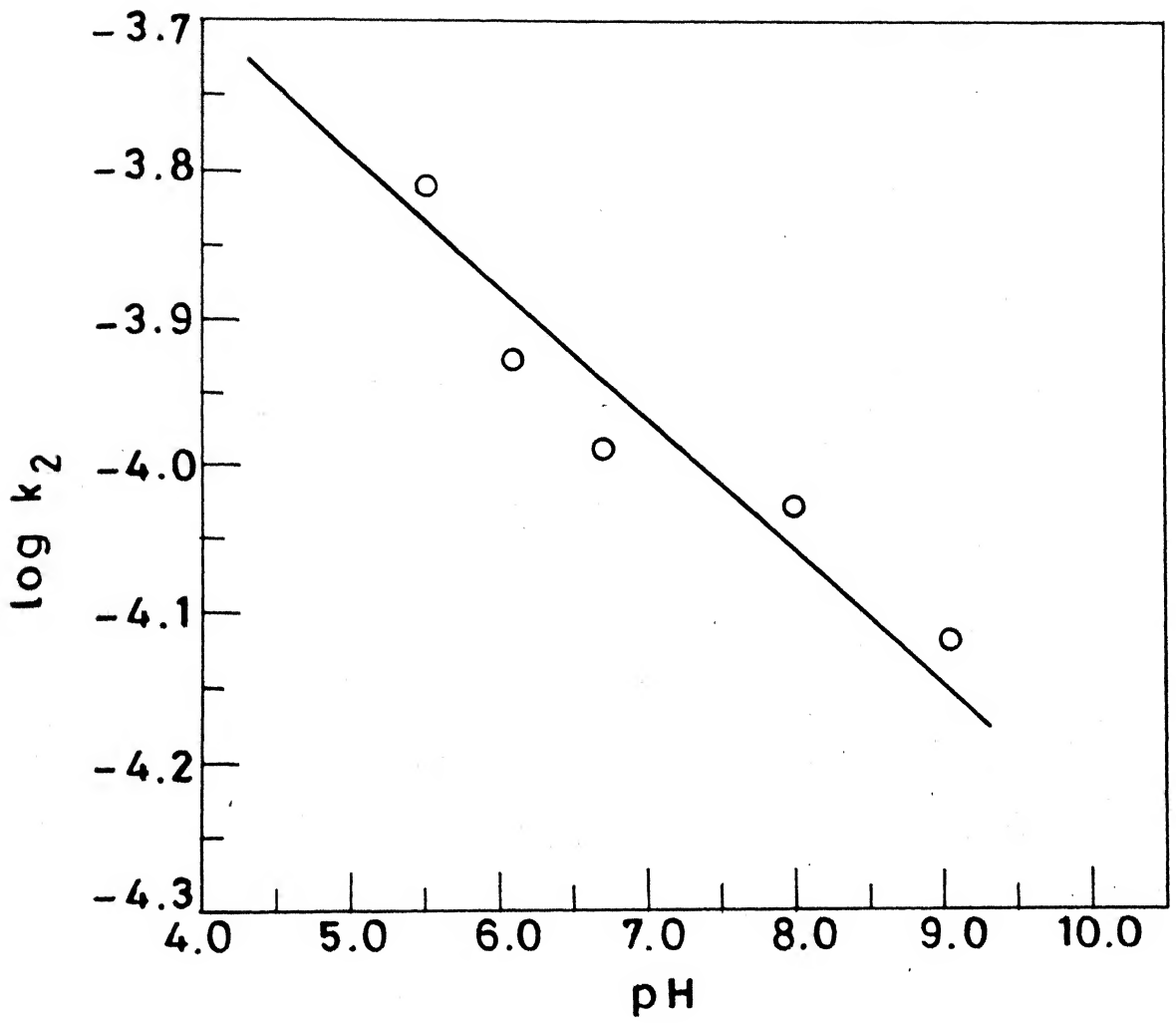


Fig.V.12 Plot of $\log k_2$ versus pH for the decomposition of $[\text{PdIDA}\cdot\text{TTHA}]^{4-}$. Reaction conditions as in Fig.V.10.

TABLE V.8. Activation parameters

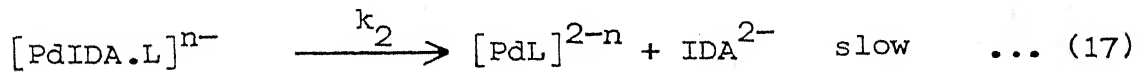
Formation of mixed ligand complex $[\text{PdIDA} \cdot \text{L}]^{n-}$	Formation of $[\text{PdL}]^{2-n}$
(A) $[\text{PdIDA}] + \text{EDTA}$ reaction	
$E_a = 24.0 \pm 0.3 \text{ kJ mol}^{-1}$	$E_a = 32.9 \pm 0.3 \text{ kJ mol}^{-1}$
$\Delta H^{\circ\neq} = 21.5 \pm 0.3 \text{ kJ mol}^{-1}$	$\Delta H^{\circ\neq} = 30.4 \pm 0.3 \text{ kJ mol}^{-1}$
$\Delta S^{\circ\neq} = -137.1 \pm 1.1 \text{ JK}^{-1} \text{mol}^{-1}$	$\Delta S^{\circ\neq} = -171.3 \pm 1.1 \text{ JK}^{-1} \text{mol}^{-1}$
$p_z = 4.7 \times 10^5 \text{ cm}^{-1}$	$p_z = 7.3 \times 10^3 \text{ cm}^{-1}$
(B) $[\text{PdIDA}] + \text{TTHA}$ reaction	
$E_a = 48.3 \pm 0.1 \text{ kJ mol}^{-1}$	$E_a = 55.5 \pm 0.6 \text{ kJ mol}^{-1}$
$\Delta H^{\circ\neq} = 45.8 \pm 0.1 \text{ kJ mol}^{-1}$	$\Delta H^{\circ\neq} = 53.2 \pm 0.6 \text{ kJ mol}^{-1}$
$\Delta S^{\circ\neq} = -57.1 \pm 0.4 \text{ JK}^{-1} \text{mol}^{-1}$	$\Delta S^{\circ\neq} = -73.5 \pm 1.9 \text{ JK}^{-1} \text{mol}^{-1}$
$p_z = 6.6 \times 10^9 \text{ cm}^{-1}$	$p_z = 1.2 \times 10^9 \text{ cm}^{-1}$

V.3.7 Effect of temperature

Both the reaction systems viz. PdIDA-EDTA and PdIDA-TTHA were studied over a temperature range of 25-45°C. Activation parameters for the fast and slow steps have been calculated from Arrhenius plots and are given in Table V.8.

V.4 Discussion

The reactions of [PdIDA] with EDTA^{4-} and TTHA^{6-} are thermodynamically favoured. On the basis of experimental observations it is proposed that both reactions proceed through the rapid formation of intermediates in which both the incoming and outgoing ligands are bonded simultaneously to the metal centre (equation 16). The stoichiometry for these ternary intermediates was established to be 1:1:1 by the mole ratio method. These dissociate to give $[\text{PdL}]^{2-n}$ with the release of IDA^{2-} according to equation (17).



Pd(II) forms square planar complexes with most ligands. Substitution of square planar complexes of Pd(II) proceeds by an associative pathway implicating five coordinated intermediates. Again, these intermediate species decompose to finally give square planar Pd(II) complexes. Pearson²⁶ has proposed a mechanism for

substitution of one dithiolate ligand $(S-S)^-$ in a complex of nickel(II), $[Ni(S-S)_2]$, by a different dithiolate ligand, $(S'-S')^-$, which involves the bimolecular formation of a five coordinated intermediate. Similar intermediates have been proposed and identified in other studies of substitution reactions of nickel(II)^{26,27}, palladium(II)²⁸ and platinum(II)²⁹ complexes.

The values of ΔS^\neq for the first stage of the reaction is less negative compared to the second stage of the reaction (Table V.8). Iminodiacetate is a tridentate ligand. During formation of mixed ligand complex, $[PdIDA \cdot L]^{n-}$ some binding sites of IDA and L^{n-} remain uncomplexed causing some increase of disorder and consequent increase in entropy. During the second stage, however, the partly chelated ligand viz. IDA starts dissociating to give, perhaps, a more orderly and highly solvated activated complex accounting for the large decrease in entropy in the second stage of reaction. The enthalpy of activation for the first stage is low as is expected in an associative additive process and higher for the second stage consistent with a bond breaking event. It is not too high, ofcourse, because along with dissociation of IDA some new bonds are also formed with EDTA or TTHA. The effect of ionic strength on the rate of first stage was negligible as expected. In the second stage, dissociation of the mixed complexes is involved and the effect of ionic strength on this rate is again expected to be negligible.

Evidence for these reactions is provided by repetitive scans of the reaction mixtures at suitable intervals. The repetitive scans for PdIDA-EDTA and PdIDA-TTHA systems are given in Fig. V.13 and 14. Immediately on mixing the reactants a band appears at 325 nm due to formation of mixed complexes $[PdIDA \cdot L]^{n-}$, which decreases continuously for about thirty minutes. In the later part of the reactions the 325 nm band shifts to 337 nm which is accounted for due to the formation of $[PdEDTA]^{2-}$ or $[PdTTHA]^{4-}$. Some similar reactions of palladium have been studied by Fayyaz and Grant.²⁸ There is also a corresponding appearance and increase in the 240 nm peak height due to the gradual release of iminodiacetic acid during the course of reaction indicating the conversion of $[PdIDA \cdot L]^{n-}$ to $[PdL]^{2-n}$.

It may be interesting to speculate on the possible pathways of these substitution reactions. The structure of $[PdIDA]$ has not been reported so far according to our information. In keeping with known square planar geometry of most Pd(II) complexes, the fourth equatorial site will be occupied by water molecule as shown in structure I of Fig. V.15. The structure of $[PdEDTA]^{2-}$ has been proposed by Gonzalez-Vilchez et al.³⁰ on the basis of nmr studied. A plausible pathway for transformation of $[PdIDA]$ to $[PdEDTA]^{2-}$ is depicted in Fig. V.15. This, however is not to the exclusion of other alternatives. The transformation to form $[PdTTHA]^{4-}$ may also follow similar path.

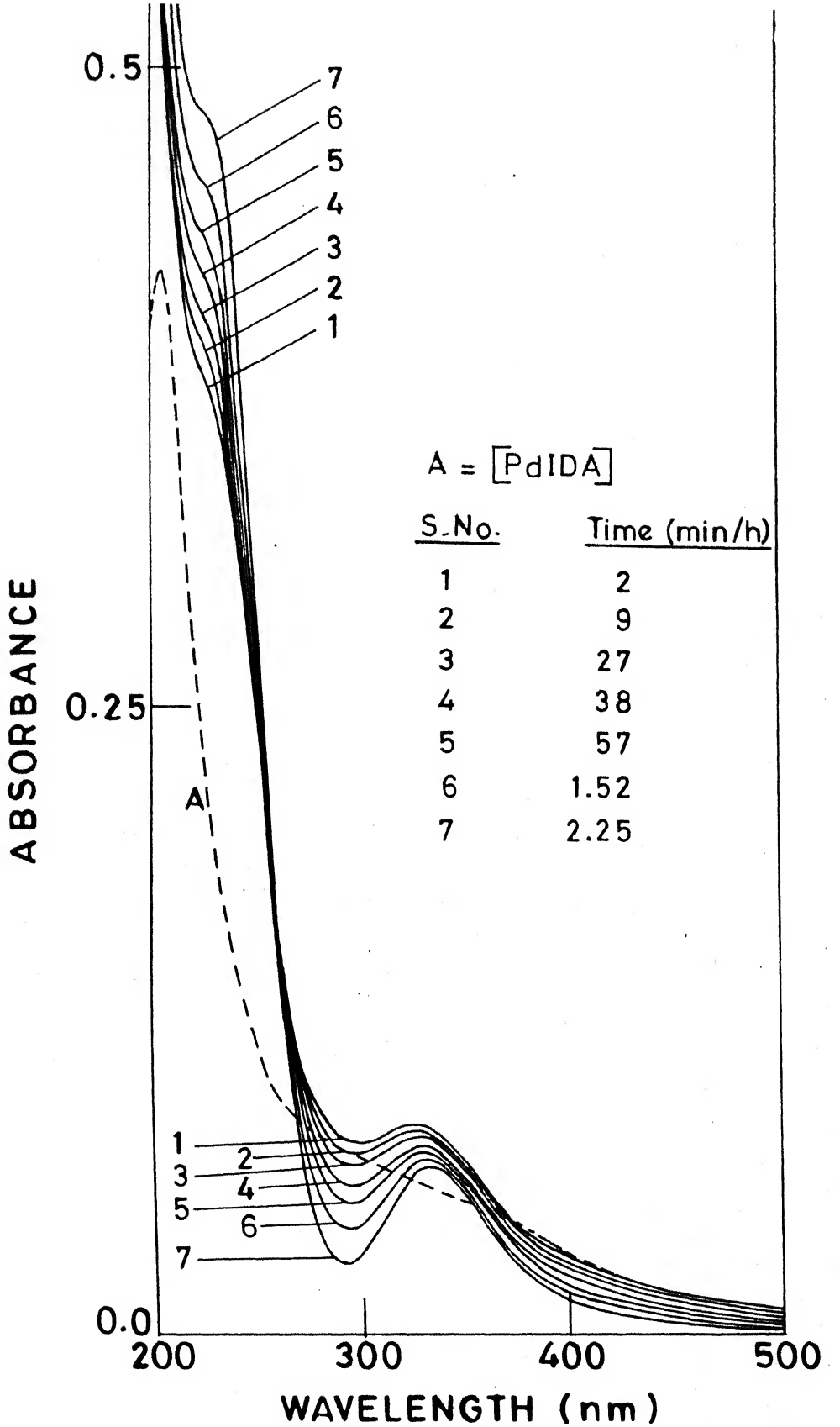


Fig.V.13 Spectral scan of the reaction between $[PdIDA]$ and EDTA. $[PdIDA] = 2.88 \times 10^{-5} M$, $[EDTA] = 5.0 \times 10^{-4} M$, $pH = 5.0 \pm 0.02$, $A = [PdIDA]$

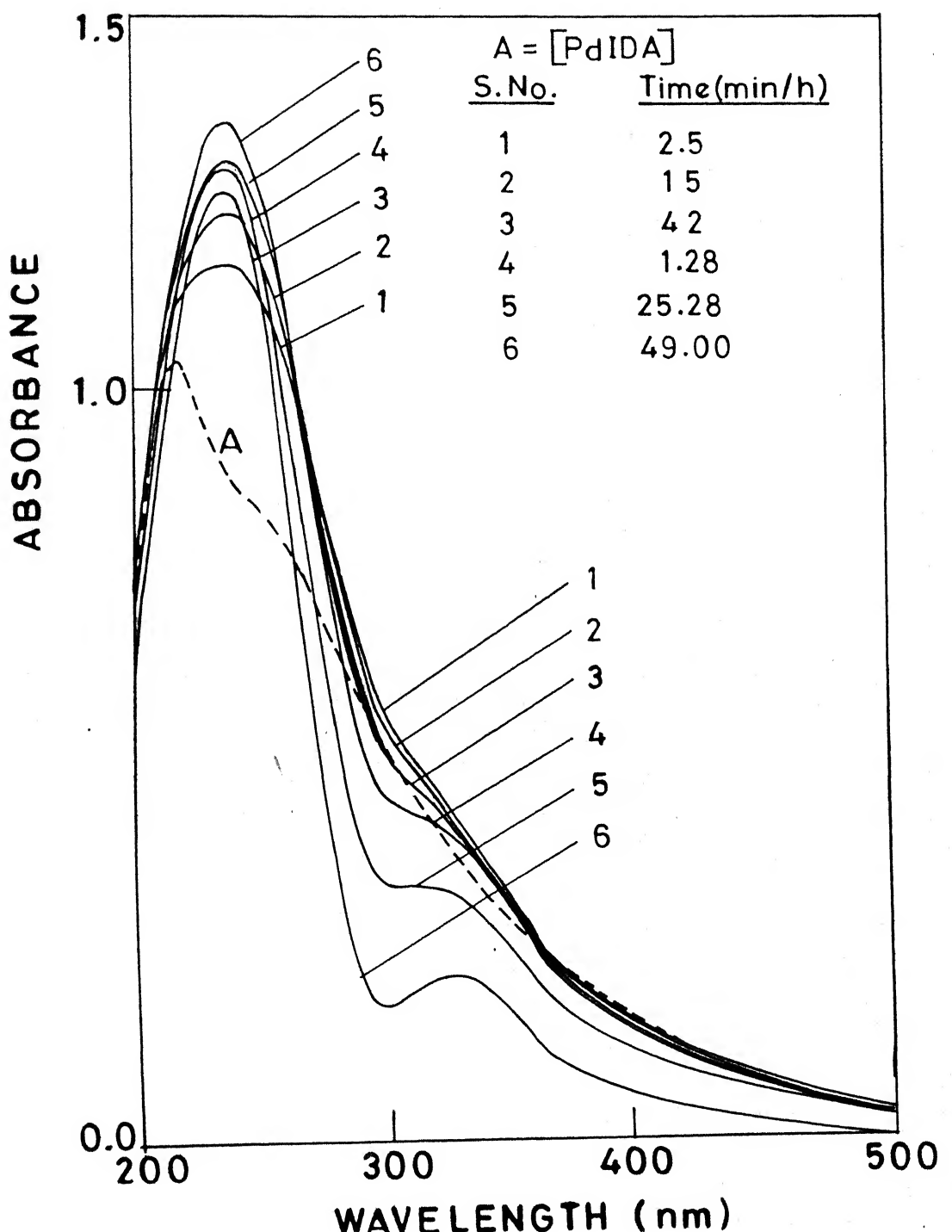


Fig.V.14 Repetitive scan of the reaction between $[\text{PdIDA}]$ and TTHA. $[\text{PdIDA}] = [\text{TTHA}] = 1.0 \times 10^{-4} \text{ M}$, $\text{pH} = 8.0 \pm 0.02$, $A = [\text{PdIDA}]$.

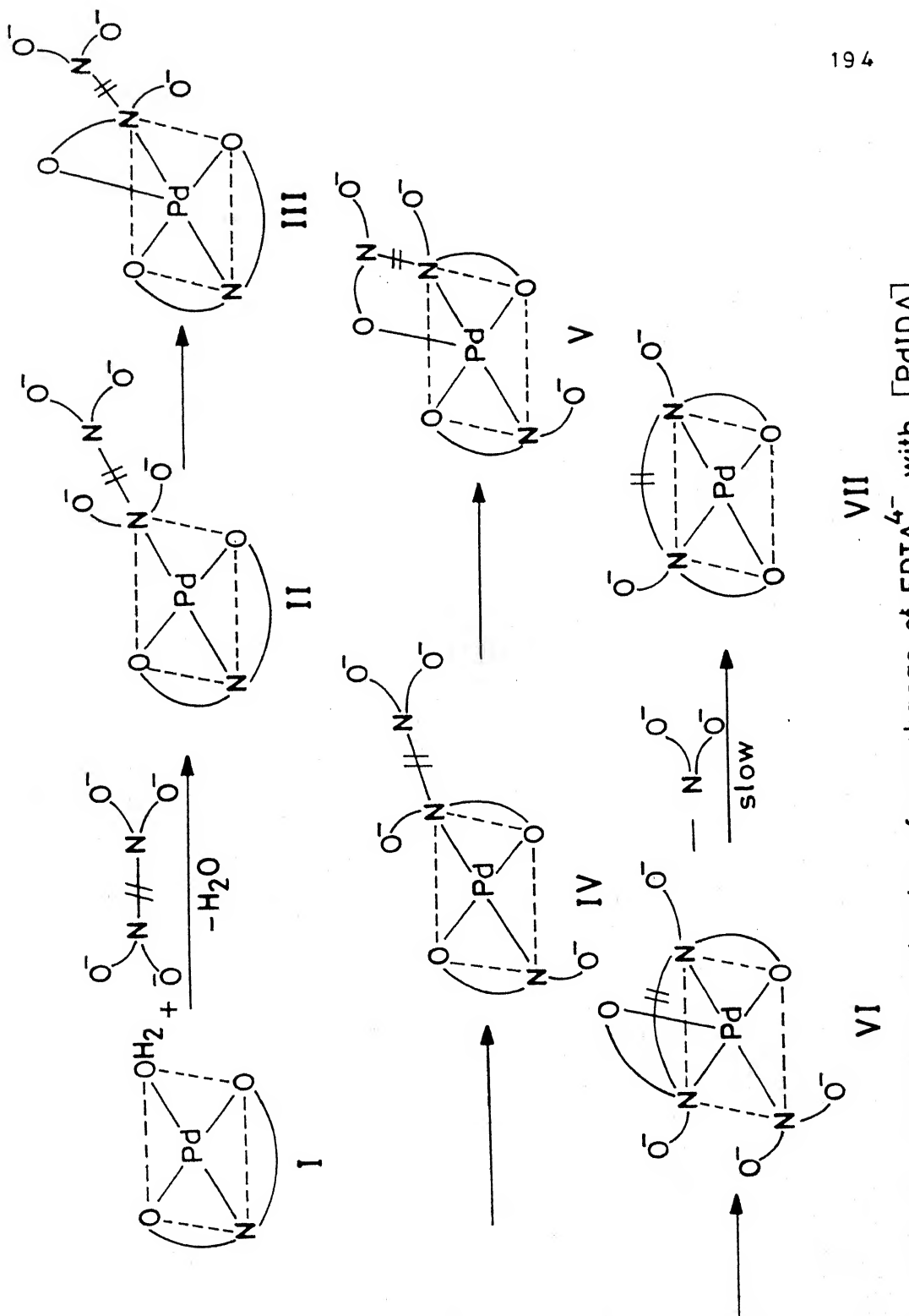


Fig. V.15 Proposed mechanism for exchange of EDTA^{4-} with $[\text{Pd}(\text{II})]$.

To summarize, the reactions between $[PdIDA]$ and $EDTA^{4-}$ or $TTHA^{6-}$ take place in two stages (equations 16 and 17) through the rapid formation of mixed ligand complex intermediates $[PdIDA \cdot L]^{n-}$ in the first stage followed by a slow dissociation of this mixed complex to give $[PdL]^{2-n}$ and IDA finally.

REFERENCES

1. O.C. Olson and D.W. Margerum, *J. Am. Chem. Soc.*, 1963, 85, 297.
2. D.B. Rorabacher and D.W. Margerum, *Inorg. Chem.*, 1964, 3, 382.
3. R.J. Kula and G.H. Reed, *Anal. Chem.*, 1966, 38, 697.
4. L.J. Sudmeir and C.N. Reilley, *Inorg. Chem.*, 1966, 5, 1047.
5. M. Kodama, S. Karasawa and T. Watanabe, *Bull. Chem. Soc. Jpn.*, 1971, 44, 1815.
6. M. Kodama, M. Hashimoto and T. Watanabe, *Bull. Chem. Soc. Jpn.*, 1972, 45, 2761.
7. M. Kodama, *Bull. Chem. Soc. Jpn.*, 1969, 42, 3330.
8. M. Kodama and K. Hagiya, *Bull. Chem. Soc. Jpn.*, 1973, 46, 3151.
9. K. Kumar and P.C. Nigam, *Ind. J. Chem.*, 1981, 20, 1623.
10. H.C. Bajaj, K. Kumar and P.C. Nigam, *Ind. J. Chem.*, 1981, 19A, 1070.
11. H.C. Bajaj and P.C. Nigam, *Ind. J. Chem.*, 1984, 23A, 8.
12. R.M. Naik and P.C. Nigam, *Ind. J. Chem.*, 1987, 26A, 205.
13. R.K. Steinhause and J.A. Boersma, *Inorg. Chem.*, 1972, 11, 1505.
14. A.J. Cohen and J. Davidson, *J. Am. Chem. Soc.*, 1951, 73, 1955.
15. A.I. Vogel, "Quantitative Inorganic Analysis", 4th edn., Longman Green, London, 1985, p.474.
16. D.D. Perrin and I.G. Sayce, *Talanta*, 1967, 14, 833.
17. A.E. Martell and R.M. Smith, "Critical Stability Constants", Vol. 1, Plenum Press, New York and London, 1974, p. 116.

18. H. Wikberg and A. Ringbom, *Suomen Kem*, 1968, B41, 177.
19. A.N. Ermakov, I.N. Marov, and N.B. Kalinicheuko, *Russ. J. Inorg. Chem.*, 1966, 11, 1404 (2614).
20. T.A. Bohigian and A.E. Martell, *J. Amer. Chem. Soc.*, 1967, 89, 832.
21. T.A. Bohigian and A.E. Martell, *J. Inorg. Nuclear Chem.*, 1967, 29, 453.
22. G.H. Carey and A.E. Martell, *J. Amer. Chem. Soc.*, 1968, 90, 32.
23. F.A. Gonzalez-Vilchez and M. Castillo, *J. Inorg. Nucl. Chem.*, 1975, 37, 316.
24. W.M. MacNevin and O.H. Kriegl, *J. Am. Chem. Soc.*, 1955, 77, 6149.
25. A. Napoli, *Talanta*, 1984, 31, 153.
26. R.G. Pearson and D.A. Sweigart, *Inorg. Chem.*, 1970, 9, 1167.
27. M.J. Hynes and P.F. Brannick, *J. Chem. Soc. Dalton Trans.*, 1977, 2281.
28. M.U. Fayyaz and M.W. Grant, *Aust. J. Chem.*, 1979, 32, 2159.
29. M.J. Hynes and A.J. Moran, *J. Chem. Soc. Dalton Trans.*, 1973, 2280.
30. M.G. Basallote, R. Vilaplana, F. Gonzalez-Vilchez, *Polyhedron*, 1987, 6, 571.

CHAPTER - VI

- A. KINETICS AND MECHANISM OF CATALYTIC DECOMPOSITION OF HYDROGEN PEROXIDE IN PRESENCE OF $[\text{FeTrien}]^{3+}$ COMPLEX (TRIEN = TRIETHYLENETETRAMINE) AND TRACE DETERMINATION OF IRON(III) BY A KINETIC METHOD
- B. KINETICS AND MECHANISM OF OXIDATION OF DIETHYLENE-TRIAMINEPENTAACETIC ACID BY HEXACYANOFERRATE(III)

ABSTRACT

The kinetics of decomposition of hydrogen peroxide in presence of triethylenetetramine complex of iron(III) has been investigated at $\text{pH} = 10.0 \pm 0.1$, $\text{temp.} = 25 \pm 0.1^\circ\text{C}$, $[(\text{Trien})-\text{Fe}(\text{OH})_2^+] = 3.15-6.3 \times 10^{-7} \text{M}$ over a wide range of hydrogen peroxide concentration. The reaction follows a Michaelis-Menten type mechanism in which the complex displays a "catalase-like" activity. The constant K_m has been determined from Lineweaver-Burk plots. The mechanism of catalytic activity has been discussed. This reaction has been further used for an analytical application described in the following paragraph.

A sensitive kinetic method is developed for the trace determination of Fe(III) based on the above described reaction. In presence of moderately high concentration of hydrogen peroxide, the initial rate is linearly related to the catalyst concentration. A "fixed-time procedure" is used to obtain a linear calibration curve between the initial rate and the catalyst concentration in the range $(1.0 \times 10^{-8} - 4.9 \times 10^{-6} \text{ M})$ for ferric ions. The detection limit is $1 \times 10^{-8} \text{ M}$ and maximum percentage error is 12.5% in the lower concentration limit. The method is sensitive, accurate, inexpensive and rapid. The interferences from a large number of cations with the exception of Mn^{2+} are negligible.

VI.A.2 INTRODUCTION

The decomposition of hydrogen peroxide in aqueous solution is known to be catalysed by many transition metal ions including Fe^{3+} . In recent years, there have been reports that many complex of transition metals are more effective catalysts than the corresponding aquo metal ions. The discovery by Wang¹ that the trien complex of Fe(III) possesses a "catalase" like activity, through of a lesser order (catalase has four active sites while this complex has two) for the decomposition of hydrogen peroxide prompted us to investigate the reaction and test the analytical possibilities of this reaction for trace determination of Fe(III). Wang¹ had also proposed a mechanism for the catalytic action and tested it in many ways. He pointed out that the trien complex

was a much more effective catalyst compared to the complexes of en, dien, tetren or aquo complexes. He advanced arguments to explain these observations. Later Wada and coworkers² observed that at relatively low concentration of H_2O_2 the ligands en, dien and H_2O provided greater reactivity compared to trien. Their experiments, however, were conducted at pH 3 while Wang¹ had carried out his investigation in pH range 6-10.

One observation of considerable analytical interest to us was that, barring Mn(II), the presence of many cations does not affect the rates of decomposition reaction materially. In this chapter we report the results of our investigations on the trace determination of Fe(III) at the ppm level in the presence of a large number of cations. The proposed method is rapid, sensitive, specific and inexpensive.

VI.A.3 MATERIALS AND METHODS

VI.A.3.1 Reagents

Hydrogen peroxide 30% (AR, BDH) was purified by distillation at 60 nm Hg pressure after removing any Fe(III) and other cations by percolation through a column of acid-regenerated Dowex 50X-8 (50-100 mesh). The concentration of H_2O_2 in the distillate was determined by titration against standard potassium permanganate. Stock solutions of ferric perchlorate and trien were prepared in triply distilled water. The trien complex of ferric ions was prepared by mixing ferric perchlorate with trien taken in a

thousand-fold excess. Sodium hydroxide (AR, BDH) or perchloric acid 70% (AR, BDH) were used for maintaining pH at any desired value. Buffers were not used for fear of complicating the reaction system. The effect of ionic strength was negligible as tested by earlier workers¹ as well as by us. All glass ware were steamed before use. Scrupulous cleaning is very necessary for obtaining consistent results.

VI.A.3.2 Procedure

The reactant solutions were brought to the desired temperature by immersion in a thermostatic bath maintained at $25 \pm 0.1^{\circ}\text{C}$ for about 30 minutes. The reaction was regarded as starting when a solution of $[(\text{trien})\text{Fe}(\text{OH})_2]^+$ was quickly poured into a reaction vessel containing a solution of hydrogen peroxide also kept in the thermostatic bath. Aliquots of the reaction mixture were drawn at short intervals and dropped into excess standard ceric sulphate solution. The amount of ceric sulphate present and thus the hydrogen peroxide remaining at any time were determined by titration with standard ferrous ammonium sulphate using o-phenanthroline as an indicator.

In order to correct for traces of Fe(III) that may be present in the reagent(s) or in glass ware as an impurity, a blank determination was performed for each kinetic run with trien and H_2O_2 but without Fe(III). The initial rates corresponding to each Fe(III) concentration were determined by the plane mirror

method.³ For drawing calibration curves, the concentration changes of H_2O_2 for a fixed-time interval were plotted against concentration of the $[(\text{trien})\text{Fe}(\text{OH})_2]^+$ complex. This is often referred to as the "fixed-time procedure" for determining initial rate.

VI.A.4 RESULTS

VI.A.4.1 Effect of hydrogen peroxide and $[(\text{trien})\text{Fe}(\text{OH})_2]^+$ concentrations

Plots showing the effect of H_2O_2 concentration on the initial rate of the decomposition reaction in presence of three different concentrations of $[(\text{trien})\text{Fe}(\text{OH})_2]^+$ complex give Michaelis-Menten type saturation curves (Fig. VI.A.1). The values of initial rates (or turnover numbers) are higher than those reported by Wang¹ and are given in Table VI.A.1. If any inhibitor were present in the system the initial rates (or turnover numbers) are bound to be lower. As mentioned in the experimental section, our samples of H_2O_2 had been scrupulously purified while Wang¹ has made no mention about purifying their sample of hydrogen peroxide. At specified conditions, the initial rate is linearly related to $[(\text{trien})\text{Fe}(\text{OH})_2]^+$ concentration in the lower concentration range, attains a maximum value and then decreases (Fig. VI.A.2). This decrease can be explained if it is assumed that the given complex dimerises giving, perhaps, $[\text{Fetrien} \begin{array}{c} \diagup \\ \text{O} \\ \diagdown \end{array} \text{trienFe}]$ which is a noncatalytic species. The change in catalytic character can be understood if the mechanism proposed by Wang¹ is assumed to hold good (vide supra). An evidence

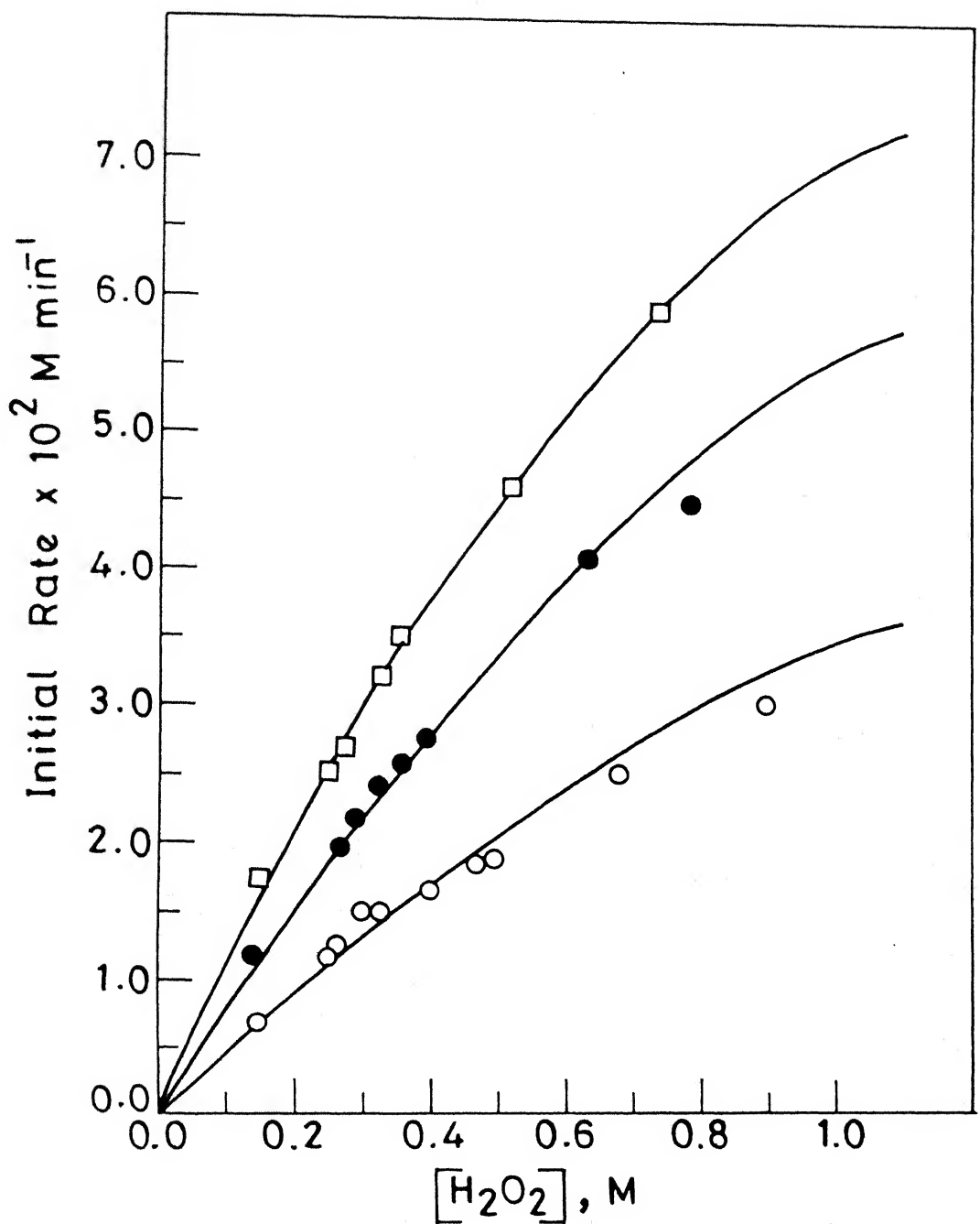


Fig. VI.A.1 Hydrogen peroxide decomposition rate as a function of H_2O_2 at $\text{pH} = 10.0 \pm 0.1$ and temp. = $25 \pm 0.1^\circ\text{C}$. $[\text{trien-Fe}(\text{OH})_2^+]$, $(\square) = 6.3 \times 10^{-7} \text{ M}$, $(\bullet) = 4.7 \times 10^{-7} \text{ M}$, $(\circ) = 3.15 \times 10^{-7} \text{ M}$.

TABLE VI.A.1. Effect of hydrogen peroxide concentration on the initial rate of decomposition of H_2O_2 at pH = 10.0 ± 0.02 and temp. = $25 \pm 0.1^\circ\text{C}$.

$10^1 \times [\text{H}_2\text{O}_2], \text{ M}$	$10^2 \times \text{Initial rate, M min}^{-1}$
A. $[(\text{trien})\text{Fe}(\text{OH})_2^+] = 3.15 \times 10^{-7} \text{ M}$,	
1.5	0.7
2.5	1.2
2.6	1.25
3.0	1.5
3.3	1.5
4.0	1.65
4.7	1.85
5.0	1.9
6.8	2.5
9.0	3.0
B. $[(\text{trien})\text{Fe}(\text{OH})_2^+] = 4.7 \times 10^{-7} \text{ M}$,	
1.4	1.2
2.7	1.95
2.9	2.2
3.3	2.45
3.5	2.5
3.9	2.75
6.3	4.05
8.0	4.3

...contd.

TABLE VI.A.1 (contd.)

$10^1 \times [H_2O_2], M$	$10^2 \times \text{Initial rate, } M \text{ min}^{-1}$
c. $[(\text{trien})\text{Fe}(\text{OH})_2^+] = 6.3 \times 10^{-7} M$,	
1.5	1.75
2.5	2.5
2.7	2.7
3.3	3.2
3.5	3.5
5.2	4.6
7.4	5.9

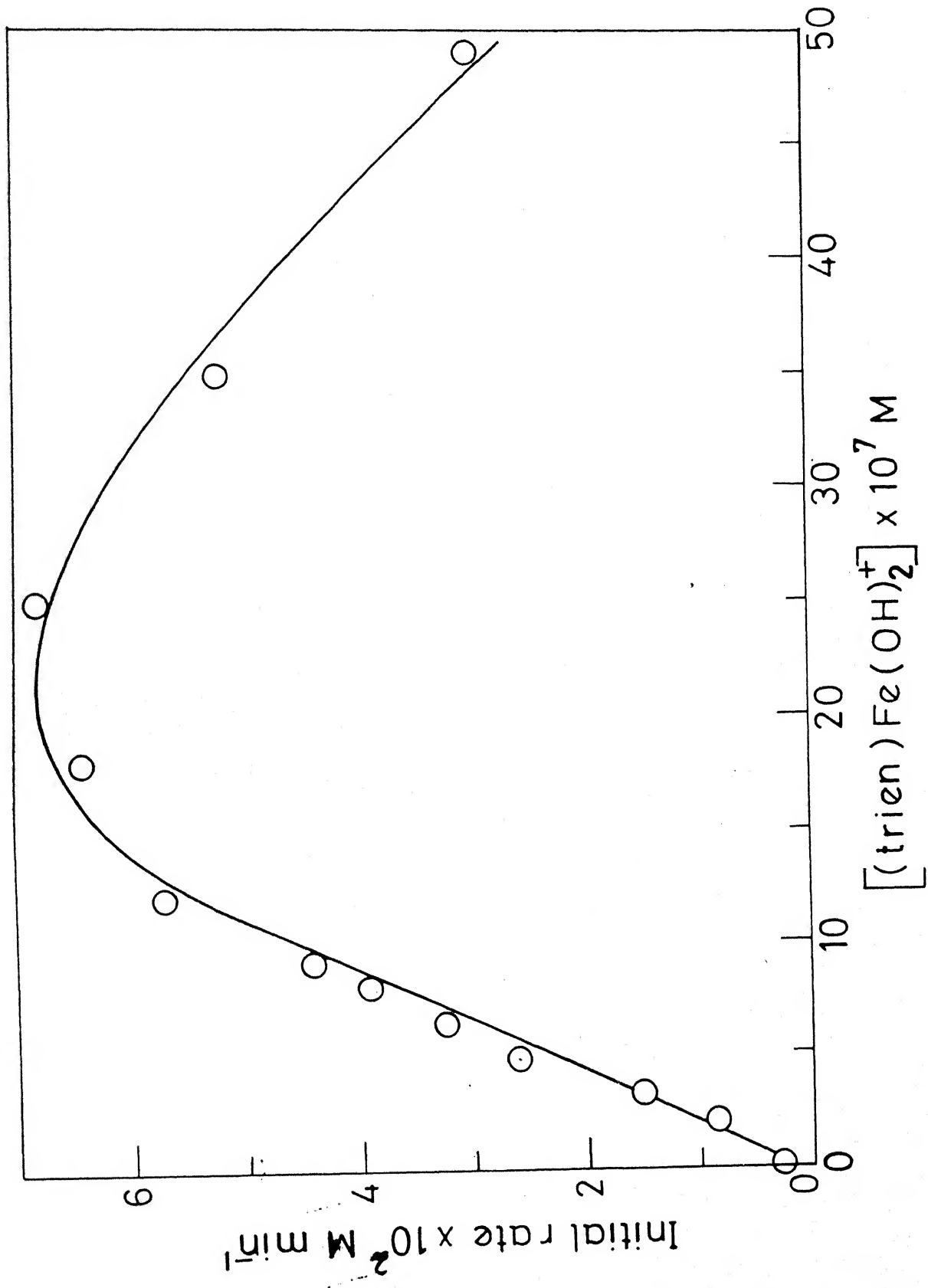


Fig.VI.A.2 Hydrogen peroxide decomposition rate as a function

for dimerization can be provided by considering the spectral changes of $[(\text{trien})\text{Fe}(\text{OH})_2]^+$ at different concentrations (Fig. VI.A.3). Of the two peaks at 310 and 330 nm observed in the spectra of the $[(\text{trien})\text{Fe}(\text{OH})_2]^+$ complex, the height of the first relative to the second enhances as the concentration of the complex changes from 9.7×10^{-7} to 7.5×10^{-6} M. If the first peak is assigned to the dimer and the second to the monomer, the ratio (A_{310}/A_{330}^2) , is measure of the equilibrium constant for the (2 Monomer \xrightleftharpoons{K} dimer) transformation. The ratio can be checked to be reasonably constant (12.7 ± 1.6) in this concentration range confirming the existence of monomer-dimer equilibrium.

It is also interesting to note that the expected Beer's law relationship between the complex concentration and absorbance at 330 nm (Fig. VI.A.4) begins to deviate from linearity above the concentration level where the catalytic activity also starts decreasing (Fig. VI.A.2). Thus our postulate about loss of catalytic power of $[(\text{trien})\text{Fe}(\text{OH})_2]^+$ at higher concentration is reasonable. Similar dimerization is known also for some other complexes of Fe(III), the most well known examples being formation of $[\text{Fe}_2(\text{CN})_{10}]^{4-}$ from $[\text{Fe}(\text{CN})_5\text{H}_2\text{O}]^{3-}$ and $[\text{Fe}_2\text{L}_2\text{O}]$ from $[\text{FeL}(\text{OH})]$ where L = EDTA, HEDTA and CYDTA.⁵

VI.A.4.2 Effect of pH

The effect of pH on the rate of decomposition of H_2O_2 is shown in Fig. VI.A.5. The rate increases linearly and then "levels

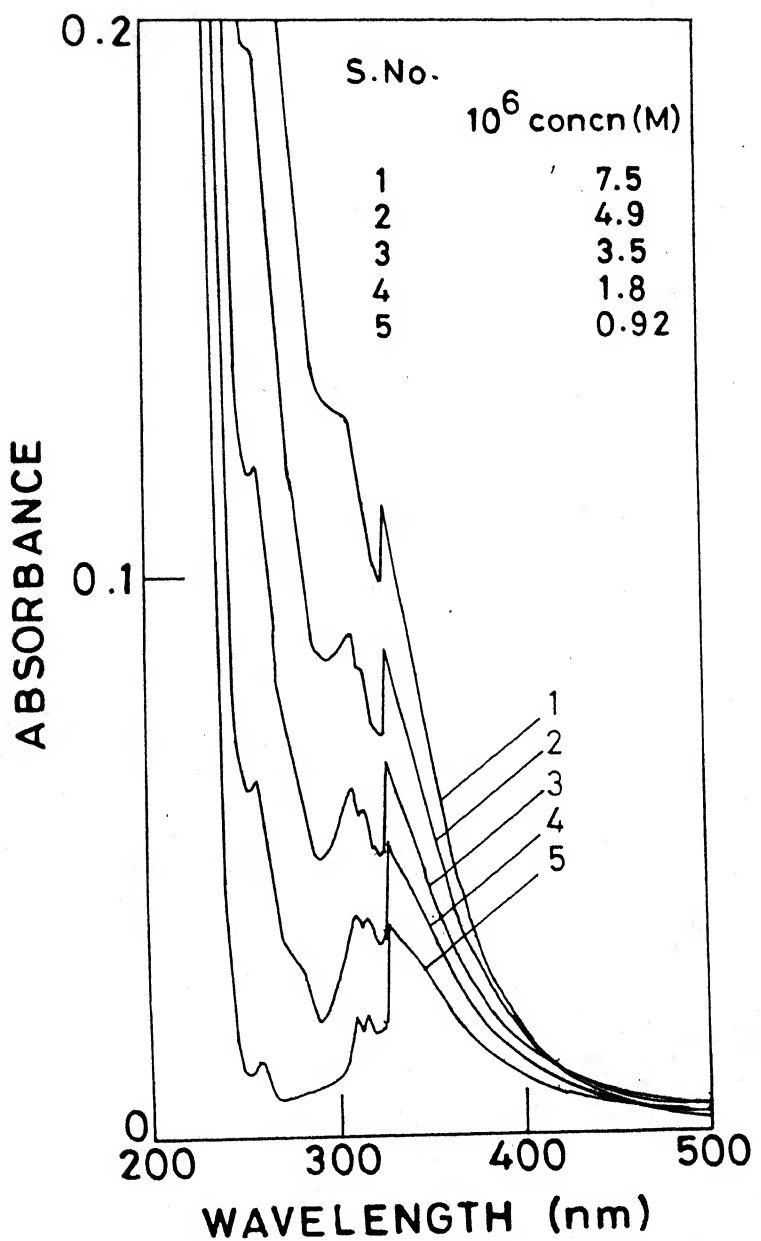


Fig.VI.A.3 Spectral changes with change in concentration of $[(\text{trien})\text{Fe}(\text{OH})_2]^+$.

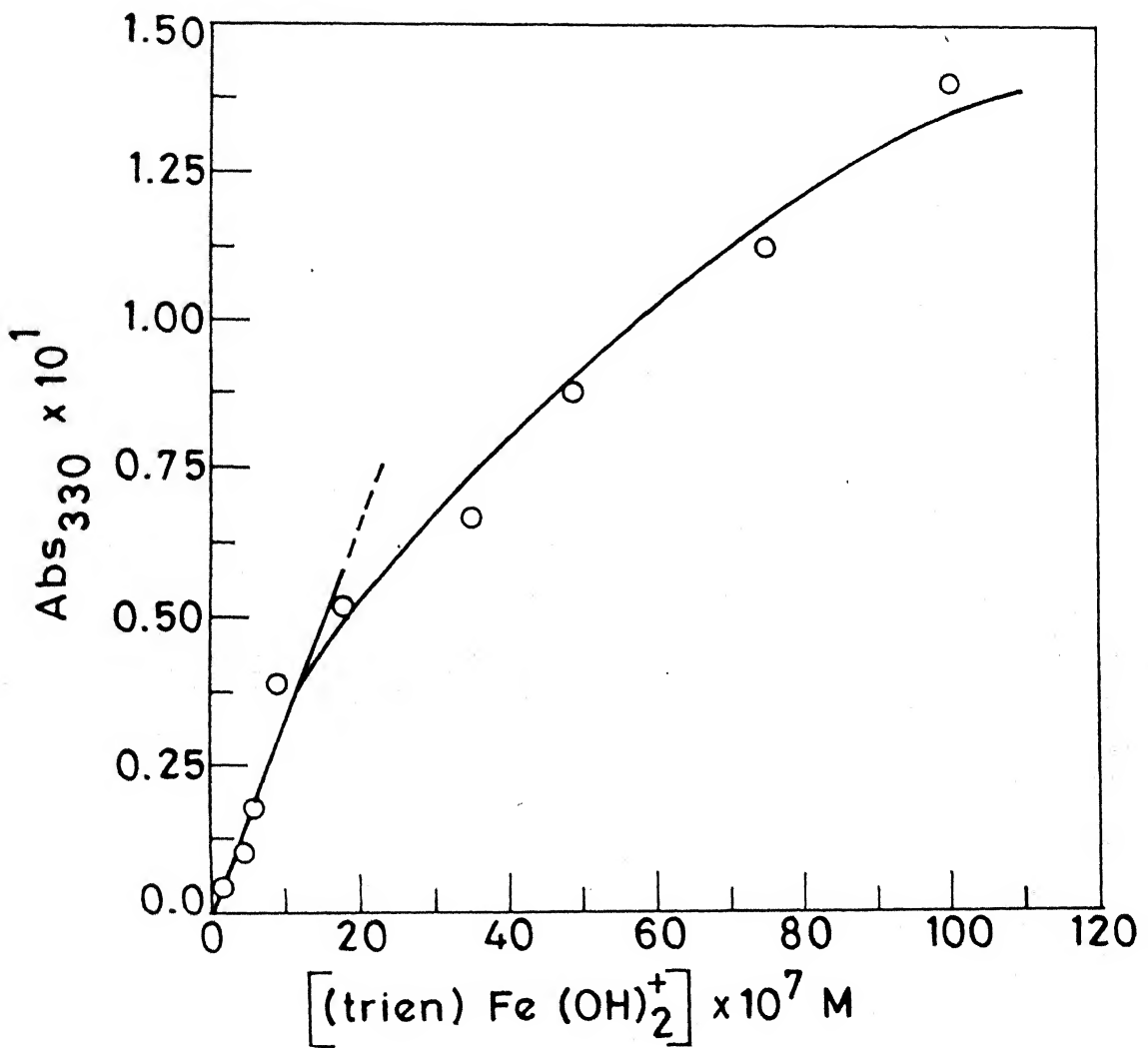


Fig. VI.A.4 Absorbance of $[(\text{trien})\text{Fe}(\text{OH})_2]^+$ at 330 nm as a function of concentration.

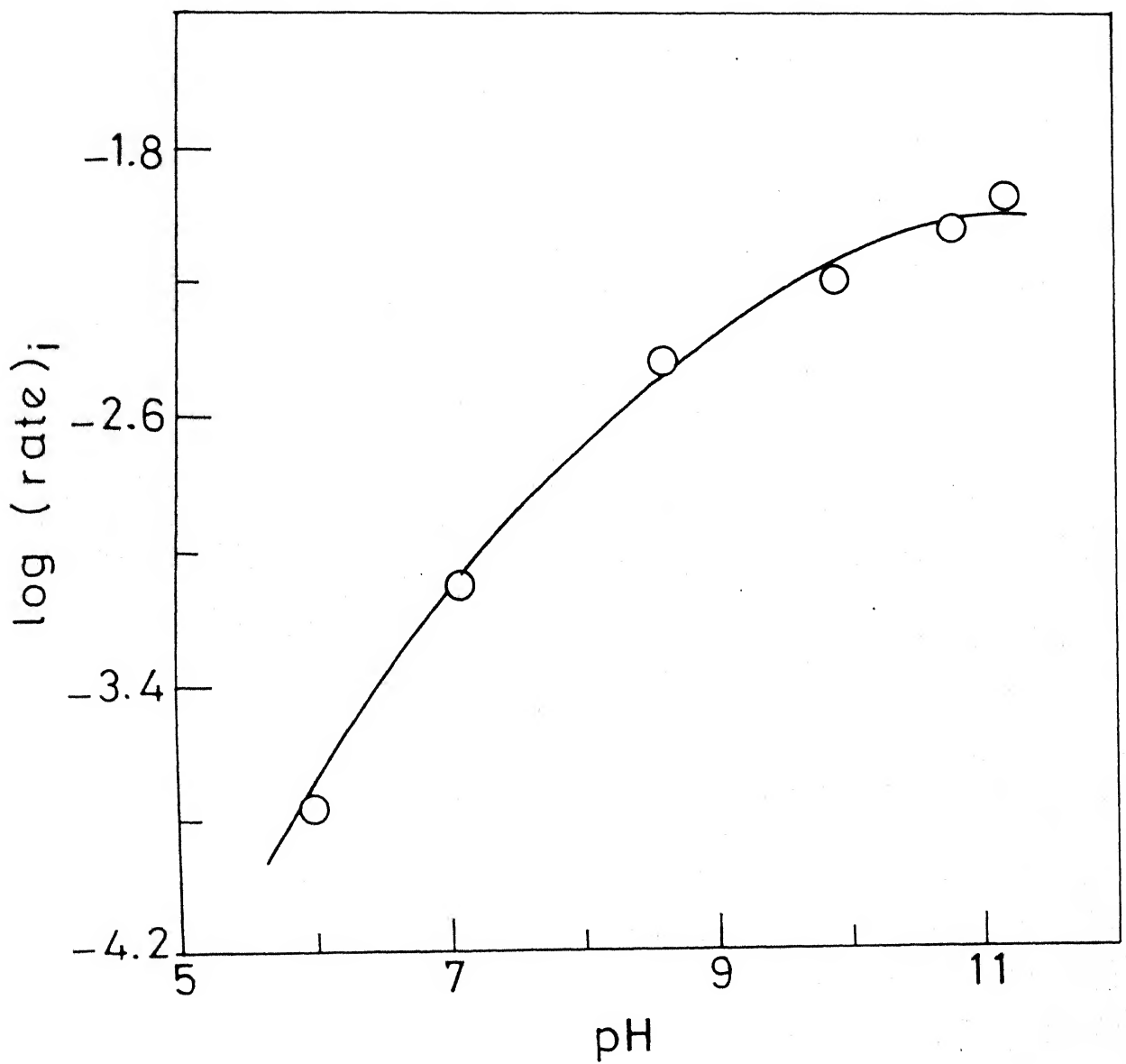


Fig.VI.A.5 Effect of pH on the decomposition rate of hydrogen peroxide.

off''. This is not unexpected and is due to a progressive increase in the relative concentration of the reactive species viz. $[(\text{trien})\text{Fe}(\text{OH})_2]^+$ complex as pH changes from seven to ten. Above pH 10 the formation of $[(\text{trien})\text{Fe}(\text{OH})_2]^+$ is complete and hence the rate attains a limiting value.

VI.A.5 DISCUSSION

Having investigated the conditions in which the decomposition rate of H_2O_2 would be most sensitive to $[(\text{trien})\text{Fe}(\text{OH})_2]^+$ and relatively insensitive to other factors such as pH and concentration of H_2O_2 , we rechecked the initial linear portion of the curve of Fig. VI.A.2 for obtaining a calibration curve between $[(\text{trien})\text{Fe}(\text{OH})_2]^+$ and concentration changes of H_2O_2 for "fixed-time" intervals of 2 and 5 minutes. Good linear plots were obtained for both time intervals (Fig. VI.A.6). The percentage errors for the two curves are given in Table VI.A.2. Considering the low level of concentration of Fe(III) that can be determined and the high specificity and sensitivity, this method can be considered to be very good.

The catalytic activities of iron(III) complexes of some other negatively charged ligands viz. NTA, EDDA and EDTA have been investigated before.¹ Though these ligands produce chelates of somewhat similar structure, they possess negligible catalytic activity compared to the trien complex. This lack of reactivity is attributed to an increase in ionic character of the Fe-O bond

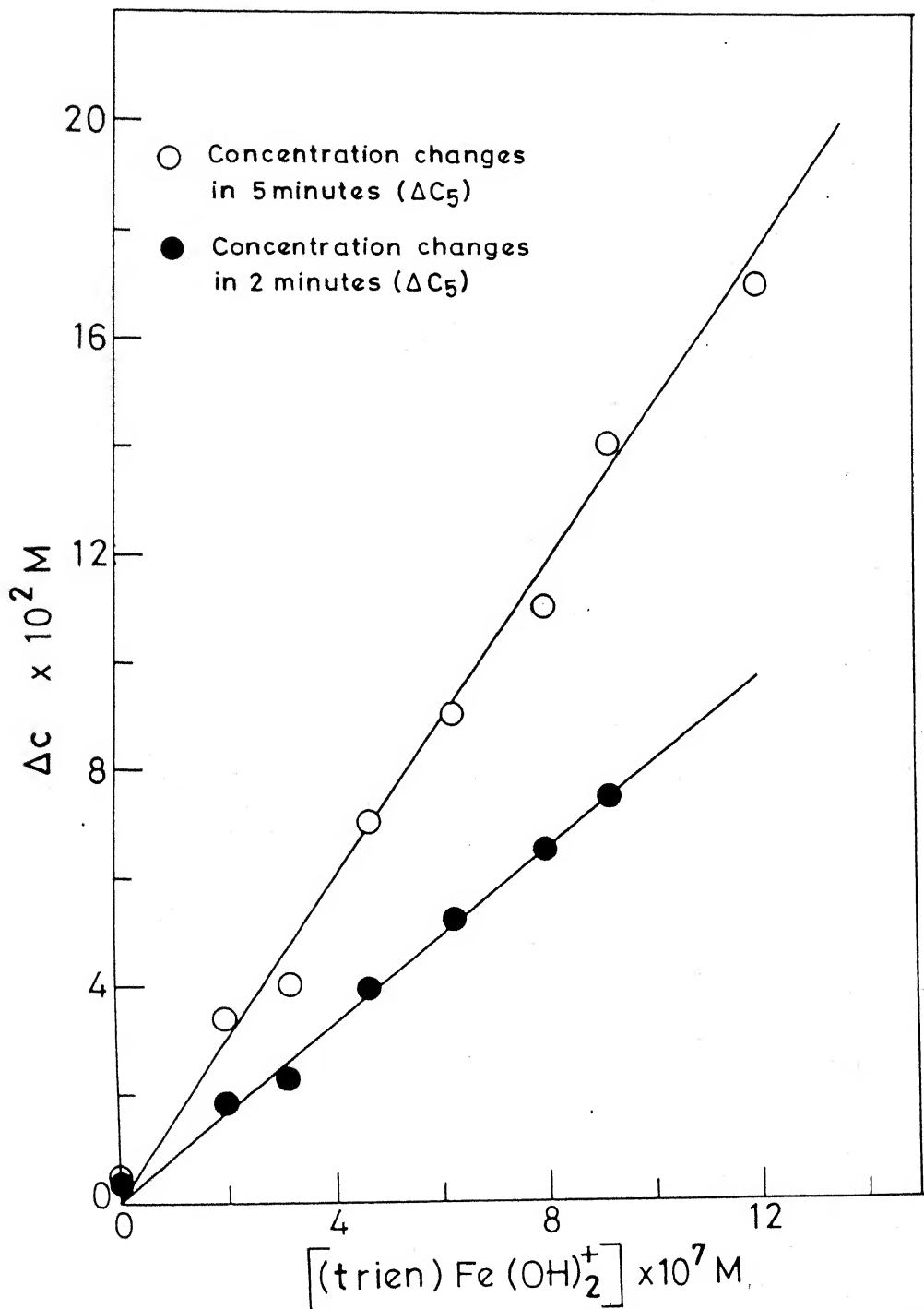


Fig.VI.A.6 Calibration curves between $[(\text{trien})\text{Fe}(\text{OH})_2^+]$ and initial rate.

TABLE VI.A.2. Concentration change of H_2O_2 at fixed time (ΔC_t) as a function of Iron(III) concentration $[\text{H}_2\text{O}_2] = 0.35 \text{ M}$, pH = 10.0 \pm 0.02, temp. = $25^\circ\text{C} \pm 0.1^\circ\text{C}$.

$[\text{Fe}^{3+}] \times 10^7, \text{M}$	$\Delta C_2 \times 10^2, \text{M}$	error	$\Delta C_5 \times 10^2, \text{M}$	error
0.1	0.4	12.2	0.5	10.0
2.0	2.25	8.2	3.4	12.5
3.15	1.90	6.1	4.0	9.5
4.7	4.0	5.1	7.0	4.4
6.3	5.2	1.9	9.0	3.3
8.0	6.5	0.8	11.0	6.2
9.2	7.45	1.35	14.0	2.9
12.0	-	-	17.0	2.9

ΔC_2 and ΔC_5 indicate the concentration changes within 2 and 5 minutes respectively.

N.B. Though higher concentration of hydrogen peroxide (limiting value) will be ideal, it would become an expensive method in that case. Since good linear curves are obtained at $[\text{H}_2\text{O}_2] = 0.35 \text{ M}$, we have chosen to stick to this concentration which gives a reasonable change in concentration in specified conditions.

in these chelates. A recent investigations by Oakes and coworkers,⁶ and Rizkalla et al.⁷ demonstrated, however, that the chelates $[\text{Fe}(\text{EDTA})(\text{OH})_2]^{2-}$ and $[\text{Fe}(\text{ENTMP})(\text{OH})]^{6-}$ respectively (EDTA = Ethylenediaminetetraacetic acid; ENTMP = Ethylenediaminetetrakis(methylphosphonic) acid) are also good catalysts for the decomposition of hydrogen peroxide.

Wang¹ also tested the catalytic activity of quite a few cations in presence of trien and came to the conclusion that only $[(\text{trien})\text{Fe}(\text{OH})_2]^+$ and to a much lesser extent $[(\text{trien})\text{Mn}(\text{OH})]^+$ show remarkable catalytic activity. According to him chelates of many other cations, however, showed negligible catalytic activity compared to chelates of Fe(III) and Mn(II). These include Mg(II), Al(III), Ca(II), Cr(III), Co(III), Ni(II), Cu(II), Zn(II), Sr(II), Ag(I), Cd(II), Ba(II), Tl(I) and Pb(II). The high degree of specificity for Fe(III) and Mn(II) is not easy to explain because many ions listed above possess same charges and comparable ionic radii. The comparative catalytic activities of both $[(\text{trien})\text{Fe}(\text{OH})_2]^+$ and $[(\text{trien})\text{Mn}(\text{OH})]^+$ is, perhaps, understandable because they are isoelectronic.

The mechanism of catalytic activity of $[(\text{trien})\text{Fe}(\text{OH})_2]^+$ for the decomposition of H_2O_2 in basic medium, as proposed by Wang¹, is given in Fig. VI.A.7. Trien forms a quadridentate chelate with ferric ion. Steric considerations favour structure I where one primary nitrogen atom is above and the other below the square plane and two hydroxyl groups occupy two adjacent $d^2\text{sp}^3$

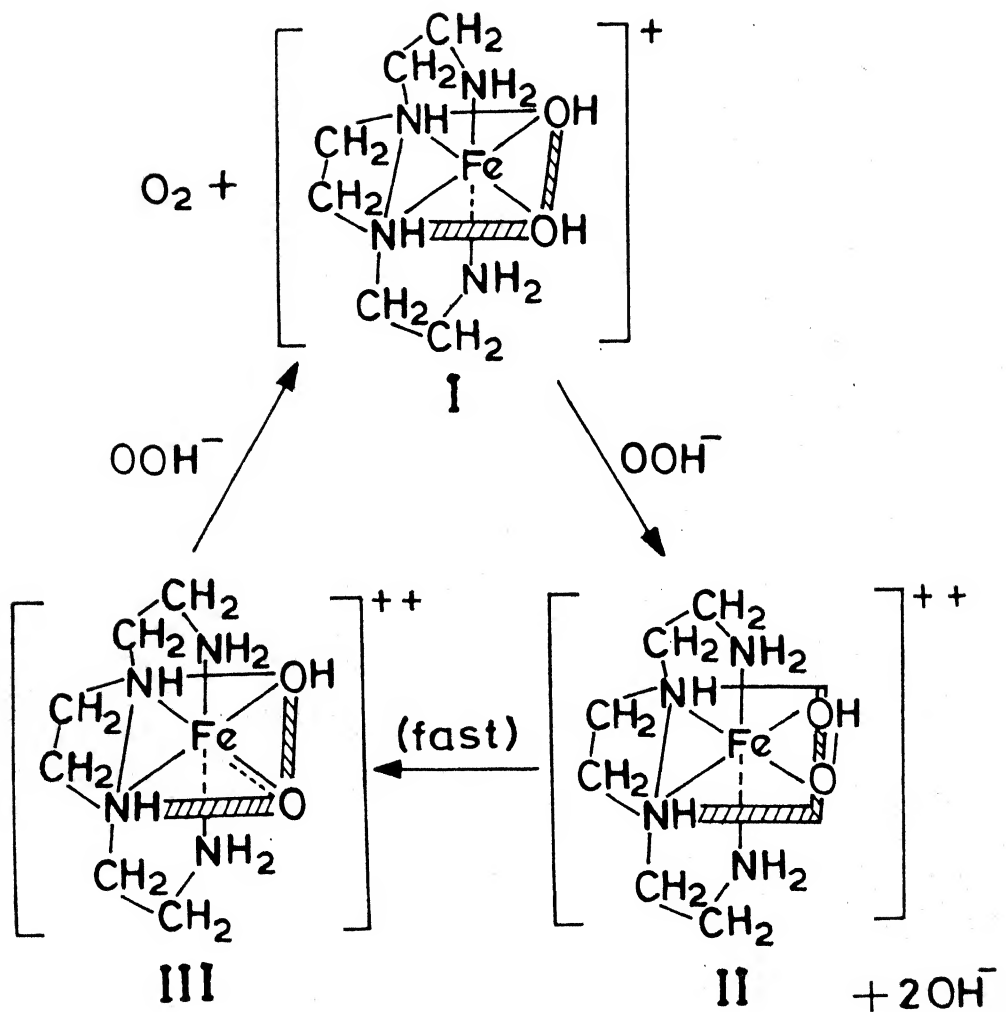


Fig.VI.A.7 Mechanism of catalytic action of $[\text{trien}]\text{Fe}(\text{OH})_2^+$ for the decomposition of hydrogen peroxide.

coordination sites. In presence of hydrogen peroxide both the hydroxyl substituents can be displaced by OOH^- ion, the latter being capable of formation of two coordinate links with Fe(III) through O atoms. The resulting chelate(II) is unstable because the original bond length of 1.3A° in peroxide ion tends to stretch until the second activated complex(III) is formed. The activation energy of about 71.4 kJ mol^{-1} for cleavage of O-O bond in hydrogen peroxide is considerably lowered to 29.4 kJ mol^{-1} in presence of $[(\text{trien})\text{Fe}(\text{OH})_2]^+$ complex⁸ because of compensation in energy provided by the simultaneous formation of a stable Fe-O bond as shown in compound (III). This compound can readily react with second OOH^- to yield oxygen and regenerate compound I. Thus the catalyst complex acts cyclically, Wang¹ also provided supporting evidence for the mechanism proposed by him.

The loss of catalytic activity on increase of concentration of $[(\text{trien})\text{Fe}(\text{OH})_2]^+$ in our study becomes understandable because dimerization, possibly to give $[\text{trien} \text{Fe} \begin{array}{c} \text{O} \\ \swarrow \quad \searrow \\ \text{O} \end{array} \text{Fe trien}]$, takes away the two adjacent hydroxyl sites where the splitting mechanism is initiated. It has been shown that replacement of the quadridentate trien by pentadentate tetren, gives a complex of practically no catalytic activity. This is due to loss of one of the hydroxyl groups necessary for the operation of the splitting mechanism discussed above. The Lineweaver-Burk plots between $1/v_o$ (reciprocal of initial rate) and $1/\text{H}_2\text{O}_2$ at three different catalyst concentrations are given in Fig. VI.A.8 and their extrapolation to abscissa intercept, enables one to estimate the value

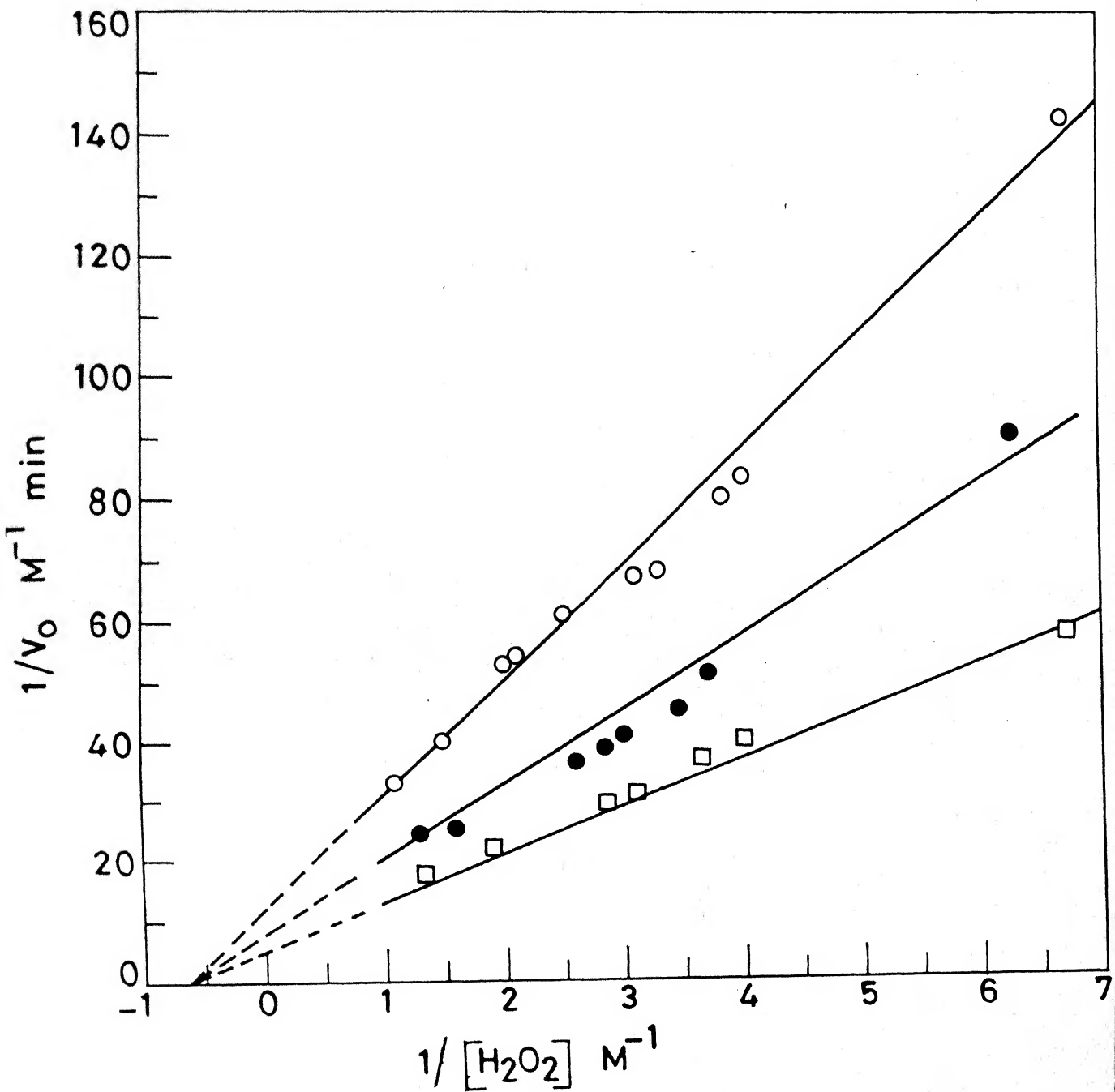


Fig. VI.A.8 Lineweaver-burk plots for estimating K_M

of $K_m = 1.56 \pm 0.2M$. This value is higher compared to that of catalase ($K_m = 0.025M$) and some other catalytic species⁹ and comparable to the value obtained by us from the data of Wang.¹

K_m is a rough measure of the affinity of the catalyst for the substrate, in this case H_2O_2 . A higher value of K_m would imply that the catalyst $[(\text{trien})\text{Fe}(\text{OH})_2]^+$ requires a relatively high concentration of the substrate $[H_2O_2]$ to attain its half maximal rate of catalysis.

Finally, we have established a kinetic method for trace determination of Fe(III) in the range $(1.0 \times 10^{-8} - 1.2 \times 10^{-6} M)$. The method is sensitive, specific, simple and inexpensive. The presence of a large number of cations in about ten fold excess causes a maximum error of 12.5% (Table VI.A.3). Even Mn(II) causes an interference comparable to other ions listed in this table at this low concentration ^{though} it may cause more serious interference if present in higher concentration. The high catalytic activity of the $[(\text{trien})\text{Fe}(\text{OH})_2]^+$ complex in low concentration range and loss of activity at higher concentration is also explained

TABLE VI.A.3. Effect of interferences

$[H_2O_2] = 0.35 \text{ M}$, $[Fe^{3+}] = 6.3 \times 10^{-7} \text{ M}$,
 $[trien] = 4.8 \times 10^{-3} \text{ M}$, $pH = 10.0 \pm 0.02$,
temp. = $25^\circ\text{C} \pm 0.1^\circ\text{C}$.

Ion	$[Fe^{3+}]$ taken 10^{-7} M	$[Fe^{3+}]$ found 10^{-7} M	Error
Ni^{2+}	6.3	5.75	8.7
Pb^{2+}	6.3	5.76	8.6
Cu^{2+}	6.3	5.56	11.8
Ag^+	6.3	5.83	7.5
Mn^{2+}	6.3	5.76	8.6
Co^{2+}	6.3	5.76	8.6
Al^{3+}	6.3	6.20	1.6

VI.B

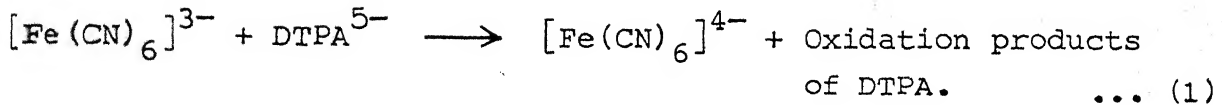
ABSTRACT

The kinetics of oxidation of Diethylenetriaminepentaacetic acid (DTPA) by hexacyanoferrate(III) has been investigated spectrophotometrically at pH = 10.5, I = 0.25M(NaClO₄) and temp. = 35 ± 0.1°C. The rate data indicate first order dependence each in $[\text{Fe}(\text{CN})_6]^{3-}$ and [DTPA], overall second order. The rate constant increases in the pH range 8.5 to 12. The reactive species of DTPA in the above pH region are H_2L^{3-} , HL^{4-} and L^{5-} . The effect of ionic strength is found to be positive. The activation parameters are evaluated from the Arrhenius plots. An electron transfer from $[\text{Fe}(\text{CN})_6]^{3-}$ to the substrate followed by decomposition of the latter is proposed.

VI.B.2 INTRODUCTION

Literature on solution kinetics is replete with reports on the kinetics and mechanism of oxidation of a number of organic and inorganic substrates by hexacyanoferrate(III). A recent work from this laboratory¹⁰ on the ligand exchange reactions between polyaminocarboxylatoferrate(III) with cyanide ion showed that these reactions consist of three observable stages. The third stage involves the oxidation of aminocarboxylates released in the first stage by $[\text{Fe}(\text{CN})_6]^{3-}$ formed in the second stage. It was, therefore, considered worthwhile to carry out an independent study of the third reaction (equation 1). In this part of chapter the

kinetics of oxidation of diethylenetriaminepentaacetic acid (DTPA) by hexacyanoferrate(III) have been reported.¹¹ To the best of our knowledge the kinetics of this reaction has not been reported so far.



VI.B.3 MATERIALS AND METHODS

Potassium hexacyanoferrate(II) (AR, Sarabhai M Chemicals), potassium hexacyanoferrate(III) (AR, SDS), sodium cyanide (May and Baker, England) and diethylenetriaminepentaacetic acid (Sigma) were used. Sodium hydroxide or perchloric acid was used to maintain pH at any desired value. Standard BDH buffers were used for standardization of pH meter. Sodium cyanide solution was standardized argentometrically.¹² Sodium perchlorate (AR, BDH) or potassium nitrate (GR, Sarabhai M Chemicals) was used to maintain ionic strength.

A Toshniwal spectrophotometer model RL-02 fitted with a circulatory arrangement for thermostating the cell compartment was used for kinetic study. The temperature could be controlled to within $\pm 0.1^\circ\text{C}$. A Shimadzu double beam spectrophotometer model UV-190 and Cary 17D spectrophotometer were used for recording the spectral changes. All pH measurements were made on an Elico digital pH meter model LI-120.

VI.B.3.1 Kinetic Measurements

The reaction between DTPA and hexacyanoferrate(III) was followed at 410 nm (broad band of $[\text{Fe}(\text{CN})_6]^{3-}$, $\epsilon = 1020 \text{ M}^{-1}\text{cm}^{-1}$), pH = 10.5 ± 0.02 , I = 0.25M(NaClO₄) and temp. = $35 \pm 0.1^\circ\text{C}$. The kinetics were studied under pseudo-first-order conditions using large excess of DTPA. Solutions of hexacyanoferrate(III) and DTPA were preequilibrated separately at the desired temperature for 30 min before mixing. Ionic strength and pH were adjusted each time before equilibrating the reactants.

The pseudo-first-order rate constants were calculated from plots of $\log C_A$ versus time, where C_A refers to hexacyanoferrate(III) remaining at any time t. The absorbance changes were observed for at least 70% of the reaction.

VI.B.4 RESULTS

The kinetic data of this reaction are given in Table VI.B.1 and the dependence of pseudo-first-order rate constant on [DTPA] is shown in Fig. VI.B.1.

VI.B.4.1 Dependence of Rate on pH

The reaction was studied in the pH range 8.5-12. The species distribution of DTPA at various pH values was calculated with an IBM 7044 computer using a programme developed by Perrin and Sayce¹³ and is shown in Fig. VI.B.2. The predominant species of DTPA in the

TABLE VI.B.1. Evaluation of pseudo-first-order rate constants and second order rate constants.

$[\text{Fe}(\text{CN})_6^{3-}] = 5 \times 10^{-4} \text{M}$, $\text{pH} = 10.5 \pm 0.02$,
 temp. = $35 \pm 0.1^\circ\text{C}$, $I = 0.25\text{M}(\text{NaClO}_4)$.

$10^3 x [\text{DTPA}]_T$ M	$10^4 x k_{\text{obsd}}$ s^{-1}	$10^2 x k_f = k_{\text{obsd}} / [\text{DTPA}]_T$ $\text{M}^{-1} \text{s}^{-1}$
5.0	4.2	8.4
7.5	6.7	8.9
10.0	7.9	7.9
12.5	9.3	7.4
15.0	10.6	7.1

$$\text{Av.} = (7.94 \pm 0.7) \times 10^{-2} \text{ M}^{-1} \text{s}^{-1}$$

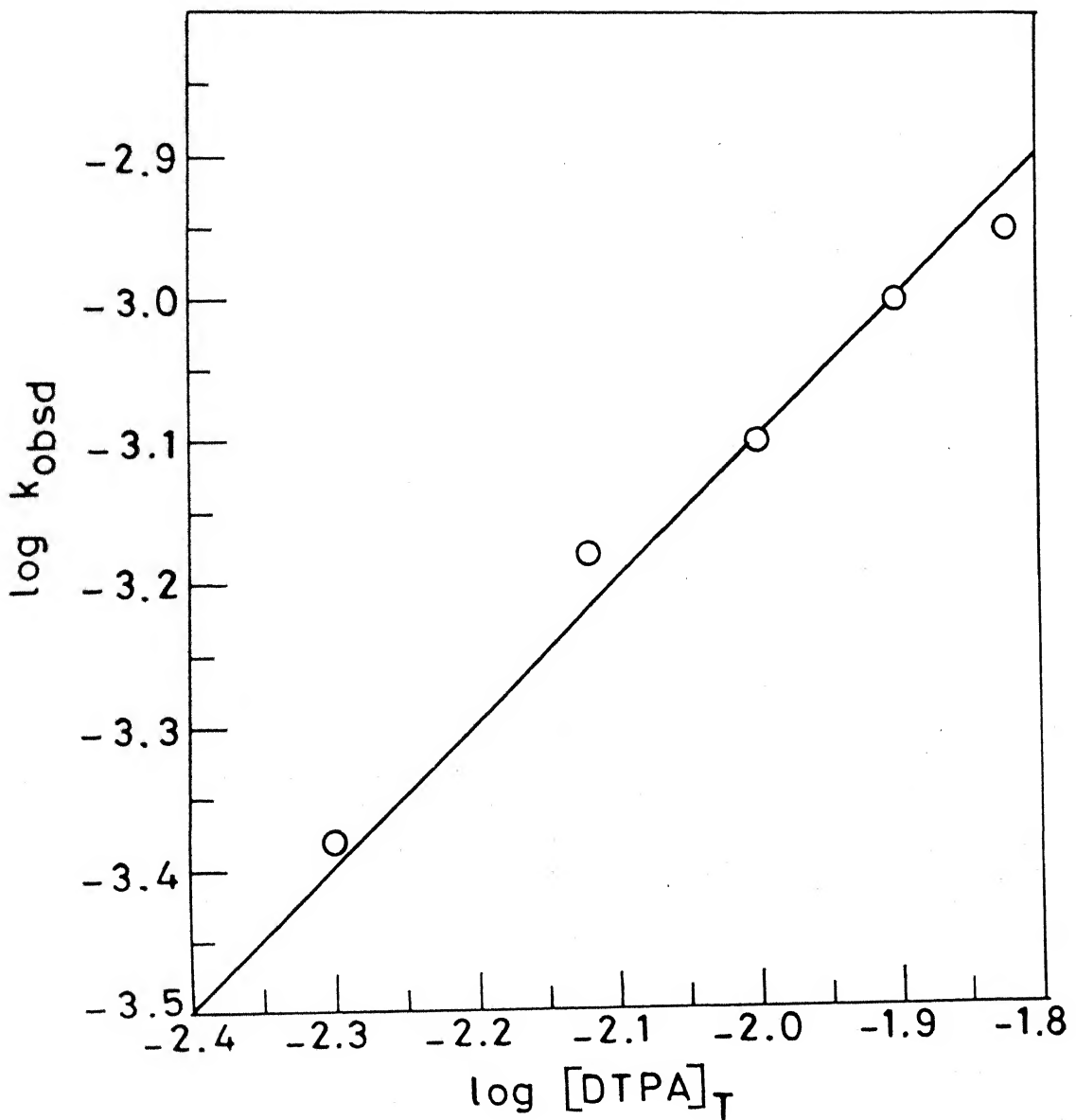


Fig.VI.B.1 Dependence of observed pseudo-first-order rate constants on $[\text{DTPA}]$. Reaction conditions as in Table VI.B.1 .

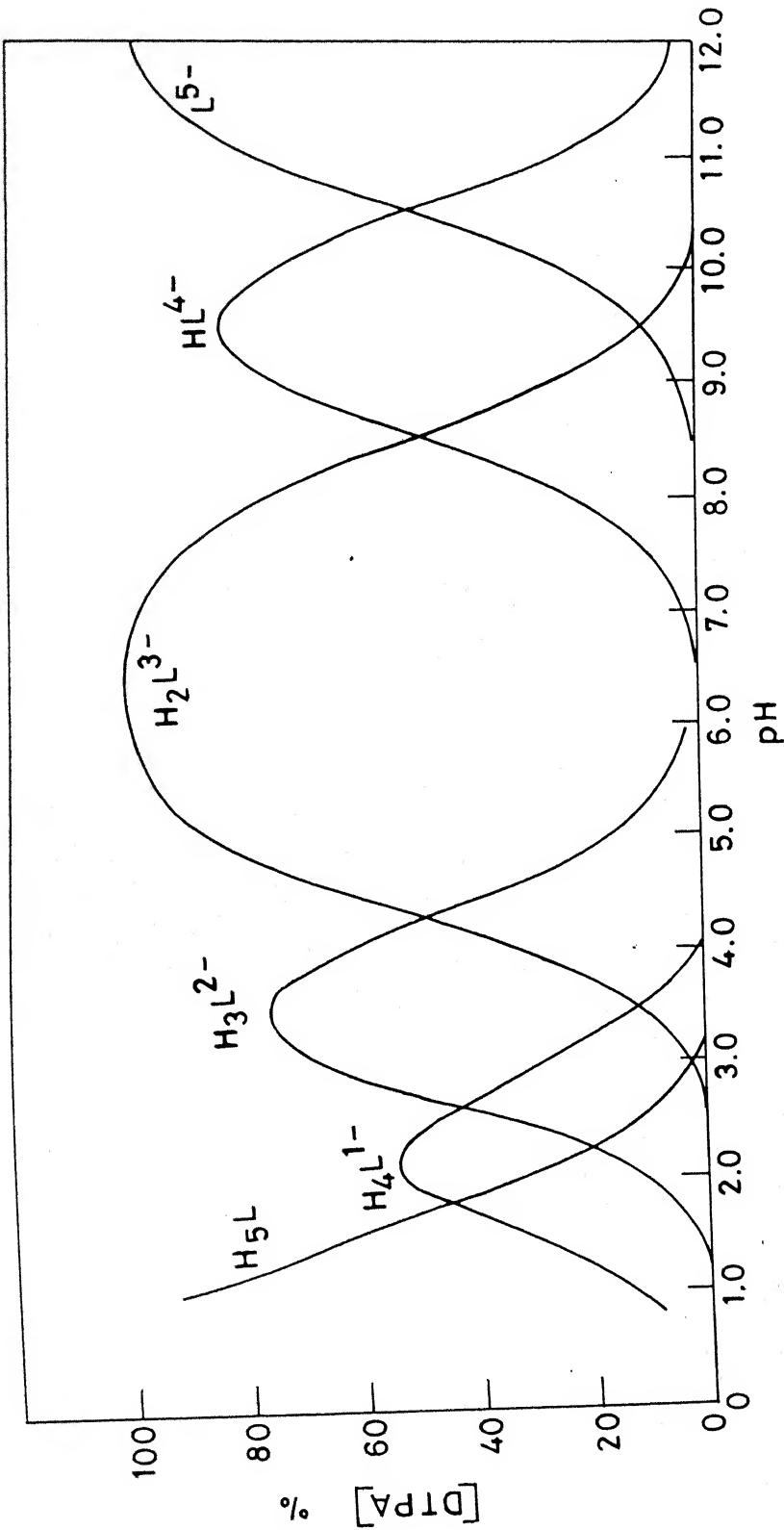


Fig. VI.B.2 Species distribution of DTPA as a function of pH; $[DTPA]_T = 5.0 \times 10^{-4} M$.

pH range of interest are H_2L^{3-} , HL^{4-} and L^{5-} in varying proportions.

It is observed that between pH 8.5 and 10.0 the reaction rate increases linearly with increase in pH and levels off at higher pH (Fig. VI.B.3 and Table VI.B.2). Below pH 8.5 the rate is extremely slow. The data on pH dependence of rate fit equation 2.

$$\text{Rate} = k_f [Fe(CN)_6^{3-}] [L]_T \quad \dots (2)$$

In equation (2) the concentration term $[L]_T$ includes all protonated and unprotonated forms of DTPA.

The rate of oxidation of DTPA can also be given by the expression (3).

$$\begin{aligned} \text{Rate} &= [Fe(CN)_6^{3-}] \{k_1 [L^{5-}] + k_2 [HL^{4-}] + k_3 [H_2L^{3-}]\} \\ &= [Fe(CN)_6^{3-}] \{k_1 [L^{5-}] + k_2 K_1 [H^+] [L^{5-}] + k_3 K_1 K_2 [H^+]^2 [L^{5-}]\} \\ &= [Fe(CN)_6^{3-}] [L^{5-}] \{k_1 + k_2 K_1 [H^+] + k_3 K_1 K_2 [H^+]^2\} \quad \dots (3) \end{aligned}$$

where k_1 , k_2 , k_3 are the rate constants for the species L^{5-} , HL^{4-} and H_2L^{3-} respectively and K_1 and K_2 are the respective protonation constants of DTPA.

Comparing equations (2) and (3) we get,

$$k_f \frac{[L]_T}{[L^{5-}]} = k_1 + k_2 K_1 [H^+] + k_3 K_1 K_2 [H^+]^2 \quad \dots (4)$$

$$\text{where } \frac{[L]_T}{[L^{5-}]} = 1 + K_1 [H^+] + K_1 K_2 [H^+]^2$$

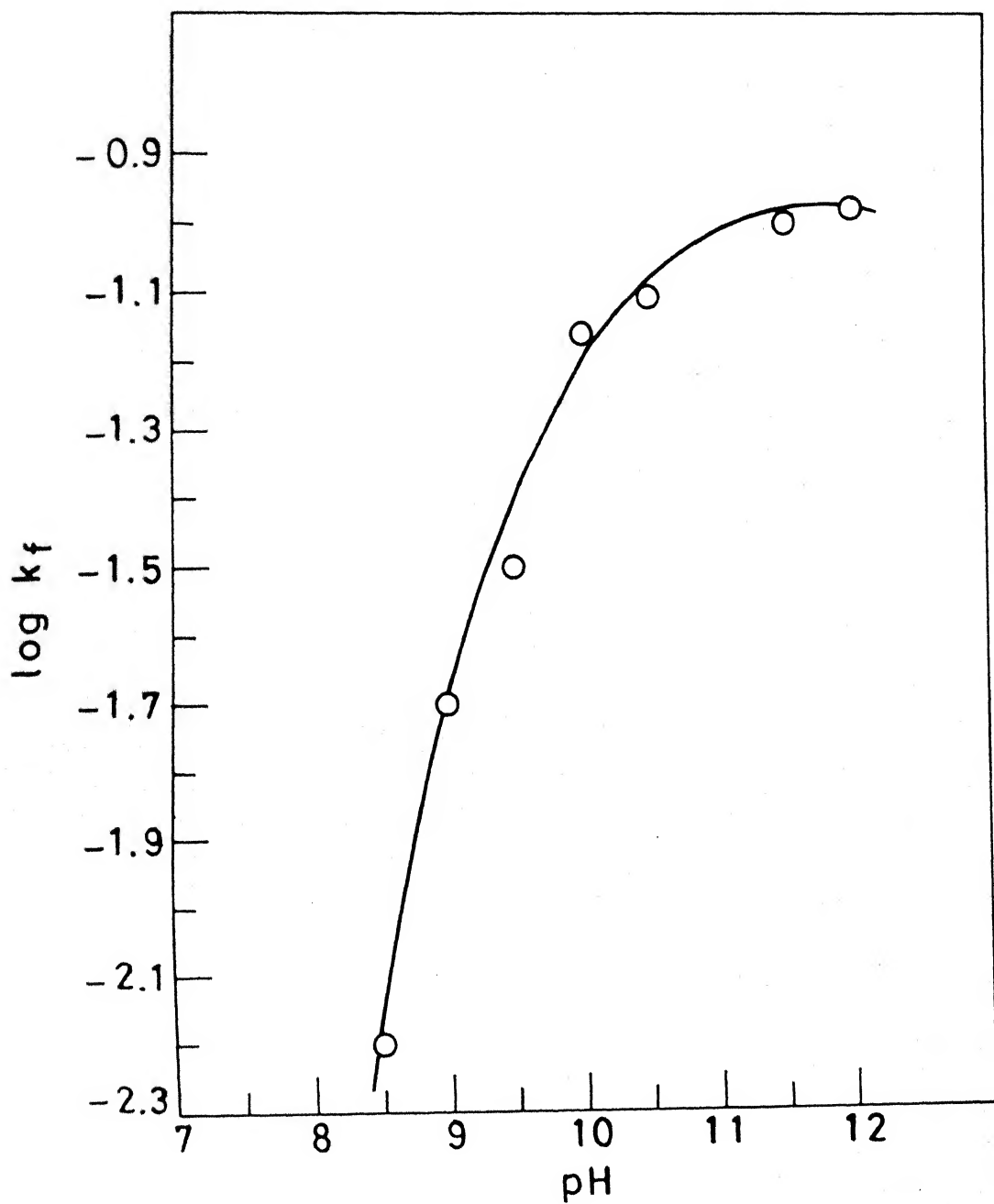


Fig. VI.B.3 Effect of pH on the reaction of $[\text{Fe}(\text{CN})_6]^{3-}$ with DTPA. Reaction conditions are given in Table VI.B.2.

TABLE VI.B.2. Effect of pH on the reaction of $[\text{Fe}(\text{CN})_6]^{3-}$ with DTPA.

$[\text{Fe}(\text{CN})_6]^{3-} = 5 \times 10^{-4} \text{M}$, $[\text{DTPA}]_T = 10^{-2} \text{M}$,
 temp. = $35 \pm 0.1^\circ\text{C}$, I = 0.25M(NaClO_4).

pH	$k_{\text{obsd}}, \text{s}^{-1}$	$k_f, \text{M}^{-1} \text{s}^{-1}$
8.5	6.3×10^{-5}	6.3×10^{-3}
9.0	2.0×10^{-4}	2.0×10^{-2}
9.5	3.2×10^{-4}	3.2×10^{-2}
10.0	7.4×10^{-4}	7.4×10^{-2}
10.5	7.8×10^{-4}	7.8×10^{-2}
11.5	1.0×10^{-3}	1.0×10^{-1}
12.0	1.1×10^{-3}	1.1×10^{-1}

At pH above 10, $[H^+]^2$ can be ignored. So equation (4) is simplified to equation (5)

$$k_f \{1 + K_1[H^+]\} = k_1 + k_2 K_1[H^+] \quad \dots (5)$$

In the higher pH region a plot of left hand side of equation (5) versus $[H^+]$ is linear (Fig. VI.B.4), the slope of which gives the value of k_2 (i.e. reaction rate between $[Fe(CN)_6]^{3-}$ and $[HL]^{4-}$) equal to $4.9 \times 10^{-2} M^{-1}s^{-1}$. The intercept of the linear plot gives k_1 (i.e. the rate constant for reaction between L^- and $[Fe(CN)_6]^{3-}$) equal to $1.05 \times 10^{-1} M^{-1}s^{-1}$. Further, transforming expression (4) and taking logarithm, we get

$$\log \frac{k_f}{[H^+]} \{1 + K_1[H^+] + K_1 K_2 [H^+]^2 - k_1 - k_2 K_1 [H^+]\} = \log(k_3 K_1 K_2) + \log [H^+] \quad \dots (6)$$

A plot of left hand side of equation (6) versus $\log [H^+]$ is linear (Fig. VI.B.5) the slope of which is close to one and the intercept gives an estimated value of k_3 equal to $6.0 \times 10^{-19} M^{-1}s^{-1}$. This is consistent with the observation that the rate below pH 8.5 is extremely slow.

VI.B.4.2 Effect of Temperature on Rate

Activation parameters for this reaction have been calculated from the Arrhenius plot in the temperature range 25–40°C and the

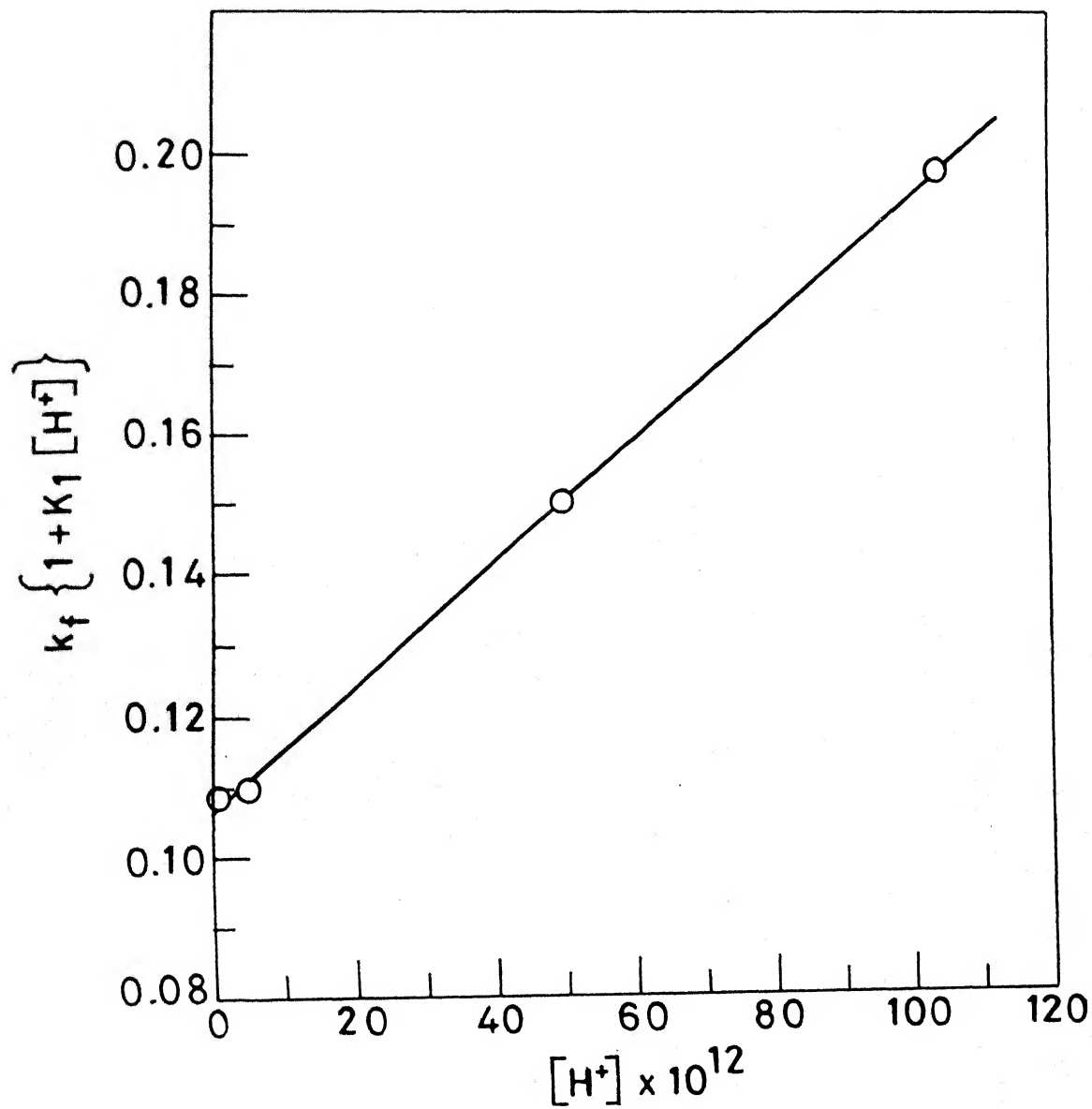


Fig.VI.B.4 Resolution of rate constants due to the reactions of $[\text{Fe}(\text{CN})_6]^{3-}$ and L^{5-} and $[\text{Fe}(\text{CN})_6]^{3-}$ and HL^{4-} .

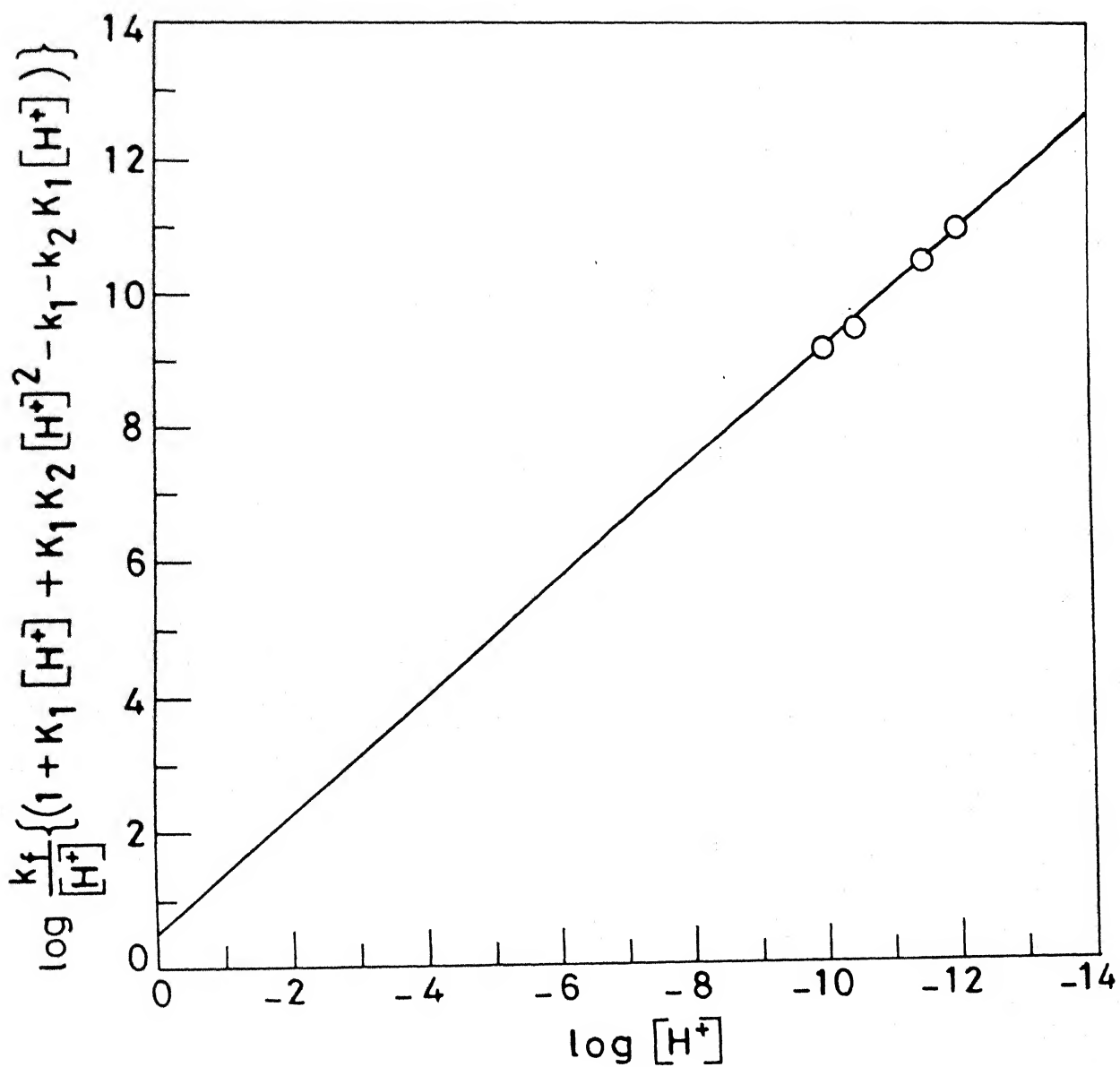


Fig. VI.B.5 Resolution of rate constants due to the reaction of $[\text{Fe}(\text{CN})_6]^{3-}$ and H_2L^{3-} .

values are: $\Delta H^{\circ f} = 28.2 \pm 0.1 \text{ kJ mol}^{-1}$ and $\Delta S^{\circ f} = -176 \pm 1 \text{ J K}^{-1} \text{ mol}^{-1}$. Fig. VI.B.6 shows a plot of enthalpies of activation versus the entropies of activation for the oxidation of a few aminocarboxylic acids, viz. DTPA, EDTA, EDTPA, IDA and NTA by $[\text{Fe}(\text{CN})_6]^{3-}$. A linear relationship indicates that the oxidation of all these substrates proceeds by a common mechanism. The slope of this line gives the isokinetic temperature as $26 \pm 3^\circ\text{C}$. At this temperature all these aminocarboxylic acids react with $[\text{Fe}(\text{CN})_6]^{3-}$ at comparable rates. It may be pointed out that our conditions were not identical with the conditions used for other aminocarboxylate reactions.¹⁴

VI.B.4.3 Effect of Ionic Strength on Rate

The rate of reaction between $[\text{Fe}(\text{CN})_6]^{3-}$ and DTPA was studied over a range of ionic strength. The second order rate constants were found to obey equation (7) given by Bronsted and Bjerrum.¹⁵

$$\log k_f = \log k_o + 1.018 Z_A Z_B \cdot \sqrt{I} / (1 + \sqrt{I}) \quad \dots (7)$$

The value of the product $Z_A Z_B$ has been calculated from the slope of this plot (Fig. VI.B.7).

VI.B.5 DISCUSSION

The kinetic data given in Table VI.B.1 and plotted in Figure VI.B.1 are consistent with the interaction of L^{5-} with

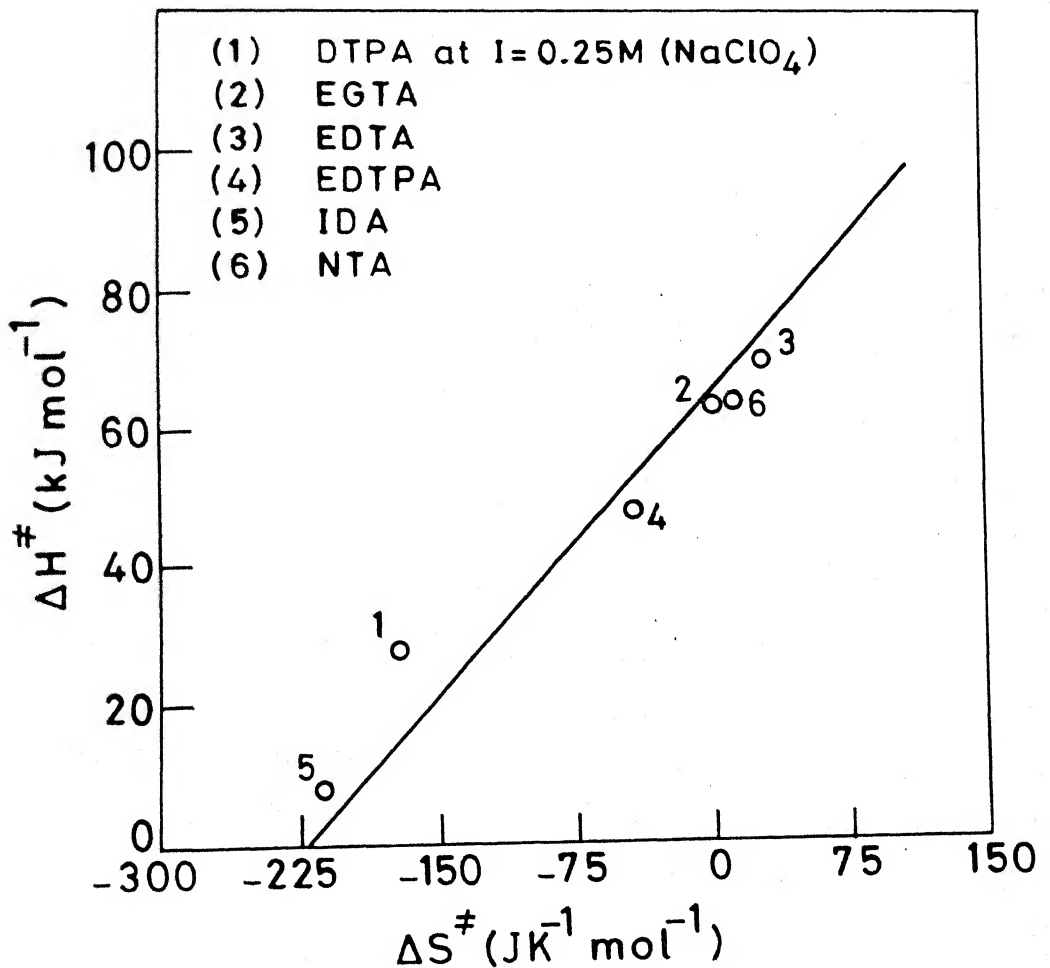


Fig. VI.B.6 A plot of enthalpy of activation versus entropy of activation for the oxidation of some amino-carboxylates by $[\text{Fe}(\text{CN})_6]^{3-}$ at 25°C and $I=0.45\text{M}$.

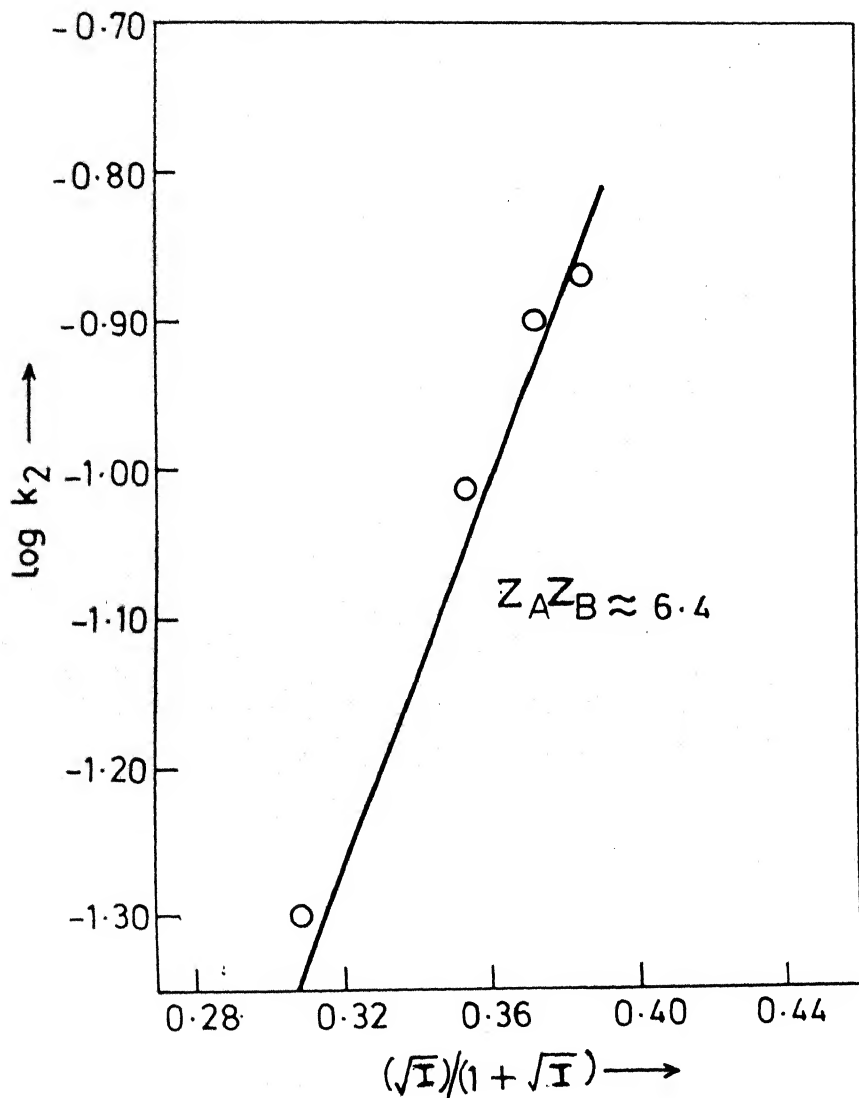


Fig. VI.B.7 Effect of ionic strength on the reaction of $[\text{Fe}(\text{CN})_6]^{3-}$ with DTPA: $[\text{Fe}(\text{CN})_6]^{3-} = 5 \times 10^{-4} \text{ M}$, $[\text{DTPA}]_T = 10^{-2} \text{ M}$, $\text{pH} = 11.0 \pm 0.02$, temp = $35 \pm 0.1^\circ\text{C}$

hexacyanoferrate(III) in the rate-determining step. Addition of hexacyanoferrate(II) in the concentration range 5×10^{-4} to 5×10^{-3} M does not retard the reaction rate indicating that the reaction is essentially irreversible. The presence of cyanide in the concentration range 2.5×10^{-2} to 7.5×10^{-2} M also does not materially affects the forward rate ruling out the possibility of prior dissociation.

The effect of ionic strength on the rate constant presents an interesting feature in that the value of $Z_A Z_B \approx 6.4$ is smaller than the expected value if the only reactants were $[\text{Fe}(\text{CN})_6]^{3-}$ and $[\text{DTPA}]^{5-}$. This is not entirely unexpected because DTPA and other aminocarboxylates are known to form complexes with alkali metals of moderate stabilities ($K_{\text{NaDTPA}} = 10.0$, $K_{\text{KDTPA}} = 4.84$).¹⁶ In the presence of three K^+ ions released from dissociation of $\text{K}_3[\text{Fe}(\text{CN})_6]$ and large excess of Na^+ present due to addition of NaClO_4 , significant concentration of DTPA is present as complexes of either Na^+ or K^+ and hence smaller effective value of $Z_A Z_B$.

Specific salt effects have also been observed in the present reaction system. The second order rate constants increase on changing Na^+ or K^+ at constant ionic strength. A similar behaviour has been observed in the hexacyanoferrate(III) oxidation of EDTA^{14} and also in the hexacyanoferrate(III)-hexacyanoferrate(II) exchange reaction.¹⁷ The values of rate constants in the presence of Na^+ or K^+ ions (2.5×10^{-1} M each) are $7.93 \times 10^{-2} \text{ M}^{-1} \text{ s}^{-1}$ and $2.5 \times 10^{-1} \text{ M}^{-1} \text{ s}^{-1}$ respectively. A third factor, which appears to affect the

values of $Z_A Z_B$, is the possible formation of ion pairs between $[\text{Fe}(\text{CN})_6]^{3-}$ and/or DTPA⁵⁻ with the cations present in sufficiently high concentration in the reaction medium.

The spectral changes occurring during a typical kinetic run have been recorded and the results are shown in Figure VI.B.8. There is a continuous decrease of absorbance at 410 nm and a corresponding decrease in the peak height at 303 nm as well. $[\text{Fe}(\text{CN})_6]^{4-}$ has a weak absorption band at 325 nm but is not observed because it gets lost in a shoulder of $[\text{Fe}(\text{CN})_6]^{3-}$ at 325 nm.

As isosbestic point at 281 nm indicates coexistence of two species, viz. $[\text{Fe}(\text{CN})_6]^{3-}$ and $[\text{Fe}(\text{CN})_6]^{4-}$. The absence of any new peak points to the fact that no reaction intermediate is possibly present in any appreciable concentration. The absorption peaks of other products are likely to be in the UV region where DTPA absorbs strongly and are, therefore, not identifiable. The oxidation products of EDTA have been identified as iminodiacetic acid and glycollic acid.¹⁴ Two specific tests for hexacyanoferrate(II), viz. ammonium molybdate and thorium nitrate tests confirm the formation of $[\text{Fe}(\text{CN})_6]^{4-}$ as one of the reaction products.

The results presented above point to an outer sphere mechanism of electron transfer from hexacyanoferrate(III) to the DTPA in a bimolecular step. Under the conditions employed the reactants are $[\text{Fe}(\text{CN})_6]^{3-}$ on the one hand and DTPA⁵⁻ and HDTPA⁴⁻ on the other

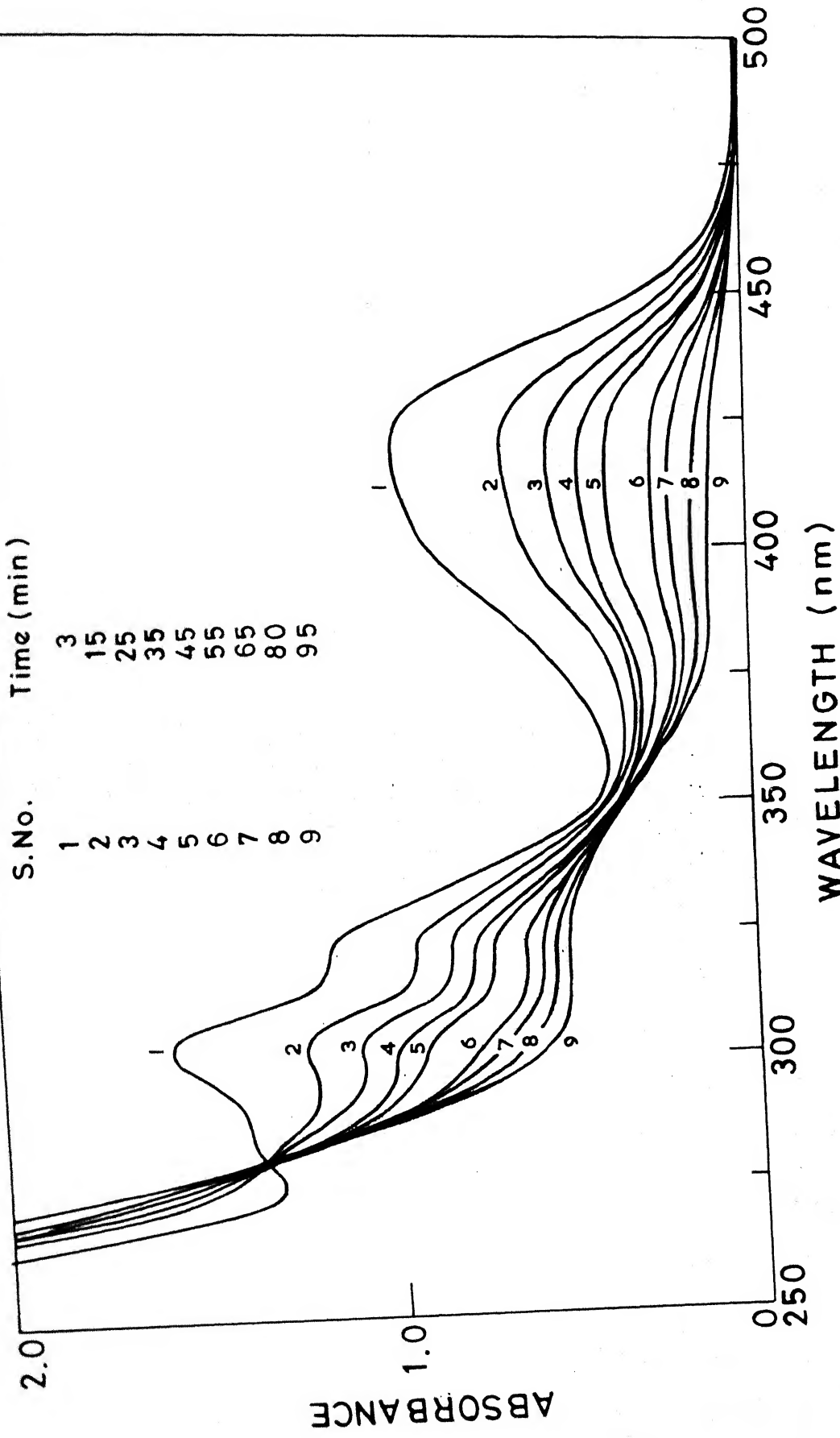


Fig. VII.B.8 Repetitive scan of the reaction mixture during a typical kinetic run : $[\text{Fe}(\text{CN})_6^{3-}] = 5 \times 10^{-4} \text{ M}$, $[\text{DTPA}]_T = 10^{-2} \text{ M}$, $\text{pH} = 11.0$, $\text{I} = 0.25 \text{ M} (\text{NaClO}_4)$, temp = $26 \pm 0.1^\circ \text{C}$.

237

depending upon pH of the medium. The presence of Na^+ and K^+ in the reaction medium complicates the reaction due to the formation of complexes of DTPA with Na^+ and K^+ and possibly ion pairs also. Specific salt effects are also observed. The highly negative value of entropy of activation shows that the activated complex obtained in the bimolecular process is highly charged.

REFERENCES

1. J.H. Wang, J. Am. Chem. Soc., 1955, 77, 4715.
2. G. Wada, T. Nakamura, K. Terauchi and T. Nakai, Bull. Chem. Soc. Jpn., 1964, 37, 447.
3. A.R. Frost and R.G. Pearson, "Kinetics and Mechanism", John Wiley and Sons Inc. New York, N.Y. (1970).
4. J.H. Espenson and S.G. Walenuk, J. Inorg. Chem., 1972, 11, 2035.
5. R.G. Wilkins and R.E. Yelin, Inorg. Chem., 1969, 8, 1470.
6. K.C. Francis, D. Cummins and J.J. Oakes, J. Chem. Soc. Dalton, 1985, 493.
7. E.N. Rizkalla, S.S. Anis and M.N. Ramsis, J. Coord. Chem., 1987, 15, 307.
8. I. Tinoco, Jr., K. Sauer and J.C. Wang, "Physical Chemistry", Prentice Hall Inc, New Jersey, USA, 1978, p. 328.
9. A.L. Lehninger, "Principles of Biochemistry" CBS Publishers and Distributors, Delhi, India, 1984, p. 216.
10. R.M. Naik and P.C. Nigam, Trans. Met. Chem., 1987, 12, 261 and references contained therein.
11. (Ms) Nishi Gupta, P.C. Nigam and R.M. Naik, Ind. J. Chem., 1986, 25A, 39.
12. A.I. Vogel, "Text book of Quantitative Analysis", Longman Green, London, 1962, p. 270.
13. D.D. Perrin and I.G. Sayce, Talanta, 1967, 14, 833.
14. D. Lambert and M.M. Jones, J. Am. Chem. Soc., 1966, 88, 4615.

15. F. Basolo and R.G. Pearson, "Mechanism of Inorganic Reactions", 2nd edn., John Wiley and Sons, New York, London and Sydney, 1967, p. 34.
16. K. Kumar, Ph.D. Thesis, I.I.T. Kanpur, 1979.
17. M. Shoporer, G. Ron, A. Loewenstein and G. Navon, Inorg. Chem., 1965, 4, 361.

reactions are NTA and HEDTA. On the basis of experimental observations a three step mechanism has been proposed. The effect of temperature and pH is also investigated and used to elucidate the mechanism.

The fourth chapter is concerned with reactions of the bis complex $[\text{CdR}_2]^{2-}$ and the reaction of $[\text{PdR(OH)}]^-$ with cyanide ions, where R represents Par. Kinetic results show that the first stage of these reactions proceeds via two paths: (i) a slow cyanide-independent dissociation of $[\text{CdR}_2]^{2-}$ and $[\text{PdR(OH)}]^-$ into their corresponding mono complexes and release of R and OH^- respectively and (ii) a fast cyanide-assisted dissociation of $[\text{CdR}_2]^{2-}$ and $[\text{PdR(OH)}]^-$ complexes to give the intermediates $[\text{CdR}(\text{CN})_x]^{x-}$ and $[\text{PdR}(\text{CN})_x]^{x-}$ ($x = 1$ to 3) and finally $[\text{Cd}(\text{CN})_4]^{2-}$ and $[\text{Pd}(\text{CN})_4]^{2-}$ respectively.

Chapter five deals with the results of investigations on the multidentate ligand exchange reactions of $[\text{PdIDA}]$ with L ($L = \text{EDTA}^{4-}$ and TTHA^{6-}). An interesting feature of these reactions is the fast formation of a mixed ligand intermediate $[\text{PdIDA}.L]$ which decomposes slowly to give respective products i.e. $[\text{PdEDTA}]^{2-}$ and $[\text{PdTTHA}]^{4-}$. The effect of pH and temperature on the formation and dissociation of mixed-ligand complexes have also been discussed.

The sixth chapter consists of two parts. The first part describes the kinetics and mechanism of catalytic decomposition of hydrogen peroxide in presence of $[(\text{trien})\text{Fe}(\text{OH})_2]^+$ complex and

trace determination of Fe(III) by a kinetic method based on this indicator reaction. The second part is concerned with the oxidation of DTPA by hexacyanoferrate(III). The effect of pH, ionic strength and temperature on the rate have been investigated. The pH dependence has been used to resolve the rate constants due to different reactivities of the reactants by an algebraic procedure.

VII.2 SUGGESTIONS FOR FURTHER WORK

It is realized that the present investigations can be extended to many new systems on Fe(III), Cd(II), Pd(II) and other centres in order to enhance our understanding of the ligand substitution processes. The following investigations are suggested.

- (i) Study of the reactions of some mono-, binuclear- and bis-polyamine complexes of Fe(III) with cyanide ion.
- (ii) A kinetic study of the reactions of complexes of some macromolecules of Fe(III) with monodentate cyanide and other multidentate ligands.
- (iii) Study of the reactions of CN^- with some binuclear Ni(II) chelates such as Ni_2TPHA (TPHA is tetraethylenepentaamine-heptaacetic acid).
- (iv) Investigation of the reactions of polyaminocarboxylato complexes of Pd(II) and Cd(II) with cyanide ion.

- (v) Study of some exchange reactions on aminocarboxylato-ruthenate(III) complexes with cyanide ion and to compare their behaviour with corresponding Fe(III) and other metal chelates.
- (vi) Exploration of possibilities of using ligand substitution reactions as a kinetic tool for the determination of metal ions and ligands.
- (vii) Study of the reactions of some amino acid complexes of Fe(III) and Ni(II) with mono and multidentate ligands.
- (viii) Study of the kinetics and mechanism of formation of octacyanomolybdate(V) and octacyanotungstate(V) from polyaminocarboxylato and polyamine complexes of Mo(V) and W(V).

LIST OF PUBLICATIONS

Part of the work embodied in the thesis has been published or communicated in scientific journals. A list of communications is given below:

1. Kinetics of oxidation of Diethylenetriaminepentaacetic acid by Hexacyanoferate(III),
Nishi Gupta, R.M. Naik and P.C. Nigam,
Ind. J. Chem., 1986, 25A, 39-43.
2. Kinetics and Mechanism of the reaction between bis 4-(2-pyridylazo)resorcinol ferrate(II) complex and cyanide ion,
Nishi Gupta and P.C. Nigam,
Trans. Met. Chem., 1988 (in press).
3. Kinetics and Mechanism of the reaction between bis 4-(2-pyridylazo)resorcinol ferrate(III) complex and cyanide ion,
Nishi Gupta and P.C. Nigam,
Trans. Met. Chem., 1988 (in press).
4. Trace determination of Iron(III) by a Kinetic Method based on "Catalase" like activity of $[(\text{trien})\text{Fe}(\text{OH})_2]^+$ complex on the decomposition rate of Hydrogen peroxide,
Nishi Gupta and P.C. Nigam,
Ind. J. Chem., 1988 (in press).
5. Multidentate ligand exchange kinetics: Reactions of amino-carboxylatoferate(III) complexes with 4-(2-pyridylazo)-resorcinol,
Nishi Gupta and P.C. Nigam,
J. Coord. Chem., 1988 (communicated).

6. Multidentate ligand exchange kinetics: Substitution reactions of Ethylenediaminetetraacetate and Triethylenetetraminehexaacetate anions with Iminodiacetatopalladium(II),
Nishi Gupta and P.C. Nigam,
Trans. Met. Chem., 1988 (communicated). (O, 000)

7. The Study of Kinetics and Mechanism of reactions of $[PdPar(OH)]^-$ and $[Cd(Par)_2]^{2-}$ with cyanide ions by Stopped Flow Technique,
Nishi Gupta, R.M. Naik and P.C. Nigam,
Inorg. Chim. Acta, 1988 (communicated). (O, 000)

8. A survey of mechanistic studies on ligand substitution reactions of transition metal complexes.
Nishi Gupta, R.M. Naik and P.C. Nigam,
T Coord. Chem. Rev., 1989 (communicated).